DISS. ETH. No. 15180

METHYLGLYOXAL, CREATINE AND MITOCHONDRIAL MICRO-COMPARTMENTS

A dissertation submitted to the
SWISS FEDERAL INSTITUTE OF TECHNOLOGY ZÜRICH
For the degree of
Doctor of natural sciences

Presented by

Oliver Speer

Dipl.-Biologe, Universität Konstanz, Germany
** 08.01.1973, Villingen-Schwenningen, Germany*
German citizen

Prof. Dr. Theo Wallimann, examiner
Prof. Dr Sabine Werner, co-examiner
Ove Eriksson, MD, PhD, co-examiner

Zürich, June 2003

ACKNOWLEDGEMENTS

While writing up my thesis, it became very clear to me, that I could not have done my PhD without the help of so many. Meeting many people who helped and invested their time and knowledge in me has marked my time as PhD student. For me these are the most valuable experiences.

First of all I want to thank Prof. Dr. Theo Wallimann. He agreed immediately when I asked him in December 1999 whether I could carry out my PhD in his lab. He was always present and gave good advice and help in both scientific and more "normal life" questions. He always gave me the freedom to develop own ideas. He never gave up his patience, even during times filled with conflicts. Thanks a lot for all the valuable discussions about scientific careers, the future and private life.

Many thanks to Prof. Dr. Sabine Werner for examining my thesis.

Many, many thanks to all the coworkers in the lab, for a great atmosphere and good teamwork over the years: Tanja Buerklen, Dr. Kate Adcock, Dr. Max Dolder, Dr. Dietbert Neumann, Dr. Isabelle Gerber, Roland Türk, Flurina Meiler, Dr. Bernd Walzel, Dr. Thorsten Hornemann, Dr. Silke Wendt, Nadine Straumann, Dr. Marianne Suter, Tina Leuenberger, Dr. Uwe Schlattner, Dr. Malgorzata Tokarska-Schlattner.

Special thanks to Lukas Neukomm, with him I spent nice 9 months, an intense working period, we had a lot to laugh and a lot to think about. His diploma work is most of chapter 6.
Special thanks go to Dr. Max Dolder for his great work on the permeability transition (Chapter 3), discussions about mitochondria and teaching.
Special thanks, Kate and Theo, for reading the manuscript during the last days of writing.

I want to thank Tina and Nadine, who are doing great experiments with expressing CrT in mammalian cell. These results gave me the last proof and impulse to write down the very last pages of Chapter 6.

Big thanks go to Dr. Ove Eriksson. We both met 1998 in Padova. Ever since, we have stayed in contact. Theo Wallimann gave me the possibility to start my PhD in Ove's lab in Helsinki. Thus, in 2000, I spent four months in Helsinki, and again two months in 2002. I learned a lot from Ove: critical thinking, lab setup, electron microscopy, MALDI-TOF, etc…thanks a lot also for the marvelous trip to northern Norway (and arctic surfing). Thank you for being my supervisor and teacher. Thanks a lot to Ove's family: Anne-Kathryn, Jens, Tom and Binx. We all had some nice time together in Helsinki and Öby. Tak so muke!!
I want to thank Dr. Nils Beck from the Institute of pathology (Helsinki), who helped me a lot with the immuno EM techniques, Kaija Niva for all the technical support in the lab in Helsinki. Many thanks for the profound teaching of a variety of electron microscopy techniques by Dr. Peter Engelhard, thanks also for some nice hours out on Pihlasaari. Thanks to Dr. Sarah Butcher at the Biocenter Viiki (Helsinki) for introducing me to cryo-electron microscopy. And I want to thank all the people in the lab at the Biomedicum Helsinki: Sarune Morkunaite, Linn Hensbo, Julius Liobikas, Marina Franck. I think we made a very nice teamwork, seen in Chapter 2; special thanks to Prof. Dr. Paavo Kinnunen for letting me work in his lab. Kiitos!

Thanks a lot, Mesieurs Dr. Hugues Henry & Dr. Olivier Braissant, for all the help with starting up 2D gels, discussing all the nasty questions about the creatine transporter, which gave rise to major results in Chapter 6. Thanks for letting me visit the lab at the CHUV in Lausanne, Prof. Dr. Bachmann. Merci beacoup!

Thanks to Dr. Torsten Kleffmann for the introduction to the ESI-MS/MS (functional genomics center Zürich) and valuable tips, which lead to important experiments and insights, all seen in chapter 6.

Thanks for your friendship, nice evenings, the splendid life in Zürich: Doro, Dietmar & Claire & Klara, Raffa & Chiara & Thorsten & Janno, Tini, Till, Max & Julia, Johannes, Nina & Gerri, Jens, Michela, Vitto, Urs, Justine, Susanne & Babsi, Alessandra, Martijn, the Akitiv theatre team, especially Lukas Schmocker.

Thanks to Erhard Wagner, my flat mate, for his brilliant playing Bach on the cembalo, which was incredibly helpful while writing! Thanks a lot for your friendship, a lot of nice evenings with Raclette, Fondue or your marvelous Sushi!

Thanks to Urs Hartmann for the encouragement to go on painting, teaching me perspective viewing and using colour. That was in a way harder than my PhD.

Not to forget: Many thanks to my teachers in Konstanz: Prof. Dr. Dieter Brdiczka. He was my first employer, it was him how introduced me to mitochondria. Thanks to Birgit Riede, Dr. Gisela Beutner and Dr. Alex Rück for teaching me how to use a pipette, photometer and oxygraph.
Thanks also for the nice time I had in the lab of Prof Dr. Paolo Bernardi (University of Padova). Here I met Drs Ove Eriksson, Francois Ichas, Eric Fontaine, Luca Scorrano, Paola Constantini. Thanks a lot to you all for teaching me so much about mitochondria, enjoy Italian life and for discussing science.

Dr. Eugenio Fava, thanks for your friendship, uncountable pasta diners, and holidays in Italy, for introducing me to Italian music. Grazie al mio fratello di pasta, per momenti pieno di gioia, con quatro capelli e quatro neuroni. Abraccio grande, spirito libero.
Dr. Berna Simon, for the great work on the GD3 story. Thanks to you both Berna & Eugenio for always opening up your house and hearts, especially helpful in difficult times! Grazie und danke!

Special thanks go to Moni for her friendship, love and support (especially during the last troublesome year!), patience and for being there and keeping up my spirits in joyful and difficult situations.

Most important:
Special thanks go to my parents, Camilla and Walter, and all the family, for all your love, support and encouragement, the basis for everything!

This work was carried out in the time between April 2000 and June 2003 in the group of Prof. Dr. Theo Wallimann at the Institute of Cell Biology at the Swiss Federal Institute of Technology Zurich.

Publications represented in this work:

Chapter 2
Oliver Speer, Sarune Morkunaite-Haimi, Julius Liobikas, Marina Franck, Linn Hensbo, Matts D. Linder, Paavo J. K. Kinnunen, Theo Wallimann, and Ove Eriksson
Rapid Suppression of Mitochondrial Permeability Transition by Methylglyoxal, Role of Reversible Arginine Modification. *J Biol Chem*, 2003 Jun 18 [Epub ahead of print]
Contributed figures 1; 2; 3; 5; 6 and table 1.

Chapter 6
Oliver Speer, Lukas J. Neukomm, Robyn M. Murphy, Elsa Zanolla, Uwe Schlattner, Rodney J. Snow, and Theo Wallimann
Creatine transporter isoenzymes: a reappraisal. *Moll Cell Biochem* in press.
Contributed figures 1- 8; 10 and table 1.

Chapter 3
Max Dolder, Bernd Walzel, Oliver Speer, Uwe Schlattner, and Theo Wallimann
Inhibition of the mitochondrial permeability transition by creatine kinase substrates: requirement for microcompartmentation. *J. Biol. Chem* 2003 May 16;278(20):17760-17766.
Contributed animals, isolated mitochondria, intellectual support.

Chapter 5
Bernd Walzel, Oliver Speer, Else Zanolla, Ove Eriksson, Paolo Bernardi, and Theo Wallimann
Novel Mitochondrial Creatine Transport Activity: Implications for Intracellular Creatine Compartments and Bioenergetics. *J Biol Chem* 2002 Oct 4;277(40):37503-37511
Contributed figures 1; 2; 3; 4; 5; 7; 8 and table 1.

Contributions to other studies:

Tarnopolsky M, Parise G, Fu MH, Brose A, Parshad A, Speer O, Wallimann T.
Acute and moderate-term creatine monohydrate supplementation does not affect creatine transporter mRNA or protein content in either young or elderly humans. *Mol Cell Biochem*. 2003 Feb; 244(1-2):159-66.

Peral MJ, Garcia-Delgado M, Calonge ML, Duran JM, De La Horra MC, Wallimann T, Speer O, Ilundain A.
Human, rat and chicken small intestinal Na+ - Cl- -creatine transporter: functional, molecular characterization and localization. *J Physiol.* 2002 Nov 15;545(Pt 1):133-44.

Bernd Walzel, Oliver Speer, Ernie Boehm, Soren Kristiansen, Sharon Chan, Kierian Clarke, Josef P. Magyar, Erik A. Richter, and Theo Wallimann
New creatine transporter assay and identification of distinct creatine transporter isoforms in muscle. *Am J Physiol Endocrinol Metab.* 2002 Aug;283(2):E390-401.

Wendt S, Dedeoglu A, Speer O, Wallimann T, Beal MF, Andreassen OA.
Reduced creatine kinase activity in transgenic amyotrophic lateral sclerosis mice. *Free Radic Biol Med* 2002 May 1;32(9):920-6

Schlattner U, Mockli N, Speer O, Werner S, Wallimann T.
Creatine kinase and creatine transporter in normal, wounded, and diseased skin. *J Invest Dermatol.* 2002 Mar;118(3):416-23.

Castro-Palomino JC, Simon B, Speer O, Leist M, Schmidt RR. Synthesis of ganglioside GD3 and its comparison with bovine GD3 with regard to oligodendrocyte apoptosis mitochondrial damage. *Chemistry* 2001 May 18;7(10):2178-84

ABBREVIATIONS

AGAT	arginine glycine armino-transferase
AGEs	advanced glycation end products
ANT	adenine nucleotide translocator
Ap_5A	P^1,P^5-di(adenosine 5')-pentaphosphate (an inhibitor of adenylate kinase)
α-HCA	α-cyano-4-hydroxycinnamic acid
α-KGDH	α-ketoglutarate dehydrogenase
BAD	2,3-butanedione
BB-CK	cytosolic brain-type creatine kinase
BC-KADH	branched chain keto acid dehxdrogenase
β-GPA	β-guanidinopropionic acid
CK	creatine kinase
COX	cytochrome oxidase
Cr	creatine
CRT, CrT	creatine transporter
CsA	cyclosporin A
CyCr	cyclocreatine
DNFB	2,4-dinitro-1-fluorobenzene
DTNB	5,5'-dithiobis(2-nitrobenzoic acid)
$\Delta\Psi_m$	mitochondrial transmembrane electrical potential difference
FCCP	carbonyl cyanide *p*-trifluoromethoxyphenylhydrazone
GAA	guanidine acetic acid
GAMT	guanidine-acetate methyl-transferase
GD3	1-O-[O-(N-acetyl-α-neuraminosyl)-(2→8)-O-(N-acetyl-α-neuraminosyl)-(2→3)-O-β-D-galactopyranosyl-(1→4)-β-D-glucopyranosyl-ceramide
GPA	β-guanidinopropionic acid
IMS	intermembrane space
LC-ESI-MS/MS	liquid-chromatograph-electro-(nano)spray-ionization tandem mass spectroscopy
MALDI TOF	matrix-assisted laser desorption-ionisation and time-of-flight
MCK	muscle type creatine kinase
MG	methylglyoxal
Mops	4-morpholinepropanesulfonic acid
MPT, mPT, PT	mitochondrial permeability transition
MtCK	mitochondrial creatine kinase
NEM	*N*-ethylmaleimide
OH-PGO	p-hydroxyphenylglyoxal
PBS	phosphate-buffered saline
PCr	phosphocreatine
PDH	pyruvate dehydrogenase
PGO	phenylglyoxal
PKC	protein kinase C
PT, MPT, PT	mitochondrial permeability transition
PTP	permeability transition pore
PKC	protein kinase C
RFI	relative fluorescence intensity
TCA	trichloric acid
TFA	trifluoroacetic acid
TMRM	tetramethyl-rhodamine methyl ester
VDAC	outer membrane anion channel

SUMMARY

SUMMARY

In recent years mitochondria have been recognized as centers of cell death regulation. The release of several pro-apoptotic proteins from the mitochondrial inter-membrane space leads to programmed cell death. For the release of apoptogenic proteins, such as cytochrome c, the mitochondrial permeability transition (mPT) is essential.

(I) In the first part of the presented thesis, the effects of methylglyoxal (MG), a new permeability transition inhibitor, are described. MG was able to reversibly inhibit Ca^{2+}- and ceramide GD3-induced swelling of mitochondria, as well as the release of cytochrome c. However, MG did not interfere with substrate transport, respiration or oxidative phosphorylation. MG is a physiological carbonyl compound formed as an intermediate by the glycolytic enzyme triose phosphate isomerase. Thus, in addition the effect of 29 other physiological carbonyl compounds were also tested on mPT. Except for glyoxal and MG none of these related compounds showed neither mPT-inducing nor mPT-inhibiting characteristics. The effect of MG is probably due to a reversible covalent modification of arginine residues in proteins that are crucial for mPT regulation.

(II) In the second part of the thesis the role of ubiquitous mitochondrial creatine kinase (mt_uCK) in mitochondria was studied. Mitochondrial CK, among other things, is a regulator of mPT. However, the role and interaction partners of mt_uCK during mPT regulation have not yet been characterised completely. Transgenic liver expressing mt_uCK, which is not present in wild type liver, is used as a model to study the function of mt_uCK. The effects of creatine and its analoges, cyclo-creatine and β-guanidinopropionic acid (β-GPA) were investigated. It was shown by standard mitochondrial swelling measurements that mt_uCK in concert with creatine and cyclocreatine is able to protect mitochondria from swelling and going into mPT pore opening. However β-GPA, which is not phosphorylated by mtCK was ineffective in this respect. The creatine and cyclo-creatine effected mPT inhibition was Mg^{2+} dependent. The mt_uCK inhibitory effects were observed without externally added nucleotides. By thin layer chromatography, the incorporation of ^{32}P into phosphocreatine, after the addition of creatine without additional nucleotides was observed.

These data indicate that an internal mitochondrial nucleotide pool must exist and a nucleotide cycling facilitated by functional coupling of adenine nucleotide translocator (ANT) and mt_uCK. An mt_uCK / ANT micro-compartment is therefore suggested. To test this hypothesis, BBCK, a cytosolic creatine kinase isoform, as well as mt_uCK, were both added to isolated wild type mitochondria not containing mt_uCK. As expected, unlike BBCK, mt_uCK did bind to the mitochondrial surface. However, in both cases neither creatine nor cyclocreatine were able to inhibit mPT. Thus, a stringent closely coupled micro-compartment between mtCK and ANT seems to be prerequisite for the protective function of CK in concert with the latter protein complex.

(III) To visualize the above reported effects of mt_uCK, the morphology of transgenic liver was studied by electron microscopy. Over-expressed mt_uCK in liver formed inclusions inside the mitochondrial christae. Mt_uCK increased significantly the number of contact sites, thus harbouring additional potential mPT regulators. Also, the resistance of mitochondria to the detergent digitonin increased, as seen by light scattering. It was possible to isolate detergent-resistant membrane domains by ultra-centrifugation. These contained besides mt_uCK also the adenine nucleotide translocator (ANT), the outer membrane voltage-dependent anion channel (VDAC), as well as certain components of the respiratory chain.

In conclusion I hypothesize that mt_uCK besides being concentrated in contact sites is also buried within christae inside mitochondria. In order to supply mt_uCK with its substrate creatine, a mitochondrial transport mechanism for creatine might be proposed.

(IV) Indeed a mitochondrial creatine uptake mechanism could be identified and characterised in the fourth part of this thesis. Antibodies against synthetic peptides derived

from the sequence of the creatine transporter (CrT) gene recognize two distinct polypeptides at ~55 and ~70 kDa (3, 5). Here the mitochondrial localisation of these proteins was investigated. By electron microscopy and sub-mitochondrial fractionation it was shown that those localised to the inner mitochondrial membrane. After assuming that the α-CrT reactive proteins represent creatine transporter; isolated mitochondria were incubated with radioactively labelled creatine. In fact, a mitochondrial creatine uptake with a high K_m of approximately 15 mM was observed. Unlike plasma membrane creatine transport (4, 5), mitochondrial creatine uptake was not inhibited by the creatine analogue β-GPA. However, the creatine precursor arginine was a significant competitive inhibitor for mitochondrial creatine uptake. Finally α-CrT antibodies inhibited mitochondrial creatine uptake.

The mitochondrial creatine uptake was significant. However, as the mitochondrial Cr uptake properties vary substantially from the reported plasma membrane Cr uptake (4, 5) the molecular identity of the mitochondrial creatine uptake system needed to be clarified.

(V) In the fifth part of the thesis, the α-CrT antibody reactive protein species were characterised in more detail. Proteins of enriched inner mitochondrial membrane were separated by 2D gel electrophoresis. After excision from the 2D gel and tryptic digestion, they were identified by LC-ESI-MS/MS. Four α-CrT immuno reactive protein species could be identified as subunits of mitochondrial dehydrogenase complexes. High pH carbonate washing of inner mitochondrial membrane fractions revealed that these α-CrT reactive proteins were not genuine membrane proteins. However, another α-CrT reactive polypeptide at higher molecular weight revealed typical membrane protein behaviour. Consequently, by MALDI-TOF a potential membrane protein was determined as carboamoyl phosphate synthase, a membrane bound mitochondrial enzyme of the urea cycle. As there was no mitochondrial creatine transporter protein found, the creatine uptake was studied again. After mitochondrial volume measurements, mitochondria appeared not to enrich creatine: the creatine concentration in mitochondria increased significantly, yet remained at ~30 % of the external creatine concentration. Pulse chaise experiments showed that creatine was migrating freely into and out of mitochondria. This indicates that there is no active creatine uptake system within mitochondria.

(VI) I propose that creatine diffuses freely into the inter-membrane spaces and into the mitochondrial christae where mtCK is located. For this creatine uptake no specific Cr transporter is needed. I suggest that a classical low K_m, high affinity creatine transporter is only present in the plasma membrane.

The complete micro-compartments inside christae on the one hand or between MOM and MIM on the other hand, containing mt_uCK, ANT, creatine and Mg^{2+} protects against mPT. In accordance to Eric Fontaine et al. (2) and Paul S. Brookes et al. (1) components of the respiratory chain were found in context with the mPT.

SUMMARY

ZUSAMMENFASSUNG

In den letzten Jahren wurden Mitochondrien als Zentren der Zelltodregulation erkannt. Die Freisetzung einiger Proteine aus dem mitochondrialen Zwischenmembranraum führt zum programmierten Zelltod. Für die Freisetzung mitochondrialer apoptogener Proteine, wie zum Beispiel Cytochrome c, ist die mitochondriale Permeabilitäts-Transition (mPT) entscheidend.

(I) Im ersten Teil der vorgestellten Arbeit werden die Effekte von Methyl-Glyoxal (MG), eines neuen Hemmstoffes der mPT beschrieben. MG inhibierte reversibel, durch Ca^{2+} und Ceramide GD3 verursachtes Schwellen von Mitochondrien. MG störte jedoch weder den Substrattransport, die Atmung, noch die oxidative Phosphorylierung. MG ist eine physiologische Verbindung, welche als Zwischenprodukt durch das glycolytische Enzym Triosephosphat Isomerase gebildet wird. Folglich wurde die Wirkung von 29 weiteren physiologisch relevante Carbonyl Verbindung auf die mPT untersucht. Außer Glyoxal zeigte keine der untersuchten Substanzen einen mPT-fördernden oder einen mPT-hemmenden Einfluss. Der Effekt von MG wird der reversiblen kovalenten Bindung an Arginine Reste in Proteinen, die entscheidend für die mPT Regulation sind, zugeschrieben.

(II) Im zweiten Teil dieser Dissertation wurde die Rolle der ubiquitären Kreatin Kinase (mt_uCK) in Mitochondrien untersucht. Unter anderem ist die mt_uCK ein Regulator der mPT. Die Rolle der mt_uCK und deren Interaktionspartner bei der mPT wurden jedoch noch nicht vollständig charakterisiert. Mt_uCK ist normalerweise in Lebergewebe nicht nachweisbar. Deshalb wird transgene Leber, welche mt_uCK expremiert, als Modell zur Funktionsuntersuchung der mt_uCK verwendet. Die Wirkung von Kreatin und dessen Analoge Cyclo-Kreatin und β-Guanidino-Propion Säure (β-GPA) wurde untersucht. Mittels Standart Schwell-Messungen an Mitochondrien wurde gezeigt, dass mt_uCK zusammen mit Kreatin oder Cyclo-Kreatin das Öffnen der mPT Pore verhindern konnte. β-GPA, dass von mt_uCK nicht phosphoryliert werden kann, zeigt hier keinen Effekt. Die Wirkung von Kreatine und Cyclo-Kreatine auf die mPT war Mg^{2+} abhängig, und wurde ohne den Zusatz von Nukleotiden beobachtet. Mittels Dünnschicht-Chromatographie wurde nach der Zugabe von Kreatin ohne zusätzlich Nukleotide der Einbau von ^{32}P in Phospho-Kreatine nachgewiesen.

Diese Daten deuten darauf hin, dass es einen internen mitochondrialen Pool an Nukleotiden geben muss, und dass eine Zyklisierung der Nukleotide durch die funktionelle Kopplung des Adenin-Nukleotid Translokators (ANT) und der mt_uCK ermöglicht wird. Deshalb wird eine ANT / mt_uCK Mikro-Kompartmentierung vorgeschlagen. Um diese Hypothese zu testen wurde zu isolierten Wildtyp-Mitochondrien (ohne mt_uCK), sowohl gereinigt mt_uCK als auch BBCK, ein zytosolisches Isoenzym, zugesetzt. Wie erwartet band mt_uCK im Gegensatz zur BBCK and die Oberfläche der Mitochondrien. In beiden Fällen waren jedoch weder Kreatin noch Cyclo-Kreatin in der Lage mPT zu hemmen. Deshalb scheint eine direkt Nachbarschaft von ANT und mt_uCK in einem Mikro-Kompartment notwendig um die schützende Wirkung der mt_uCK zu ermöglichen.

(III) Um die oben berichteten Wirkungen der mt_uCK sichtbar zu machen wurde die Morphologie der transgenen Leber im Elektronenmikroskop untersucht. In Leber über-expremierte mt_uCK führte zu Einschlüssen innerhalb der mitochondrialen Christae. MtuCK erhöhte signifikant die Anzahl der Kontaktstellen, welche vermutlich einige mögliche mPT Regulatoren beherbergen. Ebenso erhöhte sich die Beständigkeit der Mitochondrien gegenüber dem Detergents Digitonin. Dies wurde bei Lichtstreuungs-Messungen festgestellt. Es war außerdem möglich durch Ultra-zentrifugation Detergents resistente Membran-Domänen zu isolieren. Diese enthielten außer mt_uCK auch ANT, spannungsabhängigen Ionenkanäle (VDAC) und Bestandteile der Atmungskette.

mt_uCK ist folglich sowohl in den Kontaktstellen, als auch in den unzugänglichen Christae lokalisiert ist. Um mt_uCK mit Kreatin zu versorgen schlage ich hier einen mitochondrialen Kreatin-Transport-Mechanismus vor.

(IV) Tatsächlich konnte im vierten Teil dieser Doktorarbeit ein mitochondrialer Kreatin Aufnahme Prozess identifiziert und charakterisiert werden. Antikörper, die gegen synthetische Peptide, abgeleitet von der Gen-Sequenz des Kreatin Transporters (CrT), hergestellt wurden,

erkannten zwei verschiedene Polypeptide mit der molekularen Größe von ca. 55 und 70 kDa (3, 5). Hier wurde die mitochondriale Lokalisierung dieser Proteine untersucht. Mittels Elektronenmikroskopie und Sub-Fraktionierung von mitochondrialen Membranen wurde gezeigt, dass sich diese Proteine in der mitochondrialen Innenmembran befinden. Nach der Annahme, dass diese α-CrT reaktiven Proteine CrT seien, wurden isolierte Mitochondrien mit radioaktiv markiertem Kreatin inkubiert. Tatsächlich wurde ein Kreatin-Aufnahme mit hohem Km (ca. 15 mM) gemessen. Im Gegensatz zum Kreatin Transport über der Plasmamembran (4, 5), wurde der mitochondrial Kreatine Transport nicht durch β-GPA gehemmt. Arginine war jedoch ein signifikanter Inhibitor der mitochondrialen Kreatin Aufnahme. Schließlich inhibierte der α-CrT Antikörper die mitochondriale Kreatin Aufnahme.

Die mitochondriale Kreatin Aufnahme war eindeutig. Ihre Eigenschaften gegenüber der des Plamamembran Transportes waren jedoch substanziell verschieden (4, 5). Die molekulare Identität dieser mitochondrialen Kreatin Aufnahme bedurften der Klärung.

(V) Im fünften Teil dieser These wurden die α-CrT reaktiven Protein näher untersucht. Proteine aus hochangereicherter mitochondrialer Innenmembran wurden durch 2D Gel-Elektrophorese aufgetrennt. Nach dem Ausschneiden aus den Gelen und dem tryptischen Verdau, wurden sie mittels LC-ESI-MS/MS identifiziert. Vier Proteine konnten als Untereinheiten von mitochondrialen Dehydrogenase Komplexen identifiziert werden. Carbonat-Extraktionen bei hohem pH zeigten, dass es sich tatsächlich nicht um Membranproteine handelte. Eine weiter α-CrT reaktive Proteinbande bei einem Molekulargewicht von >100 kDa zeigte jedoch typische Eigenschaften eines Membranproteins. Mittels MALDI-TOF wurde dieser Kandidat aber als Karboamoyl-Phosphat Synthase, einem hypothetischen Membranprotein des Harnstoff Zyklus identifiziert. Da kein mitochondrialer CrT gefunden werden konnte wurde die mitochondriale Kreatin Aufnahme nochmals untersucht. Nach der Messung des mitochondrialen Volumens ergab es sich bei der Konzentrationsberechnung, dass Mitochondrien Kreatin nicht anreichern. Die Kreatinkonzentration in Mitochondrien stieg zwar eindeutig an, blieb jedoch immer bei 30 % der außen vorgelegten Konzentration. „Pulse chaise“ Experimente zeigten weiterhin, dass Kreatin sich frei in Mitochondrien hinein und herausbewegen kann. Summa summarum zeigen diese Ergebnisse, dass es keinen aktiven mitochondrialen Kreatintransport gibt.

(VI) Ich schlage vor, dass Kreatin frei zur mt_uCK in die Cristae hinein diffundieren kann. Für diese Aufnahme in die Mitochondrien ist jedoch kein spezifischer Transport notwendig. Ein klassischer hochaffiener Kreatin Transporter mit niedrigem K_m-Wert kommt vermutlich nur in der Plasma-Membran vor.

Weiterhin stelle ich vor, dass intakte Micro-Kompartimente in den Christae auf der einen Seite, und zwischen Außen- und Innenmembran auf der anderen Seite, mt_uCK, ANT, Mg^{2+} und Nukleotide enthalten, und als funktionelle Einheit mPT verhindern können. In Übereinstimmung mit Eric Fontaine (2) und Paul S. Brooks (1) konnten im Zusammenhang mit mPT Teile der Atmungskette nachgewiesen werden.

References:

1. **Brookes PS, Pinner A, Ramachandran A, Coward L, Barnes S, Kim H, and Darley-Usmar VM.** High throughput two-dimensional blue-native electrophoresis: a tool for functional proteomics of mitochondria and signaling complexes. *Proteomics* 2: 969-977, 2002.

2. **Fontaine E, Eriksson O, Ichas F, and Bernardi P.** Regulation of the permeability transition pore in skeletal muscle mitochondria. Modulation By electron flow through the respiratory chain complex i. *J Biol Chem* 273: 12662-12668, 1998.

3. **Guerrero-Ontiveros ML WT.** Creatine supplementation in health and disease. Effects of chronic creatine ingestion in vivo: down-regulation of the expression of creatine transporter isoforms in skeletal muscle. *Mol Cell Biochem* 184: 427-437, 1998.

4. **Peral MJ, Garcia-Delgado M, Calonge ML, Duran JM, De La Horra MC, Wallimann T, Speer O, and Ilundain A.** Human, rat and chicken small intestinal Na(+)-Cl(-)-creatine transporter: functional, molecular characterization and localization. *J Physiol* 545: 133-144., 2002.

5. **Walzel B, Speer O, Boehm E, Kristiansen S, Chan S, Clarke K, Magyar JP, Richter EA, and Wallimann T.** New creatine transporter assay and identification of distinct creatine transporter isoforms in muscle. *Am J Physiol Endocrinol Metab* 283: E390-401, 2002.

SUMMARY

Brain mitochondrium, Oliver Speer, 12.04.2001

INTRODUCTION

- Mitochondrial architechture, structure and function
- Mitochondrial electron transport and oxidative phosphorylation
- Mitochondrial outer membrane
- The mitochondrial inter membrane space
- Mitochondrial integration of metabolic and signaling pathways
- Phospho transfer networks
- Mitochondrial permeability transition
- Mitochondrial creatine kinase and creatine shuttle
- Creatine metabolism
- Inborn errors in Creatine metabolism

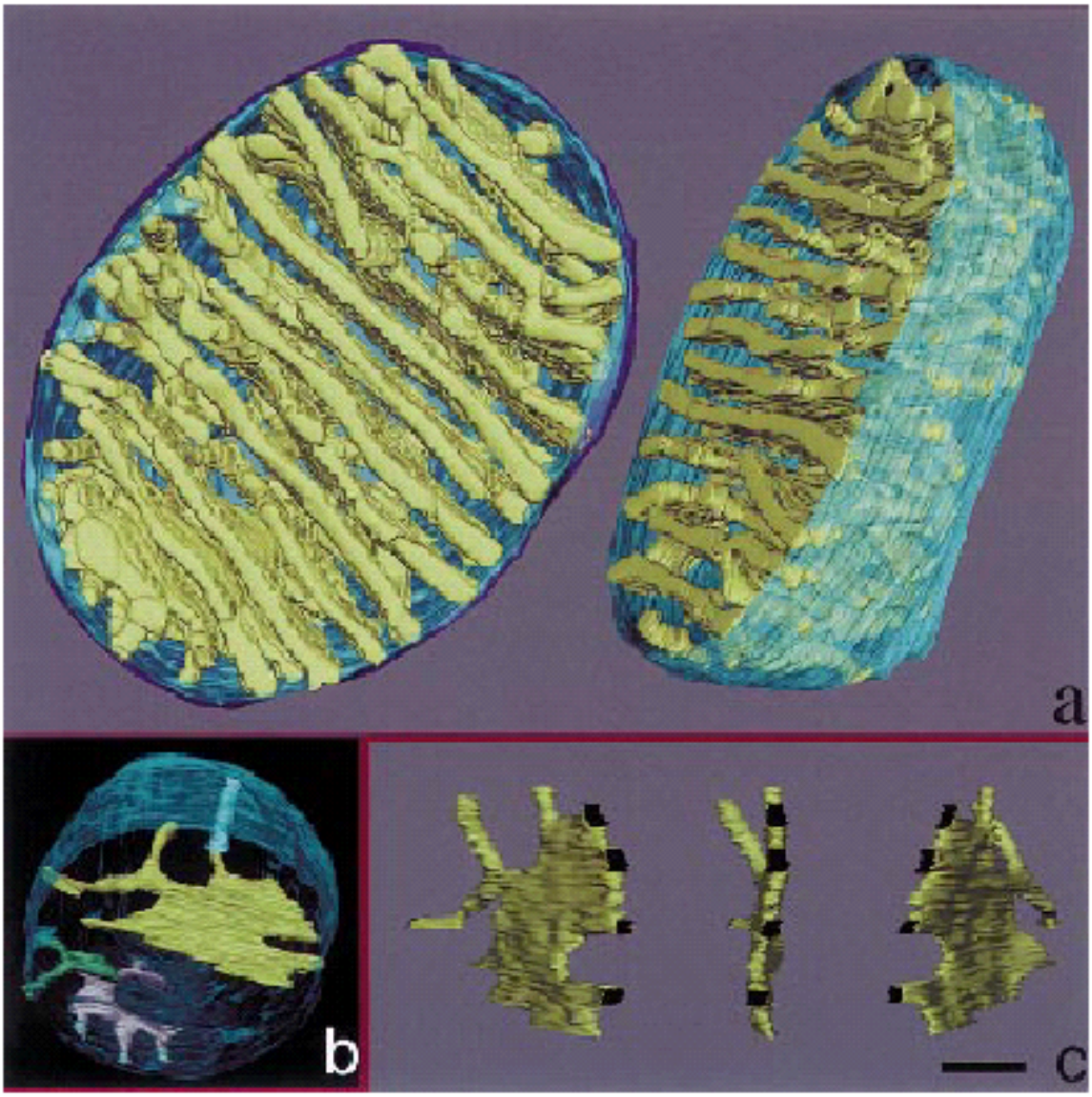

Figure 1. Electron tomography of mitochondria. (a) Two views of a 3D reconstruction of a Purkinje cell dendritic mitochondrion imaged in situ. Electron tomography was performed on 0.5 mm slices of rat brain tissue using a 400 kV microscope. The outer membrane is shown in dark blue, the inner boundary membrane in light blue, and the crista membranes in yellow. The inner boundary and crista membranes are continuous surfaces but were segmented independently to highlight their separate topographies. (b) Four cristae were segmented independently to demonstrate crista morphology and connectivity and are displayed together with the inner boundary membrane. The yellow crista is an example of a lamellar compartment with multiple crista junctions connecting it to the inner boundary membrane. The gray crista has seven tubes that connect to the inner boundary membrane on different sides. Three tubes connect to the boundary in the foreground and four tubes connect in the background, which is obscured by the lamellar portion of this crista and the green crista. A tubular crista with only one junction is displayed in blue near the top of the mitochondrion just right of center. (c) Three edge views of the yellow (lamellar) crista (from b) showing the four junctions (black openings) on this side of the crista. Scale bar = 120 nm. Adopted from G. A. Perkins and T. G. Frey (77)

This chapter is not meant to give a detailed bibliographical introduction into the literature. It is more a guide for you – the reader. This guide should lead you through the chapters. In the beginning of each chapter you will find a detailed introduction. In the following pages, however, background information is given, which is not present in the individual chapters. The main focus of this PhD thesis are, no doubt; mitochondria. In the first part of my thesis, new results on the regulation of mitochondrial permeability transition are presented, whereas in the second part novel aspects of mitochondria in creatine metabolism are illuminated.

Mitochondria - powerplants of the cell

Around 1850, microscopists used the words "*chondros"* (Greek), "*grain"* (English) or "*Korn"* (German) to describe distinct sub-cellular structures seen in the light microscope. Improved staining techniques yielded more accurate descriptions; grains were seen as "*threads"*, ***"mitos"*** in Greek, "*Faden"* in German. Hence, those structures were called Fadenkörper or **mitochondria** (C. Benda, 1898).

In the early part of the twentieth century cell biologists were eager to provide geneticists with a cellular entity, which could transmit genetic information. For a short time mitochondria were favoured as carriers of this function. The discovery by Kingsbury and Warburg that mitochondria were associated with respiration challenged this role in genetics. Another forty years of biochemical analysis lead to the characterization of mitochondria as the power plant of the cell.

Mitochondrial architecture, structure and function

Mitochondrial shape turned out to be highly dynamic and variable, but was generally described either as spherical (0,5 – 5 µm in diameter) or cylindrical (0.2 µm in diameter and 20 µm long) (Perkins et al., 2001). Mitochondria are organelles with two distinct compartments: the matrix surrounded by the inner membrane (MIM) and the intermembrane space (IMS) between the MIM and the mitochondrial outer membrane (MOM). The old *baffle model* describes the MIM protruding into the matrix space in a "baffle-like" manner. The lamellae or leaves forming these baffles are dubbed "cristae", and are aligned more or less orthogonally to the long axis of the mitochondrion (76-78).

However, scanning electron microscope studies suggest that the baffle model might be inaccurate (58, 59) and during recent years based on progress made in the field of cryo-electron microscopic tomography and image reconstruction of ultra thin frozen tissue section tilting series (for review see (5, 63)), our picture of the mitochondrial structure has been refined with a new *cristae junction model* (71, 77-79) (Fig. 1). In this model, cristae are stacks of independent membranous lamellae or "septae", and the cristae feature both a flat lamellar and a tubular part. Tubular openings connecting cristae membranes to the outer boundary membrane are named cristae junctions (76), whereas the flat lamellar cristae are located centrally in the mitochondrion (64, 78). With a few exceptions, this model proposes that there is no continuity between the cristae and peripheral inner membranes (64, 77). The functional consequence of this junctional architecture is a microcompartmentation of macromolecules inside the cristae (78). All these new structural features seem to suit mitochondrial function which is central to numerous cellular processes, such as the generation of ATP from ADP and inorganic phosphate by the process called oxidative phosphorylation (for review see (87)), regulation of the cytosolic Ca^{2+} homeostasis (43, 44) or β-oxidation of fatty acids.

The mitochondrial inner membrane: Mitochondrial electron transport and oxidative phosphorylation

The complexes of the respiratory chain are localised within the MIM together with ubiquinones, cytochromes and the ATP-synthase. The mitochondrial MIM is impermeable to most of the solutes under physiological conditions. Most of the metabolites enter the matrix under control by specific carriers in exchange for those metabolites, which must leave the mitochondria (reviewed in (99)) Among these carriers the adenine nucleotide translocase (ANT) is responsible for the exchange of ADP and ATP.

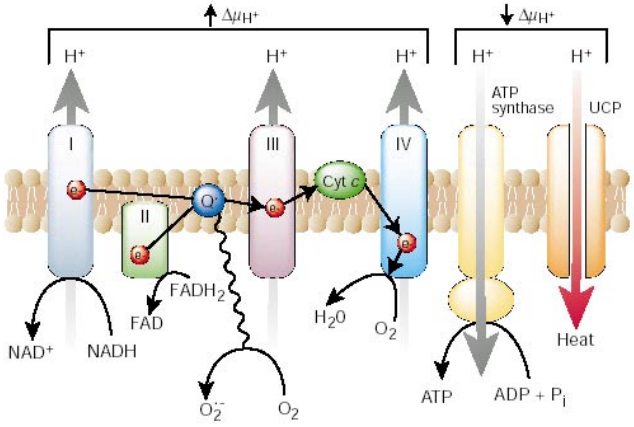

Figure 2. Chemisomotic proton circuit. Electrons from NADH and FADH2 enter respiratory chain at, respectively, complex I and II. Electrons are then transferred via ubiquinone to complex III. However Ubiquinone can transfer electrons to oxygen, producing radical oxygen species. Complexes I, III, and IV function as proton pumps, in series with respect to protons and in parallel with respect to proton circuit. Proton reentry can occur through ATP synthase to generate ATP and also through uncoupling protein (UCP), which serves for heat production. Adopted from M. Brownlee, Nature, 2001.

The mitochondrial respiratory chain is an assembly of more than twenty electron carriers grouped into four protein complexes (Fig 2). These four inner-membrane-associated enzyme complexes, with cytochrome c and the mobile carrier ubiquinone (117, 118), carry out electron flow through the mitochondrial electron transport chain. NADH derived from both cytosolic glucose oxidation and mitochondrial TCA cycle activity donates electrons to NADH:ubiquinone oxidoreductase (complex I). Complex I ultimately transfers its electrons to ubiquinone. Ubiquinone can also be reduced by electrons donated from several $FADH_2$-containing dehydrogenases, including succinate:ubiquinone oxidoreductase (complex II) and glycerol-3-phosphate dehydrogenase. Electrons from reduced ubiquinone are then transferred to ubiquinol:cytochrome c oxidoreductase (complex III) by the ubisemiquinone radical-generating Q-cycle. Electron transport then proceeds through cytochrome c to cytochrome c oxidase (complex IV), which produces water, consuming oxygen.

The mitochondrial respiratory chain catalyses the "downhill" transfer of electrons from substrates to the final acceptor, oxygen. Complexes I, III and IV pump protons across the MIM resulting in the accumulation of protons in the intermembrane space. This proton motive force is used by ATP-synthase to produce ATP using Pi + ADP. ATP is produced in the matrix compartment and exported through the ANT into the intermembrane space in exchange for ADP from the latter space. Electrons are shuttled between the complexes by specialised molecules, such as ubiquinones and cytochromes. Among the cytochromes, cytochrome c (cyt c) is important in apoptosis. Cyt c (MW 14.5 kDa) is present in the intermembrane space as well as in the christae. Cyt c is known to bind to cardiolipin, a specific lipid component of the mitochondrial MIM (88, 89), and is relative mobile within the inner membrane (3).

Mitochondrial outer membrane

The MOM is relatively selective but not as impermeable as the MIM. The major protein present in the MOM is the so-called voltage dependent anion channel (VDAC). VDAC belongs to the family of porin proteins and is permeable to solutes of < 1.5 kDa. VDAC interacts with hexokinase on the cytoplasmic surface of the MOM (11, 12). On the IMS face of the MOM VDAC interacts with mitocondrial creatine kinase (mtCK) (90).

The rotenone-insensitive NADH oxidase (RiNADHOX) is located within the outer membrane. RiNADHOX transfers electrons from cytosolic NADH to iron sulfur complexes within the MOM. Finally Cytochrome b5 transfers the electron to cytochrome c in the inter membrane space (7). The enzyme mono amino oxidase is also located at the MOM. Similar to RiNADHOX it feeds electrons to complex IV via cytochrome b5 and cytochrome c (19).

The mitochondrial inter-membrane space

The inter-membrane space (IMS) is the anteroom of mitochondria. Several apoptogenic proteins are located here, hidden from the cytoplasm. These are cytochrome c (65), part of the respiratory chain (see above), apoptosis inducing factor (AIF) (25), DIABLO/Smac (28, 114) and several procaspases (25, 47). All those factors are released if the outer membrane becomes permeable either by **mitochondrial permeability transition** (see below and **Chapter 2; 3; and 4 of the presented work**), or channel forming proteins as Bax and Bid (47).

The IMS is also a mitochondrial workshop. Proteins synthesized in the cytoplasm are imported via translocases (TOM) through the outer membrane. They are further built into the MIM or transported into the matrix for which chaperons located in the IMS are essential (94, 98, 112).

Mitochondrial membranes separate the cytosolic compartment from the mitochondrial matrix compartment. Trapped between mitochondrial matrix and the cell-cytosol, the IMS forms a third compartment, with own characteristics. On the one side IMS is restricted by the rather impermeable MIM. The outer membrane forms the other boundary of IMS. Although VDAC-containing MOM is quite permeable for small solutes, it is selective for larger charged molecules, such as nucleotides, especially ADP due to the channel's voltage dependence (33, 36, 57).

Kinases such as mitochondrial creatine kinase (mtCK) and mitochondrial adenylate kinase (mtAK) are present in the inter-membrane space. MtCK produces phosphocreatine from creatine derived from the cytoplasm plus ATP coming from the matrix. CK releases ADP into IMS like the other kinases and forms a part of the creatine shuttle (for details see **chapter 3 and 4**). While mtCK is reversibly attached to the inner membrane (82, 83), mtAK is generally considered as a marker of the aqueous phase of the IMS (17).

Several *in vitro* and *in situ* studies have shown that mitochondrial kinases are functionally linked to and prefer access to ATP derived from mitochondrial oxidative phosphorylation ((9, 10, 34, 35, 52, 56). Similarly, it was demonstrated that ADP supply to oxidative phosphorylation proceeded more effectively via mitochondrial kinases than via extra mitochondrial kinases (35, 52, 56). ADP-regeneration within the intermembrane space by mtCK and mtAK (35, 52, 56) results in high local ADP concentrations, which are greater than extra mitochondrial bulk ADP concentrations. This suggests the MOM separates kinases in the intermembrane space from the extra-mitochondrial space. This is achieved by inhibiting diffusion of adenine nucleotides and other metabolites through VDAC. The functional consequences of this compartmentation are reflected in the creatine / phosphocreatine shuttle (for details see below and **chapter 3 and 4**).

Mitochondrial integration of metabolic and signaling pathways: Phospho transfer networks

Part of intracellular energy transfer proceeds in the narrow mitochondrial inner membrane infoldings, known as cristae (Fig. 1). The cristae arrangement increases, by several folds, the capacity of mitochondrial ATP production without occupying additional intracellular space. However, it creates difficulties in ATP export from the mitochondrial intracristal space, as diffusional flux requires a significant concentration gradient. Accordingly, ATP accumulation in the mitochondrial intracristal space would inhibit export of ATP from the mitochondrial matrix by locking the adenine nucleotide translocator (64).

In principle, this limitation can be overcome by either placing in the intracristal space near-equilibrium phosphotransfer systems, capable of accelerating ATP export/ADP import, and/or by establishing high-throughput contact sites between inner and outer membranes, thereby providing direct access to ATP in the mitochondrial matrix (Fig.3). Available data

suggest that in mitochondrial physiology both possibilities are employed, and their functional significance may vary depending on the physiological conditions or functional load (37, 125). This view is supported by the observation that the presence of creatine kinase, adenylate kinase and nucleoside diphosphate kinase in the intermembrane space facilitates ATP/ADP exchange between mitochondria and cytosol (56, 81, 84).

Conversely, disruption of the adenylate kinase gene impedes ATP export from mitochondria (4). Taken together, this would indicate that in the absence of facilitating mechanisms, cell architecture and diffusional hindrances would obstruct free movement of molecules, impeding efficient intracellular communication.

Glycolytic integration

Intracellular glucose oxidation begins with glycolysis in the cytoplasm, which generates NADH and pyruvate. Cytoplasmic NADH can donate reducing equivalents to the mitochondrial electron transport chain through two shuttle systems, the malat-glutamate shuttle and cytochrome b5 in the outer membrane, which can reduce cytochrome c. Pyruvate can also be transported into the mitochondria, where it is oxidized by the tricarboxylic acid (TCA) cycle to produce carbon dioxide, water, four molecules of NADH and one molecule of

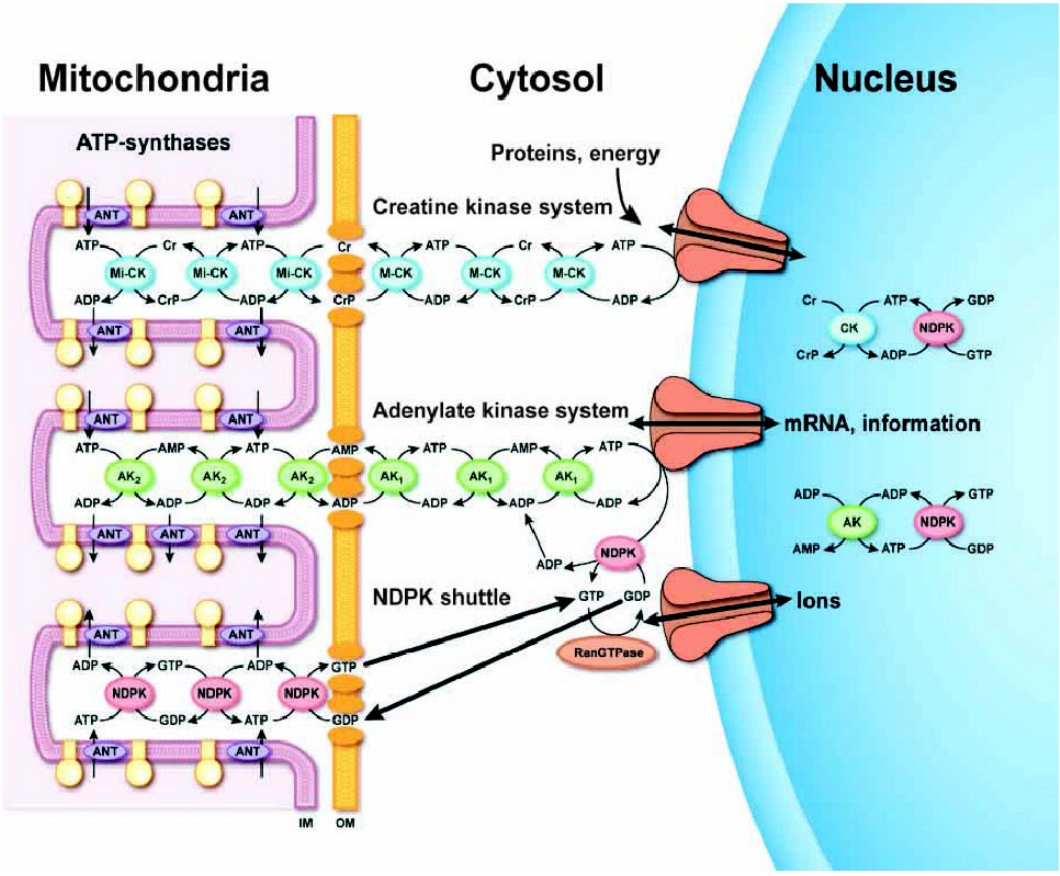

Figure 3. Energy support relays for nucleocytoplasmic communication. Mitochondria clustered around the nucleus generate the majority of ATP required for nuclear processes. Export of ATP from the mitochondrial intracristal space is facilitated by near-equilibrium reactions catalyzed by mitochondrial isoforms of adenylate kinase (AK2), creatine kinase (Mi-CK) and nucleoside diphosphate kinase (NDPK). Subsequently, highenergy phosphoryls are navigated through the diffusionally restricted perinuclear space to ATP consumption sites at the nuclear envelope and inside the nucleus by cytosolic and nuclear isoforms of AK, CK and NDPK. Interaction and complementation between these systems secure proper nucleotide ratios at and across the nuclear envelope, sustaining the high energy of ATP and GTP hydrolysis. Adopted from Dzeja &Terzic 2003 J Exp Biol

FADH2. Mitochondrial NADH and FADH2 provide energy for ATP production through oxidative phosphorylation by the electron transport chain.

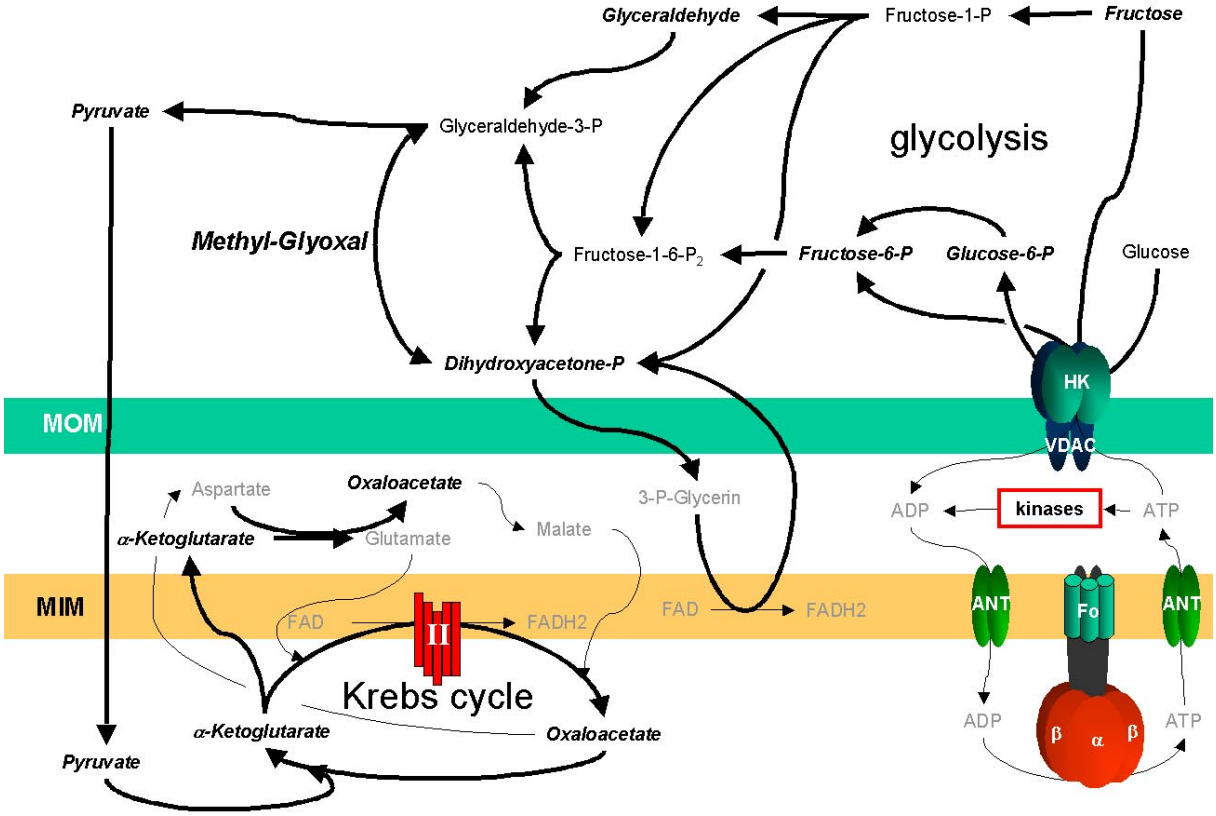

Figure 4. Compartmentation of sugar metabolism. Shown are carbonyl compounds (bold black, investigated in Chapter 2) formed in glycolysis and Krebs cycle. Note that the carbonyl compounds migrate across mitochondrial outer membrane (MOM) and mitochondrial inner membrane (MIM). Shown are also possibilities for metabolic cross-talk between mitochondria and cytoplasm, e.g. Hexokinase (HK) at the outside attached to the MOM, and other kinases, such as creatine kinase or adenylate kinase in the inter-mebrane space (see text).

The urea cycle

The keto acids α-ketoglutarate and oxaloacetate can be withdrawn from the Krebs cycle to form amino acids by transamination or added to the cycle. α-Ketoglutarate enters the Krebs cycle providing nitrogen. This nitrogen is recaptured when oxaloacetate is converted to aspartate. Those reactions are reversible.

A significant role of mitochondria in amino acid metabolism is the partition in the urea cycle. Via the urea cycle excess amino acids, e.g. aspartate coming from the Krebs cycle can be converted into urea in the liver and excreted in kidneys. Two reactions are taking place in mitochondria, the formation of carbamoyl phosphate from ammonia and bicarbonate consuming ATP, and the condensation of carbamoyl phosphate with ornithine to from citrulline.

Mitochondria – Cell Communication via permeability transition

Although the mitochondria inner membrane is permeable to certain metabolites and ions in a highly controlled and selective mode (6), it happens transiently that under certain conditions, MIM becomes unselectively permeable. This phenomenon is described as permeability transition (PT), e.g. in isolated mitochondria after addition of Ca2+. At the end of the 1970s, Haworth and Hunter obtained the first evidence that a pore (PTP) was involved in permeability transition, but the molecular nature of the PTP is still controversial (46).

During PT, the mitochondrial IM becomes permeable to solutes up to about 1,500 Da. Induction of PT is sufficient to promote apoptosis (55, 109). It is known that prolonged opening of the PT pore causes mitochondrial membrane potential ($\Delta\Psi_m$) dissipation, ATP depletion, Ca^{2+} release, impairment of Ca^{2+} buffering, mitochondria swelling and mitochondrial protein release (48, 49) such as cytochrome c, AIF, Smac/DIABLO and several proteases (47).

Several substances can induce PT such as physiological signalling agents Ca^{2+} and NO (21, 24). In addition, mitochondrial depolarisation is another general stimulus that induces PT (6, 32, 50). Most recently it was shown that the ganglioside GD3, an intracellular mediator, is able to trigger PT in isolated mitochondria and tumour cells line (53, 54, 97). GD3 is also able to induce depolarisation in some type of primary neuronal cells (oligodendrocytes), but fail to produce depolarisation on microglia cell (22).

The PT pore is inhibited by cyclosporin A (6) through its binding to cyclophillin D and also by ADP and Mg^{2+} (20). High $\Delta\Psi$, CsA, ADP, H^+, and BKA stabilize the closed conformation of the PTP, whereas low $\Delta\Psi$, intramitochondrial Ca^{2+}, low Pi, and carboxy-atractyloside (CATR) promote the open conformation (6) and chemical agents reacting with vicinal dithiol such as tributyltin are also inducers of PT (108).

The molecular machinery of the PTP is not understood in great detail. The present model of the PTP involves the outer membrane VDAC and ANT as the two major components (8, 18, 66, 67). Other proteins such as hexokinase, mitochondrial creatine kinase and cyclophilin D are involved in the regulation of the PT.

A mitochondrial multiconductance channel, measured by patch clamping of mitoplasts and considered to be the electrophysiological counterpart of the MPT (110), was also detected in an ANT-deficient yeast strain, indicating that ANT may not be involved directly as the MPT channel (61). Finally, it has been shown that the MPT is highly influenced by electron flux through respiratory complex I. MPT inhibition occurs if the electron flux is suppressed by quinones (32). This led to the suggestion that the MPT may reside within complex I (31, 32). Thus, there are some serious arguments against ANT being the sole MPT pore-forming channel

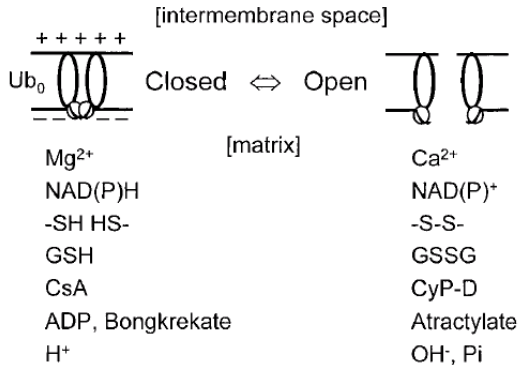

Figure 5. Modulation of the mitochondrial permeability transition by matrix and membrane effectors (see text). Adopted from P. Bernardi (6).

The identification of functionally important amino acids residues by the use of amino acid-specific covalent reagents has provided some clues on the mechanism of the PTP. Covalent modification has revealed the role of histidine-residues that react with diethylpyrocarbonate and may be involved in CyP-D binding and pH sensing (72); cysteines-residues controlling the PTP conformation have been characterized by thiol-disulfide interconversions (24); and arginine residues that react with synthetic dicarbonyl compounds phenylglyoxal and 2,3-butanediol favoring the closed conformation of the PTP (29, 30, 60). In contrast to phenylglyoxal, and despite their structural similarity, hydroxy-phenylglyoxal strongly promoted the open conformation of the PTP. The PT inducing effect of hydroxy-phenylglyoxal was strongly favored by mitochondrial de-energization, indicating that arginine-residues might be involved in the PTP voltage dependence (29, 30, 60). In the present work (see Chapter 2) a physiological, non-synthetic arginine reagent was investigated. Methylglyoxal, a dicarbonyl compound, is an intermediate formed by the glycolytic enzyme triose phosphate isomerase (please see chapter 2). Another organic molecule that is involved in PT regulation is creatine and its phosphorylated derivative.

Mitochondrial creatine kinase and the phospho-creatine shuttle

Creatine (Cr) and phospho-creatine (PCr) are guanidino compounds. Creatine kinase (CK) isoforms and Cr/PCr are part of the cellular energy network e.g. in skeletal muscle, brain and other tissues and cells with fluctuating high-energy demand. In these tissues, Cr is the substrate of CK, which transfers a phosphate group from ATP to PCr at sites of energy production (mitochondria) and recycles ATP by consuming the PCr at sites of high energy turnover (for review see (9, 120)). The sites of high-energy consumption are e.g. Na-K-ATPase, which is functional coupled with CK, as shown in kidney epithelia (41). Another important aspect involving CK is the sensing of ATP fluctuations. Very recently, the ATP-sensitive K+ (K(ATP)) channel was co-immuno precipitated with MCK, a prototypic metabolic sensor (1). The dynamics of high energy phosphoryl transfer through the creatine kinase permitted the transmission of energetic signals into the submembrane compartment synchronizing K(ATP) channel activity with cell metabolism. Knock-out of the creatine kinase M-CK gene disrupted signal delivery to K(ATP) channels and generated a cellular phenotype with increased electrical vulnerability (1). Further more, an interaction of CK with a metabolic master switch AMP activated protein kinase (AMPK) was proposed (80).

It seems that creatine is also crucially involved in regulation of cellular calcium homeostasis (102), subsequently of cell death ((18, 73, 119) for recent review see (25)). I have cited some cases of CK involvement. Thus it becomes clear that it will be important to learn more about the different metabolic- and signalling pathways – biosynthesis, uptake, transport and physiological functions of creatine in organisms and cells.

The vertebrate genome codes for two distinct an tissue-specific mtCK isoforms sharing 82-85 % amino acid sequence identity (68). Ubiquitous mt_uCK is found in several non-muscle organs like kidney or brain, and sarcomeric mt_sCK which expression is restricted to sarcomeric muscle tissue. Both mtCK isoforms form dimeric, as well as highly ordered octameric structures with a molecular weight of approx. 66 and 340 kD, respectively (93, 123). The prevalent species of mtCK under normal conditions in vivo is the octamer (92). The octamer / dimer ratio of Mt-CK in vitro was shown to be influenced by enzyme concentration, pH, ionic strength and the presence of substrates (40).

MtCK is localized in the IMS and the cristae, where they bind to mitochondrial membranes. Octameric mtCK is able to cross-link membranes at mitochondrial contact sites (82, 83) and also cross-links phospholipid vesicle in vitro (101). Human Mt-CK iso-enzymes from heart and brain have been shown to differ in octamer stability and membrane binding (91). The direct transphosphorylation of intramitochondrially produced ATP into PCr is probably the primary function of mtCK (120, 124). The functional coupling mtCK to oxidative phosphorylation via the adenine nucleotide translocator (ANT) has been reported *in vivo and vitro* (51, 52, 85).

It is discussed that the binding of mtCK to VDAC (90), and the functional coupling to ANT (12, 13, 52, 66, 67) is part of the PT regulation. Creatine prevents mitochondria to open the PTP after appropriate stimuli (27, 73). The PTP inhibiting characteristic, the coupling of ANT and mtCK within a micro-compartment have been studied in detail (see chapter 3). Furthermore the localization and the impact of mitochondrial structure have been investigated (see chapter 4).

Creatine metabolism

In mammals, Cr is synthesized mainly in liver and pancreas by the enzyme guanidine-acetate methyl-transferase (GAMT) from its precursor guanidine acetic acid (GAA). GAA on the other hand is synthesised mainly in kidney pancreas by arginine glycine armino-transferase (AGAT) ((38, 62, 115, 116)). However, tissues, which contain the highest concentrations of PCr, do not synthesize their own creatine or do so only to a limited extent (16). Most of the creatine is absorbed from the plasma into the respective tissues by a specific creatine transporter (CrT) ((74, 121), for review see (42, 100)).

Inborn errors in Creatine metabolism.

Recent reports describe inborn errors in creatine metabolism pathways resulting from a deficiency of hepatic GAMT activity (95, 96, 104, 105). GAMT mutations were detected in children suffering from neurological disorders. The patients have an accumulation of GAA and a severe creatine deficiency. From this patient group, one male patient exhibits an extra pyramidal movement disorder starting at the age of 5 months. At the age of 22 months, he displayed severe muscular hypotonia and developmental delay. The EEG showed abnormally low background activity with multifocal spikes. Another patient, a girl aged 4 yr, presented a dystonic-dyskinetic syndrome, developmental delay, and epilepsy with myoclonic and astatic seizures and grand mal. The third patient, a five-year-old boy, displayed global developmental delay and experienced frequent tonic seizures, associated with apnea. GAMT deficiency was identified as the underlying metabolic basis of the disease by finding considerably increased brain, cerebrospinal fluid, serum, and urine concentrations of GAA; low Cr concentrations in plasma, cerebrospinal fluid, and urine; a virtual absence of Cr and PCr in the brain. Patients carrying a GAMT mutation, treated with oral Cr demonstrate a remarkable improvement of both the clinical symptoms and of the biochemical abnormalities (103-107, 113).

Several mutations in CRT (14, 23, 45, 86) were found in humans suffering from an X-linked Cr deficiency syndrome with developmental delay, hypotonia, severe delay in both speech and expressive language function, and epilepsy. Those patients are described as having an absent PCr peak in their brain MRS spectra, elevated Cr plasma levels and elevated creatinine in urine. Fibroblasts from these patients contained hemizygous nonsense mutations in the CRT gene and were defective in Cr uptake (23, 86). Interestingly, the Xq28 locus - where the *crt1* gene is localized – has been linked to the genes for several neuromuscular disorders, as Barth syndrome (2, 15), (26, 111), causing several authors (39, 42, 70) to speculate that dysfunctional *crt1* gene may be responsible for some of these diseases.

After the generation of different peptide antibodies (42), CRT protein was shown to be expressed in liver, small intestine, skeletal and heart muscle, (69, 75, 121, 122). In those tissues CRT is not only located in the plasma-lemma but also in mitochondria (69, 121, 122). As there is little known about the exact localisation of CrT, I decided to study the CrT in muscle tissue. The localisation and physiological characterisation of CrT is the second focus of my thesis. Therefore one will find detailed information about the molecular identity, tissue specific expression, regulation, and about CrT mutations in humans in the chapters 5 & 6.

References

1. Abraham MR, Selivanov VA, Hodgson DM, Pucar D, Zingman LV, Wieringa B, Dzeja PP, Alekseev AE, and Terzic A. Coupling of cell energetics with membrane metabolic sensing. Integrative signaling through creatine kinase phosphotransfer disrupted by M-CK gene knock-out. *J Biol Chem* 277: 24427-24434., 2002.

2. Ades LC, Gedeon AK, Wilson MJ, Latham M, Partington MW, Mulley JC, Nelson J, Lui K, and Sillence DO. Barth syndrome: clinical features and confirmation of gene localisation to distal Xq28. *Am J Med Genet* 45: 327-334., 1993.

3. Ardail D, Privat JP, Egret-Charlier M, Levrat C, Lerme F, and Louisot P. Mitochondrial contact sites. Lipid composition and dynamics. *J Biol Chem* 265: 18797-18802, 1990.

4. Bandlow W, Strobel G, Zoglowek C, Oechsner U, and Magdolen V. Yeast adenylate kinase is active simultaneously in mitochondria and cytoplasm and is required for non-fermentative growth. *Eur J Biochem* 178: 451-457, 1988.

5. Baumeister W, Grimm R, and Walz J. Electron tomography of molecules and cells. *Trends Cell Biol* 9: 81-85, 1999.

6. Bernardi P. Mitochondrial transport of cations: channels, exchangers, and permeability transition. *Physiol Rev* 79: 1127-1155., 1999.

7. Bernardi P and Azzone GF. Cytochrome c as an electron shuttle between the outer and inner mitochondrial membranes. *J Biol Chem* 256: 7187-7192, 1981.

8. Bernardi P and Petronilli V. The permeability transition pore as a mitochondrial calcium release channel: a critical appraisal. *J Bioenerg Biomembr* 28: 131-138., 1996.

9. Bessman SP and Carpenter CL. The creatine-creatine phosphate energy shuttle. *Annu Rev Biochem* 54: 831-862, 1985.

10. Bessman SP and Geiger PJ. Transport of energy in muscle: the phosphorylcreatine shuttle. *Science* 211: 448-452., 1981.

11. Beutner G, Ruck A, Riede B, and Brdiczka D. Complexes between hexokinase, mitochondrial porin and adenylate translocator in brain: regulation of hexokinase, oxidative phosphorylation and permeability transition pore. *Biochem Soc Trans* 25: 151-157., 1997.
12. Beutner G, Ruck A, Riede B, and Brdiczka D. Complexes between porin, hexokinase, mitochondrial creatine kinase and adenylate translocator display properties of the permeability transition pore. Implication for regulation of permeability transition by the kinases. *Biochim Biophys Acta* 1368: 7-18., 1998.
13. Beutner G, Ruck A, Riede B, Welte W, and Brdiczka D. Complexes between kinases, mitochondrial porin and adenylate translocator in rat brain resemble the permeability transition pore. *FEBS Lett* 396: 189-195., 1996.
14. Bizzi A, Bugiani M, Salomons GS, Hunneman DH, Moroni I, Estienne M, Danesi U, Jakobs C, and Uziel G. X-linked creatine deficiency syndrome: a novel mutation in creatine transporter gene SLC6A8. *Ann Neurol* 52: 227-231., 2002.
15. Bolhuis PA, Hensels GW, Hulsebos TJ, Baas F, and Barth PG. Mapping of the locus for X-linked cardioskeletal myopathy with neutropenia and abnormal mitochondria (Barth syndrome) to Xq28. *Am J Hum Genet* 48: 481-485., 1991.
16. Braissant O, Henry H, Loup M, Eilers B, and Bachmann C. Endogenous synthesis and transport of creatine in the rat brain: an in situ hybridization study(1). *Brain Res Mol Brain Res* 86: 193-201., 2001.
17. Brdiczka D. Contact sites between mitochondrial envelope membranes. Structure and function in energy- and protein-transfer. *Biochim Biophys Acta* 1071: 291-312, 1991.
18. Brdiczka D, Beutner G, Ruck A, Dolder M, and Wallimann T. The molecular structure of mitochondrial contact sites. Their role in regulation of energy metabolism and permeability transition. *Biofactors* 8: 235-242, 1998.
19. Brdiczka D and Schumacher D. Iodination of peripheral mitochondrial membrane proteins in correlation to the functional state of the ADP/ATP carrier. *Biochem Biophys Res Commun* 73: 823-832., 1976.
20. Broekemeier KM, Klocek CK, and Pfeiffer DR. Proton selective substate of the mitochondrial permeability transition pore: regulation by the redox state of the electron transport chain. *Biochemistry* 37: 13059-13065, 1998.
21. Brooks KJ, Hargreaves IP, and Bates TE. Nitric-oxide-induced inhibition of mitochondrial complexes following aglycaemic hypoxia in neonatal cortical rat brain slices. *Dev Neurosci* 22: 359-365, 2000.
22. Castro-Palomino JC, Simon B, Speer O, Leist M, and Schmidt RR. Synthesis of ganglioside GD3 and its comparison with bovine GD3 with regard to oligodendrocyte apoptosis mitochondrial damage. *Chemistry* 7: 2178-2184, 2001.
23. Cecil KM, Salomons GS, Ball WS, Jr., Wong B, Chuck G, Verhoeven NM, Jakobs C, and DeGrauw TJ. Irreversible brain creatine deficiency with elevated serum and urine creatine: a creatine transporter defect? *Ann Neurol* 49: 401-404., 2001.
24. Chernyak BV and Bernardi P. The mitochondrial permeability transition pore is modulated by oxidative agents through both pyridine nucleotides and glutathione at two separate sites. *Eur J Biochem* 238: 623-630, 1996.
25. Cohen I, Castedo M, and Kroemer G. Tantalizing Thanatos: unexpected links in death pathways. *Trends Cell Biol* 12: 293-295., 2002.
26. Consalez GG, Thomas NS, Stayton CL, Knight SJ, Johnson M, Hopkins LC, Harper PS, Elsas LJ, and Warren ST. Assignment of Emery-Dreifuss muscular dystrophy to the distal region of Xq28: the results of a collaborative study. *Am J Hum Genet* 48: 468-480., 1991.
27. Dolder M, Walzel B, Speer O, Schlattner U, and Wallimann T. Inhibition of the mitochondrial permeability transition by creatine kinase substrates: requirement for microcompartmentation. *J Biol Chem*, 2003.
28. Du C, Fang M, Li Y, Li L, and Wang X. Smac, a mitochondrial protein that promotes cytochrome c-dependent caspase activation by eliminating IAP inhibition. *Cell* 102: 33-42, 2000.
29. Eriksson O, Fontaine E, and Bernardi P. Chemical modification of arginines by 2,3-butanedione and phenylglyoxal causes closure of the mitochondrial permeability transition pore. *J Biol Chem* 273: 12669-12674, 1998.
30. Eriksson O, Fontaine E, Petronilli V, and Bernardi P. Inhibition of the mitochondrial cyclosporin A-sensitive permeability transition pore by the arginine reagent phenylglyoxal. *FEBS Lett* 409: 361-364, 1997.
31. Fontaine E and Bernardi P. Progress on the mitochondrial permeability transition pore: regulation by complex I and ubiquinone analogs. *J Bioenerg Biomembr* 31: 335-345, 1999.
32. Fontaine E, Eriksson O, Ichas F, and Bernardi P. Regulation of the permeability transition pore in skeletal muscle mitochondria. Modulation By electron flow through the respiratory chain complex i. *J Biol Chem* 273: 12662-12668, 1998.
33. Gellerich FN KM, Kunz W, Neumann W, Kuznetsov A, Brdiczka D, Nicolay K. The influence of the cytosolic oncotic pressure on the permeability of the mitochondrial outer membrane for ADP: implications for the kinetic properties of mitochondrial creatine kinase and for ADP channelling into the intermembrane space. *Mol Cell Biochem* 133-134: 85-104, 1994.
34. Gellerich FN, Laterveer FD, Korzeniewski B, Zierz S, and Nicolay K. Dextran strongly increases the Michaelis constants of oxidative phosphorylation and of mitochondrial creatine kinase in heart mitochondria. *Eur J Biochem* 254: 172-180, 1998.

35. Gellerich FN, Laterveer FD, Zierz S, and Nicolay K. The quantitation of ADP diffusion gradients across the outer membrane of heart mitochondria in the presence of macromolecules. *Biochim Biophys Acta* 1554: 48-56, 2002.
36. Gellerich FN, Wagner M, Kapischke M, Wicker U, and Brdiczka D. Effect of macromolecules on the regulation of the mitochondrial outer membrane pore and the activity of adenylate kinase in the inter-membrane space. *Biochim Biophys Acta* 1142: 217-227, 1993.
37. Gerbitz KD GK, Brdiczka D. Mitochondria and diabetes. Genetic, biochemical, and clinical implications of the cellular energy circuit. *Diabetes* 45: 113-126, 1996.
38. Grazi E, Magri E, and Balboni G. On the control of arginine metabolism in chicken kidney and liver. *Eur J Biochem* 60: 431-436., 1975.
39. Gregor P, Nash SR, Caron MG, Seldin MF, and Warren ST. Assignment of the creatine transporter gene (SLC6A8) to human chromosome Xq28 telomeric to G6PD. *Genomics* 25: 332-333., 1995.
40. Gross M and Wallimann T. Kinetics of assembly and dissociation of the mitochondrial creatine kinase octamer. A fluorescence study. *Biochemistry* 32: 13933-13940, 1993.
41. Guerrero ML, Beron J, Spindler B, Groscurth P, Wallimann T, and Verrey F. Metabolic support of Na+ pump in apically permeabilized A6 kidney cell epithelia: role of creatine kinase. *Am J Physiol* 272: C697-706, 1997.
42. Guerrero-Ontiveros ML WT. Creatine supplementation in health and disease. Effects of chronic creatine ingestion in vivo: down-regulation of the expression of creatine transporter isoforms in skeletal muscle. *Mol Cell Biochem* 184: 427-437, 1998.
43. Gunter TE. Cation transport by mitochondria. *J Bioenerg Biomembr* 26: 465-469, 1994.
44. Gunter TE, Gunter KK, Sheu SS, and Gavin CE. Mitochondrial calcium transport: physiological and pathological relevance. *Am J Physiol* 267: C313-339, 1994.
45. Hahn KA, Salomons GS, Tackels-Horne D, Wood TC, Taylor HA, Schroer RJ, Lubs HA, Jakobs C, Olson RL, Holden KR, Stevenson RE, and Schwartz CE. X-linked mental retardation with seizures and carrier manifestations is caused by a mutation in the creatine-transporter gene (SLC6A8) located in Xq28. *Am J Hum Genet* 70: 1349-1356., 2002.
46. Haworth RA and Hunter DR. Allosteric inhibition of the Ca2+-activated hydrophilic channel of the mitochondrial inner membrane by nucleotides. *J Membr Biol* 54: 231-236, 1980.
47. Hengartner MO. The biochemistry of apoptosis. *Nature* 407: 770-776, 2000.
48. Hirsch T, Marchetti P, Susin SA, Dallaporta B, Zamzami N, Marzo I, Geuskens M, and Kroemer G. The apoptosis-necrosis paradox. Apoptogenic proteases activated after mitochondrial permeability transition determine the mode of cell death. *Oncogene* 15: 1573-1581, 1997.
49. Hirsch T, Marzo I, and Kroemer G. Role of the mitochondrial permeability transition pore in apoptosis. *Biosci Rep* 17: 67-76, 1997.
50. Isenberg JS and Klaunig JE. Role of the mitochondrial membrane permeability transition (MPT) in rotenone-induced apoptosis in liver cells. *Toxicol Sci* 53: 340-351, 2000.
51. Jacobus WE. Respiratory control and the integration of heart high-energy phosphate metabolism by mitochondrial creatine kinase. *Annu Rev Physiol* 47: 707-725, 1985.
52. Kay L, Nicolay K, Wieringa B, Saks V, and Wallimann T. Direct evidence for the control of mitochondrial respiration by mitochondrial creatine kinase in oxidative muscle cells in situ. *J Biol Chem* 275: 6937-6944, 2000.
53. Kristal BS and Brown AM. Apoptogenic ganglioside GD3 directly induces the mitochondrial permeability transition. *J Biol Chem* 274: 23169-23175, 1999.
54. Kristal BS and Brown AM. Ganglioside GD3, the mitochondrial permeability transition, and apoptosis. *Ann N Y Acad Sci* 893: 321-324, 1999.
55. Larochette N, Decaudin D, Jacotot E, Brenner C, Marzo I, Susin SA, Zamzami N, Xie Z, Reed J, and Kroemer G. Arsenite induces apoptosis via a direct effect on the mitochondrial permeability transition pore. *Exp Cell Res* 249: 413-421, 1999.
56. Laterveer FD, Nicolay K, and Gellerich FN. Experimental evidence for dynamic compartmentation of ADP at the mitochondrial periphery: coupling of mitochondrial adenylate kinase and mitochondrial hexokinase with oxidative phosphorylation under conditions mimicking the intracellular colloid osmotic pressure. *Mol Cell Biochem* 174: 43-51, 1997.
57. Laterveer FD NK, Gellerich FN. Experimental evidence for dynamic compartmentation of ADP at the mitochondrial periphery: coupling of mitochondrial adenylate kinase and mitochondrial hexokinase with oxidative phosphorylation under conditions mimicking the intracellular colloid osmotic pressure. *Mol Cell Biochem* 174: 43-51, 1997.
58. Lea PJ and Hollenberg MJ. Mitochondrial structure revealed by high-resolution scanning electron microscopy. *Am J Anat* 184: 245-257, 1989.
59. Lea PJ and Hollenberg MJ. Mitochondrial structure revealed by scanning electron microscopy (SEM). *Prog Clin Biol Res* 295: 63-70, 1989.
60. Linder MD, Morkunaite-Haimi S, Kinnunen PK, Bernardi P, and Eriksson O. Ligand-selective modulation of the permeability transition pore by arginine modification. Opposing effects of p-hydroxyphenylglyoxal and phenylglyoxal. *J Biol Chem* 277: 937-942, 2002.
61. Lohret TA, Murphy RC, Drgon T, and Kinnally KW. Activity of the mitochondrial multiple conductance channel is independent of the adenine nucleotide translocator. *J Biol Chem* 271: 4846-4849, 1996.
62. Magri E, Baldoni G, and Grazi E. On the biosynthesis of creatine. Intramitochondrial localization of transamidinase from rat kidney. *FEBS Lett* 55: 91-93., 1975.

63. Mannella CA. Application of electron tomography to mitochondrial research. *Methods Cell Biol* 65: 245-256, 2001.
64. Mannella CA, Pfeiffer DR, Bradshaw PC, Moraru II, Slepchenko B, Loew LM, Hsieh CE, Buttle K, and Marko M. Topology of the mitochondrial inner membrane: dynamics and bioenergetic implications. *IUBMB Life* 52: 93-100, 2001.
65. Martinou JC DS, Antonsson B. Cytochrome c release from mitochondria: all or nothing. *Nat Cell Biol* 2: E41-E43, 2000.
66. Marzo I, Brenner C, Zamzami N, Jurgensmeier JM, Susin SA, Vieira HL, Prevost MC, Xie Z, Matsuyama S, Reed JC, and Kroemer G. Bax and adenine nucleotide translocator cooperate in the mitochondrial control of apoptosis. *Science* 281: 2027-2031, 1998.
67. Marzo I, Brenner C, Zamzami N, Susin SA, Beutner G, Brdiczka D, Remy R, Xie ZH, Reed JC, and Kroemer G. The permeability transition pore complex: a target for apoptosis regulation by caspases and bcl-2-related proteins. *J Exp Med* 187: 1261-1271., 1998.
68. Muhlebach SM, Gross M, Wirz T, Wallimann T, Perriard JC, and Wyss M. Sequence homology and structure predictions of the creatine kinase isoenzymes. *Mol Cell Biochem* 133-134: 245-262, 1994.
69. Murphy R, McConell G, Cameron-Smith D, Watt K, Ackland L, Walzel B, Wallimann T, and Snow R. Creatine transporter protein content, localization, and gene expression in rat skeletal muscle. *Am J Physiol Cell Physiol* 280: C415-C422., 2001.
70. Nash SR, Giros B, Kingsmore SF, Rochelle JM, Suter ST, Gregor P, Seldin MF, and Caron MG. Cloning, pharmacological characterization, and genomic localization of the human creatine transporter. *Receptors Channels* 2: 165-174, 1994.
71. Nicastro D, Frangakis AS, Typke D, and Baumeister W. Cryo-electron tomography of neurospora mitochondria. *J Struct Biol* 129: 48-56, 2000.
72. Nicolli A, Petronilli V, and Bernardi P. Modulation of the mitochondrial cyclosporin A-sensitive permeability transition pore by matrix pH. Evidence that the pore open-closed probability is regulated by reversible histidine protonation. *Biochemistry* 32: 4461-4465, 1993.
73. O'Gorman E BG, Dolder M, Koretsky AP, Brdiczka D, Wallimann T. The role of creatine kinase in inhibition of mitochondrial permeability transition. *FEBS Lett* 414: 253-257, 1997.
74. Peral MJ, Garcia-Delgado M, Calonge ML, Duran JM, De La Horra MC, Wallimann T, Speer O, and Ilundain A. Human, rat and chicken small intestinal Na(+)-Cl(-)-creatine transporter: functional, molecular characterization and localization. *J Physiol* 545: 133-144., 2002.
75. Peral MJ, Garcia-Delgado M, Calonge ML, Duran JM, De La Horra MC, Wallimann T, Speer O, and Ilundain A. Human, rat and chicken small intestinal Na+ - Cl- -creatine transporter: functional, molecular characterization and localization. *J Physiol* 545: 133-144, 2002.
76. Perkins G, Renken C, Martone ME, Young SJ, Ellisman M, and Frey T. Electron tomography of neuronal mitochondria: three-dimensional structure and organization of cristae and membrane contacts. *J Struct Biol* 119: 260-272, 1997.
77. Perkins GA and Frey TG. Recent structural insight into mitochondria gained by microscopy. *Micron* 31: 97-111, 2000.
78. Perkins GA, Renken CW, Frey TG, and Ellisman MH. Membrane architecture of mitochondria in neurons of the central nervous system. *J Neurosci Res* 66: 857-865, 2001.
79. Perkins GA, Renken CW, Song JY, Frey TG, Young SJ, Lamont S, Martone ME, Lindsey S, and Ellisman MH. Electron tomography of large, multicomponent biological structures. *J Struct Biol* 120: 219-227, 1997.
80. Ponticos M, Lu QL, Morgan JE, Hardie DG, Partridge TA, and Carling D. Dual regulation of the AMP-activated protein kinase provides a novel mechanism for the control of creatine kinase in skeletal muscle. *Embo J* 17: 1688-1699., 1998.
81. Roberts J, Aubert S, Gout E, Bligny R, and Douce R. Cooperation and Competition between Adenylate Kinase, Nucleoside Diphosphokinase, Electron Transport, and ATP Synthase in Plant Mitochondria Studied by 31P-Nuclear Magnetic Resonance. *Plant Physiol* 113: 191-199, 1997.
82. Rojo M, Hovius R, Demel R, Wallimann T, Eppenberger HM, and Nicolay K. Interaction of mitochondrial creatine kinase with model membranes. A monolayer study. *FEBS Lett* 281: 123-129, 1991.
83. Rojo M, Hovius R, Demel RA, Nicolay K, and Wallimann T. Mitochondrial creatine kinase mediates contact formation between mitochondrial membranes. *J Biol Chem* 266: 20290-20295, 1991.
84. Saks VA, Khuchua ZA, Vasilyeva EV, Belikova O, and Kuznetsov AV. Metabolic compartmentation and substrate channelling in muscle cells. Role of coupled creatine kinases in in vivo regulation of cellular respiration--a synthesis. *Mol Cell Biochem* 133-134: 155-192, 1994.
85. Saks VA, Ventura-Clapier R, and Aliev MK. Metabolic control and metabolic capacity: two aspects of creatine kinase functioning in the cells. *Biochim Biophys Acta* 1274: 81-88, 1996.
86. Salomons GS, van Dooren SJ, Verhoeven NM, Cecil KM, Ball WS, Degrauw TJ, and Jakobs C. X-linked creatine-transporter gene (SLC6A8) defect: a new creatine- deficiency syndrome. *Am J Hum Genet* 68: 1497-1500., 2001.
87. Saraste M. Oxidative phosphorylation at the fin de siecle. *Science* 283: 1488-1493, 1999.
88. Schlame M, Brody S, and Hostetler KY. Mitochondrial cardiolipin in diverse eukaryotes. Comparison of biosynthetic reactions and molecular acyl species. *Eur J Biochem* 212: 727-735, 1993.
89. Schlame M and Haldar D. Cardiolipin is synthesized on the matrix side of the inner membrane in rat liver mitochondria. *J Biol Chem* 268: 74-79, 1993.

90. Schlattner U, Dolder M, Wallimann T, and Tokarska-Schlattner M. Mitochondrial creatine kinase and mitochondrial outer membrane porin show a direct interaction that is modulated by calcium. *J Biol Chem* 276: 48027-48030, 2001.
91. Schlattner U and Wallimann T. Octamers of mitochondrial creatine kinase isoenzymes differ in stability and membrane binding. *J Biol Chem* 275: 17314-17320, 2000.
92. Schlegel J, Wyss M, Schurch U, Schnyder T, Quest A, Wegmann G, Eppenberger HM, and Wallimann T. Mitochondrial creatine kinase from cardiac muscle and brain are two distinct isoenzymes but both form octameric molecules. *J Biol Chem* 263: 16963-16969, 1988.
93. Schlegel J, Zurbriggen B, Wegmann G, Wyss M, Eppenberger HM, and Wallimann T. Native mitochondrial creatine kinase forms octameric structures. I. Isolation of two interconvertible mitochondrial creatine kinase forms, dimeric and octameric mitochondrial creatine kinase: characterization, localization, and structure-function relationships. *J Biol Chem* 263: 16942-16953, 1988.
94. Schneider HC, Berthold J, Bauer MF, Dietmeier K, Guiard B, Brunner M, and Neupert W. Mitochondrial Hsp70/MIM44 complex facilitates protein import. *Nature* 371: 768-774, 1994.
95. Schulze A, Hess T, Wevers R, Mayatepek E, Bachert P, Marescau B, Knopp MV, De Deyn PP, Bremer HJ, and Rating D. Creatine deficiency syndrome caused by guanidinoacetate methyltransferase deficiency: diagnostic tools for a new inborn error of metabolism. *J Pediatr* 131: 626-631., 1997.
96. Schulze A, Mayatepek E, Bachert P, Marescau B, De Deyn PP, and Rating D. Therapeutic trial of arginine restriction in creatine deficiency syndrome. *Eur J Pediatr* 157: 606-607., 1998.
97. Scorrano L, Petronilli V, Di Lisa F, and Bernardi P. Commitment to apoptosis by GD3 ganglioside depends on opening of the mitochondrial permeability transition pore. *J Biol Chem* 274: 22581-22585., 1999.
98. Sirrenberg C, Bauer MF, Guiard B, Neupert W, and Brunner M. Import of carrier proteins into the mitochondrial inner membrane mediated by Tim22. *Nature* 384: 582-585, 1996.
99. Sluse FE. Mitochondrial metabolite carrier family, topology, structure and functional properties: an overview. *Acta Biochim Pol* 43: 349-360, 1996.
100. Snow RJ and Murphy RM. Creatine and the creatine transporter: a review. *Mol Cell Biochem* 224: 169-181., 2001.
101. Stachowiak O, Dolder M, and Wallimann T. Membrane-binding and lipid vesicle cross-linking kinetics of the mitochondrial creatine kinase octamer. *Biochemistry* 35: 15522-15528, 1996.
102. Steeghs K, Benders A, Oerlemans F, de Haan A, Heerschap A, Ruitenbeek W, Jost C, van Deursen J, Perryman B, Pette D, Bruckwilder M, Koudijs J, Jap P, Veerkamp J, and Wieringa B. Altered Ca2+ responses in muscles with combined mitochondrial and cytosolic creatine kinase deficiencies. *Cell* 89: 93-103., 1997.
103. Stockler S and Hanefeld F. Guanidinoacetate methyltransferase deficiency: a newly recognized inborn error of creatine biosynthesis. *Wien Klin Wochenschr* 109: 86-88., 1997.
104. Stockler S, Hanefeld F, and Frahm J. Creatine replacement therapy in guanidinoacetate methyltransferase deficiency, a novel inborn error of metabolism. *Lancet* 348: 789-790., 1996.
105. Stockler S, Holzbach U, Hanefeld F, Marquardt I, Helms G, Requart M, Hanicke W, and Frahm J. Creatine deficiency in the brain: a new, treatable inborn error of metabolism. *Pediatr Res* 36: 409-413., 1994.
106. Stockler S, Isbrandt D, Hanefeld F, Schmidt B, and von Figura K. Guanidinoacetate methyltransferase deficiency: the first inborn error of creatine metabolism in man. *Am J Hum Genet* 58: 914-922., 1996.
107. Stockler S, Marescau B, De Deyn PP, Trijbels JM, and Hanefeld F. Guanidino compounds in guanidinoacetate methyltransferase deficiency, a new inborn error of creatine synthesis. *Metabolism* 46: 1189-1193., 1997.
108. Stridh H, Fava E, Single B, Nicotera P, Orrenius S, and Leist M. Tributyltin-induced apoptosis requires glycolytic adenosine trisphosphate production. *Chem Res Toxicol* 12: 874-882, 1999.
109. Susin SA, Zamzami N, and Kroemer G. Mitochondria as regulators of apoptosis: doubt no more. *Biochim Biophys Acta* 1366: 151-165, 1998.
110. Szabo I, Bernardi P, and Zoratti M. Modulation of the mitochondrial megachannel by divalent cations and protons. *J Biol Chem* 267: 2940-2946, 1992.
111. Thomas NS, Williams H, Cole G, Roberts K, Clarke A, Liechti-Gallati S, Braga S, Gerber A, Meier C, Moser H, and et al. X linked neonatal centronuclear/myotubular myopathy: evidence for linkage to Xq28 DNA marker loci. *J Med Genet* 27: 284-287., 1990.
112. Ungermann C, Neupert W, and Cyr DM. The role of Hsp70 in conferring unidirectionality on protein translocation into mitochondria. *Science* 266: 1250-1253, 1994.
113. van der Knaap MS, Verhoeven NM, Maaswinkel-Mooij P, Pouwels PJ, Onkenhout W, Peeters EA, Stockler-Ipsiroglu S, and Jakobs C. Mental retardation and behavioral problems as presenting signs of a creatine synthesis defect. *Ann Neurol* 47: 540-543., 2000.
114. Verhagen AM, Ekert PG, Pakusch M, Silke J, Connolly LM, Reid GE, Moritz RL, Simpson RJ, and Vaux DL. Identification of DIABLO, a mammalian protein that promotes apoptosis by binding to and antagonizing IAP proteins. *Cell* 102: 43-53, 2000.
115. Walker JB. Creatine: biosynthesis, regulation, and function. *Adv Enzymol Relat Areas Mol Biol* 50: 177-242, 1979.
116. Walker JB and Hannan JK. Creatine biosynthesis during embryonic development. False feedback suppression of liver amidinotransferase by N-acetimidoylsarcosine and 1- carboxymethyl-2-iminoimidazolidine (cyclocreatine). *Biochemistry* 15: 2519-2522., 1976.

117. Wallace D. Diseases of the mitochondrial DNA. *Annu Rev Biochem* 61: 1175-1212, 1992a.
118. Wallace D. Mitochondrial genetics: a paradigm for aging and degenerative diseases? *Science* 256: 628-632, 1992b.
119. Wallimann T, Dolder M, Schlattner U, Eder M, Hornemann T, O'Gorman E, Ruck A, and Brdiczka D. Some new aspects of creatine kinase (CK): compartmentation, structure, function and regulation for cellular and mitochondrial bioenergetics and physiology. *Biofactors* 8: 229-234, 1998.
120. Wallimann T, Wyss M, Brdiczka D, Nicolay K, and Eppenberger HM. Intracellular compartmentation, structure and function of creatine kinase isoenzymes in tissues with high and fluctuating energy demands: the 'phosphocreatine circuit' for cellular energy homeostasis. *Biochem J* 281: 21-40, 1992.
121. Walzel B, Speer O, Boehm E, Kristiansen S, Chan S, Clarke K, Magyar JP, Richter EA, and Wallimann T. New creatine transporter assay and identification of distinct creatine transporter isoforms in muscle. *Am J Physiol Endocrinol Metab* 283: E390-401., 2002.
122. Walzel B, Speer O, Zanolla E, Eriksson O, Bernardi P, and Wallimann T. Novel mitochondrial creatine transport activity. Implications for intracellular creatine compartments and bioenergetics. *J Biol Chem* 277: 37503-37511., 2002.
123. Wyss M, James P, Schlegel J, and Wallimann T. Limited proteolysis of creatine kinase. Implications for three-dimensional structure and for conformational substrates. *Biochemistry* 32: 10727-10735, 1993.
124. Wyss M and Kaddurah-Daouk R. Creatine and creatinine metabolism. *Physiol Rev* 80: 1107-1213., 2000.
125. Ziegelhoffer-Mihalovicova B, Ziegelhoffer A, Ravingerova T, Kolar F, Jacob W, and Tribulova N. Regulation of mitochondrial contact sites in neonatal, juvenile and diabetic hearts. *Mol Cell Biochem* 236: 37-44, 2002.

CHAPTER 1

Heart mitochondrium, Oliver Speer, April 2001

Chapter 2

RAPID SUPPRESSION OF MITOCHONDRIAL PERMEABILITY TRANSITION BY METHYLGLYOXAL

ROLE OF REVERSIBLE ARGININE MODIFICATION

Oliver Speer‡§, Sarune Morkunaite-Haimi‡, Julius Liobikas‡**, Marina Franck‡, Linn Hensbo‡, Matts D. Linder‡¶, Paavo J. K. Kinnunen‡, Theo Wallimann§, and Ove Eriksson‡‖

§Swiss Federal Institute Of Technology, ETH-Zürich, Institute of Cell Biology, ETH-Hönggerberg, CH-8093 Zürich, Switzerland

‡Helsinki Biophysics and Biomembrane Group, Institute of Biomedicine, University of Helsinki, FIN-00014 Finland, and

CHAPTER 2

Published in
The Journal of Biological Chemistry, 18th June 2003
(epub ahead of print)

Acknowledgments— We thank Prof Paolo Bernardi for critical reading of the manuscript and Ms Kaija Niva for excellent technical assistance. We thank Dr Eeva Penttilä for helpful advice on mass spectroscopy of gangliosides.

This study was supported by grants from the Rector of the University of Helsinki, Sigrid Juselius Foundation, Finska Läkaresällskapet and Perklén Memorial Foundation. O.S. and T.W. were supported by Swiss Foundation for the Research on Muscle Diseases.

The abbreviations used are: AGEs, advanced glycation end products; ANT, adenine nucleotide translocator; α-HCA, α-cyano-4-hydroxycinnamic acid; BAD, 2,3-butanedione; CsA, cyclosporin A; $\Delta\Psi_m$, mitochondrial transmembrane electrical potential difference; fwhm, full width at half maximum; GD3, 1-O-[O-(N-acetyl-α-neuraminosyl)-(2→8)-O-(N-acetyl-α-neuraminosyl)-(2→3)-O-β-D-galactopyranosyl-(1→4)-β-D-glucopyranosyl-ceramide; MALDI TOF, matrix-assisted laser desorption-ionisation and time-of-flight; MG, methylglyoxal, OH-PGO, p-hydroxyphenylglyoxal; PGO, phenylglyoxal; PTP, permeability transition pore; PKC, protein kinase C; RFI, relative fluorescence intensity; TFA, trifluoroacetic acid; TMRM, tetramethyl-rhodamine methyl ester; VDAC, outer membrane anion channel.

Summary

Methylglyoxal (MG) (pyruvaldehyde) is a reactive carbonyl compound produced in glycolysis. MG can form covalent adducts on proteins resulting in advanced glycation end products that may alter protein function. Here we report that MG covalently modifies the mitochondrial permeability transition pore (PTP), a large-conductance channel involved in the signal transduction of cell death processes. Incubation of isolated mitochondria with MG for a short period of time (5 min), followed by removal of excess free MG, prevented both ganglioside GD3- and Ca2+-induced PTP opening and the ensuing membrane depolarisation, swelling and cytochrome c release. Under these conditions MG did not significantly interfere with mitochondrial substrate transport, respiration or oxidative phosphorylation. The suppression of permeability transition was reversible following extended incubation in MG-free medium. Of the 29 physiological carbonyl and dicarbonyl compounds tested only MG and its analogue glyoxal were able to specifically alter the behaviour of the PTP. Using a set of arginine-containing peptides we found that the major MG-derived arginine adduct formed following short time exposure was the 5-hydro-5-methylimidazolone-derivative. These findings demonstrate that MG rapidly modifies the PTP covalently, which stabilizes the PTP in the closed conformation. This is probably due to the formation of an imidazolone-adduct on a critical arginine residue involved in the control of the PTP conformation (Linder, M.D., Morkunaite-Haimi, S., Kinnunen, P.J.K., Bernardi, P., and Eriksson, O. (2002) J. Biol. Chem. 277, 937-942.). We deduce that the permeability transition constitutes a potentially important physiological target of MG.

Introduction

MG is a reactive dicarbonyl compound that is formed during glucose metabolism. MG binds covalently to proteins resulting in the formation of advanced glycation end products (AGEs)[1], which are involved in several pathologic processes including cellular proliferative disorders (1) and diabetes mellitus (2). Increased formation of AGEs owing to hyperglycemia is a key factor in the development of diabetic complications such as microvascular disease and atherosclerosis (2). Inhibition of glycation reactions slows the progression of diabetic vascular disease manifestations (3, 4).

During glucose metabolism triose phosphates may undergo either spontaneous (5) or enzyme-facilitated decomposition to yield MG (6, 7). Triose phosphate isomerase catalyses the interconversions of dihydroxyacetone phosphate and glyceraldehyde phosphate and has a flexible loop surrounding enzyme-bound reaction intermediate on the active site. This loop flickers continuously between open and closed state leading to a small but constant leakage of the unstable intermediate enediolate phosphate (8), which immediately undergoes phosphate elimination to yield MG. Triose phosphate isomerase is a very efficient catalyst that is present at high concentration in tissues (9, 10), and therefore significant amounts of MG and MG-modified proteins may be produced (11).

At physiological concentrations of MG it primarily targets arginine residues of proteins (12), resulting initially in the formation of reversible adducts, which consequently may undergo a series of rearrangements that yields several possible end-products that contain either imidazolone- or pyrimidine-based ring systems (13, 14, 15). MG is known to target several proteins involved in the regulation of cell growth and differentiation (16, 17, 18, 19) although the coupling between MG-induced alterations and subsequent cellular effects remains incompletely understood.

Mitochondria play an important role in programmed cell death by releasing proteins from the inter-membrane compartment, where they are normally confined, to cytosol and nucleus (20). These proteins include cytochrome c and Smac/DIABLO, which activate caspases, endonuclease G that induces DNA fragmentation, and apoptosis inducing factor (AIF) which promotes caspase-independent chromatin condensation and DNA fragmentation (21). The release of these pro-apoptotic proteins may be triggered by mitochondrial permeability transition (22). This event is induced by upstream apoptotic signals such as formation of the ganglioside GD3 (23, 24, 25) or mitochondrial Ca^{2+} uptake (22). Permeability transition is due to opening of the permeability transition pore (PTP), which under normal cell life remains closed. In open conformation the PTP permits free diffusion of solutes with a molecular mass <1.5 kDa across the mitochondrial membrane. Permeability transition leads to mitochondrial depolarisation and equalization of matrix and cytosolic ion and metabolite concentrations. Concomitant osmotic swelling of the mitochondrial matrix may lead to rupture of the outer membrane and release of proteins from the inter-membrane compartment. According to the prevalent model, permeability transition pores are composed of the adenine nucleotide translocator, the voltage dependent anion channel and mitochondrial matrix cyclophilin (26, 27).

Mitochondrial Ca^{2+} uptake does not elicit permeability transition in isolated mitochondria after treatment of mitochondria with the synthetic dicarbonyl compounds phenylglyoxal (PGO) or 2,3-butanedione (BAD) (28, 29, 30 below, 31 below). These compounds react specifically with the guanidino group of arginine, indicating that modification of a critical arginine residue by PGO or BAD stabilizes the PTP in its closed conformation. Interestingly, modification with the PGO analogue

OH-PGO results in an arginine adduct that induces the open conformation of the PTP (31). The profound effect of arginine modification demonstrates that structural rearrangements of a critical arginine are of key importance for the control of the PTP conformation although the location of that arginine residue is still unclear. The possibility that physiological PTP regulators act through that site prompted us investigate whether the natural dicarbonyl compound MG was capable of inducing changes in the function of the PTP.

In this study we have identified the mitochondrial permeability transition as a novel target of MG. Brief incubation of isolated rat liver mitochondria with MG lead to complete suppression of both ganglioside GD3- and Ca^{2+}-induced permeability transition, with inhibition of its downstream events including cytochrome c release. Moreover, suppression of permeability transition by MG could be reversed by incubation in MG-free media. These results demonstrate that MG induced a reversible covalent PTP-modification, most likely an imidazolone-derivative on a critical arginine residue involved in the control of the PTP conformation (28, 29, 30, 31). These findings raise the possibility that MG reacts with the PTP under physiological conditions and that the concomitant deregulation of the PTP perturbs the cell death program.

Experimental procedures

Chemical modification of mitochondria.

Preparation of liver mitochondria from male Wistar rats was performed as described previously (29). Mitochondria (1 mg protein/ml) were preincubated either with MG or in its absence in modification medium containing 250 mM sucrose, 100 µM EGTA, 10 mM Hepes-KOH pH 8.0, for 5 min at 34ºC. The modification reaction was terminated by adjusting the pH to 6.8 with Hepes, cooling to 4°C and sedimentation of mitochondria by centrifugation at 8000x *g* for 5 min. Mitochondria were resuspended at a concentration of approximately 50 mg protein/ml in 250 mM sucrose, 100 µM EGTA and 10 mM Hepes-KOH pH 7.4. Unless otherwise stated experiments were carried out at room temperature in assay medium containing 125 mM KCl, 5 mM succinate, 5 mM Pi-Tris, 2 mM Mg^{2+}, 5 µM EGTA, 2 µM rotenone, 10 mM Hepes-Tris pH 7.4. In one experimental series MG was substituted by PGO. Oxygen consumption was measured using a Clark electrode (Yellow Springs Instruments).

PTP assays.

Permeability transition was assayed measuring membrane potential, Ca^{2+} transport and swelling. Medium [Ca^{2+}] was measured using the fluorescent indicator dye Fluo 4FF (ex 494 nm, em 516 nm). Membrane potential was measured by TMRM fluorescence (ex 550 nm, em 565 nm) and swelling was monitored as a decrease in mitochondrial light scattering at 540 nm. Measurements were performed using a 96 well Tecan Spectrafluoplus plate reader or a Perkin-Elmer Luminescence Spectrometer LS50B. In swelling experiments, measured light scattering (I) was normalized setting the initial scattering of the mitochondrial suspension to one unit. Permeability transition was quantified using the initial change in 90º light scattering following addition of Ca^{2+}. The initial change in light scattering for mitochondria preincubated in the absence of MG was set to 100 per cent permeability transition. The initial change in light scattering for mitochondria preincubated in the absence of MG but supplemented with 1 µM CsA was set to zero per cent permeability transition. GD3 was dissolved to 5 mM in water and sonicated in a water bath for 5 min before use. To test compounds containing the carbonyl group for effects on the PTP, mitochondria were incubated at 1 mg protein/ml for 15 min at room temperature in modification medium supplemented with the compound of interest at the following concentrations: 10, 30, 100 and 300 nM, 1, 3, 10, 30, 100, 330 µM and 1, 3 and 10 mM. Mitochondria were diluted five times by addition of assay medium and the effect of the compounds on the PTP was assessed following addition of Ca^{2+}. Permeability transition was quantified as rate of swelling.

Cytochrome c release.

Release of cytochrome c was determined by immunoblotting. The mitochondrial suspension was removed from the photometer cuvette, cooled to + 4ºC degrees and centrifugated for 3 min at 21 000 x *g*. The pellet and the supernatant were separated and proteins were precipitated by addition of 10% trichloroacetic acid. Precipitated proteins were separated by SDS-PAGE using 12% gels and electrotransferred to polyvinylidene fluoride membrane. Immunoblotting was performed using a monoclonal cytochrome c antibody (Zymed Laboratories) and visualized by the ECL system (Pharmacia).

Mass spectrometry.

For MALDI TOF mass spectrometry of MG-derived arginine adducts 100 µM of the test peptides was allowed to react with 2 mM MG in 10 mM Hepes-KOH, 100 µM EGTA pH 8.0, at 34ºC. The reaction was stopped by addition of 0.1% trifluoroacetic acid and cooling to 4ºC. The reaction mixture was desalting using a Zip Tip C18 silica bead microcolumn (Millipore). Peptides were eluted with 33% acetonitrile in 0.1% trifluoroacetic acid and the eluate was mixed with an equal volume of saturated α-HCA in acetonitrile/0.1% trifluoroacetic acid 1:2. Half a microliter of this solution was applied on the target. MALDI TOF mass spectra were recorded on a Bruker Autoflex spectrometer using the linear

detector in positive mode. Calibration of the machine was performed using the peaks of α-HCA and peptides of known masses. The resolving power (fwhm) was 3000. For mass analysis of the GD3 ganglioside 0.5 nanomole was mixed with 1 µl 1 mM 2,4,6-trihydroxyacetophenone in acetonitrile/20 mM ammonium citrate 1:1 and applied on the target. Mass spectra were recorded using the linear detector in negative mode.

Electron microscopy.

Fixation of mitochondria was performed by adding 1% glutaraldehyde directly to the suspension. Embedding, sectioning and staining were performed as described previously (29). Sections were viewed in a Jeol 1200 transmission electron microscope at a magnification of 10 000 x.

Chemicals.

CsA was a gift from Novartis, OH-PGO was from Pierce, 3-deoxyglucosone was from Toronto Research Chemicals, TMRM and Fluo-4FF from Molecular Probes. Ganglioside GD3 (bovine buttermilk) was from Calbiochem. Analysis of GD3 by MALDI TOF demonstrated that the C-2 *N*-fatty acyl-sphingosine moiety was a C18 fatty acid in 9%, C19 in 15%, C20 in 25%, C21 in 31%, and C22 in 20%. Other chemicals were from Sigma. Δ-pyrroline 5-carboxylate was regenerated from its 2,4-dinitrophenylhydrazone derivative as described (32).

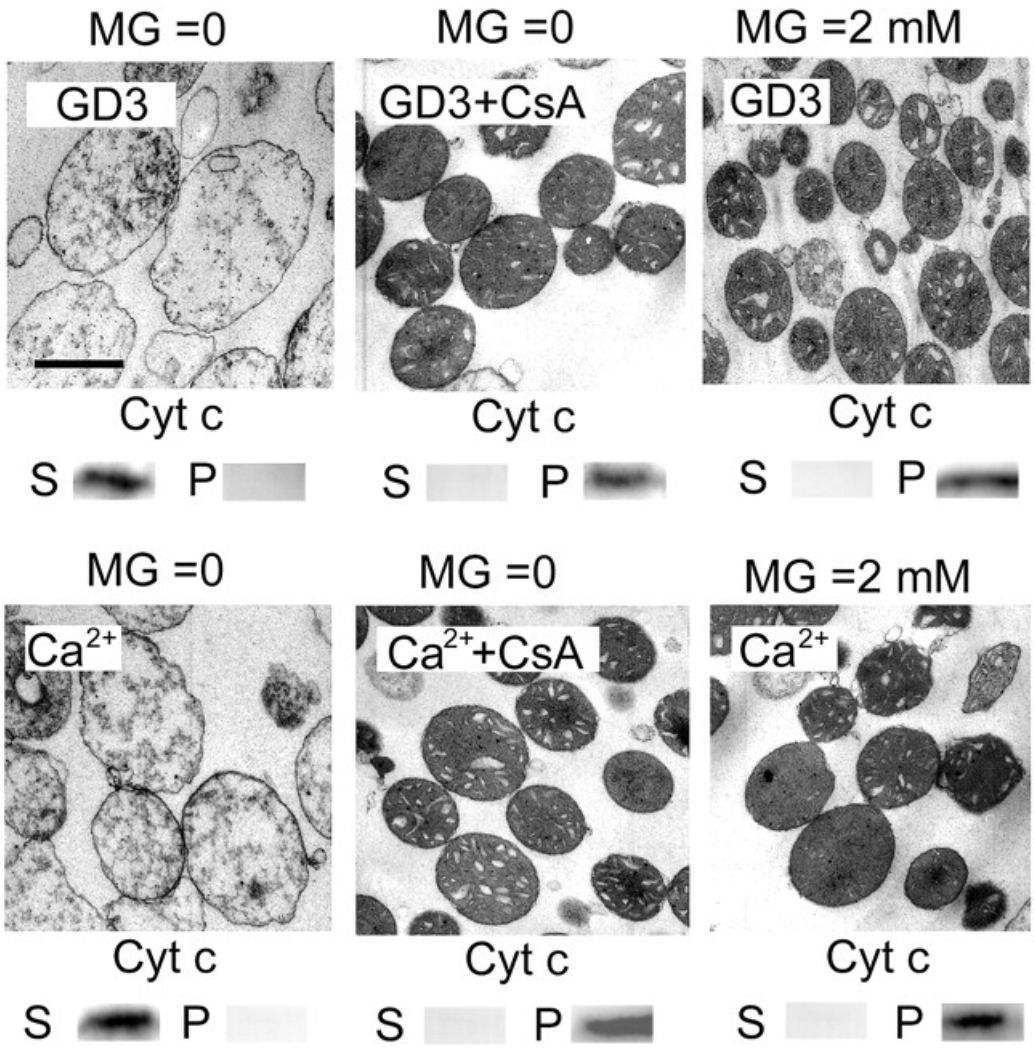

Figure 1. Prevention of mitochondrial swelling and cytochrome c release by MG. Mitochondria were preincubated for 5 min either in the presence of 2 mM MG or in its absence. After that treatment mitochondria were sedimented by centrifugation and resuspended in assay medium at a concentration of 0.2 mg protein/ml. The mitochondrial suspensions were supplemented with the following compounds: 25 μM GD3, 25 μM GD3 + 1 μM CsA, 10 μM Ca^{2+}, or 10 μM Ca^{2+} + 1 μM CsA. The suspensions were incubated at room temperature for 30 min whereupon mitochondria were sedimented by centrifugation. Aliquots of the supernatant and pellets were taken for SDS-PAGE and immunoblotting of cytochrome c. S and P indicate cytochrome c detected in the supernatant and pellet respectively. Chemical fixation of mitochondria was performed using 1% glutaraldehyde followed by embedding, thin-sectioning and staining. Sections were viewed at a magnification of 20 000 x. The scale bar is 1 μm.

Results

We first studied the effect of MG on permeability transition induced by the ganglioside GD3 or Ca^{2+}. Mitochondria were preincubated for 5 min in the presence or absence of 2 mM MG followed by removal of free MG by centrifugation. These mitochondria were incubated for 30 min in assay medium containing 25 μM GD3 or 10 μM Ca^{2+} whereupon mitochondria were processed for ultrastructural analysis by transmission EM and for analysis of cytochrome c release by immunoblotting. The results, shown in fig. 1, demonstrated that both GD3 and Ca^{2+} caused extensive swelling and cytochrome c release in mitochondria preincubated in the absence of MG. Supplementing the medium with CsA, a selective high-affinity inhibitor of permeability transition, prevented mitochondrial swelling and cytochrome c release, showing

that both effects were due to permeability transition. Likewise, preincubation of mitochondria in the presence of MG completely prevented GD3- and Ca^{2+}-induced swelling and cytochrome c release. This finding demonstrated that brief MG-treatment effectively suppressed mitochondrial permeability transition.

The onset of permeability transition is dependent on Ca^{2+}-uptake and production of $\Delta\Psi_m$ by substrate oxidation under the conditions used in fig 1. We verified that MG acted directly on the PTP, and not via these factors, investigating the effect of MG-treatment on $\Delta\Psi_m$ and Ca^{2+}-transport. The membrane potential-sensitive dye TMRM was used to measure $\Delta\Psi_m$ and Ca^{2+}-uptake was assessed by measuring medium [Ca^{2+}] using the membrane impermeable dye fluo-4FF, which becomes fluorescent upon Ca^{2+}-binding. Mitochondrial swelling was monitored as a decrease in light scattering. First we studied the effect of GD3 on $\Delta\Psi_m$ and swelling (fig. 2). Mitochondria, preincubated in the presence or absence of MG, were suspended in assay medium, which was supplemented with 5 mM succinate after 2 min. This addition lead to a rapid accumulation of TMRM regardless of whether MG had been present or not during preincubation, showing that MG did not interfere with the production of $\Delta\Psi_m$ by substrate oxidation (fig. 2, panel A). However, in mitochondria preincubated in the absence of MG the addition of 25 μM GD3 caused a release of TMRM, indicating a drop in $\Delta\Psi_m$ (trace a). GD3 addition also induced a decrease in light scattering indicating that these mitochondria underwent swelling (panel B, trace a). Supplementing the medium of these mitochondria with CsA (trace b) or using MG-treated mitochondria (trace c) prevented both the GD3-induced drop in $\Delta\Psi_m$ and swelling.

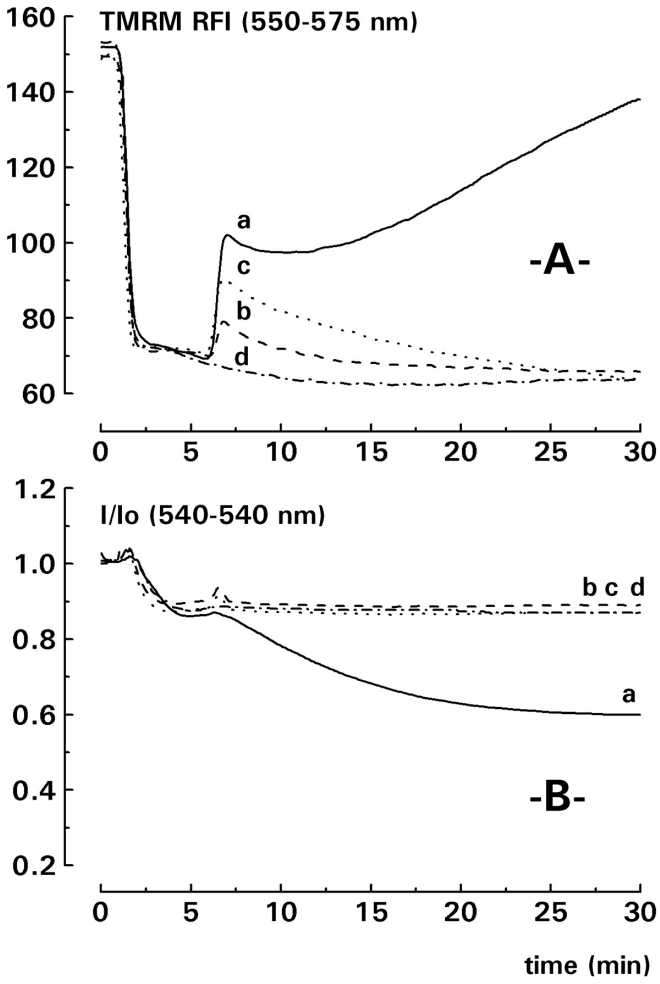

Figure 2. Suppression of GD3-induced permeability transition by MG. Mitochondria were preincubated, centrifugated and resuspended as in fig.1. Succinate (5 mM) was added to the suspension after 2 min followed by GD3 ganglioside (25 μM) after 5 min. Panel A, depicts membrane potential measured using the fluorescent dye TMRM. Panel B, depicts swelling measured as light scattering at 540 nm. The initial intensity of the scattering was set to one unit. *Traces a, b* and *d* show mitochondria preincubated in the absence of MG and *trace c* shows MG-treated mitochondria. The suspension was supplemented with 1 μM CsA in *trace b*. In *trace d* GD3 was not added.

We proceeded to study $\Delta\Psi_m$, Ca^{2+}-transport and swelling following Ca^{2+} addition (fig. 3). Mitochondria were suspended in assay medium and 10 μM Ca^{2+} was added after 2 min. The increase in medium [Ca^{2+}] resulted in an increase in fluo-4FF fluorescence (panel C). Three minutes later mitochondria were energized by the addition of 5 mM succinate. In mitochondria preincubated without MG this addition caused rapid swelling as indicated by the

decrease in light scattering (panel B, trace a). Consistently, these mitochondria failed to produce $\Delta\Psi_m$ in the presence of Ca^{2+} as indicated by the lack of both TMRM and Ca^{2+} accumulation (panel A and C, trace a). However, supplementing the medium of these mitochondria with CsA prevented swelling and the mitochondria were able both to maintain $\Delta\Psi_m$ (panel A, trace b) and take up Ca^{2+} (panel C, trace b). As expected, succinate addition to MG-treated mitochondria resulted in an immediate production of $\Delta\Psi_m$ (panel A, trace c), rapid Ca^{2+}-uptake (panel C, trace c) and prevention of swelling. These results indicate that MG acts directly on the PTP and not on $\Delta\Psi_m$ -production or Ca^{2+}-uptake.

This finding was further corroborated by measurements of respiration rate and $\Delta\Psi_m$ production by ATP hydrolysis (fig. 4). The results indicated that mitochondria retained their maximal respiration rates in the presence of ADP or the protonophoric uncoupler FCCP following preincubation with up to 2 mM MG (left panel). Similarly, preincubation with 2 mM MG had no effect on $\Delta\Psi_m$. production by ATP hydrolysis as measured by the uptake of TMRM (right panel).

In these initial experiments we used a higher MG concentration than that reported for biological systems. To investigate the physiological significance of the findings it was necessary to determine the quantitative relationship between MG concentration and suppression of permeability transition. Therefore mitochondria were preincubated with varying concentrations of MG followed by permeability transition using Ca^{2+} as the triggering signal. Permeability transition was quantified using the initial swelling rates, which were plotted against the concentration of MG used during the preincubation (fig. 5). The plot indicates that the apparent K_{50} for PTP inhibition is 600 µM and that MG already had a significant effect at 250 µM.

As MG reacts with proteins, resulting in both reversible and irreversible adducts, it was of interest to determine whether the effect of MG was reversible or not. To address this

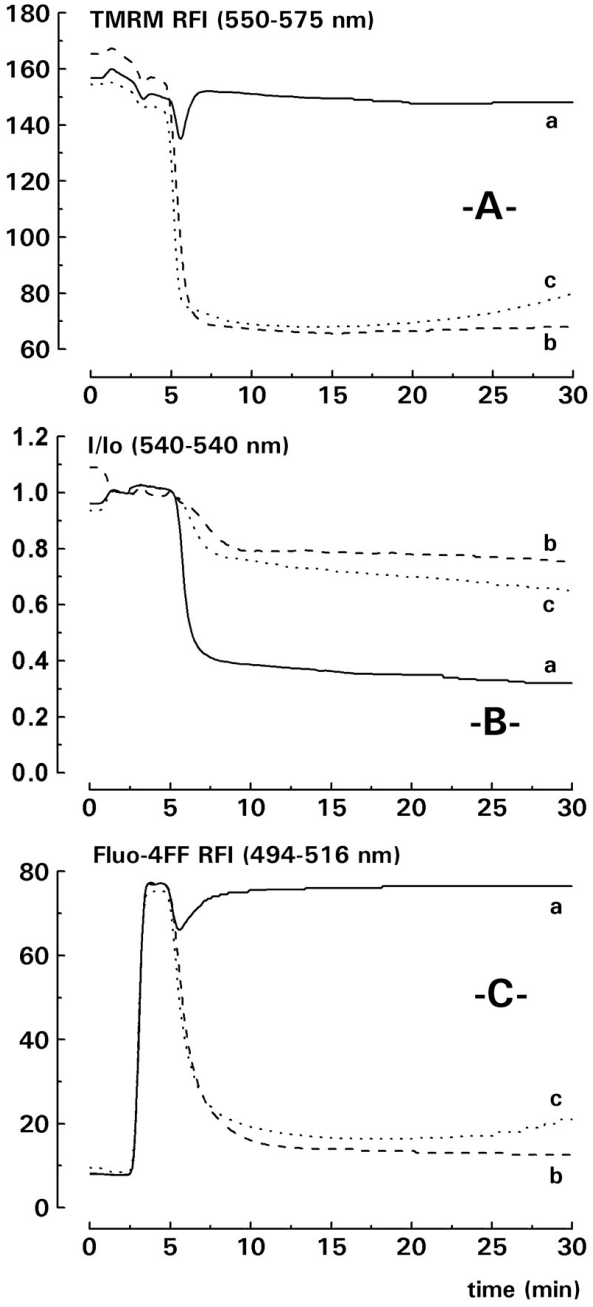

Figure 3. Suppression of Ca^{2+}-induced permeability transition by MG. Mitochondria were preincubated, centrifugated and resuspended as in fig.1. Ca^{2+} (10 µM) was added after 2 min followed by succinate (5 mM) after 5 min. Panel A, depicts membrane potential measured as in fig 2. Panel B, depicts swelling measured as in fig 2. Panel C, shows the Ca^{2+} concentration of the medium measured using the fluorescent dye Fluo-4FF. *Traces a* and *b* show mitochondria preincubated in the absence of MG and *trace c* shows MG-treated mitochondria. The suspension was supplemented with 1 µM CsA in *trace b*.

question we preincubated mitochondria with 2 mM MG or 2 mM PGO that forms an irreversible adduct (29). Following the modification reaction and removal of free reagent mitochondria were incubated in assay medium at room temperature for up to 3 hours whereupon permeability transition was measured by swelling. The results shown in fig. 5 inset indicated that suppression of permeability transition by MG was transient and disappeared after 2 hours at room temperature. As shown previously the effect of PGO was irreversible (29).

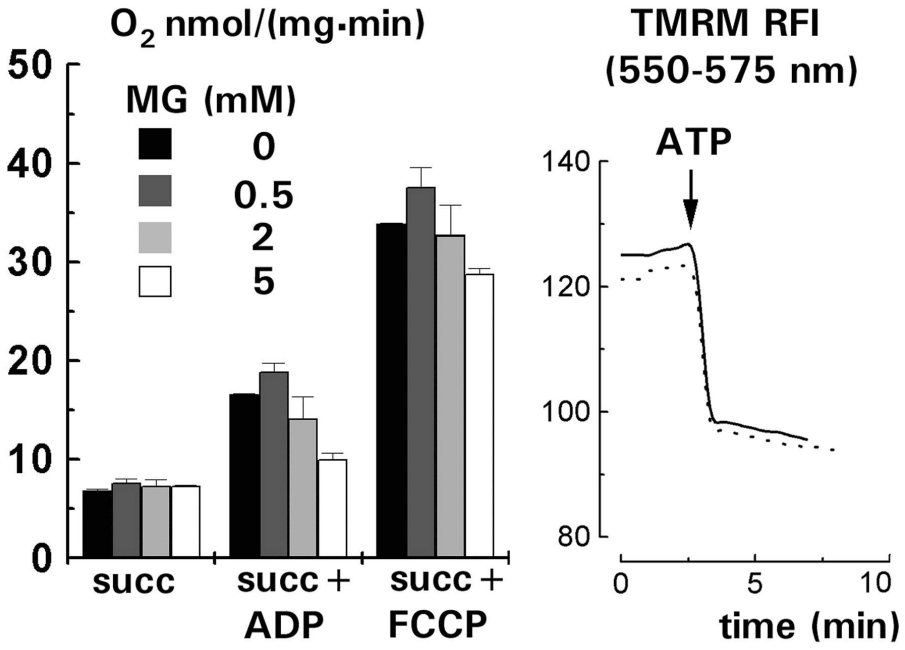

Figure 4. Effect of MG on mitochondrial respiration and production of $\Delta\Psi_m$ by ATP-hydrolysis. Left panel depicts mitochondrial oxygen consumption measured using a Clark electrode. Mitochondria were preincubated with the indicated concentrations of MG followed by centrifugation and resuspension at a concentration of 0.2 mg protein/ml in assay medium. The suspension was added to the electrode chamber and succinate (5 mM) was added immediately followed by ADP (200 µM) after 3 min and FCCP (1 µM) after 6 min. The oxygen consumption was calculated from the decrease in medium oxygen concentration following the addition of succinate, ADP and FCCP, respectively. Right panel shows membrane potential measured as in fig. 2. ATP (1 mM) was added to energize mitochondria after 3 min. *Dotted trace,* mitochondria treated with 2 mM MG. *Filled trace,* mitochondria preincubated in the absence of MG.

CHAPTER 2

We then proceeded to investigate whether any physiological carbonyl compound other than MG was able to suppress permeability transition. We selected candidate carbonyl compounds from the main pathways of carbohydrate, amino acid and fat metabolism and also some aliphatic aldehydes formed in the metabolism of alcohols. Mitochondria were incubated with each compound at concentrations of up to 10 mM in modification medium whereupon permeability transition was assayed by swelling, using Ca^{2+} as the triggering signal. The results are presented in fig 6 and table 1. We first tested the α-oxoaldehydes glyoxal and 3-deoxyglucosone, both of which are implicated in the formation of AGEs. Data showed that while glyoxal effectively suppressed permeability transition at an apparent K50 of 2 mM, 3-deoxyglucosone was completely without effect under the same conditions. CsA inhibited permeability transition in the sub-micromolar concentration range. For comparison we also used the highly toxic cross-linker glutaraldehyde, which caused an inhibition in the sub-millimolar concentration range. Other carbonyls were analyzed in a similar way, plots were constructed as in fig. 6, and data were summarized in table 1. Data show that none of the other compounds specifically altered the response of the PTP to pro-apoptotic signals, in spite of the high intrinsic chemical reactivity of several of them.

In general, formation of significant amounts of MG-derived arginine adducts on proteins requires hours or even days (12, 13, 33). In contrast, our findings showed that complete suppression of permeability transition by MG required a reaction time of only a few

minutes. It was thus of interest to clarify the nature of the MG adduct formed after the short time incubation used in this study. We therefore analyzed the products formed in the reaction of 2 mM MG with the following arginine-containing peptides: NRVYIHPFHL (A), RVYVHPF (B), pEWPRQIPP (C), YGGFMRF (D). The crude reaction mixture was subjected to desalting in C18 reversed phase Zip tips followed by MALDI TOF mass spectrometry analysis. After incubation with MG for 1 h no adduct could be detected on peptides A and B, but prominent additional peaks indicating an increase in mw of 54 could be detected on peptides C and D. Peptide D was selected for studying the time dependence of the reaction since it was the most reactive. In the absence of reagents, the native peptide D gave rise to a single peak at m/z 877.4 ($M+H^+$) (fig. 7). After incubation for 1 min the intensity of that peak had decreased markedly and new peaks appeared at m/z 931.7 corresponding to the 5-hydroxy-5-methylimidazolone-derivative, and at m/z 913.7 corresponding to the 5-methylimidazolone-derivative. Peaks corresponding to the expected molecular weight of pyrimidine- and tetrahydro-pyrimidine derivatives could not be detected. These findings demonstrate that the reaction between MG and peptidyl-arginine may proceed to completion rapidly, within minutes, and suggest that the predominating adduct formed under these conditions was the 5-hydroxy-5-methyl-imidazolone-derivative.

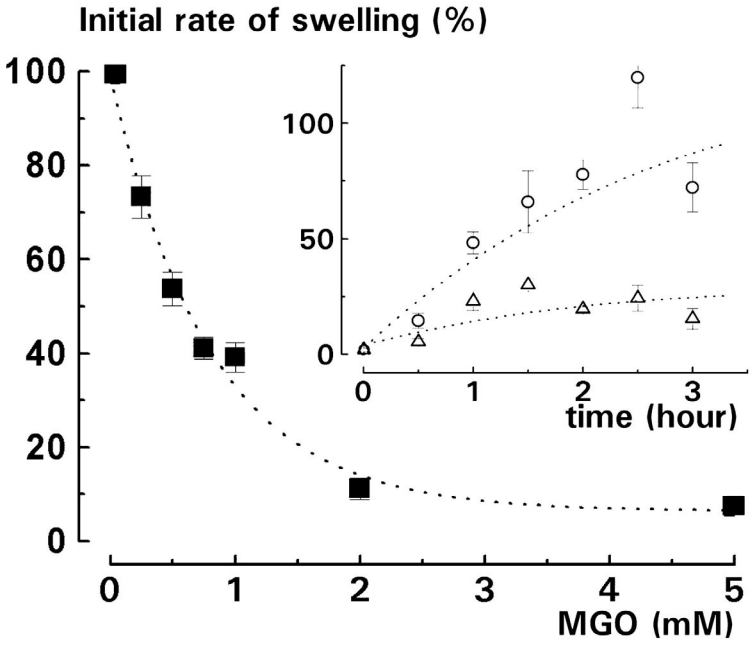

Figure 5. Concentration dependence and reversibility of MG-induced suppression of permeability transition. Mitochondria were incubated with the indicated concentrations of MG followed by centrifugation and resuspension at a concentration of 0.2 mg protein/ml in assay medium. Permeability transition was assayed exactly as in fig. 2, panel B. Swelling was quantified using the initial decrease in light scattering as described in the experimentals section. *Inset,* mitochondria preincubated either with 2 mM MG (*circles*) or 2 mM PGO (*triangles*) were suspended in assay medium at a concentration of 0.2 mg protein/ml at room temperature for the indicated time. Permeability transition was quantified as in the main figure. Experiments were performed in triplicate on three different mitochondrial preparations.

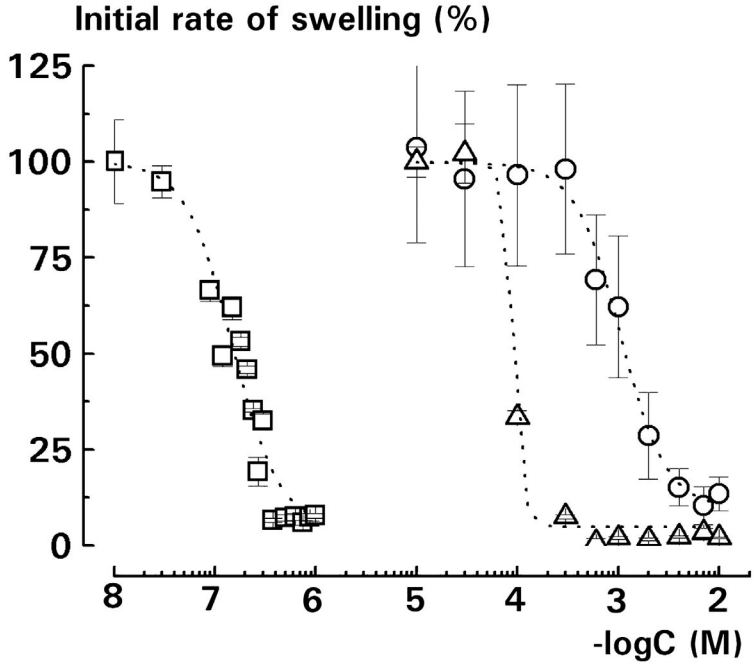

Figure 6. Effect of compounds containing the carbonyl group on permeability transition. Mitochondria were preincubated for 15 min with the indicated concentration of CsA (*squares*), glutaraldehyde (*triangles*) or glyoxal (*circles*). Permeability transition was assayed and quantified as in fig 5.

Compound	K50 (mM)	% swelling at 1 mM ± SEM		n
2-oxoaldehydes				
Glyoxal	2	56.8	9.7	6
3-deoxyglucosone	-	115.2	16.9	3
Carbohydrates and derivatives				
D, L-glyceraldehyde	-	101.4	3.2	6
D-erythrose	-	95.4	16.7	2
D-ribose	-	89.0	14	2
D-galactose	-	130.9	20.3	4
Dihydroxyacetone	-	98.5	3.7	4
D-erythrylose	-	87.5	22.4	2
D-ribulose	-	105.5	23.7	2
D-fructose	-	89.2	19.5	2
D-glucuronic acid	-	115.0	23.0	4
D-glucose 6-phosphate	-	87.4	6.6	6
D-fructose 6-phosphate	-	108.2	50.6	6
Amino acid derivatives				
Oxaloacetate	-	92.9	5.1	6
Pyruvate	-	107	8.4	2
α-ketoglutarate	-	113.7	9.1	4
p-hydroxyphenylpyruvate	-	86.9	11.0	6
phenylpyruvate	-	92.6	8.6	6
α-ketobutyrate	-	92.4	7.5	4
α-ketoadipate	-	94.2	1.8	2
Δ-pyrroline 5-carboxylate	-	105.4	5.7	3
Other aldehydes				
Formaldehyde (b)	>10(a)	78.4	6.5	2
Acetaldehyde (b)	>10(a)	76.0	12.4	2
Propionaldehyde	-	103.2	11.6	4
Glycoaldehyde	-	97.6	8.4	8
Acetone	-	78.9	12.3	3
Hydroxyacetone	-	124.0	19.3	6
Acetoacetic acid	-	124.5	9.5	3
Trans 2-hexenal	4(a)	76.9	11.2	4
Glutaraldehyde	0.02 (a)	1.7	1.4	2
CsA	0.2 µM	(b)		2

Table 1. Effect of compounds containing the carbonyl group on permeability transition. Mitochondria were incubated for 15 min at room temperature with the listed compounds at concentrations up to 10 mM. Permeability transition was assayed and quantified as described in fig. 5. (a) These compounds caused an unspecific loss of mitochondrial function. (b) The initial swelling rate for mitochondria in the presence of CsA was set to 0%.

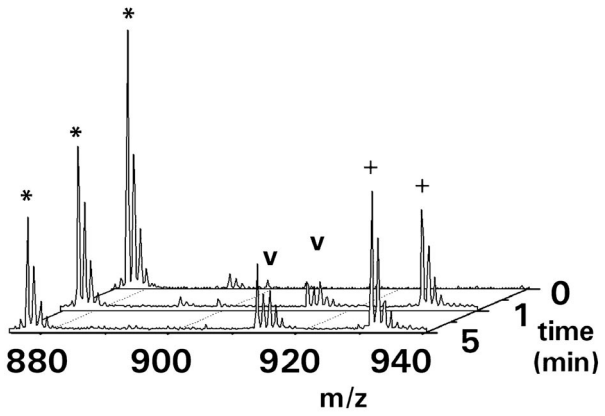

Figure 7. Time dependence of the reaction between MG and the test peptide YGGFMRF. The peptide (100 µM) was incubated with 2 mM MG for the indicated time followed by HPLC separation and analysis by MALDI TOF mass spectrometry using the linear detector in positive mode. Peaks corresponding to the native peptide (m/z 877.4) are indicated with *asterisks*. Peaks of the peptide with 5-hydro-5-methylimidazol-4-one derivative (m/z 931.7) are marked with *plus signs* and peaks of the 5-methylimidazol-4-one derivative (m/z 913.7) are marked with *arrowheads*.

Discussion

In this study we have characterized a novel target of MG: the mitochondrial permeability transition pore (PTP). We have demonstrated that incubation of isolated mitochondria with MG in the millimolar concentration range for a short time was sufficient to completely suppress permeability transition. Under these conditions MG had no significant side effects on mitochondrial substrate transport, respiration or oxidative phosphorylation demonstrating that MG acted selectively on the permeability transition. The effect of MG persisted following removal of free MG indicating that MG had formed a covalent ligand on the PTP. As MG reacts almost exclusively with arginine residues under these conditions (12, 13) we suggest that MG targets the same arginine residue(s) that reacts with the synthetic arginine reagents PGO, BAD and OH-PGO (28, 29, 30, 31).

In these experiments we have used the ganglioside GD3 or Ca^{2+} as signals to induce permeability transition. In several cell types the ganglioside GD3 is formed as a consequence of TNF-α or Fas receptor activation and functions as an apoptosis mediator by transferring from the plasma membrane to mitochondria (35) where it induces permeability transition (23, 24, 25). Influx of Ca^{2+} through the plasma membrane leading to extensive mitochondrial Ca^{2+} accumulation and subsequent permeability transition is of key importance in neuronal death (36). In all likelihood mobilization of either GD3 or Ca^{2+} during cell death processes is essential for induction of mitochondrial permeability transition. As MG suppressed both GD3- and Ca^{2+}-induced permeability transition we conclude that the effect of MG is robust and not restricted to narrowly defined conditions.

In order to investigate the central question as to whether the PTP is a potential target of MG under physiological conditions we have devised an experimental approach based on the expected behaviour of MG in the cell. In the intracellular milieu production of MG is limited and therefore several factors contribute to determine on which proteins MG-derived adducts are formed. The net production of MG is undoubtedly the most important factor influencing the total number of proteins modified by MG. However, under conditions of limiting MG generation the selection of individual targets is not a fortuitous event but is determined by the relative target reactivity, which in turn depends on the local chemical and physical environments. If free and reversibly bound MG is in dynamic equilibrium (11) the extent of modification of different targets is expected to be proportional to their respective equilibrium constants. In order to answer the question of whether the PTP is a potential target of MG under physiological conditions we have characterized several aspects modification reaction including its concentration-dependence, reversibility, and selectivity for the PTP and the specificity of MG among carbonyl compounds.

Concentration-dependence measurements showed that a significant suppression of permeability transition by MG could be observed at 250 μM after incubation for only 5 min. This concentration of free MG is far in excess of that in living systems. However, in cells the MG production goes on more or less constantly leading to equilibrium between free and protein bound MG, which is shifted far in the direction towards the bound form. Whilst the free MG concentration of cells is in the submicromolar range the total MG concentration is reported to be as high as 310 μM (11). MG-induced suppression of permeability transition was reversible indicating that the MG adduct decomposes restoring the PTP to its native state. This finding suggests that PTP-bound MG is in equilibrium with free MG and hence that the level of modification of the PTP is proportional to the prevailing MG concentration. Furthermore, MG did not affect other mitochondrial functions suggesting that the arginine of interest is exceptionally reactive and hence that MG targets primarily the PTP. MG and its structural analogue glyoxal were the only physiological carbonyl compounds, among a large number of similar compounds tested that selectively suppressed the permeability transition. Most notably the reactive α-oxoaldehyde 3-deoxyglucosone, which is an important mediator of the formation of AGEs, completely lacked effect. Our results suggest that MG and glyoxal are the only physiological carbonyl compounds that form covalent ligands on the PTP. The characteristics of the reaction between MG and the PTP, i.e. the fast rate, the reversibility, the selectivity for the PTP and specificity of MG among carbonyl compounds, lend support to the notion that MG-induced modification of the PTP can occur in cells. Furthermore, it can be argued that the PTP functions as a sensor for the MG concentration, which suggests that the modification may play a specific role.

The synthetic MG-analogues PGO and OH-PGO irreversibly modify the PTP. The resulting uncharged PGO-adduct strongly suppresses permeability transition, while the negatively charged OH-PGO adduct promotes permeability transition (31). This lead us to propose that the effect of arginine modification on the PTP conformation is determined by the electrical charge of the resulting adduct. To test this hypothesis further we investigated the reaction product of MG and a set of arginine containing test peptides under the same conditions as we used for incubating mitochondria. The molecular mass of the detected compounds indicated that the major products formed during the first minutes of the reaction were imidazolone-derivatives. This fining is consistent with our working hypothesis that uncharged adducts stabilize the closed conformation of the PTP. The results also showed that the reactivity of the arginine-peptides with MG varied largely, probably owing to the local physical and chemical environment of the respective arginine residues. For the most reactive arginine peptide studied, a second order rate constant of approximately 1.5 $M^{-1}s^{-1}$ could be estimated from the rate of consumption of the native peptide during the initial 5 minute period of the reaction. This rate constant is about 200 fold higher than that reported for the formation of the first reaction product between N-acetylarginine and MG (13). These findings demonstrate that modification of arginine residues by MG can proceed at unprecedented speed.

The major intracellular precursors of MG are the glycolysis intermediates dihydroxyacetone phosphate and glyceraldehyde 3-phosphate (5, 6, 7, 8). The former compound takes part in the glycerolphosphate shuttle, in which cytosolic NADH reduce dihydroxyacetone phosphate to glycerol 3-phosphate, which transfers across the outer mitochondrial membrane and is reoxidized by glycerolphosphate dehydrogenase of the inner membrane. Owing to this design the local concentration of triose phosphates is presumably elevated close to the mitochondria. The PTP thus constitutes a nearby target for MG formed from triose phosphates. Consequently, we hypothesize that MG reacts with the PTP in living organisms and that MG-induced suppression of permeability transition and the ensuing deregulation of the mitochondrial pathway to apoptosis is of importance in the pathogenesis of several diseases. This mechanism may come into play particularly when glycolysis is enhanced and the rate of MG production is increased over the normal level. This occurs not only during diabetic hyperglycemia (38) but also in many malignant tumors (1).

During diabetic hyperglycemia the production of MG is increased both due to the increased intracellular glucose level and to the decrease in glyceraldehyde 3-phosphate dehydrogenase activity (39) caused by reactive oxygen species formed in the mitochondrial

respiratory chain (38). This may lead to suppression of permeability transition in vascular endothelial cells and hence counteract pro-apoptotic signals. However, selective deactivation of apoptotic pathways has been shown to enforce cell death by necrosis in many models (40, 41). Death of vascular cells by necrosis would lead to release of cell content and promote inflammation, a hallmark of atherosclerosis (42). It is thus possible that MG-induced PTP deregulation, together with other mechanisms such as PKC activation, increased polyol formation and reactive oxygen species (2), plays a role in the pathogenesis of diabetic vascular disease.

In rapidly growing solid tumours the supply of oxygen by the vascular system is insufficient to cover the high demand for oxygen. This leads to tumour hypoxia which in turn results in the activation of hypoxia-inducible transcription factor (HIF-1) and other transcription factors, resulting in, among other things, increased expression of genes for glycolytic enzymes (43). The rate of glucose uptake of tumour cells is several-fold higher than of normal cells and glucose uptake correlates with tumour aggressiveness and poor prognosis (44). The increase in the rate of glycolysis is associated with an elevated MG production and over expression of glyoxalases (45). The increased MG production may suppress permeability transition and therefore perturb apoptotic-signalling processes. This provides a cancer cell with an additional mechanism to evade apoptosis, leading to increased tumour aggressiveness. Interestingly, modification of Hsp27 by MG was recently shown to prevent cytochrome c-mediated caspase activation (16). These findings thus suggest that MG acts a link between increased glycolysis rate and aggressive tumour phenotype.

The rapid onset, reversibility and specificity of the effects of MG described in the present work qualify MG as a signalling compound for the PTP. It is noteworthy that selective MG-induced protein modification plays a role in the signal transduction cascade of tumour necrosis factor (19). The question as to whether MG is a *bona fide* secondary messenger, playing a role in the physiological regulation of cell death and differentiation, as proposed previously (46), or is merely a toxic product formed as a consequence of the design of glycolysis should be the subject of future studies.

References

1. Thornalley, P. J. (1995) *Crit. Rev. Oncol. Hematol.* 99, 99-128
2. Brownlee, M (2001) *Nature* 414, 813-820
3. Nakamura, S., Makita, Z., Yasumura, S., Fujii, W., Yanagisawa, K., Kawata, T., and Koike, T. (1997) *Diabetes* 46, 895-899
4. Hammes, H-P, Martin, S., Federlin, K., Geisen, K., and Brownlee, M. (1991) *Proc. Natl. Acad. Sci. USA,* 88, 11555-11558
5. Phillips, S. A., and Thornalley, P. J. (1993) *Eur. J. Biochem,* 212, 648-655
6. Pompliano, D. L., Peyman, A., and Knowles, J. R. (1990) *Biochemistry* 29, 3186-3194
7. Richard, J P. (1991) *Biochemistry* 30, 4581-4585
8. Williams, J.C., and McDermott, A.E., (1995) *Biochemistry* 34, 8309-8319
9. Shonk, C.E., and Boxer, G. E. (1964) *Cancer Res.* 24, 709-721
10. Srivastava, D. K., and Bernhard, S. A. (1987) *Ann. Rev. Biophys. Biophys. Chem.* 16, 175-204
11. Chaplen, F. R. W., Fahl, W. E., and Cameron, D. C. (1998) *Proc. Natl. Acad. Sci. USA,* 95, 5533-5538
12. Westwood, M.E., and Thornalley, P. J.(1995) *J. Prot. Chem.* 4, 359-372
13. Lo, T. W. C., Westwood, M. E., McLellan, A. C., Selwood, T., and Thornally, P. J. (1994) *J. Biol. Chem.* 269, 32299-33005
14. Shipanova, I. N., Glomb, M. A., and Nagaraj, R. H. (1997) *Arch. Biochem. Biophys.* 344, 29-36
15. Oya, T., Hattori, N., Mizuno, Y., Miyata, S., Maeda, S., Osawa, T., and Uchida, K. (1999) *J. Biol. Chem.* 274, 18492-18502
16. Sakamoto, H., Mashima, T., Yamamoto, K., and Tsuruo, T. (2002) *J. Biol. Chem.* 277, 45770-45775
17. Portero-Otín, M., Pamplona, R., Bellmunt, M. J., Ruiz, M.C., Prat, J., Salvayre, R., and Nègre-Salvayre, A. (2002) *Diabetes* 51, 1535-1542
18. Godbout, J.P., Pesavento, J., Hartman, M. E., Manson, S. R., and Freund, G. G. (2002) *J. Biol. Chem.* 277, 2554-2561
19. Van Herreweghe, F., Mao, J., Chaplen, F. W. R., Grooten, J., Gevaert, K., Vanderkerckhofe, J., and Vankompernolle, K. (2002) *Proc. Nat. Acad. Sci. USA.* 99, 949-954
20. Hengartner, M. O. (2000) *Nature* 407, 770-776
21. Yo, S.-W., Wang, H., Poitras, M. F., Coombs, C., Bowers, W. J., Federoff, H. J., Poirier, G. G., Dawson, T. M., and Dawson, V.L. (2002) *Science,*297, 259-262.
22. Bernardi, P. (1999) *Physiol. Rev.* 79, 1127-1155
23. Kristal, B. S., and Brown, A.M. (1999) *J. Biol. Chem.* 274, 23169-23175
24. Scorrano L., Petronilli, V., Di Lisa, F., and Bernardi P. (1999) *J. Biol. Chem.* 274, 22581-22585
25. Garcìa-Ruiz, C., Colell, A., París, R., and Fernández-Checa, J., C. (2000) *FASEB J,* 14, 847-858
26. Desagher, S., and Martinou, J.-C. (2000) *Trends Cell Biol.* 10, 369-377
27. Vieira, H. L., Haouzi, D., El Hamel, C., Jacotot, E., Belzacq, A. S., Brenner, C., and Kroemer, G. (2000) *Cell Death. Diff.* 7, 1146-1154
28. Eriksson, O., Fontaine, E., Petronilli, V., and Bernardi, P. (1997) *FEBS Lett.* 409, 361-364
29. Eriksson, O., Fontaine, E., and Bernardi, P. (1998) *J. Biol. Chem.* 273, 12669-74
30. Scorrano L., Penzo, D., Petronilli, V., Pagano, F., and Bernardi P. (1999) *J. Biol. Chem.* 276, 12035-12040
31. Linder, M.D., Morkunaite-Haimi, S., Kinnunen, P.J.K., Bernardi, P., and Eriksson, O. (2002) *J. Biol. Chem.* 277, 937-942.
32. Mezl, V. A., and Knox, W. E. (1976) *Anal. Biochem.* 74, 430-440
33. Riley, M. L., and Harding, J. J. (1994) *Biochim. Biophys. Acta* 1270, 36-43
34. De Maria, R., Lenti, L., Malisan, F., d'Agostino, F., Tomassini, B., Zeuner, A., Rippo, M. R., and Testi, R (1997) *Science* 277, 1652-1655
35. Garcìa-Ruiz, C., Colell, A., Morales, A., Calvo, M., Enricj, C., and Fernández-Checa, J., C. (2002) *J. Biol. Chem.* 27, 36443-36448
36. Mattson, M., P. (2002) *Nat. Rev. Mol. Cell. Biol.* 1, 120-129
37. Niwa, T. (1999) *J. Chromatogr. B.* 731, 23-36
38. Hishikawa, T., Edelstein, D., Du, X. L., Yamagashi, S-I., Matsumura, T., Kaneda, Y., Yorek, M. A., Beebe, D., Oates, P. J., Hammes, H-P., Giardino, I., and Brownlee, M. (2000) *Nature* 404, 787-790
39. Knight, R. J., Kofoed, K. F., Schelbert, H. R., and Buxton, D. B. (1996) *Cardiovasc. Res.* 32, 1016-1023
40. Kitanaka, C., and Kuchino, Y. (1999) *Cell Death Diff.* 6, 508-515
41. Chautan, M., Chazal, G., Cecconi, F., Gruss, P., and Golstein, P. (1999) *Curr. Biol.* 9, 967-970
42. Libby, P. (2002) *Nature,* 420, 868-874
43. Harris, A. L. (2002) *Nat. Rev. Cancer,* 2, 38-47
44. Dang, C. V., and Semenza, G. L. (1999) *Trends Biochem. Sci.* 24, 68-72
45. Ranganathan, S., Walsh, E. S., Godwin, A. K., and Tew, K. D. (1993) *J. Biol. Chem.* 268, 5661-5667.
46. Egyud, L.G., and Szent-Györgyi, A. (1968) *Science* 160, 1140

Chapter 3

INHIBITION OF THE MITOCHONDRIAL PERMEABILITY TRANSITION BY CREATINE KINASE SUBSTRATES

REQUIREMENT FOR MICROCOMPARTMENTATION

Max Dolder[1], Bernd Walzel[2], Oliver Speer, Uwe Schlattner, and Theo Wallimann

Institute of Cell Biology, Swiss Federal Institute of Technology, ETH-Hönggerberg, CH-8093 Zürich, Switzerland
[1] Present address: Institute of Biotechnology, Swiss Federal Institute of Technology ETH-Hönggerberg, CH-8093 Zürich, Switzerland
[2] Present address: Coty-Lancaster Group, International Research and Development Center, Athos Palace/2, Rue de la Lùjerneta, MC-98000 Monaco

CHAPTER 3

Published in
The Journal of Biological Chemistry, 16th May 2003, 278 (20), 17760 - 66

Acknowledgments — We thank Elsa Zanolla for technical support and Dr. Alan P. Koretsky (NIH Bethesda, USA) for providing transgenic liver-mtCK mice. We thank Dr. Alan P. Koretsky, Prof. Paolo Bernardi (University of Padua, Italy), and Dr. Laurence A. Kay (Université Joseph Fourier, Grenoble, France) for valuable discussions and comments on the manuscript.

This work was supported by private sponsoring (Careal Holding AG, Zürich, and AVICENA Inc. [Dr. Rima Kaddurah-Daouk], Boston, USA) to M. D. and T. W., a grant from the Swiss Society for Research on muscle diseases (to B. W., O. S., and T. W.), and by a Swiss National Science Foundation grant (no. 31-62024.00 to T. W. and U. S.).

The abbreviations used are: CK, creatine kinase; ANT, adenine nucleotide translocase; Ap_5A, ***P*^{1},*P*^{5}**-di(adenosine 5')-pentaphosphate (an inhibitor of adenylate kinase); BB-CK, cytosolic brain-type creatine kinase; Cr, creatine; CsA, cyclosporin A; CyCr, cyclocreatine; FCCP, carbonyl cyanide *p*-trifluoromethoxyphenylhydrazone; GPA, β-guanidinopropionic acid; IMS, intermembrane space; MPT, mitochondrial permeability transition; mtCK, mitochondrial creatine kinase; PCr, phosphocreatine; Mops, 4-morpholinepropanesulfonic acid.

Summary

Mitochondria from transgenic mice, expressing enzymatically active mitochondrial creatine kinase in liver, were analysed for opening of the permeability transition pore in the absence and presence of creatine kinase substrates, but with no external adenine nucleotides added. In mitochondria from these transgenic mice, cyclosporin A-inhibited pore opening was delayed by creatine or cyclocreatine, but not by β-guanidinopropionic acid. This observation correlated with the ability of these substrates to stimulate state 3 respirations in the presence of extramitochondrial ATP. The dependence of transition pore opening on calcium and magnesium concentration was studied in the presence and absence of creatine. If mitochondrial creatine kinase activity decreased (i.e. by omitting magnesium from the medium), protection of permeability transition pore opening by creatine or cyclocreatine was no longer seen. Likewise, when creatine kinase was added externally to liver mitochondria from wild type mice that do not express mitochondrial creatine kinase in liver, no protective effect on pore opening by creatine and its analog was observed. All these findings indicate that mitochondrial creatine kinase activity located within the intermembrane and intercristae space, in conjunction with its tight functional coupling to oxidative phosphorylation, via the adenine nucleotide translocase, an modulate mitochondrial permeability transition in the presence of creatine. These results are of relevance for the design of creatine analogs for cell protection as potential adjuvant therapeutic tools against neurodegenerative diseases.

Introduction

Most vertebrate cell types express cytosolic as well as mitochondrial isoforms of the enzyme creatine kinase (CK)[1]. CK catalyzes the reversible transphosphorylation of phosphocreatine (PCr) to ATP. The findings of distinct subcellular localizations of creatine kinases have led to the formulation of the PCr-circuit concept, proposing that sites of energy production (mitochondria, glycolysis) are tightly linked via Cr/PCr shuttling to sites of energy consumption (various cellular ATPases) (1-6). ATP generated by oxidative phosphorylation in mitochondria reacts with creatine (Cr) to produce PCr, a reaction mediated by mitochondrial CK (mtCK) located in the intermembrane and intercristae space. Phosphocreatine, then, diffuses to the cytosol to locally regenerate ATP via cytosolic CK from ADP. Cr produced during this reaction is shuttled back to mitochondria for recharging it to PCr. This energy shuttling system is particularly efficient in tissues with a very high and fluctuating energy demand like skeletal and cardiac muscle, as well as in brain and neural tissues (7). Thus, in addition to the generally accepted temporal energy buffering function, PCr also provides a means to spatially buffer energy reserves (3). This holds especially true for highly polar cells like spermatozoa where the diffusion of ADP is the limiting factor (8). Studies with cultured rat hippocampal neurons have shown recently that creatine protects against glutamate and beta-amyloid toxicity (9), as well as against energetic insults in striatal neurons (10). Similarly, creatine and in some cases the related analog cyclocreatine (CyCr), exert protective effects in several animal models of neurodegenerative diseases, like Huntington's disease (11), amyotrophic lateral sclerosis (12), and a form of Parkinsonism (13). Likewise, Cr-pretreatment of cultured myotubes from dystrophic *mdx* mice enhanced myotube formation and survival (14). Recent data indicate that Cr reduces muscle necrosis and protects mitochondrial function *in vivo* in *mdx* mice (15). Treatment of patients with Cr or Cr analogs has, therefore, been proposed as a possible adjuvant therapy for such diseases (16). The protection observed with Cr in these cell and animal models may be partially explained by its function as a cellular energy buffer and transport system via the PCr shuttle as outlined above. An additional potential mechanism of Cr protection may be linked to direct effects on mitochondrial permeability transition (MPT) (17), which has been suggested to be a causative event in different *in vivo* and *in vitro* models of cell death (18-24).

In an attempt to define the role of mitochondrial creatine kinase on MPT, we have shown in an earlier study that isolated liver mitochondria from transgenic mice containing mtCK did not respond by MPT pore opening upon treatment with Ca^{2+} plus atractyloside if Cr or CyCr were present in the medium (17). In the absence of Cr and CyCr, however, MPT pore opening could be fully induced by Ca^{2+} plus atractyloside. On the other hand, in liver mitochondria from control mice without mtCK, pore opening induced by Ca^{2+} plus atractyloside was independent on the presence or absence of Cr or CyCr. In the present study we investigated these effects in more detail, asking the question of whether inhibition of MPT pore opening by CK substrates depends on mtCK activity and whether the tight functional coupling between the CK reaction and oxidative phosphorylation, demonstrated recently to take place *in situ* (25), would lead to cycling of mitochondrial adenine nucleotides, thus resulting in net production of phosphorylated CK substrates. Our results indicate that substrate channeling between mtCK and adenine nucleotide translocase (ANT) takes place in a tight functionally coupled microcompartment that seems absolutely required for protection of MPT pore opening by creatine.

Experimental procedures

Source and preparation of mitochondria

Transgenic mice expressing the ubiquitous mitochondrial creatine kinase isoform in their liver mitochondria (transgenic liver-mtCK mice) were kindly provided by Dr. Alan P. Koretsky (NIH, Bethesda USA). Mice were killed, the liver quickly removed and placed in ice-cold isolation buffer for mitochondria (10 mM Tris-HCl, pH 7.4, 250 mM sucrose) supplemented with 1 mM EDTA and 0.1% BSA. Livers were homogenized and the homogenate centrifuged at 700xg for 10 min. The supernatant was filtered through two layers of nylon gauze and centrifuged at 7000xg for 10 min. The mitochondrial pellet was washed twice with isolation buffer (without EDTA and BSA), centrifuged, and kept on ice.

Respiration and swelling measurements

Mitochondrial oxygen consumption was measured with a Cyclobios oxygraph (Anton Paar, Innsbruck, Austria) at 25 °C. The standard medium (2 ml) consisted of 10 mM Tris/Mops, pH 7.4, 250 mM sucrose, 10 mM phosphate/Tris, 2 mM MgCl2, 0.5 mM EGTA/Tris, 2 µM rotenone, and 50 µM Ap_5A. State 4 respiration was stimulated by addition of 5 mM succinate/Tris. Creatine kinase substrates (Cr, CyCr, GPA) were present at 10 mM concentration, and state 3 respiration was induced by adding 1 mM ATP. Mitochondrial protein concentration in all assays was 0.5 mg/ml. Deviations from these conditions are specified in the figure legends. Mitochondrial MPT pore opening was measured by the convenient swelling assay and carried out in a UV4 UV/VIS spectrometer (Unicam) connected to a computer. Swelling curves were recorded at 540 nm and data points were acquisited every 1/8 s using Visions© software (version 3.10, Unicam Ltd.). Cuvettes containing the mitochondrial suspension were thermostated to 25 °C. Incubation conditions and inductions of MPT are indicated in the legends to the figures.

Measurement of PCr production by quantitative thin-layer chromatography

Mitochondria were incubated under different conditions (see legend to Fig. 4) in the presence of $^{32}P_i$. Reactions were stopped after defined time intervals by addition of 1% (final concentration) sodium dodecylsulfate, centrifuged, and the supernatants applied to silica gel 60 thin-layer plates (Merck, Darmstadt, Germany). Running solvent was a mixture of isopropanol, ethanol and 25% ammonia (6:1:3, by volume). Thin-layer plates were air-dried, exposed to a Kodak storage phosphor screen SO230 and analyzed with a Phosphor Imager (Storm 820, Molecular Dynamics). The position of PCr in thin-layer chromatograms was identified in control experiments using recombinant brain-type BBCK incubated in the presence of radioactive ^{14}C-creatine and cold ATP.

Binding of exogenously added CK to mitochondria

Mouse liver mitochondria (0.5 mg/ml) were incubated in standard medium at pH 7.4 with 5 mM glutamate and 2.5 mM malate and without rotenone. Specified amounts of recombinant brain-type BB-CK or ubiquitous human mtCK (prepared as described elsewhere (26,27)) were added. After a five-minutes incubation, an aliquot of the suspension was removed (to measure total CK activity). The rest was centrifuged (5 min. at 7000xg) to separate mitochondria. CK activity was measured separately in the supernatants and mitochondrial pellets by a coupled enzymatic assay (28).

Other methods

Protein concentrations were determined by Bradford assay (Bio Rad) using BSA as a standard. Mitochondrial adenine nucleotide content was measured by reversed phase chromatography of acid extracts according to Kay *et al*. (25).

Results

To correlate the effects of the different creatine kinase substrates on MPT pore opening with their ability to stimulate oxidative phosphorylation, we first measured stimulation of state 3 respiration by ATP and CK substrates in mitochondria oxidizing succinate. The data of these experiments are summarized in Table I. In mtCK containing mitochondria from transgenic mice, substantial stimulation (about 3-fold over state 4) was observed only with Cr and CyCr (both 10 mM), but not with GPA, in the presence of externally added ATP, due to endogenous production of ADP by mitochondrial CK. The absence of a detectable stimulation with 10 mM GPA agrees with the inability of mitochondrial CK to phosphorylate this creatine analog (29,30). No Cr- or CyCr stimulated respiration was seen with mitochondria from control mice, which do not express mtCK in liver (17). These data confirm earlier findings with the same substrates given to heart mitochondria (30). In general, with respect to creatine-stimulated respiration, mitochondria from transgenic liver-mtCK mice are

	nmol $O \cdot min^{-1} \cdot mg^{-1}$ protein			
CK substrate	state 4	state 3	state3/state 4	n
None	55.7 ± 2.6	64.9 ± 2.3	1.17	6
10 mM Cr	56.5 ± 2.9	167.9 ± 7.9	2.97	8
10 mM CyCr	57.7 ± 2.2	164.7 ± 7.0	2.86	8
10 mM GPA	55.3 ± 1.2	64.5 ± 2.0	1.17	8

Table I **Oxygen consumption rates of liver mitochondria from transgenic liver-mtCK mice in the presence of different creatine kinase substrates.** Incubation conditions are specified in Materials and Methods. State 4 respiration was measured in the presence of 5 Mm succinate/Tris and state 3 was stimulated by addition of 1 mM ATP. Oxygen consumption values are means ± SD. n: number of experiments. Note that transgenic mtCK containing mitochondria show Cr- and CyCr-stimulated respiration in contrast to liver mitochondria from control mice (not shown, see ref. (17)).

behaving comparably to mtCK containing heart mitochondria (see also ref. (17).)

Next, we measured, in transgenic mtCK-liver mitochondria, the opening of the permeability transition pore induced by Ca^{2+} in the presence of CK substrates, but in the complete absence of external adenine nucleotides, and under different of conditions. To avoid any effects caused by adenylate kinase (AK) activity the specific AK inhibitor Ap_5A as included in the medium in all experiments. In the experiments shown in Fig. 1A, mitochondria were energized with glutamate and malate in the absence of rotenone. Due to the presence of 2 mM Mg^{2+} (but no EGTA) in the medium, a rather high (120 µM) Ca^{2+} pulse had to be administered to overcome MPT inhibition by magnesium. As shown in Fig. 1A, Cr and CyCr effectively inhibited pore opening within the time frame of the experiment. In the absence of CK substrates or with GPA present, MPT pore opening occurred in a significant fraction of the mitochondrial population. These effects of CK substrates were independent, at least qualitatively, on how the MPT was triggered and of the respiratory substrates used as documented in Figs. 1B and 1C. In the experiments shown in Fig. 1B, mitochondria were again energized with complex I substrates (glutamate and malate), but exposed to only 40 µM Ca^{2+} (which did not open the MPT *per se*). Subsequent depolarization with 0.2 µM FCCP led to rapid swelling of the mitochondria, both, in the absence and presence of CK substrates. Swelling was again sensitive to CsA, as well as to 50 µM ubiquinone 0, a novel and general MPT inhibitor (not shown) (31), indicating opening of the MPT pore. Remarkably however, Cr and CyCr exerted MPT protection in a significant subpopulation of mitochondria

even in the absence of external adenine nucleotides and under these very strongly pore promoting conditions (absence of EGTA, high phosphate, depolarization of mitochondria by FCCP, presence of complex I substrates). Again, GPA did not protect mitochondria from MPT pore opening. Figure 1C shows the same set of experiments, but with succinate-energized mitochondria in the presence of rotenone. Here, the same qualitative conclusions can be drawn as from the data presented in Figs. 1A and 1B. In accordance with the finding of Fontaine *et al*. (32), conditions are more restrictive for MPT pore opening with complex II linked substrates due to decreased electron flux through complex I, a general property of the MPT. With succinate as the electron donor, Cr and CyCr, but not GPA, fully protected from MPT pore opening. Next we analysed MPT protection by creatine at different calcium concentrations. In the experiments displayed in Fig. 1D the Mg^{2+} concentration was reduced to 0.5 mM to better compare the effect of Cr as a function of the calcium load. Under these conditions, 30 µM Ca^{2+} did not open the MPT pore if Cr was present. Pore opening was, however, observed at higher Ca^{2+} concentrations (90 and 150 µM, solid curves in Fig. 1D). Nevertheless, Cr still inhibited significant fractions of mitochondria when compared to conditions without Cr but equal Ca^{2+} concentrations (dashed curves in Fig. 1D).

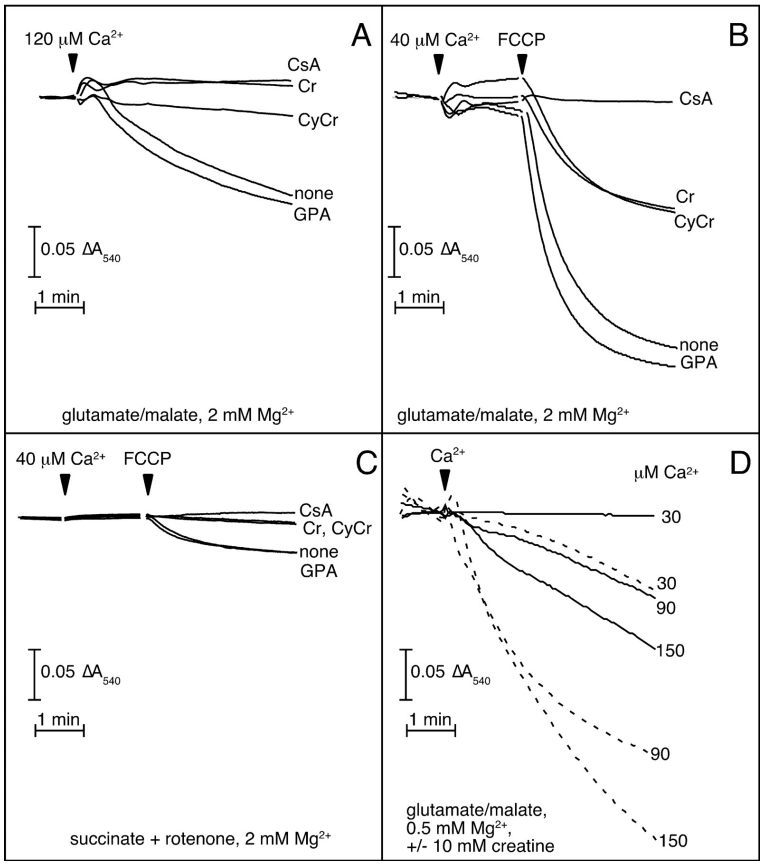

FIGURE 1 **Swelling measurements showing the effect of creatine kinase substrates on MPT pore opening of liver mitochondria from transgenic liver-mtCK mice under different conditions**. The incubation medium (1 ml) contained 10 mM Tris/Mops, pH 7.4, 250 mM sucrose, 10 mM phosphate/Tris, 2 mM (panels *A-C*) or 0.5 mM (panel *D*) $MgCl_2$, and 50 µM Ap_5A. Mitochondria were energized either with 5 mM glutamate/Tris and 2.5 mM malate/Tris (panels *A, B,* and *D*), or with 5 mM succinate/Tris in the presence of 2 µM rotenone (panel *C*). CK substrates were present at 10 mM concentration. In the uppermost traces of panels *A-C*, the medium was supplemented with 1 µM CsA. Reactions were started by addition of 0.5 mg mitochondria (not shown) and MPT was induced by Ca^{2+} or Ca^{2+} plus FCCP as indicated. In panel *D* solid and dashed traces represent conditions with and without 10 mM Cr, respectively.

Based on these observations and the data presented in Table I, we suggested that the protective effect on MPT pore opening seen with Cr and CyCr as compared to GPA could be related to the kinetic properties of these substrates, i.e. their rate of phosphorylation by mtCK. In contrast to GPA, Cr and CyCr are rapidly converted by mtCK via ATP to their respective phosphorylated compounds, PCr and CyPCr (30). If substrate phosphorylation by mtCK (with internally available ATP) were responsible for the observed effects, protection of MPT by Cr and CyCr should have been abolished under conditions where CK is inactive as an enzyme. As there is no absolutely specific K inhibitor available, we omitted Mg^{2+} instead, which is an essential cofactor for the CK reaction (33), from the medium. With no Mg^{2+}

present, creatine-stimulated respiration with ATP was almost completely absent as shown in Fig. 2A (compare slopes at arrow in *trace a* with that of *trace b*). Importantly, in the absence of exogenous Mg^{2+}, state 3 respiration was still observed after addition of ADP (disodium salt, Fig. 2A, *trace a*) indicating that sufficient matrix Mg^{2+} is available for phosphorylation of ADP by FoF1-ATP synthase, but this Mg^{2+} is not accessible to mtCK located in the inter-membrane space. As shown in Fig. 2B, in the absence of Mg^{2+}, mitochondrial swelling induced by 20 µM Ca^{2+} and 0.2 µM FCCP occurred to the same extent irrespectively of whether CK substrates were present or not, in contrast to what was observed in the presence of Mg^{2+} (see the corresponding traces in Fig. 1B). MPT pore opening was, however, still fully blocked by 1 µM CsA, even in the absence of Mg^{2+}.

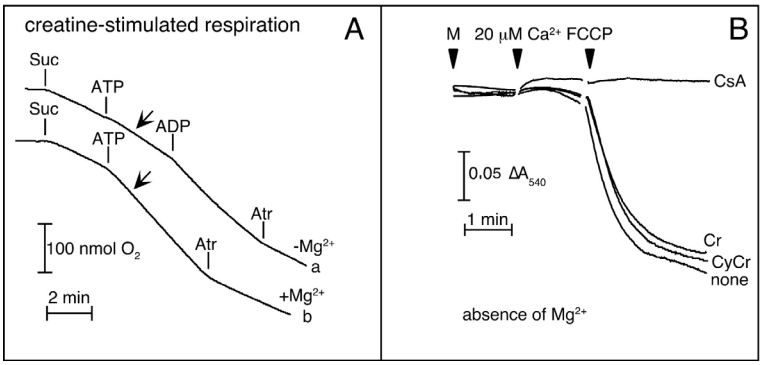

FIGURE 2 **Effect of Mg^{2+} on respiration and swelling of liver mitochondria from transgenic liver-mtCK mice in the presence of creatine kinase substrates**. *A,* respiration measurements without (*trace a*) and with 2 mM $MgCl_2$ (*trace b*). Where indicated, 5 mM succinate/Tris (*Suc*), 1 mM ATP, 50 µM ADP, or 20 µM atractyloside (*Atr*) were added. Note that CK-mediated Cr-stimulated state 3 respiration with ATP in the presence of Mg^{2+} is no longer observed in the absence of Mg^{2+} (compare slopes at *arrows* in *traces b* and *a*, respectively). *B,* Swelling measurements. Incubation conditions were as specified in the legend to Fig. 1A, except that $MgCl_2$ was omitted. CK substrates (Cr or CyCr) were present at 10 mM concentration. In the *uppermost trace*, the medium was supplemented with 1 µM CsA. Reactions were started by addition of 0.5 mg mitochondria (M) to 1 ml medium followed by Ca^{2+} and FCCP as indicated.

In a further set of experiments we analysed the effect of Mg^{2+} and Cr on MPT in more detail by varying the concentrations of these substrates and measuring mtCK activity under identical conditions. Representative swelling measurements at two different Mg^{2+} concentrations with (solid curves) and without (dashed curves) Cr are displayed in Fig. 3A. From such curves we determined the absorption difference (ΔA_{540}) before and four minutes after triggering the MPT with 120 µM Ca^{2+} (same conditions as in the experiments of Fig. 1A). The ΔA_{540} values were used to calculate the fraction of swollen mitochondria with reference to the ΔA_{540} measured with 5 µM of the channel-forming peptide alamethicin, which resulted in (not MPT-caused) swelling of 100% of the mitochondria (not shown). As shown in Fig. 3C, the fraction of swollen mitochondria, i. e., the fraction having undergone a permeability transition, decreased at increasing Mg^{2+} concentrations, also in the absence of Cr (open circles in Fig. 3C). This was to be expected, as the MPT is regulated by an external inhibitory Me^{2+} binding site (34). However, in the presence of 10 mM Cr an additional protection starting at around 0.5 mM Mg^{2+} is observed (closed circles in Fig. 3C). At this Mg^{2+} concentration, mtCK activity, as measured in the pH stat in the forward reaction with ATP plus Cr, was at about 70% of the maximum value (open triangles in Fig. 3C). Therefore, MPT protection by Cr shows up at relatively high Mg^{2+} concentrations only (>0.5 mM) with corresponding high mtCK activities. A similar analysis carried out by variation of the Cr concentration at constant [Mg^{2+}] (2 mM) revealed that MPT protection by Cr is clearly a function of mtCK activity (Figs. 3B and D).

These data are in strong support of the idea that the rate of phosphorylation of CK substrates by active mtCK is related to their effect on MPT. Phosphorylation of these CK

substrates occurs in microcompartments formed by mtCK and ANT (see below) (35). Since we did not add external adenine nucleotides, phosphorylation must occur via internally available ATP inside mitochondria, suggesting continuous cycling of internal ADP and ATP between matrix and intermembrane space mediated by ANT, if Cr or CyCr are present. As a consequence, if Cr is present, we should expect a net production of PCr even in the absence of exogenously added adenine nucleotides. This is indeed the case as shown in Fig. 4A. Mitochondria were incubated in the presence of ^{32}Pi, Mg^{2+}, and 10 mM creatine. Only with energized mitochondria and fully active mtCK, as well as with a working oxidative phosphorylation system, we could observe a generation of PCr (*lane a*). These are exactly the conditions used in the

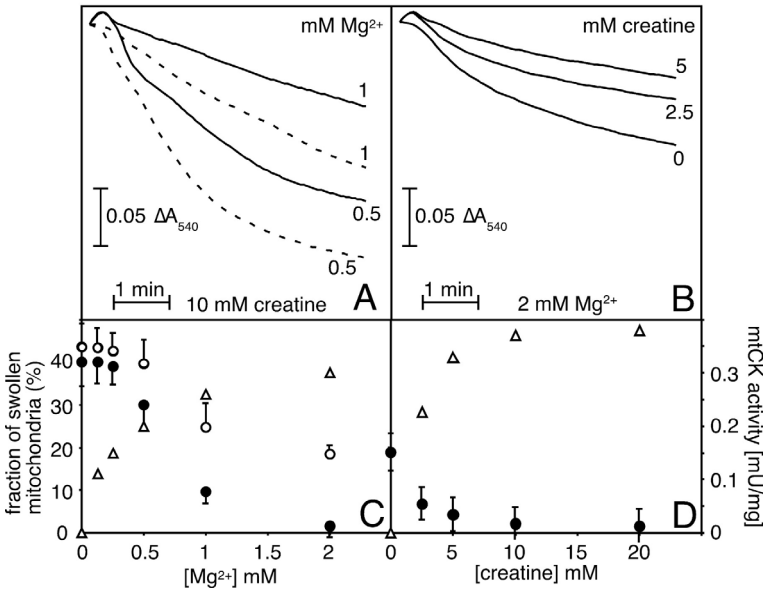

FIGURE 3 **Correlation of mtCK activity with MPT inhibition at variable substrate concentrations**. Incubation conditions for the swelling experiments (panels *A* and *B*) were as in Fig. 1A. Panel *A* effect of [Mg_{2+}] on MPT in the presence (solid traces) and absence (dashed traces) of 10 mM Cr. Panel *B* effect of Cr on MPT at constant [Mg_{2+}] (2mM). Panels *C* and *D* fraction of swollen mitochondria (calculated from •A_{540}, see text for details) in the presence (filled circles) and absence (open circles) of Cr, and mtCK activity (triangles) measured in the forward reaction at pH 7.4 with a pH stat (65).

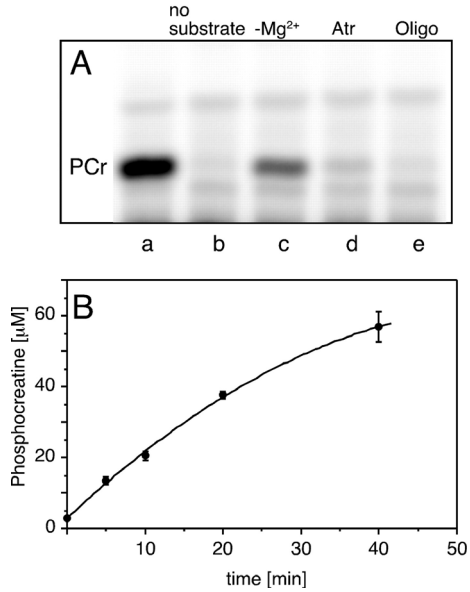

FIGURE 4 **Phosphocreatine production by mitochondria from transgenic liver-mtCK mice in the absence of exogenous adenine nucleotides**. Panel *A* Thin-layer chromatography of solubilised mitochondria after a 40 min incubation of intact mitochondria in the presence of $_{32}P_i$ (1 µCi per assay). The incubation medium (50 µl) consisted of 10 mM Tris/Mops, pH 7.4, 250 mM sucrose, 10 mM phosphate/Tris, 2 mM $MgCl_2$ (except in *lane c*), 5 mM succinate/Tris (except in *lane b*), 2 µM rotenone, and 50 µM Ap_5A. In *lane d*, the medium was supplemented with 20 µM atractyloside (Atr) and in *lane e* with 1 µM oligomycin (Oligo). panel *B* time course of PCr production by mitochondria incubated as described for *lane a* in panel *A*.

swelling experiments where MPT protection by Cr was observed (Fig. 1). With deenergized mitochondria (no substrates, *lane b*), blocked ANT (20 µM atractyloside, *lane d*), or blocked FoF1-ATP synthase (1µM oligomycin, *lane e*), no PCr was produced. Note in *lane c* (absence of Mg^{2+}), some PCr is still generated due to residual Mg^{2+} (probably bound to mtCK). Figure 4B shows a time-course experiment of net PCr production by energized mitochondria in the presence of external Cr plus Mg^{2+}, but no adenine nucleotides. The measured adenine nucleotide content is 0.11 ± 0.01 nmol per 25 µg of isolated mitochondria from transgenic liver-mtCK mice. After a 40 min incubation of succinate-energized mitochondria, 2.85 nmol of PCr were produced by 25 µg of mitochondria (Fig. 4B). Recalling

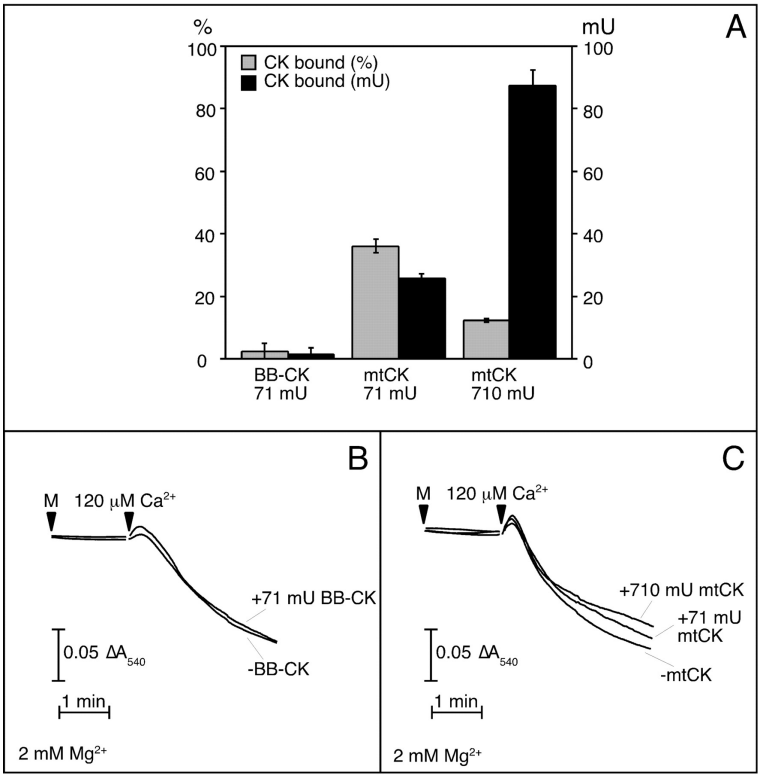

FIGURE 5 **Effect of externally added creatine kinase on MPT pore opening of liver mitochondria from control mice in the presence of 10 mM Cr**. Panel *A* Binding of different CK isoforms added externally to mitochondria from control mice. Conditions were as specified in the legend of Fig. 1A. Relative percentage (%, grey bars) and absolute amounts (mU, black bars) of bound CK are given after incubation of mitochondria with either 71 mU BB-CK, 71 mU or 710 mU mtCK. Panel *B* Swelling of liver mitochondria from control mice with 71 mU externally added BB-CK present (*lane a*), or in the absence of BB-CK. Panel *C* Same as in panel *B*, but in the presence of different amounts of externally added mtCK.

that one ATP is consumed for every molecule of PCr produced, we can estimate that this is over 25 times more than the measured adenine nucleotide content. This quantitative consideration is a strong argument for internal nucleotide cycling. Mitochondrial CK forms a microcompartment with ANT at the contact sites (together with outer membrane porin), as well as along the cristae (with ANT only (36,37)). This compartmentation allows efficient transphosphorylation of ATP to PCr and export of the latter to the cytosol at peripheral contact sites. The reaction product ADP is fed back via ANT to the matrix for rephosphorylation resulting in an overall lowering of the apparent Km of ADP for oxidative phosphorylation (38). It is conceivable that microcompartmentation of mtCK and ANT is also responsible for the observed MPT inhibition by Cr and CyCr (48). To test this idea, we measured MPT pore opening in liver mitochondria from control mice lacking mtCK, but with exogenously added recombinant human brain-type dimeric CK (BB-CK). Under the conditions used, especially at pH 7.4, this cytosolic isoform does not bind to mitochondrial outer membranes (Fig. 5A). The amount of BB-CK enzyme activity added in these experiments was equivalent to that found (based on mtCK activity) within mitochondria of transgenic liver-mtCK mice. Under these conditions, no protection of MPT pore opening of control mitochondria with externally added CK by any of the CK substrates was seen, even in the presence of Mg^{2+} (Fig. 5B, shown only for Cr). By contrast, with the same amount of ubiquitous mtCK (the isoform expressed in the liver mitochondria of the transgenic mice), significant binding of the enzyme to the surface of mitochondria was observed (Fig. 5A). However, even with mtCK bound to the outside of mitochondria, no noticeable MPT protection by Cr was observed (Fig. 5C) as was also the case for BB-CK (Fig. 5B). Even increasing the total amount of mtCK by ten-fold in the medium did not bring about detectable MPT protection by Cr, although absolute binding of mtCK to the mitochondrial surface increased by more than three-fold under these conditions (Fig. 5A). Thus, addition of CK externally or even mtCK bound to the outer membrane were not able to confer significant protection against MPT.

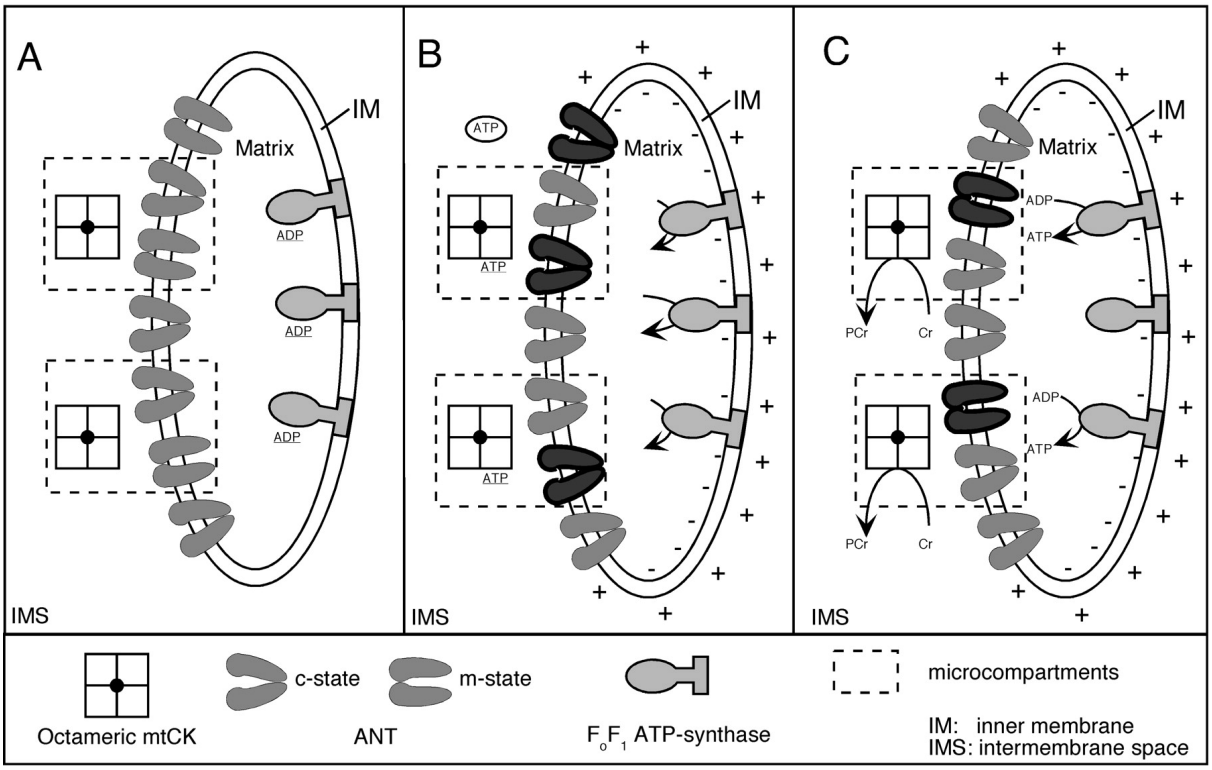

FIGURE 6 **Model for MPT protection by Cr**. For clarity, the outer mitochondrial membrane has been omitted from the scheme and only the inner membrane is shown. *Panel A* Isolated mitochondria (deenergized). Matrix ATP/ADP ratio is expected to be low and ADP presumably mostly enzyme-bound (e.g. to the ATP synthase, *underlined*). ANT-dimers are in m- as well as c-conformation. *Panel B* Energization (symbolized by *plus* and *minus* signs of membrane potential). Matrix ATP/ADP ratio is expected to be high. Formerly bound ADP is now converted to ATP (*arrows*). ATP is transported via ANT to the IMS. Some ATP (*underlined*) is trapped by octameric mtCK (symbolized as *squares*), another fraction of ATP (*encircled*) is diluted into the medium. Some of the ANT-dimers did change from m- to c-conformation (*outlined, dark*). *Panel C* In the presence of creatine, conversion of Cr to PCr by mtCK takes place. ADP produced in mtCK/ANT microcompartments is transported back into the matrix and is rephosphorylated there by the ATP synthase. Some ANT-dimers have now switched from c- to m-conformation (*outlined, dark*). The hatched rectangles in *A-C* outline mtCK-ANT-assemblies forming functionally coupled microcompartments. Further details are given in the text.

Discussion

The present study was carried out to provide a mechanistic basis for the observation that certain substrates of creatine kinase efficiently inhibit the MPT (17). Because opening of the MPT pore appears to be causally related to cell death in several models (18-24), these studies may provide the basis for novel cytoprotective drugs. We have measured MPT pore opening in isolated mitochondria by the convenient swelling assay in sucrose-based medium and under different conditions, and compared the response of transgenic mitochondria containing active or inactive CK with that of control mitochondria to which CK was added externally. These experiments revealed a major difference in MPT behavior. With liver mitochondria from transgenic mice, expressing mtCK in these organelles (39), but not with liver mitochondria from wild-type mice, we have observed MPT inhibition (based on measurements of uncoupled respiration) in the presence of Cr or CyCr in an earlier study (17). Here, using mitochondrial-swelling assays, we show that MPT protection by these CK substrates critically depends on two key factors.

The most striking new findings from the present study are that Cr-protection of MPT requires magnesium, an essential cofactor for the CK reaction, and active mtCK at its proper location in the IMS. These observations together with the finding of net PCr production by isolated mitochondria, even in the absence of exogenous adenine nucleotides, suggest that endogenous adenine nucleotides are permanently cycling via ANT between matrix and IMS, if CK substrates are present that can efficiently be phosphorylated. This is the case for Cr and CyCr but not for GPA.

The consequences for MPT modulation by CK substrates could then be explained by the influence of nucleotide binding to ANT and conformational changes of this carrier (40,41). To visualize this (see Fig. 6), during adenine nucleotide exchange, the common transport site for ADP and ATP on the ANT faces alternatively the matrix (m) and Creatine kinase substrates and mitochondrial permeability transition 15 cytosolic (c) side (42,43). Accordingly, the ANT changes its conformation between m- and c-state, if conditions allow adenine nucleotide transport. In the absence of a proton motive force, the matrix ATP/ADP ratio of isolated mitochondria is low (40,44) and it is entirely conceivable that adenine nucleotides are enzyme-bound (e.g. to the ATP synthase). Certain (unknown) fractions of transport units (shown as ANT-dimers in Fig. 6, see also ref. (45)) are locked either into the m- or c-state (Fig. 6A). Upon energization, the matrix ATP/ADP ratio rises and ATP will be liberated and transported to the IMS. There, ATP either gets diluted in the medium or is trapped by mtCK (Fig. 6B). As a consequence, more transport units would now be in the c-state than before energization. Under these conditions, MPT pore opening should be favored, as seen with no CK substrate present. This situation is likely to be similar to the effect of the strong ANT inhibitor, atractyloside, known to stabilize the c-conformation and being an inducer of the MPT (46). If, however, Cr (or CyCr) is present, the trapped ATP will be transphosphorylated and the generated ADP transported to the matrix for rephosphorylation (Fig. 6C). As this process proceeds, the time-averaged fraction of transport units occupied with adenine nucleotides and being in the m-state is expected to be higher and, therefore, conditions for MPT pore opening are less favorable. In the presence of GPA, the ATP delivered to the active site of mtCK is not used up because GPA is not phosphorylated by mtCK (29). Consequently, the ANT is largely locked into the c-conformation, again favoring MPT pore opening. At present, it is still unclear how ANT conformation would affect the MPT. An indirect effect, e.g. via the surface potential, has been proposed (41,47). Note the emphasis on microcompartmentation and functional coupling of mtCK and ANT as an essential part of the model shown in Fig. 6. This is corroborated by the fact that similar amounts of either cytosolic BB-CK or mtCK added externally to the outside of control mitochondria, as is present as mtCK in transgenic mitochondria, did not result in any significant Cr protection of MPT.

We have clearly demonstrated that in the presence of Cr, by measuring net production of PCr, oxidative phosphorylation proceeds even without adding external adenine nucleotides, although at a slow rate only. Nevertheless, besides the effect on the conformational state of the ANT, an additional contribution to MPT protection by Cr could be caused by variation of the matrix ATP/ADP ratio in favor of ADP (25), which is a strong MPT inhibitor (40,44). On the other hand, the accumulating PCr is not believed to exert MPT inhibition (e. g., via the membrane potential) as we have shown earlier (17).

As mtCK functionally interacts with ANT at mitochondrial contact sites, as well as along the cristae membranes (36), a second possibility is that the two proteins may interact, and that modulation by CK substrates may affect pore formation by the ANT. The known property of ANT to form an unspecific pore showing some of the characteristics of the MPT pore (48-50) in *in vitro* reconstituted systems has been taken by several authors as evidence that the ANT represents the central element of an MPT pore complex (51-59). However, it should be considered that pore formation is not unique to ANT, but has also been described for other members of the mitochondrial carrier family (60,61). Furthermore, mitochondria from ANT-deficient yeast still exhibit a mitochondrial multiconductance channel (MCC), which is believed to be the electrophysiological counterpart of the MPT (62). A recent study of Linder *et al*. (63), showing that arginine modification has pronounced influences on MPT pore opening that are not modulated by the ANT ligands atractyloside and bongkrekic acid, further

questions a direct involvement of the ANT in pore formation. Finally, the structural interactions between mtCK and ANT, which were postulated in models of mitochondrial contact sites (64), still await experimental proof.

Creatine has been shown to exert strong protective effects against glutamate and beta-amyloid toxicity and energetic insults in neuronal cell cultures (9,10), as well as in several animal models of neurodegenerative diseases (11-13). It is interesting to note that in the study of Brustovetsky and co-workers (10), Cr did not prevent MPT in isolated brain mitochondria, despite protection from energetic insults in cultured striatal neurons. This could be either due to the low magnesium concentration (0.5 mM) used by these authors in their assays, or to the only weak coupling of the CK reaction to oxidative phosphorylation in these particular preparations. For the latter, however, no data were provided. In any case, both interpretations are fully in line with the model concerning the effect of Cr on MPT as proposed above. Thus, the beneficial effects of Cr seen in animal disease models can be attributed to at least two mechanisms that are ultimately linked by the PCr shuttle: 1) ATP levels and local ATP/ADP ratios in the cytosol are kept high, thus sustaining membrane ion-gradients and other vital energy consuming processes at a highly efficient level, and 2), mitochondria are protected from MPT pore opening via functional coupling of the mtCK reaction to oxidative phosphorylation.

Taken together, our findings offer important clues on MPT regulation by mitochondrial ADP phosphorylation, and may have interesting implications for the design of creatine analogs to treat patients with neurodegenerative diseases. In order to fully exploit the advantages of the PCr shuttle for cell survival, such analogs would have to be substrates for CK in both, the forward and reverse direction of the reaction.

References

1. Bessman, S. P., and Geiger, P. J. (1981) *Science* 211, 448-452
2. Wallimann, T., Wyss, M., Brdiczka, D., Nicolay, K., and Eppenberger, H. M. (1992) *Biochem J* 281, 21-40
3. Wallimann, T. (1994) *Curr Biol* 4, 42-46
4. Saks, V. A., Ventura-Clapier, R., and Aliev, M. K. (1996) *Biochim Biophys Acta* 1274, 81-88
5. Ventura-Clapier, R., Kuznetsov, A., Veksler, V., Boehm, E., and Anflous, K. (1998) *Mol Cell Biochem* 184, 231-247
6. Kraft, T., Hornemann, T., Stolz, M., Nier, V., and Wallimann, T. (2000) *J Muscle Res Cell Mot* 21, 691-703
7. Wallimann, T., and Hemmer, W. (1994) *Mol Cell Biochem* 133/134, 193-220
8. Kaldis, P., Kamp, G., Piendl, T., and Wallimann, T. (1997) *Adv Develop Biol* 5, 275-312
9. Brewer, G. J., and Wallimann, T. W. (2000) *J Neurochem* 74, 1968-1978
10. Brustovetsky, N., Brustovetsky, T., and Dubinsky, J. M. (2001) *J Neurochem* 76, 425-434
11. Matthews, R. T., Yang, L., Jenkins, B. G., Ferrante, R. J., Rosen, B. R., Kaddurah-Daouk, R., and Beal, M. F. (1998) *J Neurosci* 18, 156-163
12. Klivenyi, P., Ferrante, R. J., Matthews, R. T., Bogdanov, M. B., Klein, A. M., Andreassen, O. A., Mueller, G., Wermer, M., Kaddurah-Daouk, R., and Beal, M. F. (1999) *Nat Med* 5, 347-350
13. Matthews, R. T., Ferrante, R. J., Klivenyi, P., Yang, L., Klein, A. M., Mueller, G., Kaddurah-Daouk, R., and Beal, M. F. (1999) *Exp Neurol* 157, 142-149
14. Pulido, S. M., Passaquin, A. C., Leijendekker, W. J., Challet, C., Wallimann, T., and Ruegg, U. T. (1998) *FEBS Lett* 439, 357-362
15. Passaquin, A. C., Renard, M., Kay, L., Challet, C., Mokhtarian, A., Wallimann, T., and Ruegg, U. T. (2002) *Neuromuscul Disord* 12, 174-182
16. Tarnopolsky, M. A., and Beal, M. F. (2001) *Ann Neurol* 49, 561-574 17. O'Gorman, E., Beutner, G., Dolder, M., Koretsky, A. P., Brdiczka, D., and Wallimann, T. (1997) *FEBS Lett* 414, 253-257
18. Pastorino, J. G., Simbula, G., Gilfor, E., Hoek, J. B., and Farber, J. L. (1994) *J Biol Chem* 269, 31041-31046
19. Ankarcrona, M., Dypbukt, J. M., Bonfoco, E., Zhivotovsky, B., Orrenius, S., Lipton, S. A., and Nicotera, P. (1995) *Neuron* 15, 961-973
20. Castedo, M., Hirsch, T., Susin, S. A., Zamzami, N., Marchetti, P., Macho, A., and Kroemer, G. (1996) *J Immunol* 157, 512-521
21. Marchetti, P., Hirsch, T., Zamzami, N., Castedo, M., Decaudin, D., Susin, S. A., Masse, B., and Kroemer, G. (1996) *J Immunol* 157, 4830-4836
22. Scorrano, L., Petronilli, V., Di Lisa, F., and Bernardi, P. (1999) *J Biol Chem* 274, 22581-22585
23. Jacotot, E., Ravagnan, L., Loeffler, M., Ferri, K. F., Vieira, H. L., Zamzami, N., Costantini, P., Druillennec, S., Hoebeke, J., Briand, J. P., Irinopoulou, T., Daugas, E., Susin, S. A., Cointe, D., Xie, Z. H., Reed, J. C., Roques, B. P., and Kroemer, G. (2000) *J Exp Med* 191, 33-46
24. Tafani, M., Schneider, T. G., Pastorino, J. G., and Farber, J. L. (2000) *Am J Pathol* 156, 2111-2121
25. Kay, L., Nicolay, K., Wieringa, B., Saks, V., and Wallimann, T. (2000) *J Biol Chem* 275, 6937-6944
26. Eder, M., Schlattner, U., Becker, A., Wallimann, T., Kabsch, W., and Fritz-Wolf, K. (1999) *Protein Sci* 8, 2258-2269
27. Eder, M., Fritz-Wolf, K., Kabsch, W., Wallimann, T., and Schlattner, U. (2000) *Proteins* 39, 216-225
28. Wallimann, T., Turner, D. C., and Eppenberger, H. M. (1975) *J Cell Biol* 75, 297-317
29. Clark, J. F., Khuchua, Z., Kuznetsov, A. V., Vassil'eva, E., Boehm, E., Radda, G. K., and Saks, V. (1994) *Biochem J* 300, 211-216
30. Boehm, E. A., Radda, G. K., Tomlin, H., and Clark, J. F. (1996) *Biochim Biophys Acta* 1274, 119-128
31. Fontaine, E., Ichas, F., and Bernardi, P. (1998) *J Biol Chem* 273, 25734-25740
32. Fontaine, E., Eriksson, O., Ichas, F., and Bernardi, P. (1998) *J Biol Chem* 273, 12662-12668
33. Gross, M., and Wallimann, T. (1993) *Biochemistry* 32, 13933-13940
34. Bernardi, P., Veronese, P., and Petronilli, V. (1993) *J Biol Chem* 268, 1005-1010
35. Saks, V. A., Veksler, V. I., Kuznetsov, A. V., Kay, L., Sikk, P., Tiivel, T., Tranqui, L., Olivares, J., Winkler, K., Wiedemann, F., and Kunz, W. S. (1998) *Mol Cell Biochem* 184, 81-100
36. Wegmann, G., Huber, R., Zanolla, E., Eppenberger, H. M., and Wallimann, T. (1991) *Differentiation* 46, 77-87
37. Schlattner, U., Forstner, M., Eder, M., Stachowiak, O., Fritz-Wolf, K., and Wallimann, T. (1998) *Mol Cell Biochem* 184, 125-140
38. Saks, V. A., Kuznetsov, A. V., Khuchua, Z. A., Vasilyeva, E. V., Belikova, J. O., Kesvatera, T., and Tiivel, T. (1995) *J Mol Cell Cardiol* 27, 625-645
39. Miller, K., Sharer, K., Suhan, J., and Koretsky, A. P. (1997) *Am J Physiol* 272, C1193-C1202
40. Halestrap, A. P., Woodfield, K. Y., and Connern, C. P. (1997) *J Biol Chem* 272, 3346-3354
41. Bernardi, P. (1999) *Physiol Rev* 79, 1127-1155
42. Klingenberg, M. (1985) in *The Enzymes of Biological Membranes* (Martonosi, A. N., ed) Vol. 4, pp. 511-553, Plenum, New York
43. Fiore, C., Trezeguet, V., Le Saux, A., Roux, P., Schwimmer, C., Dianoux, A. C., Noel, F., Lauquin, G. J., Brandolin, G., and Vignais, P. V. (1998) *Biochimie* 80, 137-150
44. Novgorodov, S. A., Gudz, T. I., Brierley, G. P., and Pfeiffer, D. R. (1994) *Arch Biochem Biophys* 311, 219-228
45. Huang, S. G., Odoy, S., and Klingenberg, M. (2001) *Arch Biochem Biophys* 394, 67-75
46. Zoratti, M., and Szabo, I. (1995) *Biochim Biophys Acta* 1241, 139-176

47. Bernardi, P., Colonna, R., Costantini, P., Eriksson, O., Fontaine, E., Ichas, F., Massari, S., Nicolli, A., Petronilli, V., and Scorrano, L. (1998) *Biofactors* 8, 273-281
48. Brustovetsky, N., and Klingenberg, M. (1996) *Biochemistry* 35, 8483-8488
49. Ruck, A., Dolder, M., Wallimann, T., and Brdiczka, D. (1998) *FEBS Lett* 426, 97-101
50. Brustovetsky, N., Tropschug, M., Heimpel, S., Heidkamper, D., and Klingenberg, M. (2002) *Biochemistry* 41, 11804-11811
51. Woodfield, K., Ruck, A., Brdiczka, D., and Halestrap, A. P. (1998) *Biochem J* 336, 287-290
52. Crompton, M., Virji, S., and Ward, J. M. (1998) *Eur J Biochem* 258, 729-735
53. Beutner, G., Ruck, A., Riede, B., and Brdiczka, D. (1998) *Biochim Biophys Acta* 1368, 7-18
54. Crompton, M. (1999) *Biochem J* 341, 233-249
55. Bauer, M. K., Schubert, A., Rocks, O., and Grimm, S. (1999) *J Cell Biol* 147, 1493-1502
56. Brenner, C., Cadiou, H., Vieira, H. L., Zamzami, N., Marzo, I., Xie, Z., Leber, B., Andrews, D., Duclohier, H., Reed, J. C., and Kroemer, G. (2000) *Oncogene* 19, 329-336
57. Zamzami, N., and Kroemer, G. (2001) *Nat Rev Mol Cell Biol* 2, 67-71
58. Belzacq, A. S., Vieira, H. L., Kroemer, G., and Brenner, C. (2002) *Biochimie* 84, 167-176
59. Halestrap, A. P., McStay, G. P., and Clarke, S. J. (2002) *Biochimie* 84, 153-166
60. Dierks, T., Salentin, A., Heberger, C., and Kramer, R. (1990) *Biochim Biophys Acta* 1028, 268-280
61. Indiveri, C., Tonazzi, A., Dierks, T., Kramer, R., and Palmieri, F. (1992) *Biochim Biophys Acta* 1140, 53-58
62. Lohret, T. A., Murphy, R. C., Drgon, T., and Kinnally, K. W. (1996) *J Biol Chem* 271, 4846-4849
63. Linder, M. D., Morkunaite-Haimi, S., Kinnunen, P. K., Bernardi, P., and Eriksson, O. (2002) *J Biol Chem* 277, 937-942
64. Brdiczka, D., Beutner, G., Ruck, A., Dolder, M., and Wallimann, T. (1998) *Biofactors* 8, 235-242
65. Wallimann, T., Schlosser, T., and Eppenberger, H. M. (1984) *J Biol Chem* 259, 5238-5246

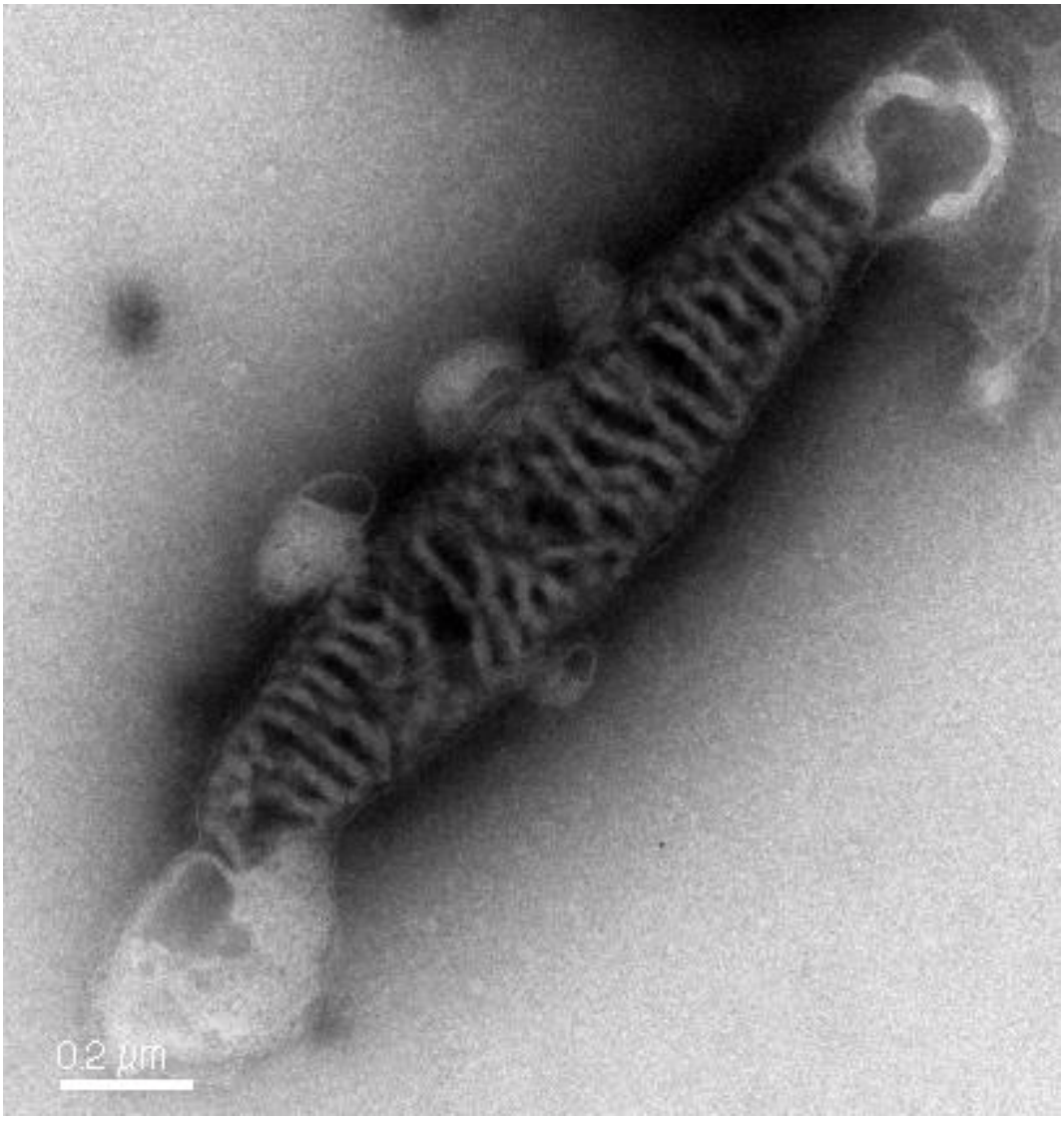

Heart mitochondriam treated with digitonin, Oliver Speer, October 2000

Chapter 4

MITOCHONDRIAL CREATINE KINASE INDUCES CONTACT SITES

CHARACTERIZATION OF TRANSGENIC MOUSE LIVER EXPRESSING MITOCHONDRIAL CREATINE KINASE

Oliver Speer[‡§], Ove Eriksson[§], Nils Beck[§], Dieter Brdiczka[#], and Theo Wallimann[‡]

[‡] Swiss Federal Institute Of Technology, ETH-Zürich, Institute of Cell Biology, ETH-Hönggerberg, CH-8093 Zürich, Switzerland,

[§] Helsinki Biophysics and Biomembrane Group, Institute of Biomedicine, University of Helsinki, FIN-00014 Finland,

and [#] Department of life sciences, University of Konstanz, Germany.

Prepared for submission

Acknowledgements – We thank Dr. Alan P. Koretsky (NIH, Bathesda, USA) for providing transgenic mt_uCK mice. We thank doctors Michael Hess, Heinz Gross, Peter Tittmann and Roland Wessicken for technical support with electron microscopy.

The Swiss National Foundation and the Swiss foundation for research on muscle diseases support T.W. and O.S.. The Rector of the University of Helsinki, Sigrid Juselius Foundation, Finska Läkaresällskapet and Perklén Memorial Foundation funds all to O.E. are thankfully acknowledged.

Abbreviations: ANT, adenine nucleotide translocator; COX, cytochrome oxidase; MIM, mitochondrial inner membrane; MOM, mitochondrial outer membrane; mt_uCK, ubiquitous mitochondrial creatine kinase; VDAC, voltage-dependant anion channel

Abstract

Mitochondrial creatine kinase is found in contact sites between mitochondrial inner and outer membrane, and also between cristae membranes (12, 13, 33, 40). Overexpression of ubiquitous mitochondiral creatine kinase (mt_uCK) in murine liver, containing no mtCK in wild type animals, increased the number of contact sites between mitochondrial inner and outer membranes at least three fold, as seen by standard electron microscopy. Immuno electron microscopy revealed the location of mt_uCK within contact sites as well as in inter cristae inclusions. Mitochondrial disintegration monitored by $OD_{540\ nm}$ after digitonin addition decreased to baselinelevels in the presence of over-expressed mt_uCK. Negative staining of digitonin treated mitochondria under iso-osmotic conditions revealed the destruction of wild type mitochondria, whereas mt_uCK-containing liver mitochondria showed a broken outer membrane but no other visible changes in mitochondrial structure. By detergent resistant membrane floating, mt_uCK-containing micro-compartments could be isolated. Besides mt_uCK, those vesicles contained also the outer membrane voltage dependant anion channel (VDAC), the inner membrane adenine nucleotide translocator (ANT), as well as cytochrome oxidase (COX). We conclude that mt_uCK is sufficient to induce contact site formation in mitochondria by cross-linking mitochondrial membranes, leading to an increased stability of mitochondrial structure. Phospholips, VDAC, ANT, as well as parts of the respiratory chain form the mt_uCK containing contact sites. We suggest that such detergent resistant micro-comparments might contain the entire mtiochondrial permeability transition pore complex.

Introduction

Cells with high and fluctuating energy metabolism usually co-express a cytosolic and a mitochondrial creatine kinase isoenzyme (CK, EC 2.7.3.2). Cytosolic CK transphosphorylates the high-energy phosphocreatine (PCr), used as an energy-storage and -transport metabolite, to ADP, thereby restoring the cellular ATP-pool (7, 61, 64, 67, 68). Since the concentrations of ATP and ADP control many metabolic processes, these parameters have to be kept constant within their physiological range. At rest, ATP and ADP are present in the 3–5 mM range and 10–30 µM range, respectively. At times of high workload, the cell can immediately regenerate ATP, as it is consumed, from the PCr pool (30–40 mM) via the action of creatine kinase. This so called temporal energy buffering provided by the CK system leads to increased metabolic capacity (30, 48, 57). Furthermore, by using the CK system, the cell is able to provide facilitated diffusion of high-energy phosphate from sites of energy production to sites of energy demand thereby creating spatial buffering. This concept is especially important for polar cells, e.g. spermatozoa and photoreceptor cells where diffusion distances from mitochondria to sites of energy consumption are long (61) (30, 62). To exert these functions in an optimized manner, the CK system is compartmentalized. There are dimeric CK isoforms, which are exclusively found in the cytosolic compartment, whereas mitochondrial CK (mtCK) isoforms are strictly localized within the intermembrane and christae space of mitochondria (28, 68) (29). In contrast to the cytosolic isoforms, which are always dimeric, mtCKs can occur as dimers and octamers, the latter being built up by association of two dimers into instable tetramers, which then react in a fast association step to form rather stable octamers (26). The cytosolic CK isoforms mainly uses PCr to reproduce ATP at sites of high-energy consumption, such as the myofibrillar actomyosin ATPase in muscle (63), the Ca^{2+}-ATPase of the sarcoplasmic reticulum (45) or the rods of photoreceptor cells (27).

In conjunction with the adenine nucleotide translocator the mitochondrial CK isoform is mainly responsible for the conversion of mitochondrial ATP into PCr, which is exported into the cytosol via outer membrane voltage dependant anion channel (VDAC). PCr is then used at sites of high-energy demand by the reverse CK reaction yielding ATP and Cr. This exchange of PCr/Cr and ATP/ADP between the cytosol and mitochondria is referred to as ‘phosphocreatine shuttle’ (7, 6) or PCr circuit (64).

The mitochondrial envelope can form contact sites, a close superposition of the mitochondrial outer membrane (MOM) and the mitochondrial boundary inner membrane (MIM). Contact sites are dynamic structures and their formation correlates with activity of oxidative phosphorylation (32, 37) and they are regulated by [ADP] (18). Mitochondrial contact sites are enriched in mtCK, andenyl nucleotide translocator (ANT) and VDAC (1, 8-10, 33). VDAC is responsible for the permeability of the outer mitochondrial membrane (2-4) but can adopt a low conductance cation-selective state, which can account for a metabolic compartmentation of nucleotides in the inter-membrane space, especially at the contact sites (3). Extra-mitochondrial creatine, which can permeate cation-selective VDAC, effectively stimulates mitochondrial phosphocreatine synthesis via mtCK and finally oxidative phosphorylation *in vitro* (46, 47) and in vivo (31). The physical interaction between mtCK and VDAC was shown *in vitro* (49).

It was proposed that contact sites operate as micro-compartments or multi-enzyme complexes for energy export (11, 12). Such a compartment would confer a thermodynamic advantage to the mtCK reaction, since products of the mtCK reaction, phosphocreatine and ADP, are constantly removed via VDAC and ANT (14). The micro-compartment model suggests that mtCK, which is in general only attached to the inner mitochondrial membrane, binds in contact sites to the outer mitochondrial membrane as well. It should be noted, however, that mtCK is not a prerequisite for contact site formation, which also occurs in tissues exempt from mtCK, e.g. the liver. The micro-compartment-model of mtCK is strongly supported by *in situ* localization of mtCK showing mtCK along the cristae membranes and between inner and outer membranes (66) as well as by *in vitro* studies demonstrating that mtCK interacts not only with inner but also with outer mitochondrial membrane preparations

(43) and, most importantly, is able to bridge two membranes (44). By this bridging capability, mtCK is well suited for contact site formation.

Interference with the Cr / CrP circuit can lead to pathologic changes in the cell. For example in Cr depleted animal models, mtCK-rich crystalline mitochondrial inclusion bodies (39) (40) are formed. In addition, an increase in aerobic capacity (54), an increase in the glucose transporter (GLUT4) expression (42), a decrease in AMP aminase activity (41), as well as an increase in slow twitch fibres in skeletal muscle with a subsequent shift in the expression of fast to slow myosin isoforms (42) have been shown. Emphasising the importance of the Cr /CrP system, patients suffering form miotchondrial myopathies (58-60) show enlarged mitochondria with paracrystaline inclusion bodies, enriched with sarcomeric mtCK. Those mitochondria are found predominantly in "ragged red fibres" seen in muscle biopsies from these patients, as well as in HIV patients treated with Zidovudine (20).

Furthermore, it is discussed that mtCK plays a role for preventing cytochrome C release from mitochondria during the initiation of apoptosis (12, 23, 38). It was shown that neurons, over-stimulated by different proapototic factors could be protected by creatine supplementation (15). However it is still not clear whether mtCK interacts in a molecular way with other molecules or whether mtCK may have other impacts on the cellular energy metabolism. Consequently a model system of mitochondria from the same tissue, with and without mtCK should open a new way to collect more information. One possible model was liver, normally not expressing mtCK, from transgenic mice, over-expressing ubiquitus mtCK (mt_uCK). Alan Koretsky and coworkers produced such transgenic animals (36). In fact the presence of mt_uCK in mitochondria from such transgenic liver together with creatine reduced the mPT inducing effects of calcium and atractylate on wild type mitochondria, which do not contain mt_uCK (21, 38).

In this work, morphological changes due to the presence of mt_uCK in liver mitochondria were characterised. Therefore liver tissue from transgenic and control mice were investigated by standard electron microscopy procedures. After immuno-gold decoration it seems clear that mt_uCK is located between inner and outer mitochondrial membranes, but also forms rather big inclusions inside the cristae. Further, the impact of mt_uCK on the overall mitochondrial structure and resistance to digitonin, which permeabilises the outer mitochondrial membrane independent of the permeability transition, is demonstrated: under those conditions liver mitochondria containing mt_uCK did not disintegrate. We conclude that over-expressed mt_uCK located at the expected places within mitochondria that are between MOM and MIM, induces contact sites. Finally since certain proportions of mt_uCK is located inside cristae, and thus cross-links the MIM, it thereby contributes to enhancing mitochondrial structure, integrity and stability.

Material and Methods

Animals

Transgenic mice, which over-express mt_uCK in liver, were kindly provided by Alan Koretsky (NIH). Those mice carry a mt_uCK gene under a liver specific promotor and enhancer regions from the mouse transthyretin gene (36).

Western blotting

Extracts were separated in 10-12 % polyacrylamide SDS-gels and trans-blotted onto nitrocellulose membranes (Schleicher & Schuell, Germany; Geneworks, Australia). Membranes were blocked with 5 % fat-free milk powder in TBS(T) buffer (150 mM NaCl, 25 mM Tris-HCl, pH 7.4, [0.05% Tween]) for 1 hr at room temperature. After washing for 30 min, membranes were incubated with 1:1.000 to 5,000 diluted anti-CrT peptide antibody in TBS buffer for 2 hrs at room temperature. After washing with TBS(T) buffer, the blots were incubated again with a 1:10,000 dilution of goat HRP-conjugated anti-rabbit secondary antibody (Amersham Pharmacia Biotech, Sweden; Silenus, Australia). The immunoreactive bands were visualized using the Renaissance Western Blot Chemiluminescence Reagent Plus Kit (NEN, USA).

Fixation of liver tissue and immunodecoration for electron microscopy

Liver tissue was fixed during vascular perfusion with 2% paraformaldehyde, 2% Glutaraldehyde, 2% DMSO and 0.1 % Acrolein in PBS. Tissue slices were stored at room temperature in the same fixative. After 2h, they were brought to 0.3 M Sucrose in PBS. Tissue was postfixed with 1% tannic acid, then embedded in sucrose-polyvinylpyrrolidone over night. The embedded tissue was sectioned at –100°C. Tissue sections were blocked in 1% FCS/PBS, decorated with antibody against mt_uCK or pre immune serum (PIS) (1:200 diluted serum) for 1h and then washed 3 times 10min in PBS. Sections were stained with 10 nm colloidal gold-conjugated protein A for 1h. The primary antibody / Protein A complexes were fixed with 4% Formaldehyde and 1% Glutaraldehyde and washed again in PBS. The sections were finally embedded in methyl-cellulose and post stained with 1% uranyl acetate. The preparations were examined in a JEOL s100 TEM at 80kV.

Tissue extracts and isolation of mitochondria

Mice (3-4 month of age) were killed by a short exposure to carbon dioxide, followed by cervical dislocation. Liver, brain and cardiac muscle was taken and immediately transferred to ice-cold HEPES-sucrose buffer containing 250 mM sucrose, 10 mM HEPES-HCl pH 7.4, 0.5 % BSA (essentially free of fatty acids) and 1 mM EDTA and homogenized by a teflon/glass potter (Braun-Melsungen, Germany). The homogenate was centrifuged for 10 min at 700 x g to remove heavy debris as platelets, as well as nuclei. An aliquot from the supernatant was taken as total tissue extract for further analysis. The supernatant was centrifuged for 10 min at 7,000 x g. The pellet containing mitochondria was resuspended in 30 ml 250 mM sucrose, 10 mM Tris/HCl pH 7.4, 100 µM EGTA, 25 % Percoll^{TM} (Amersham Pharmacia Biotech, Sweden) and centrifuged for 35 min at 100,000 x g. Percoll^{TM} fractions containing highly purified mitochondria were washed twice with 250 mM sucrose, 10 mM HEPES-HCl pH 7.4, 100 µM EGTA by centrifugation at 7,000 x g for 10 min. Washed mitochondria were then recovered from the pellet and resuspended in 200 µl of the washing buffer.

Disintegration measurements

Mitochondrial protein concentration in all assays was kept at 0.5 mg/ml. Mitochondria were diluted in the washing buffer. Mitochondrial disintegration was measured by adding 100µg Digitonin / mg mitochondrial protein to mitochondrial suspension and recorded in a UV4 UV/VIS spectrometer (Unicam) connected to a computer. Traces were recorded at 540

nm and data points were acquisited every 30 seconds using Visioṇs Software (version 3.10, Unicam Ltd.). Cuvettes containing the mitochondrial suspension were always thermostated to 25 °C. After the assays, mitochondria were layered on nickel grids suitable for electron microscopy, contrasted with 2% ammonium-molybdate (iso-osmotic), air-dried, visualized and recorded with a Jeol 200 transmission electron microscope at 80 kV.

Preparation of mt_uCK containing microdomains

Isolated liver and kidney mitochondria were diluted with chilled washing buffer to 20 mg/ml mitochondrial protein, adding 0.75 % Triton X-100 to final concentration. Mitochondria were dissolved on ice in a glass/glass homogeniser. The Triton homogenate was diluted resulting in 40 % Sucrose and 10 mg/ml mitochondrial protein in washing buffer. This 40 % sucrose solution was layered under a linear sucrose gradient (38%- 15%) and centrifuged for at least 20h at 100'000 x g at 4°C. The resulting gradient was fractionated into 500 µl aliquots. After the protein determination, 20 µg protein from each sample was precipitated by standard TCA precipitation, dissolved in SDS buffer, and processed for Western blotting (see above).

Results

Mitochondrial creatine kinase plays a role in regulation of mitochondrial permeability transition (9, 10, 12, 21, 35, 38). In contrast to wild type, mitochondria from transgenic animals that express mtCK in their livers do not swell after calcium addition (21, 38). We were interested whether mtCK also has an influence on the structural integrity of mitochondria. To compare mitochondria with and without mtCK we took transgenic mice, overexpressing ubiquitous mtCK (mt_uCK) in liver as a model.

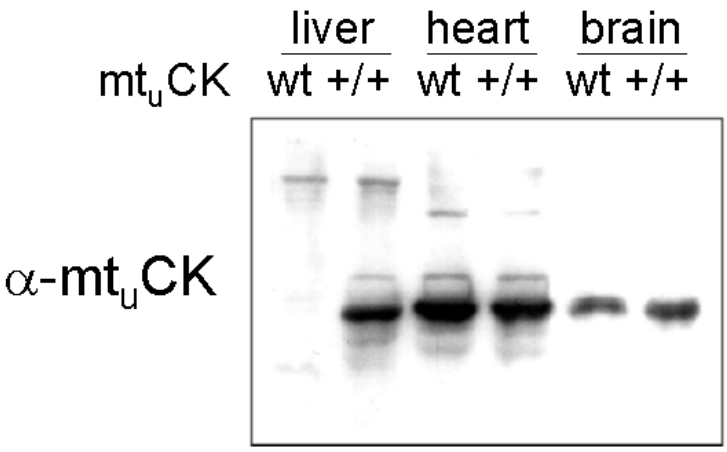

Figure 1 **Western blot of mouse tissues**. Liver, heart and brain from wild type mice (wt) and from mice expressing mt_uCK in liver (+/+) were homogenized. Protein extracts were separated by SDS PAGE and transferred to nitro-cellulose membranes. mt_uCK was detected by polyclonal rabbit anti chicken serum. Primary antibodies were detected by secondary anti-rabbit IgG antibodies coupled to horseradish peroxidase and were visualized by ECL kit (Amersham). Transgenic liver (+/+) was expressing mt_uCK comparable to heart or brain. Note, that in wt liver no mt_uCK was detected.

To test the over-expression model, the expression of mt_uCK in liver of transgenic mice was first tested by Western blots. As seen in figure 1, in wild type liver there was no detectable mt_uCK, however, in liver from transgenic mice high amounts of mt_uCK were expressed, confirming earlier results (36). Western Blot analysis from different tissues show that the expression level of mt_uCK in transgenic liver was approximately equivalent to the expression mtCK in tissues like muscle and neurons (figure 1).

Over-epressed mt_uCK induces contact sites in vivo

To gain more information on a sub-cellular level about the expression and localization of mt_uCK and its impact in mouse liver, tissue was fixed, embedded, cut and stained after standard procedures. Electron microscopical studies revealed surprisingly clear-cut differences in the general morphological appearance between mitochondria from control and transgenic liver tissue. The transgenic tissue contained a lot of mitochondria with changed morphology.

In contrast to wild type (figure 2A), the lumen of one or two cristae in a significant proportion of mitochondria from transgenic liver was electron dense and immensely enlarged (figure 2B). Furthermore, we observed that the number of contact points where the MOM and MIM were in close vicinity, forming contact sites (18), were significantly increased in comparison to mitochondria from wild type liver (figure 2C). To quantify this observation, the circumference of mitochondrial sections from both animal groups was measure and the number of clearly discernible contact sites was counted per µm. The number of contact sites in liver mitochondria containing mt_uCK was 3 times higher than in wild type liver mitochondria (figure 2D). We claim, that the presence of mtCK is inducing the formation of contact sites in vivo. We have shown elsewhere, that over-expressed mtCK is enzymatically active and directly converts creatine into phosphocreatine which is then expelled into the medium (21). Furthermore over-expressed mt_uCK inhibits the mitochondrial permeability transition (21, 38).

To determine, whether mt_uCK is responsible for forming the inclusions inside cristae (figure 2A) and whether mt_uCK is indeed directly localized also between MOM and MIM within the contact sites, as observed in the transgenic liver mitochondria (figure 2B), we performed an immuno-decoration of cryo-fixed tissue samples. In fact, the electron dense inclusions inside cristae were strongly labeled with mt_uCK antibody (figure 3). Also the inter-membrane space between MOM and MIM was significantly decorated with gold particles (figure 3), whereas the control with the pre-immune sera (PIS) showed only few gold particles.

These data coroborate, that mt_uCK, if over-expressed is located in the expected mitochondrial compartments: between MOM and MIM, but also forms dramatic alterations by occupying the intra-cristae lumen. However, it seems that these cristae inclusions do not form regular mtCK-crystals as it was observed in muscular myopathies or after creatine depletion (39, 40, 56). This was determined by Furrier transformation analysis of such inclusions observed here (data not shown). The mt_uCK inclusions shown in this work do not present with the typical furrier scattering known from crystalline mt_uCK inclusions in those cases reported above.

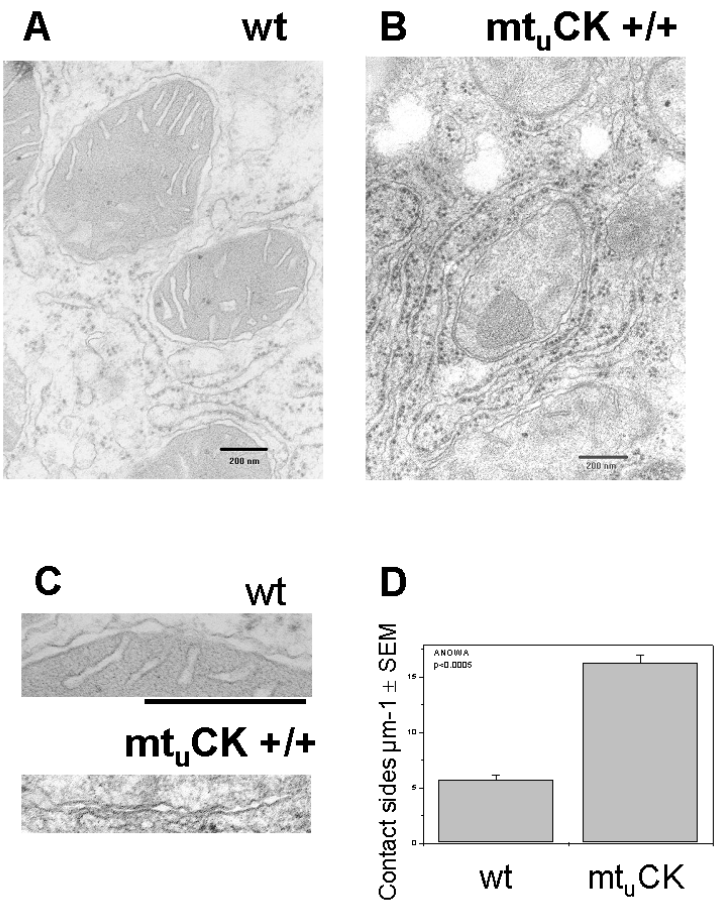

Figure 2 **Electron microscopic study of wild type (wt) and transgenic (mt_uCK +/+) liver**. Tissue was fixed by immersion in triple aldehyde (see material and methods), embedded and cut by standard procedures. A) Representative image of wild type liver tissue, B) representative picture of mt_uCK over expressing liver. A characteristic electron dense inclusion in an enlarged crista is seen. C) Sections of MOM and peripheral MIM are enlarged, increased number of contact sites are seen, which have been quantified from 20 mitochondria in D) The circumference of each mitochondrium trans section was measured by NIHimage, contact sites were counted and plotted as contact sites per µm circumference, significance was tested with ANOVA. Bar = 200 nm

Over-expressed mtCK increases mitochondrial structural integrity and stability

mt_uCK interacts with mitochondrial membranes in vitro (50, 51, 55) (49). The presence of mt_uCK within mitochondria is expected to lead to a stabilization of mitochondrial structure in contrast to mitochondria containing no mt_uCK, as the enzyme is able to cross-link MOM with the peripheral MIM, but also the central MIM forming cristae. To find an approach, which was independent of mitochondrial swelling after permeability transition (PT) induction, we measured the direct effect of the presence of mtCK on the structural stability of mitochondria by simple mitochondrial swelling after addition of digitonin, without any addition of PT stimulating agents. With such an approach the impact of mt_uCK on the structural integrity of mitochondria should become clear independent of any changes of the inner membrane. Therefore 100 µg digitonin per mg mitochondrial protein were added to isolated

mouse liver mitochondria and the mitochondrial disintegration followed at 540 nm. After the recording was completed, mitochondria were visualized by electron microscopy after contrasting the organelles with 2 % ammonium molybdate.

The absorption of mitochondria at 540 nm from transgenic liver, over-expressing mt$_u$CK did not change after the addition of digitonin (Figure 4). By electron microscopy we could confirm that digitonin did not have a deleterious effect on mt$_u$CK containing mitochondria. Detached vesicles were observed, which we interpreted as detached MOM. However, the overall mitochondrial appearance seemed to bemore or less unchanged. The MIM was able to keep its integrity, as the ammonium molybdate solution did not enter the matrix, still seen as white areas inside mitochondria (figure 5).

In contrast, wild type mitochondria were almost completely destroyed under the very same conditions. First, the absorption of liver mitochondria from wild type mice did decrease significantly after the addition of digitonin, due to disintegration of the MOM followed by disintegration of MIM. As seen in the EM the typical mitochondrial structure was lost. The negative stain was leaking into the matrix, due to the lost MIM integrity. Thus, the electron dense ammonium molybdate was seen also inside the mitochondrial vesicles (Figure 5).

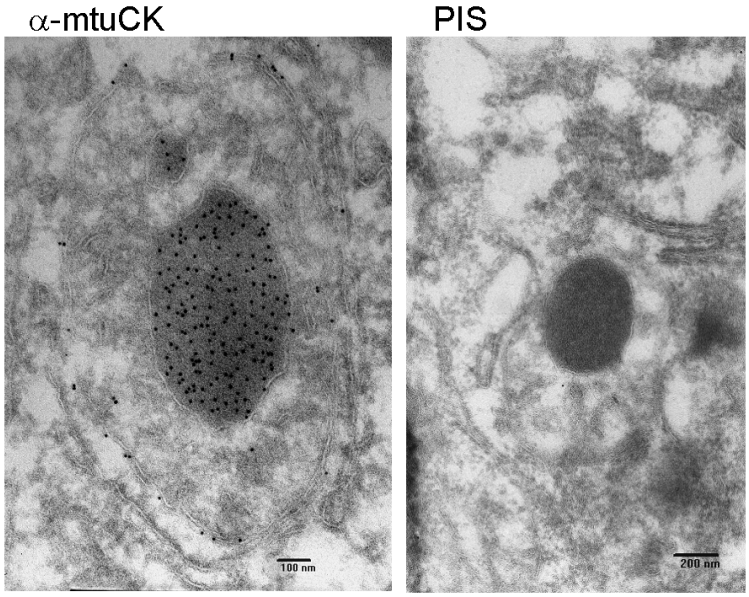

Figure 3 **Immuno-electron microscopy of transgenic liver**. Liver tissue was fixed as in Figure 2, embedded in sucrose-polyvinylpyrrolidone over night and sectioned at -100°C. Sections were taken on a copper grid suitable for electron microscopy and blocked with PBS containing 10% FCS for at least 2h. mt$_u$CK was detected with anti-mt$_u$CK antibody (1:200) for 1h in PBS, followed by 10nm colloidal gold-conjugated protein A 1:70 for 1h in PBS. Sections were fix again with 4% formaldehyde and 1% glutaraldehyde to stabilize the antibody-protein A complexes, followed by embedding in methylcellulose and contrasting with 2% uranyl acetate. The control (right panel) was treated identically, but using rabbit pre immune serum with no significant immuno-staining visible. With anti-mt$_u$CK-antibody (left hand panel), a strong labelling within the enlarged cristae, but also between the MOM and the outer boundary MIM was seen. The cristae inclusions are clearly highly enriched with mt$_u$CK. However, there is also mt$_u$CK located between MOM and MIM.

We conclude as seen already before (13, 21, 22, 33, 43, 44, 50), that mtCK is interacting with mitochondrial membranes and proteins thereof. This is obviously leading to an overall stabilization of mitochondrial structure. In the case of liver mitochondria, normally the MOM is mostly responsible for the structural integrity. Once destroyed e.g. with digitonin, also MIM looses its structure and mitochondria fall apart (figure 4 and 5, wt + digitonin). Whereas in the presence of mt$_u$CK, central MIM membranes, forming cristae, are cross-linked by symmetrical mtCK octamers and are thus stabilized. This increased stability of mitochondrial cristae membranes by mt$_u$CK even persists after disruption of the MOM.

Biochemical isolation of contact sites

MtCK interacts with VDAC (49) and is attached also to the inner mitochondrial membrane close to ANT (13, 21). This interaction is likely mediated by cardiolipin (crompton halestrap). It was consequently shown that mtCK forms contact sites between outer and inner membrane (1, 9-13, 33-35). We were looking for a method to isolate contact sites that

still could contain mtCK. We postulated that contact sites are embedded in rigid membrane formations. Furthermore, we postulated that these macro-molecular assemblies should be detergent resistant, as seen previous with plasma membrane micro-domains (17, 52, 53). Therefore, kidney mitochondria were homogenized at 4°C in 0.75 % Triton X-100 (see figure 6 and material and methods). The homogenates were layered below continuous sucrose gradients and ultra-centrifuged at 100'000 g. The gradients were fractionated and analyzed by Western blotting.

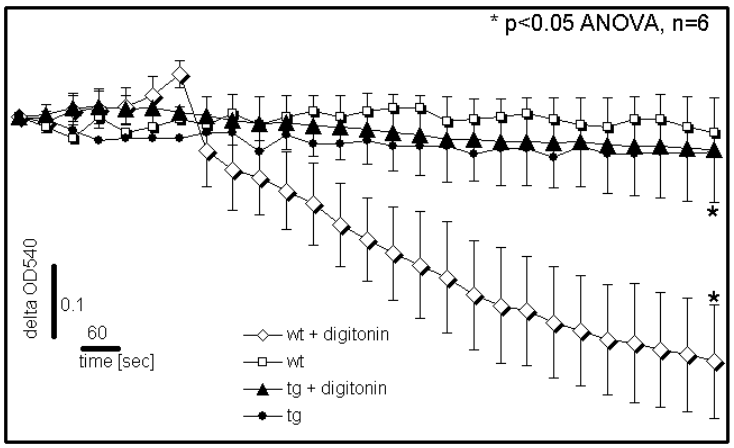

Figure 4 **Digitonin induced disintegration of mitochondria**. Liver mitochondria from wild type mouse liver (wt) and from transgenic mtuCK expressing liver (mtuCK +/+) were isolated in sucrose buffer (see material and methods). The absorption of mitochondria diluted in sucrose buffer (0,5 mg/ml) was recorded at 540 nm. For each, wt and tg mitochondria a baseline without digitoni was recorded. In parallel samples, digitonin (100µg/mg mitochondrial protein) was added. Only the wt mitochondria showed a significant decrease in absorption, which was interpreted as swelling and disintegration of mitochondrial structure, leading to a lower optical density. Mitochondria containing mt_uCK showed no significant loss in optical density.

Astonishingly, we found most of the mitochondrial VDAC in low-density parts of the gradients. VDAC was "floating" (figure 7). The inner membrane ANT was partly within the floating, detergent resistant fractions together with VDAC, but also remained within the high-density parts of the gradient, and in addition some ANT was also precipitated. The matrix-located pyruvate dehydrogenase was completely precipitated (figure 7).

Within the detergent insoluble parts, which we called "contact sites", mt_uCK was located, as well as cytocrome oxidase subunit 4 (COX IV). COX (IV) could not be detected in any other fractions. However cytochrome c was distributed equally within all analyzed fractions (data not shown).

To control the method, we incubated mitochondria after the homogenization with Triton, for 10 min at room temperature. This warming resulted in the distribution of VDAC all over the gradient, which otherwise was concentrated under 4°C-conditions predominantly in the low-density sucrose parts of the gradient (figure 7).

Detergent resistant, floating protein complexes were formed at least out of VDAC, mt_uCK, ANT and parts of the respiratory chain. This could mean that they were still enveloped with phospholipids. We thus suggest that we have developed a method to prepare mitochondrial contact sites within their more or less natural membrane environment. By this technique we could see the close localization of mt_uCK with the outer membrane protein VDAC. The interaction between both purified mtCK and VDAC could be shown in vitro (49). However the coupling between mt_uCK and ANT was proposed several times, but direct experimental evidence for a direct interaction between mtCK and ANT has not been published, but indirect interaction via functional coupling of the two proteins is evident (9, 10, 31, 48).

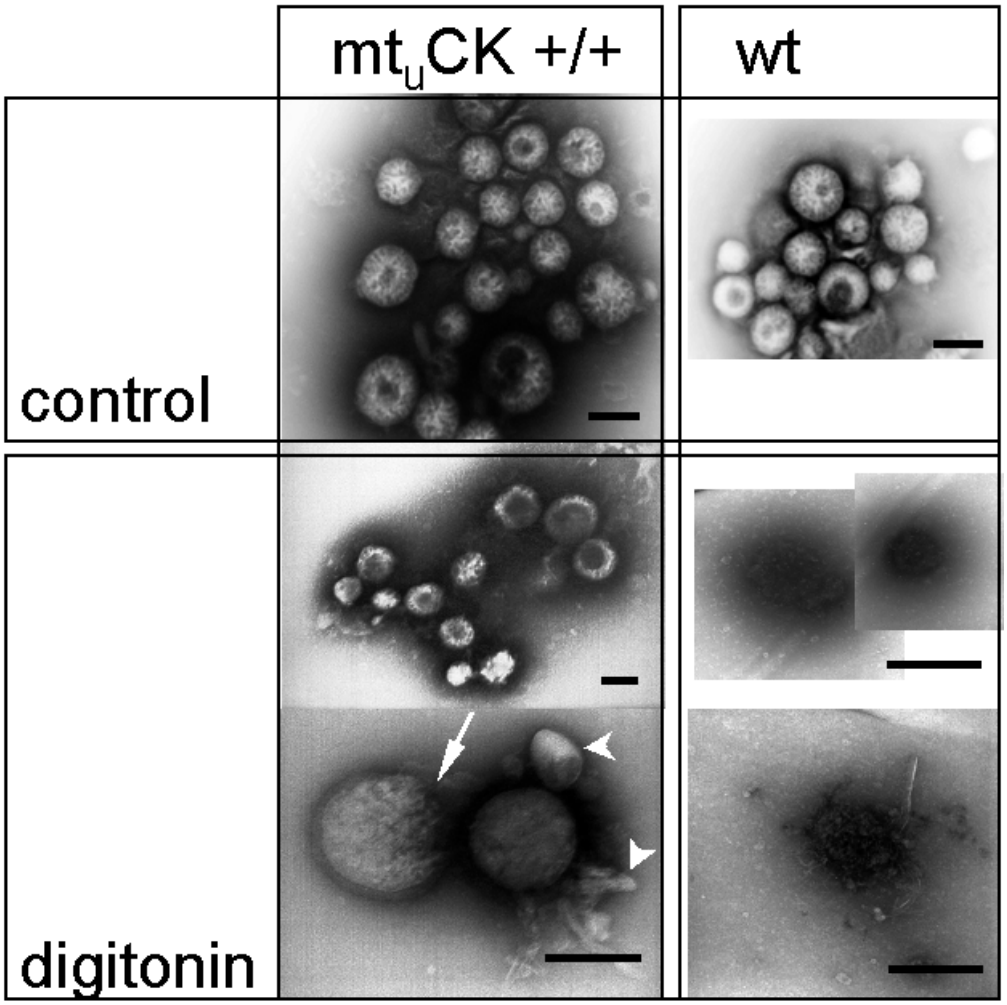

Figure 5 **Negatively stained mitochondria with and without digitonin**. Mitochondria were taken after the recording of the optical density (figure 4), layered on a carbon-coated cupper grid and contrasted with 2% ammonium molybdate solution (pH 7.4). Pictures were taken in a Jeol electron microscope at 80 kV. Untreated mitochondria showed clearly the typical round structure with visible cristae, both in transgenic (*upper panel*, mtuCK +/+) and wild type (*upper panel*, wt) mitochondria. After digitonin treatment (100 µg/mg protein, as in figure 4) wild type mitochondria lost their structure. It was hard to detect any remaining structure other than vesicular structure (*lower panel on the right hand*). By contrast, transgenic liver mitochondria kept their round shape even after digitonin addition (*lower panel on the left hand*). However, some were opened at one side (*arrow*) other seemed to stripped from their MOM (*arrow head*). The mere presence of mtuCK rescued mitochondria from the deleterious effect by digitonin.

Discussion

In a previous study, we have shown that mtuCK forms a functionally coupled micro compartment with ANT on the one hand (21), and on the other hand is directly interacting with VDAC in a calcium dependant manner (49). Furthermore, it became clear in recent years that mtCK is able to interact with, and cross-link membranes (43, 44, 50, 51). We have also seen in previous studies that mtCK in the presence of creatine inhibits mitochondrial permeability transition (21, 38). This protection towards the permeability transition, however,

is based on a functional coupling between mtCK and ANT and might not be due to a direct physical interaction between the two proteins. A direct physical interaction of mtCK was shown with VDAC (49), as well as with mitochondrial membranes (43, 44).

(I) In the present study, we could show that the mitochondrial protection by mtCK is not only due to a functional coupling between mtCK and ANT. This coupling seems to have also a direct structural basis: Immuno electron microscopy revealed that over-expressed mt_uCK is able to increase the number of contact sites in situ (figure 2). Over-expressed mt_uCK localizes directly between outer and inner membrane, and also inside cristae (figure 3).

To test whether mt_uCK was cross-linking mitochondrial membranes directly and independently from the permeability transition also in a physiological state, mitochondria were treated with the detergent digitonin. Digitonin is interacting with cholesterol, thereby leading to disruption of the MOM. Due to the fact that MIM contains none or very little cholesterol, less or no damage should occur on the MIM. In wild type mitochondria disruption of the MOM is leading to a loss of integrity, MIM is expanding, and mitochondria are loosing their typical structure (figure 5).

(II) Although upon digitonin treatment mitochondria containing mt_uCK loose their MOM, which remains as vesicles sticking to the MIM, the mitochondrial structure is largely preserved. The mitochondrial appearance with the cristae and the round shape, typical for isolated liver mitochondria (37) is still maintained. This is due to the cross-linking of mitochondrial membranes by mtCK. Mitochondrial CK interacts with VDAC at the inner side of the MOM (49) and with cardiolipin at the outside of the MIM (19) close to ANT (21). So mtCK is able to cross-link cristae membranes, thus stabilizing cristae architecture also under otherwise rather devastating conditions, as digitonin treatment, or maybe also after a heavy calcium load.

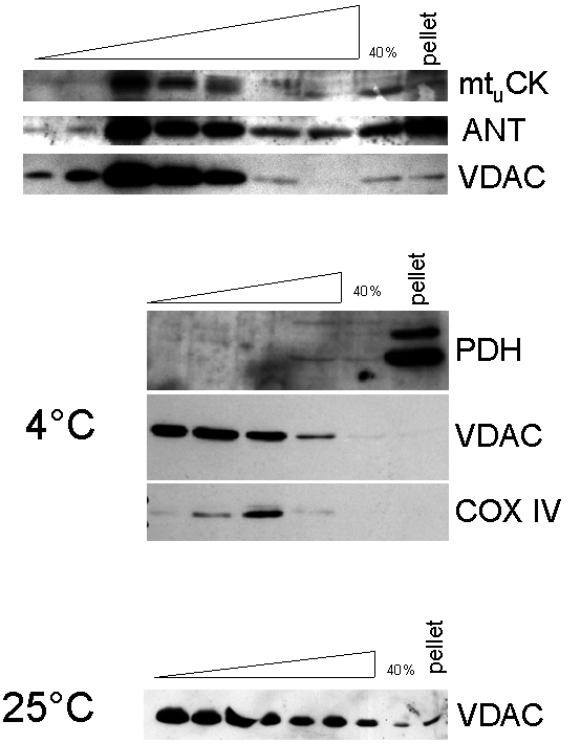

Figure 6 **Contact side preparation**. Isolated mitochondria were homogenized in 0.75 % Triton containing sucrose buffer strictly at 4°C. Dissolved mitochondrial membranes and proteins were mixed 1:1 in 80 % sucrose (40% final concentration) and layered below a continuous sucrose gradient (15 – 38 %). The gradient was centrifuged for at least 16 hours at 100'000 x g at 4 °C. (See figure 7) Upper panel distribution of the outer membrane VDAC, soluble inter-membrane space located mtuCK, and inner membrane ANT within the sucrose gradient. Middle panel distribution of the soluble matrix located PDH, outer membrane VDAC, and soluble inner membrane associated subunit IV of COX. Lower Panel contact site preparation at room temperature. Note that VDAC, ANT, mtuCK and COX are floating. At 25 °C VDAC is distributed all over the gradient in contrast to 4 °C.

Assuming the formation of a micro-compartment (21), or better a complex formed out of VDAC (in the MOM), mt_uCK, cardiolipin and ANT (in the MIM), we developed a new method to enrich those micro-compartments, also referred to as contact sites. Recently, detergent resistant micro-domains within the plasma membrane were described (17, 52, 53). In analogy to the described method, mitochondria were dissolved with Triton X-100 on ice. Against our expectations, a visible white fraction was floating to lower density within the sucrose gradient (figure 6). This floating fractions, which contained clearly membrane vesicles as seen in the electron microscope (figure 7) were positive for VDAC, mt_uCK, and

ANT on Western blots. These three proteins are postulated to form complexes relevant for the regulation of the mitochondrial permeability transition (8-10, 34, 35). Thus it seems that an enrichment of in situ contact sites is possible by using this detergent solubilization technique.

(III) Apparently, these complexes can be isolated within their in situ membrane envelope. It was found that also parts of the respiratory chain, here cytochrome oxidase, are components of the contact site complex. If such a macromolecular protein assembly acts as a permeability transition pore, it might explain, why ubiquinones and electron flow also regulate PT (5, 24, 25, 65). In line with such reasoning is the fact that very recently mtCK has been found in a proteomics approach to be associated with complex IV and complex I (16). If the latter would be a key player in mPT, such an association of mtCK with complex I could possibly also explain the protective effects of creatine on PTP opening (21, 38). However, other proteins as the soluble pyruvate dehydrogenase (PDH) were not found to be part of such a complex, since PDH was collected entirely in the pellet after Triton extraction. This argues for the specificity of this method. Also the hydrophobic carbamyl phosphate synthase (CPS) was not part of this complex (see chapter 7, figure x).

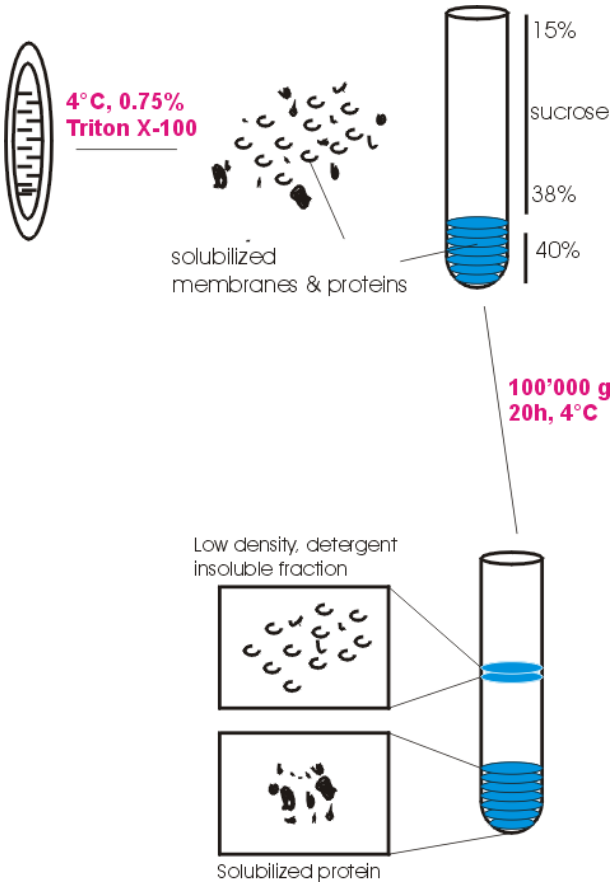

Figure 7 **Sketch of contact side preparation**. Isolated mitochondria were homogenized in 0.75 % Triton containing sucrose buffer strictly at 4°C. Dissolved mitochondrial membranes and proteins were mixed 1:1 in 80 % sucrose (40% final concentration) and layered below a continuous sucrose gradient (15 – 38 %). The gradient was centrifuged for at least 16 hours at 100'000 x g at 4 °C. After centrifugation a white fluffy band could be seen in the upper half of the gradient. The gradient was fractionated in fractions of 500 µl each.

In this work, we have found mt_uCK to be responsible for the physical rigidity and structural integrity of mitochondria. Due to its molecular symmetry octameric mt_uCK is able to interact with all mitochondrial membranes, thereby cross-linking them. Mt_uCK can be isolated with in this lipid-protein complex, which contains as additional components VDAC, ANT and COX, and probably also cyclophilin D. The use of such a method, together with the comparison of wild type liver mitochondria and liver mitochondria containing over-expressed mt_uCK, may lead to the molecular identification of proteins within the mitochondrial permeability transition pore complex in future.

References

1. Adams V, Bosch W, Schlegel J, Wallimann T, and Brdiczka D. Further characterization of contact sites from mitochondria of different tissues: topology of peripheral kinases. *Biochim Biophys Acta* 981: 213-225, 1989.
2. Benz R. Permeation of hydrophilic solutes through mitochondrial outer membranes: review on mitochondrial porins. *Biochim Biophys Acta* 1197: 167-196, 1994.
3. Benz R and Brdiczka D. The cation-selective substate of the mitochondrial outer membrane pore: single-channel conductance and influence on intermembrane and peripheral kinases. *J Bioenerg Biomembr* 24: 33-39, 1992.
4. Benz R, Kottke M, and Brdiczka D. The cationically selective state of the mitochondrial outer membrane pore: a study with intact mitochondria and reconstituted mitochondrial porin. *Biochim Biophys Acta* 1022: 311-318, 1990.
5. Bernardi P. Mitochondrial transport of cations: channels, exchangers, and permeability transition. *Physiol Rev* 79: 1127-1155., 1999.
6. Bessman SP and Carpenter CL. The creatine-creatine phosphate energy shuttle. *Annu Rev Biochem* 54: 831-862, 1985.
7. Bessman SP and Geiger PJ. Transport of energy in muscle: the phosphorylcreatine shuttle. *Science* 211: 448-452., 1981.
8. Beutner G, Ruck A, Riede B, and Brdiczka D. Complexes between hexokinase, mitochondrial porin and adenylate translocator in brain: regulation of hexokinase, oxidative phosphorylation and permeability transition pore. *Biochem Soc Trans* 25: 151-157., 1997.
9. Beutner G, Ruck A, Riede B, and Brdiczka D. Complexes between porin, hexokinase, mitochondrial creatine kinase and adenylate translocator display properties of the permeability transition pore. Implication for regulation of permeability transition by the kinases. *Biochim Biophys Acta* 1368: 7-18., 1998.
10. Beutner G, Ruck A, Riede B, Welte W, and Brdiczka D. Complexes between kinases, mitochondrial porin and adenylate translocator in rat brain resemble the permeability transition pore. *FEBS Lett* 396: 189-195., 1996.
11. Brdiczka D. Contact sites between mitochondrial envelope membranes. Structure and function in energy- and protein-transfer. *Biochim Biophys Acta* 1071: 291-312, 1991.
12. Brdiczka D, Beutner G, Ruck A, Dolder M, and Wallimann T. The molecular structure of mitochondrial contact sites. Their role in regulation of energy metabolism and permeability transition. *Biofactors* 8: 235-242, 1998.
13. Brdiczka D, Kaldis P, and Wallimann T. In vitro complex formation between the octamer of mitochondrial creatine kinase and porin. *J Biol Chem* 269: 27640-27644, 1994.
14. Brdiczka D WT. The importance of the outer mitochondrial compartment in regulation of energy metabolism. *Mol Cell Biochem* 133-134: 69-83, 1994.
15. Brewer GJ and Wallimann TW. Protective effect of the energy precursor creatine against toxicity of glutamate and beta-amyloid in rat hippocampal neurons. *J Neurochem* 74: 1968-1978, 2000.
16. Brookes PS, Pinner A, Ramachandran A, Coward L, Barnes S, Kim H, and Darley-Usmar VM. High throughput two-dimensional blue-native electrophoresis: a tool for functional proteomics of mitochondria and signaling complexes. *Proteomics* 2: 969-977, 2002.
17. Brown DA and Rose JK. Sorting of GPI-anchored proteins to glycolipid-enriched membrane subdomains during transport to the apical cell surface. *Cell* 68: 533-544, 1992.
18. Bucheler K AV, Brdiczka D. Localization of the ATP/ADP translocator in the inner membrane and regulation of contact sites between mitochondrial envelope membranes by ADP. A study on freeze-fractured isolated liver mitochondria. *Biochim Biophys Acta* 1056: 233-242, 1991.
19. Cheneval D and Carafoli E. Identification and primary structure of the cardiolipin-binding domain of mitochondrial creatine kinase. *Eur J Biochem* 171: 1-9, 1988.
20. Dalakas MC Il, Pezeshkpour GH, Laukaitis JP, Cohen B, Griffin JL. Mitochondrial myopathy caused by long-term zidovudine therapy. *N Engl J Med* 322: 1098-1105, 1990.
21. Dolder M, Walzel B, Speer O, Schlattner U, and Wallimann T. Inhibition of the mitochondrial permeability transition by creatine kinase substrates: requirement for microcompartmentation. *J Biol Chem*, 2003.
22. Dolder M, Wendt S, and Wallimann T. Mitochondrial creatine kinase in contact sites: interaction with porin and adenine nucleotide translocase, role in permeability transition and sensitivity to oxidative damage. *Biol Signals Recept* 10: 93-111., 2001.
23. Ferri KF and Kroemer G. Organelle-specific initiation of cell death pathways. *Nat Cell Biol* 3: E255-263., 2001.
24. Fontaine E and Bernardi P. Progress on the mitochondrial permeability transition pore: regulation by complex I and ubiquinone analogs. *J Bioenerg Biomembr* 31: 335-345, 1999.
25. Fontaine E, Eriksson O, Ichas F, and Bernardi P. Regulation of the permeability transition pore in skeletal muscle mitochondria. Modulation By electron flow through the respiratory chain complex i. *J Biol Chem* 273: 12662-12668, 1998.
26. Gross M and Wallimann T. Kinetics of assembly and dissociation of the mitochondrial creatine kinase octamer. A fluorescence study. *Biochemistry* 32: 13933-13940, 1993.

27. Hemmer W, Riesinger I, Wallimann T, Eppenberger HM, and Quest AF. Brain-type creatine kinase in photoreceptor cell outer segments: role of a phosphocreatine circuit in outer segment energy metabolism and phototransduction. *J Cell Sci* 106: 671-683, 1993.
28. Jacobus WE. Respiratory control and the integration of heart high-energy phosphate metabolism by mitochondrial creatine kinase. *Annu Rev Physiol* 47: 707-725, 1985.
29. Jacobus WE and Lehninger AL. Creatine kinase of rat heart mitochondria. Coupling of creatine phosphorylation to electron transport. *J Biol Chem* 248: 4803-4810, 1973.
30. Kaldis P, Stolz M, Wyss M, Zanolla E, Rothen-Rutishauser B, Vorherr T, and Wallimann T. Identification of two distinctly localized mitochondrial creatine kinase isoenzymes in spermatozoa. *J Cell Sci* 109: 2079-2088, 1996.
31. Kay L, Nicolay K, Wieringa B, Saks V, and Wallimann T. Direct evidence for the control of mitochondrial respiration by mitochondrial creatine kinase in oxidative muscle cells in situ. *J Biol Chem* 275: 6937-6944, 2000.
32. Knoll G and Brdiczka D. Changes in freeze-fractured mitochondrial membranes correlated to their energetic state. Dynamic interactions of the boundary membranes. *Biochim Biophys Acta* 733: 102-110, 1983.
33. Kottke M, Adams V, Wallimann T, Nalam VK, and Brdiczka D. Location and regulation of octameric mitochondrial creatine kinase in the contact sites. *Biochim Biophys Acta* 1061: 215-225, 1991.
34. Marzo I, Brenner C, Zamzami N, Jurgensmeier JM, Susin SA, Vieira HL, Prevost MC, Xie Z, Matsuyama S, Reed JC, and Kroemer G. Bax and adenine nucleotide translocator cooperate in the mitochondrial control of apoptosis. *Science* 281: 2027-2031, 1998.
35. Marzo I, Brenner C, Zamzami N, Susin SA, Beutner G, Brdiczka D, Remy R, Xie ZH, Reed JC, and Kroemer G. The permeability transition pore complex: a target for apoptosis regulation by caspases and bcl-2-related proteins. *J Exp Med* 187: 1261-1271., 1998.
36. Miller K, Sharer K, Suhan J, and Koretsky AP. Expression of functional mitochondrial creatine kinase in liver of transgenic mice. *Am J Physiol* 272: C1193-1202, 1997.
37. Munn EA. On the structure of mitochondria and the value of ammonium molybdate as a negative stain for osmotically sensitive structures. *J Ultrastruct Res* 25: 362-380, 1968.
38. O'Gorman E BG, Dolder M, Koretsky AP, Brdiczka D, Wallimann T. The role of creatine kinase in inhibition of mitochondrial permeability transition. *FEBS Lett* 414: 253-257, 1997.
39. O'Gorman E FK, Tittmann P, Gross H, Wallimann T. Crystalline mitochondrial inclusion bodies isolated from creatine depleted rat soleus muscle. *J Cell Sci* 110: 1403-1411, 1997.
40. O'Gorman E, Piendl T, Muller M, Brdiczka D, and Wallimann T. Mitochondrial intermembrane inclusion bodies: the common denominator between human mitochondrial myopathies and creatine depletion, due to impairment of cellular energetics. *Mol Cell Biochem* 174: 283-289, 1997.
41. Ren JM HJ. Adaptation of rat skeletal muscle to creatine depletion: AMP deaminase and AMP deamination. *J Appl Physiol* 73: 2713-2716, 1992.
42. Ren JM, Semenkovich CF, and Holloszy JO. Adaptation of muscle to creatine depletion: effect on GLUT-4 glucose transporter expression. *Am J Physiol* 264: C146-150., 1993.
43. Rojo M, Hovius R, Demel R, Wallimann T, Eppenberger HM, and Nicolay K. Interaction of mitochondrial creatine kinase with model membranes. A monolayer study. *FEBS Lett* 281: 123-129, 1991.
44. Rojo M, Hovius R, Demel RA, Nicolay K, and Wallimann T. Mitochondrial creatine kinase mediates contact formation between mitochondrial membranes. *J Biol Chem* 266: 20290-20295, 1991.
45. Rossi AM, Eppenberger HM, Volpe P, Cotrufo R, and Wallimann T. Muscle-type MM creatine kinase is specifically bound to sarcoplasmic reticulum and can support Ca2+ uptake and regulate local ATP/ADP ratios. *J Biol Chem* 265: 5258-5266, 1990.
46. Saks VA, Belikova YO, and Kuznetsov AV. In vivo regulation of mitochondrial respiration in cardiomyocytes: specific restrictions for intracellular diffusion of ADP. *Biochim Biophys Acta* 1074: 302-311, 1991.
47. Saks VA, Belikova YO, Kuznetsov AV, Khuchua ZA, Branishte TH, Semenovsky ML, and Naumov VG. Phosphocreatine pathway for energy transport: ADP diffusion and cardiomyopathy. *Am J Physiol* 261: 30-38, 1991.
48. Saks VA, Ventura-Clapier R, and Aliev MK. Metabolic control and metabolic capacity: two aspects of creatine kinase functioning in the cells. *Biochim Biophys Acta* 1274: 81-88, 1996.
49. Schlattner U, Dolder M, Wallimann T, and Tokarska-Schlattner M. Mitochondrial creatine kinase and mitochondrial outer membrane porin show a direct interaction that is modulated by calcium. *J Biol Chem* 276: 48027-48030, 2001.
50. Schlattner U and Wallimann T. Octamers of mitochondrial creatine kinase isoenzymes differ in stability and membrane binding. *J Biol Chem* 275: 17314-17320, 2000.
51. Schlegel J, Wyss M, Eppenberger HM, and Wallimann T. Functional studies with the octameric and dimeric form of mitochondrial creatine kinase. Differential pH-dependent association of the two oligomeric forms with the inner mitochondrial membrane. *J Biol Chem* 265: 9221-9227, 1990.
52. Schroeder R, London E, and Brown D. Interactions between saturated acyl chains confer detergent resistance on lipids and glycosylphosphatidylinositol (GPI)-anchored proteins: GPI-anchored proteins in liposomes and cells show similar behavior. *Proc Natl Acad Sci U S A* 91: 12130-12134, 1994.
53. Schroeder RJ, Ahmed SN, Zhu Y, London E, and Brown DA. Cholesterol and sphingolipid enhance the Triton X-100 insolubility of glycosylphosphatidylinositol-anchored proteins by promoting the formation of detergent-insoluble ordered membrane domains. *J Biol Chem* 273: 1150-1157, 1998.

54. Shoubridge EA, Challiss RA, Hayes DJ, and Radda GK. Biochemical adaptation in the skeletal muscle of rats depleted of creatine with the substrate analogue beta-guanidinopropionic acid. *Biochem J* 232: 125-131, 1985.
55. Stachowiak O, Schlattner U, Dolder M, and Wallimann T. Oligomeric state and membrane binding behaviour of creatine kinase isoenzymes: implications for cellular function and mitochondrial structure. *Mol Cell Biochem* 184: 141-151, 1998.
56. Stadhouders AM, Jap PH, Winkler HP, Eppenberger HM, and Wallimann T. Mitochondrial creatine kinase: a major constituent of pathological inclusions seen in mitochondrial myopathies. *Proc Natl Acad Sci U S A* 91: 5089-5093, 1994.
57. Sweeney HL. The importance of the creatine kinase reaction: the concept of metabolic capacitance. *Med Sci Sports Exerc* 26: 30-36, 1994.
58. Wallace D. Diseases of the mitochondrial DNA. *Annu Rev Biochem* 61: 1175-1212, 1992a.
59. Wallace D. Mitochondrial genetics: a paradigm for aging and degenerative diseases? *Science* 256: 628-632, 1992b.
60. Wallace DC LM, Shoffner JM, Brown MD. Diseases resulting from mitochondrial DNA point mutations. *J Inherit Metab Dis* 15: 472-479, 1992c.
61. Wallimann T. Bioenergetics. Dissecting the role of creatine kinase. *Curr Biol* 4: 42-46, 1994.
62. Wallimann T and Hemmer W. Creatine kinase in non-muscle tissues and cells. *Mol Cell Biochem* 133-134: 193-220, 1994.
63. Wallimann T, Schlosser T, and Eppenberger HM. Function of M-line-bound creatine kinase as intramyofibrillar ATP regenerator at the receiving end of the phosphorylcreatine shuttle in muscle. *J Biol Chem* 259: 5238-5246, 1984.
64. Wallimann T, Wyss M, Brdiczka D, Nicolay K, and Eppenberger HM. Intracellular compartmentation, structure and function of creatine kinase isoenzymes in tissues with high and fluctuating energy demands: the 'phosphocreatine circuit' for cellular energy homeostasis. *Biochem J* 281: 21-40, 1992.
65. Walter L, Miyoshi H, Leverve X, Bernard P, and Fontaine E. Regulation of the mitochondrial permeability transition pore by ubiquinone analogs. A progress report. *Free Radic Res* 36: 405-412, 2002.
66. Wegmann G, Huber R, Zanolla E, Eppenberger HM, and Wallimann T. Differential expression and localization of brain-type and mitochondrial creatine kinase isoenzymes during development of the chicken retina: Mi-CK as a marker for differentiation of photoreceptor cells. *Differentiation* 46: 77-87, 1991.
67. Wyss M and Kaddurah-Daouk R. Creatine and creatinine metabolism. *Physiol Rev* 80: 1107-1213., 2000.
68. Wyss M, Smeitink J, Wevers RA, and Wallimann T. Mitochondrial creatine kinase: a key enzyme of aerobic energy metabolism. *Biochim Biophys Acta* 1102: 119-166, 1992.

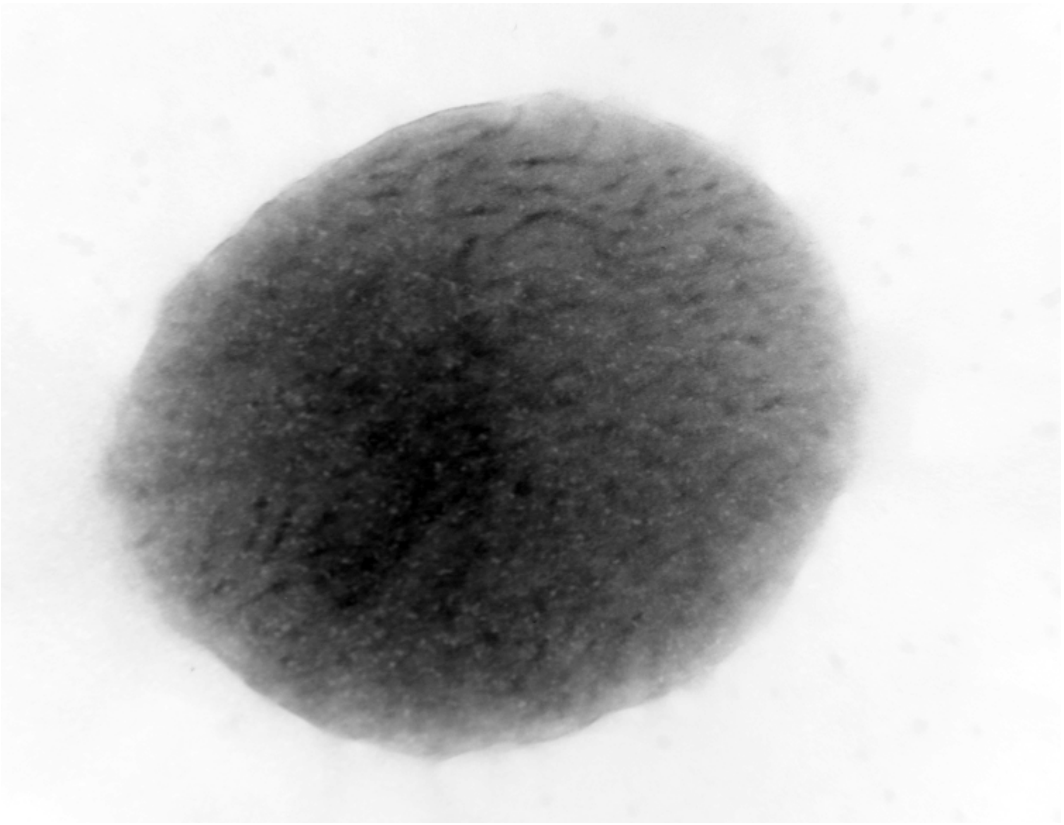

Kidney mitochondrium, Oliver Speer, April 2001

Chapter 5

NOVEL MITOCHONDRIAL CREATINE TRANSPORT ACTIVITY

IMPLICATIONS FOR INTRACELLULAR CREATINE COMPARTMENTS AND BIOENERGETICS

**Bernd Walzel‡§, Oliver Speer‡§,
Else Zanolla‡, Ove Eriksson¶,
Paolo Bernardi‡‡, and Theo Wallimann‡**

§ These authors have contributed equally to this work.

From the ‡Swiss Federal Institute of Technology, ETH-Zürich, Institute of Cell Biology, ETH-Hönggerberg, CH-8093 Zurich, Switzerland,

the ¶Institute of Biomedicine/Biochemistry, Biomedicum, Haartmaninkatu 8, University of Helsinki, FIN-00014 Helsinki, Finland,

and the ‡‡Department of Biomedical Sciences, University of Padova, Viale Giuseppe Colombo 3, I-35131 Padova, Italy

Published in
The Journal of Biological Chemistry, 4th October 2002, 277(40),37503 - 11

Acknowledgments—We are indebted to all members of our research group (Cell Biology, ETH), especially to Dr. Max Dolder, Dr. Uwe Schlattner, Dr. Laurence Kay, Dr. Thorsten Hornemann, Dr. Dietbert Neumann, and Lukas Neukomm for help and stimulating discussion, as well as to Dr. Peter Engelhard (Hartman Institute, Helsinki, Findland) and Mats Linder (Biomedicum Helsinki) for helpful discussion and excellent technical co-work. We would also like to thank Dr. Nils Beck (Biomedicum Helsinki), who provided protein A conjugated with 10 nm gold.

This work was supported by the Swiss Society for Research on Muscle Diseases (to B. W. and O. S.), the parents organization Benni & Co., Germany, the German Muscle Society and the ETH-Zurich, as well as by the Swiss National Foundation (Grant 31-62024.00 (to T. W.)). Parts of this work have been published in abstract form (45).

The abbreviations used are: Cr, creatine; PCr, phosphocreatine; CRT, creatine transporter; DTNB, 5,5'-dithiobis(2-nitrobenzoic acid); DNFB, 2,4-dinitro-1-fluorobenzene; NEM, *N*-ethylmaleimide; COX, cytochrome oxidase core complex; PBS, phosphate-buffered saline; FCCP, carbonyl cyanide *p*-(trifluoromethoxy) phenylhydrazone; β-GPA, β-guanidinopropionic acid.

Abstract

Immunoblotting of isolated mitochondria from rat heart, liver, kidney, and brain with antibodies made against N- and C-terminal peptide sequences of the creatine transporter, together with in situ immunofluorescence staining and immunogold electron microscopy of adult rat myocardium, revealed two highly related polypeptides with molecular masses of ~ 70 and ~ 55 kDa in mitochondria. These polypeptides were localized by immunoblotting of inner and outer mitochondrial membrane fractions, as well as by immunogold labeling in the mitochondrial inner membrane. In addition, a novel creatine uptake via a mitochondrial creatine transport activity was demonstrated by [^{14}C]creatine uptake studies with isolated mitochondria from rat liver, heart, and kidney showing a saturable low affinity creatine transporter, which was largely inhibited in a concentrationdependent manner by the sulfhydryl-modifying reagent NEM, as well as by the addition of the above anti-creatine transporter antibodies to partially permeabilized mitochondria. Mitochondrial creatine transport was to a significant part dependent on the energetic state of mitochondria and was inhibited by arginine, and to some extent also by lysine, but not by other creatine analogues and related compounds. The existence of an active creatine uptake mechanism in mitochondria indicates that not only creatine kinase isoenzymes, but also creatine transporters and thus a certain proportion of the creatine kinase substrates, might be subcellularly compartmentalized. Our data suggest that mitochondria, shown here to possess creatine transport activity, may harbor such a creatine/phosphocreatine pool.

Introduction

Creatine (Cr) and phosphocreatine (PCr) play fundamental roles in cellular energetics (for reviews, see Refs. 1–3). Cells that do not synthesize Cr, like skeletal and cardiac muscle, must take it up from the blood through an active Cr transport system (CRT) (4). cDNA and gene sequencing of the CRTs from rabbit, rat, mouse, human, and the electric ray (Torpedo) (5– 10) have shown that CRTs are composed of 611–636 amino acid residues with a calculated molecular mass of ~ 70 kDa. The CRT sequences (Protein Data Bank accession number for rat CRT = P28570 and for human CRT = P48029) are most closely related to the γ-aminobutyric acid, taurine / betaine transporter subfamily (46–53% amino acid sequence identity), while the homology to the glycine, proline, catecholamine, and serotonin transporters is less pronounced (38–34%). Computational analysis revealed that these CRTs, like other neurotransmitter transporters, are integral membrane proteins containing 12 putative transmembrane domains (8). CRT expression has been studied by a few research groups (11–16). The presence of two different gene products expressed in various tissues corresponding to two major polypeptides of ~55 and ~70 kDa has been described. The two polypeptides are most likely generated by alternative splicing (12). This assumption is supported by the fact that antipeptide antibodies generated against the N and C-terminal region of the cDNA-derived CRT polypeptide sequence, all recognize the same two proteins with molecular masses of ~55 and ~70 kDa on Western blots (11–16). Furthermore, the existence of CRT splice variants has recently been suggested, based on genetics studies using rapid amplification of cDNA ends methods (17). Recent immuno-fluorescence studies have indicated a high degree of intracellular CRT localization (16), which is consistent with a mainly mitochondrial localization (15). This finding is in contrast to the general view that CRT, represented here by two major ~55- and ~70-kDa CRT-related proteins, is localized exclusively in the plasma membrane. Instead, it was also recently reported that only a minor CRT protein species with an intermediate apparent molecular mass of ~58 kDa is located in the plasma membrane (15). This ~58-kDa polypeptide has been identified by surface biotinylation of intact cardiomyocytes, followed by Western blotting with anti-CRT antibodies, or alternatively by Western blotting of highly enriched plasma membrane fractions (15). Also in contrast to the prevailing view that mitochondria do not contain Cr, PCr uptake into isolated rat heart mitochondria had been reported earlier (18) and was attributed, however, to the activity of adenine nucleotide translocase. The same authors also studied changes in the subcellular distribution of ATP, ADP, Cr, and PCr depending on the physiological state in rat fast twitch gastrocnemius and slow twitch soleus muscles by fractionation of freeze-clamped and freeze-dried tissue in non-aqueous solvents (19). It was found that during isotonic contraction of gastrocnemius muscles, the mitochondrial content of total Cr and PCr decreased with a parallel increase in extramitochondrial total Cr, indicating a net transfer of Cr across the mitochondrial membranes. In line with the above observation, *in vivo* isotope tracing studies with labeled Cr have shown that creatine kinase does not have access to the entire cellular Cr and PCr pool(s) (20), which indicates that intracellular Cr and PCr pools may exist that are not in immediate equilibrium with one another. Such interpretations are in agreement with a number of ^{31}P NMR magnetization transfer studies (21, 22), as well as with recent ^{1}H NMR spectroscopy data (23), where monitoring the Cr and PCr levels in human muscle pointed to the existence of a pool of Cr that is not NMR “visible” in resting muscle, but appears in NMR spectra of muscle in ischemic fatigue or post mortem (23). From these studies, it was also concluded that the total PCr / Cr pool must be

divided into physical compartments, or chemical entities, without fast exchange, and the authors even mentioned that increased flux through mitochondria could provide an explanation for their experimental results (23). It is, however, important to emphasize that by the above experimental approaches, no specific information neither on the nature or the direction of Cr shuttling pathways nor on the identity of such putative Cr compartments could be inferred. These findings led us to search for a potential mitochondrial Cr transport activity in muscle and non-muscle tissues, which would be associated with corresponding CRT protein(s), by using cell fractionation techniques, confocal immunofluorescence, immunoelectron microscopy, as well as substrate transport studies. Here we show that the mitochondrial inner membrane possesses active CRT activity, which seems to be associated with distinct CRT-related polypeptides.

Experimental procedures

Materials

If not otherwise stated all chemicals were purchased from Sigma. Male Wistar rats (250–300 g) were purchased from Invitrogen BRL, (Füllinsdorf, Switzerland). The characterization of our rabbit anti-CRT peptide antibodies has been described earlier (12).

Immunofluorescence of sections from rat ventricle

Freshly excised rat ventricles were fixed for 3 h at room temperature in PBS containing 3% paraformaldehyde. Tissues were dehydrated and embedded in paraffin by standard techniques. Ten-µm slices were cut with a microtome, paraffin was removed with xylene, and sections were washed with 70% ethanol and stored in PBS. For immunofluorescence staining, tissue sections were permeabilized first with 0.2% Triton X-100 for 15 min, then with 0.1% SDS for 30 s and subsequently washed in PBS for 30 min. The sections were blocked in 5% goat serum albumin and 1% bovine serum albumin in PBS. Primary antibodies (rabbit anti-CRT peptide antibody 1:200, mouse anti-cytochrome oxidase subunit IV (COX, Molecular Probes) 1:200, both diluted in PBS containing 2% fat-free dry milk powder) were incubated at 4°C overnight. Subsequently, the tissue sections were washed extensively six times. Secondary antibodies (fluorescein isothiocyanate-conjugated mouse-anti-rabbit IgG 1:500 and Cy3-conjugated goat-anti-mouse IgG, both diluted 1:500 in PBS), were incubated 1 h at room temperature in the dark. The stained sections were washed again extensively in PBS, followed by embedding in an antifading medium containing 70% glycerol, 240 Mm N-propylgallate, 30 mM Tris/HCl at pH 9.5. Sections were analyzed with a confocal fluorescence microscope (Zeiss Axiophot, equipped with an argon/krypton mixed gas laser), a Bio-Rad MRC-600 confocal scanner unit and a Silicon Graphics Iris 4D/25 work station, using Imaris (Bitplane AG, Zurich, Switzerland) software. Images were recorded with oil immersion objectives (Zeiss).

Immunoelectron microscopy of ventricle sections

Rat heart ventricles were fixed with 4% glutaraldehyde/PBS by immersion fixation at room temperature for 3 h. Tissue was washed with 0.1 M cacodylate buffer, pH 7.4, and fixed again in the presence of 1% OsO_4 for 2 h at room temperature. Tissues were dehydrated with increasing concentrations of ethanol, stained en bloc with 2% uranyl acetate, and embedded in Epon-Araldite. Sections of 80–100 nm were cut with an Ultra-microtome (Reichert, München, Germany), adsorbed onto copper electron microscope grids, incubated for etching of the plastic on drops of saturated sodium perjodate for 1 h, rinsed with double distilled H_2O, incubated in boiling 10 mM citric acid NaOH, pH 6, for 20 min and rinsed again extensively. Subsequently, the sections were blocked in buffer 1 (PBS containing 0.1% acetylated bovine serum albumin and 0.1% Tween) for 20 min, followed by incubation with anti-CRT peptide antibody in buffer 1 for 70 min, washed, incubated for 45 min with goat-anti-rabbit IgG conjugated with 10 nm colloidal gold, washed with buffer 1 again, and finally with double distilled H_2O. After contrasting sections with 2% uranyl acetate and 2% lead citrate, pictures were taken by a transmission electron microscope JEOL200 at 100 kV.

Tissue extracts and isolation of mitochondria

Male Wistar Rats (3–4 month of age) were anesthetized with diethyl ether and killed by cervical dislocation. Tissue of liver, skeletal and cardiac muscle, kidney, and brain were taken and immediately transferred to ice-cold buffer. Liver, brain, and kidney tissues were homogenized by a Teflon/glass potter (Braun, Melsungen, Germany), whereas skeletal and heart muscle was homogenized by a Polytron mixer in 40 ml HEPES-sucrose buffer containing 250 mM sucrose, 10 mM HEPES KOH, pH 7.4, 0.5% bovine serum albumin (essentially free of fatty acids) and 1 mM EDTA. The homogenate was centrifuged for 10 min at 700 x g to remove heavy debris as platelets and nuclei. An aliquot from the supernatant was taken for further analysis as the total tissue extract. The supernatant was centrifuged for 10 min at 7,000 x g, and the resulting supernatant was stored for subsequent analysis as the

soluble cytosolic fraction, while the pellet containing mitochondria was resuspended in 60 ml of 250 mM sucrose, 10 mM Tris/HCl, pH 7.4, 100 µM EGTA, 25% PercollTM (Amersham Biosciences) and centrifuged for 35 min at 100,000 x g. PercollTM fractions containing highly purified mitochondria were washed twice with 250 mM sucrose, 10 mM HEPES KOH, pH 7.4, 100 µM EGTA by centrifugation at 7,000 x g for 10 min. Washed mitochondria were then recovered from the pellet and resuspended in 200 µl of the washing buffer.

Western blotting

Extracts were separated in 10% polyacrylamide SDS gels and trans-blotted onto a nitrocellulose membrane (Schleicher & Schuell, Bottmingen, Germany). The membrane was blocked with 5% ft-free milk powder in TBS buffer (150 mM NaCl, 25 mM Tris-HCl, pH 7.4) for 1 h at room temperature. After washing for 30 min, membranes were incubated with 1:5,000 diluted anti-CRT peptide antibodies in TBS buffer for 2 h at room temperature. After washing with TBS buffer, the blot was incubated again with a 1:10,000 dilution of goat horseradish peroxidase-conjugated anti-rabbit secondary antibody (Amersham Biosciences). The immunoreactive bands were visualized using the Renaissance Western blot chemiluminescence reagent plus kit (PerkinElmer Life Sciences).

Isolation of outer and inner membrane from rat liver mitochondria

The isolation of the mitochondrial membranes was done according to Ref. 41. Briefly, rats were anesthetized with diethyl ether and killed by cervical dislocation. The liver was taken and immediately transferred to ice-cold homogenization buffer (250 mM sucrose, 10 mM HEPES-KOH, pH 7.4, 0.5% bovine serum albumin, 1 mM EDTA) and freed from fat and connective tissue. The tissue was homogenized using a glass-Teflon potter in homogenization buffer at 0 °C. Nuclei and cell debris were pelleted by centrifugation at 700 _ g for 10 min, and crude mitochondria were pelleted from the post-nuclear supernatant by centrifugation at 7,000 x g for 10 min. Enriched mitochondria were resuspended in 250 mM sucrose, 10 mM HEPES-KOH, pH 7.4, 0.1 mM EGTA and purified in a 25% PercollTM density gradient. Highly enriched mitochondria were carefully collected from the gradient and washed twice in sucrose/HEPES buffer. Protein determination was performed with the BCL Kit from Pierce. Fifty mg of mitochondria were then resuspended in 6 ml of 10 mM KH_2PO_4 buffer, pH 7.5, at 0 °C. After 15 min to allow swelling, 6 ml of 10 mM KH_2PO_4 containing 30% sucrose, 30% glycerol, 10 mM $MgCl_2$, 4 mM ATP were added. After 60 min of incubation at 0 °C to allow shrinking (turbidity appears) the mitochondrial suspension was treated with sonic oscillation using a Brandson device at position 3A for three times (cycles of 15 s each with 60 s between each cycle for cooling). A first crude inner membrane fraction was pelleted at 12,000 x g for 10 min. The pellet was resuspended in 3 ml of 10 mM KH_2PO_4 buffer. Pellet and supernatant were layered onto a discontinuous sucrosegradient consisting out of 51%, 37 and 25% sucrose and centrifuged in a swinging bucket rotor (SW 40) at 100,000 x g for at least 12 h at 4 °C. The clear top of the gradient contained the soluble protein fraction, the 25–37% interphase contained the light outer membrane subfraction, and the 37–51% interphase contained the pure inner membrane subfraction. The membrane fractions were collected carefully from the gradient, diluted 1:10 in sucrose/HEPES buffer, and pelletedat 100,000 x g, 4 °C for 1 h. The pellets were solubilized in sucrose/ HEPES containing 0.01% SDS and analyzed.

Immunolabeling and negative staining of isolated mitochondria

Mitochondria (0.5 mg/ml) were incubated for 1 h at room temperature with anti-CRT peptide antibody under a variety of osmotic conditions (between 50 and 250 mOsmol/kg). Subsequently, these mitochondria were washed with buffer containing 250 mM sucrose, 10 mM HEPES-KOH, pH 7.4, 100 µM EGTA and incubated with protein A-10 nm colloidal gold. After several washing steps, a drop of the mitochondrial suspension was transferred onto a carbon-coated electron microscope grid and washed with 2% ammonium molybdate as negative stain (250 mosmol, pH 7.4). The grid was blotted with Whatman Filter #1 and air-dried (42, 43). Pictures of negatively stained mitochondria were then taken in a transmission

electron microscope JEOL100 at 80 kV. Counting of gold grains was automated with the NIH-image program. Analysis of variance statistics was done with Origin 4.1 software.

Measurement of Cr transport into mitochondria

Standard conditions — All Cr uptake assays were performed at room temperature using highly enriched, PercollTM gradient-purified mitochondrial preparations (adjusted to 10 mg ml^{-1} protein concentration). The reaction was started by the addition of 10 µl of the mitochondria suspension to 90 µl of transport buffer (10 mM Tris/HCl, pH 7.4, supplemented with 250 mM sucrose, 20 mM Cr, and 5 µCi ml^{-1} [^{14}C] Cr (American Radiolabeled Chemicals), 10 µCi ml^{-1} [^{3}H] sucrose, 5 mM succinate/Tris, 2 µM rotenone, 2 mM $MgCl_2$, 10 mM Pi/Tris, 100 µM EGTA, and 2 mM ADP).

Time course measurement — Cr uptake was stopped after 1.5, 2.5, 3.5, 6, 7.5, 10, 15, and 20 min, respectively, and the amount of Cr taken up was plotted against time (Fig. 6A).

K_m and V_{max} determination — Cr uptake was determined as a function of Cr concentration at room temperature for 3 min at 0.53, 1, 2, 10, and 20 mM Cr, respectively, and fitted to an Eadie-Hofstee plot (Fig. 6B).

NEM, DTNB, and DNFB inhibition — Mitochondria were preincubated for 10 min at room temperature with increasing concentrations of NEM, DTNB, or DNFB followed by uptake measurements for 15 min under standard conditions.

Dependence on membrane potential — Cr transport assays were performed under standard conditions but without succinate and ADP. Mitochondrial substrates (5 mM succinate, 1 mM ADP) and uncoupler (100 nM FCCP) were added sequentially (Fig. 7).

Inhibition by anti-CRT antibodies — Mitochondria (100 µg/ml mitochondrial protein) were preincubated for 1h at 22 °C either in 250 mM or 50 mM sucrose alone or in 250 mM or 50 mM sucrose together with anti-CRT or preimmune serum (at 1:100 final dilution). Subsequently, mitochondria were washed three times in 250 mM sucrose, 10 mM Tris/HCl, pH 7.4, 0.1 mM EDTA, and uptake was measured understandard conditions.

Competitive Cr uptake measurements — Transport was measured in buffer containing 10 mM Tris/HCl, pH 7.4, supplemented with 250 mM sucrose and 5 µCi ml^{-1} [^{14}C] Cr, 10 µCi ml^{-1} [^{3}H] sucrose, 2 µM rotenone, 2 mM $MgCl_2$, 10 mM Pi/Tris, and 100 µM EGTA (serving as control), and in the additional presence of 1 mM concentration of each of either PCr, Cr analogues, other guanidino compounds, amino acids, or related compounds added as potential competitors or inhibitors (see Table I). In all cases, Cr uptake was stopped by a quick centrifugation step at 16,000 x g for 1 min and removal of the supernatant. The mitochondrial pellets were solubilized in 100 µl of 1% SDS and counted in 4 ml of scintillation mixture “Ultima Gold XR” (Packard) in a Packard 1500 Tri-CarbTM liquid scintillation counter. Double isotope measurement settings were 0–18 eV for the [^{3}H] isotope and 18–256 eV for the [^{14}C] isotope. The amount of Cr uptake was calculated as the difference of total Cr measured, subtracted by the Cr present in the sucrose accessible space.

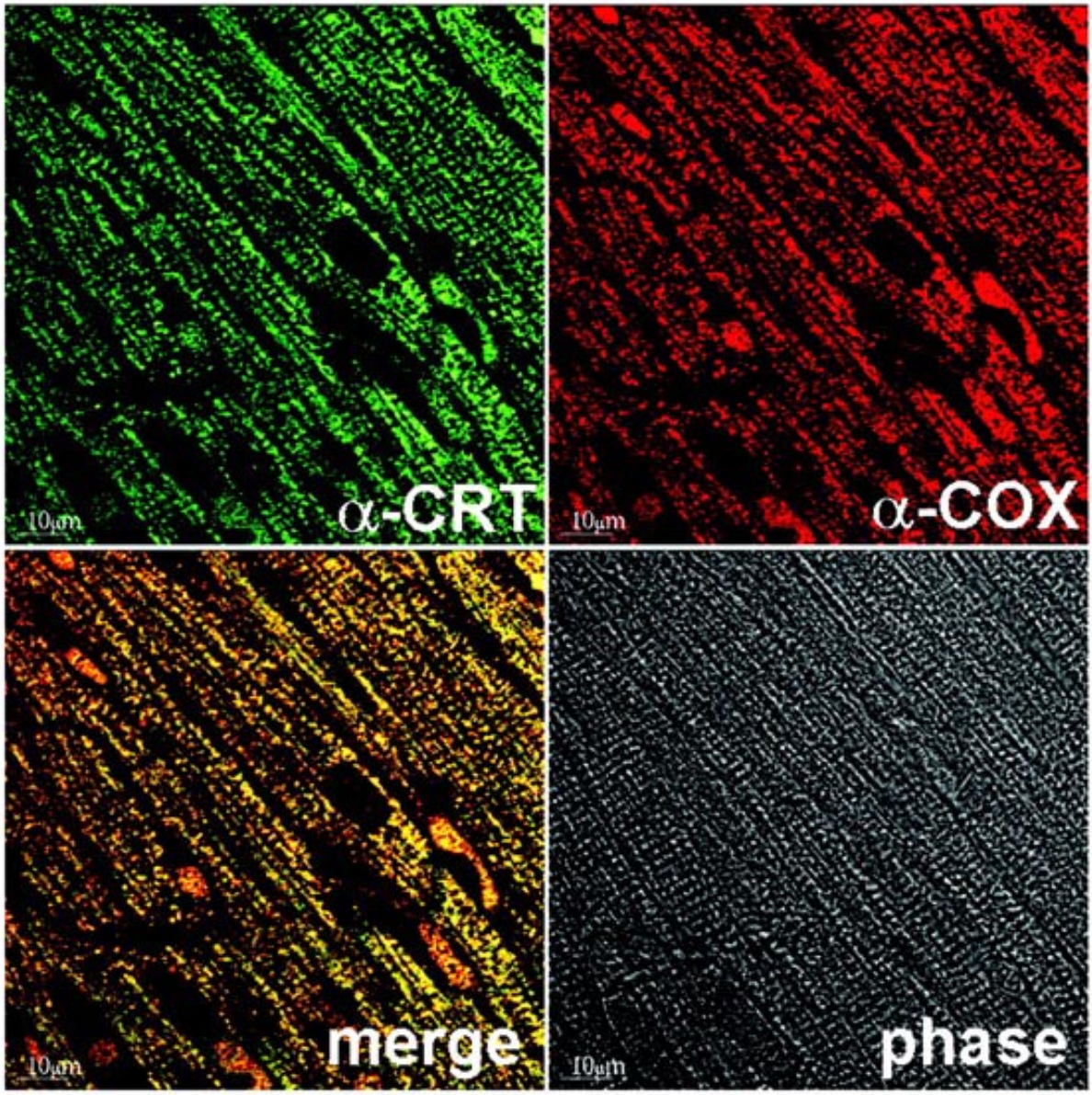

FIGURE 1 **Localization of CRT-related protein in rat heart by confocal microscopy.** Sections of 10 μm of paraffin-embedded rat left ventricle, after fixation and permeabilization (see "Experimental Procedures"), shown as phase contrast picture (phase, lower right), were stained for 1 h at room temperature with polyclonal rabbit anti-CRT peptide antibodies, followed by incubation for 1 h with fluorescein isothiocyanate-conjugated goat anti-rabbit IgG and double stained by a monoclonal mouse anti-COX antibody (_-COX) followed by a Cy3-conjugated donkey anti-mouse secondary antibody. The presence of CRT in mitochondria was verified by merging both fluorescence channels (merge). Sections were analyzed with a Leica TCS SP laser confocal microscope with a He/Ne/Ar laser and Leica scanning electronics and software. Image processing was done on a Silicon Graphics Iris 4D/25 work station, using Imaris (Bitplane AG) software.

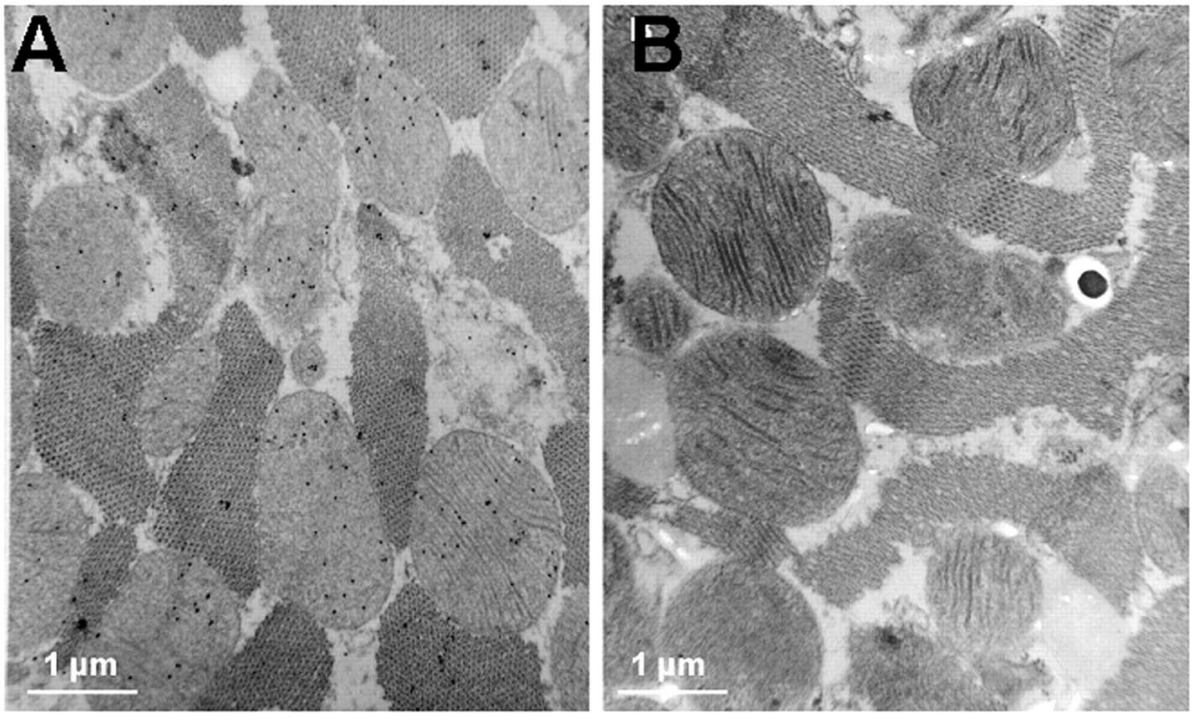

FIGURE 2 **Intracellular localization of CRT-related protein in rat heart by immunoelectron microscopy**. Rat left ventricles were fixed in 2.5% glutaraldehyde and embedded in Epon. Sections of 80–100 nm were cut and adsorbed onto carbon-coated electron microscope grids, treated with saturated sodium per-jodate, and boiled in 10 mM citric acid NaOH at pH 6 and subsequently labeled for 1 h at room temperature with polyclonal rabbit anti-CRT peptide antibodies (A) or preimmune serum (B), followed by a 1-h incubation with a goat antirabbit IgG conjugated to 10 nm colloidal gold. Pictures were taken by a transmission electron microscope (JEOL, Aksihima, Tokyo, Japan).

Results

Intracellular location of CRT in rat heart

Indirect immunofluorescence staining of rat heart sections with anti-CRT antibodies directed against a 15-mer C-terminal peptide of CRT revealed a predominantly intracellular localization of CRT-related protein (Fig. 1, α-CRT). The spotted pattern of the immunofluorescence signal suggests that the distribution of the protein within the cell is not homogeneous and might be associated to intracellular organelles. The remarkably ordered and regular alignment of small, anti-CRT-positive spots along the contractile apparatus suggests a periodic association with regular structures of the myofibrillar apparatus that is typical for mitochondria in muscle. Co-staining with the mitochondrial marker COX, a mitochondrial trans-membrane protein and thus a marker for mitochondria (24), indeed displayed an identical immuno fluorescence pattern (Fig. 1, α-COX), as indicated by the co-localization of anti-CRT and anti-COX staining (Fig. 1, merge). Essentially the same immunolocalization was obtained also with antibodies directed against a 15-mer N-terminal synthetic peptide of CRT (12) (not shown).

To precisely identify the site(s) of intracellular CRT localization, we performed immunoelectron microscopy studies on sections of the adult rat myocardium, treated with anti-CRT antibodies followed by colloidal gold-conjugated secondary antibodies. Fig. 2A clearly demonstrates specific labeling of mitochondria by anti-CRT antibodies that are evenly distributed within the muscle fibers, with some non-mitochondrial and otherwise very low background staining, as compared with staining with preimmune serum (Fig. 2B).

Expression of CRT-related Polypeptides in Mitochondria from Different Organs

Next, we examined whether CRT was expressed in mitochondria of different tissues by Western blotting. In the experiments reported in Fig. 3, protein extracts of mitochondria (m) from brain, heart, kidney, and liver were separated in SDS-PAGE together with the corresponding cytosolic fractions (c) and total tissue extracts (t), transferred to nitrocellulose membranes and probed with two different anti- CRT antisera raised against synthetic peptides corresponding to the C-terminal (A) and N-terminal (B) sequences of the cDNA-derived CRT sequence (12). Mitochondrial purification was assessed in parallel with an anti-COX antibody (C). The result clearly demonstrates that the ~55- and ~70-kDa CRTrelated proteins are both recognized by both the anti-N-terminal, as well as the anti-C-terminal, CRT antibodies (12) and that both of these immunoreactive polypeptides are predominantly localized in mitochondria of all tissues tested, where they are highly enriched relative to the total extracts.

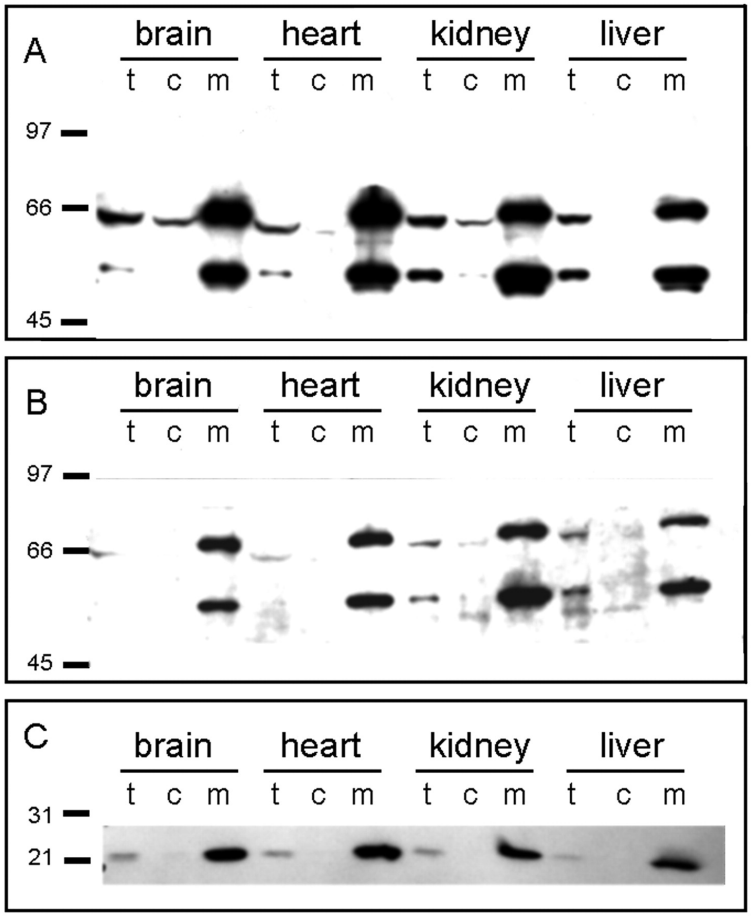

FIGURE 3 **Immunoreactivity of rabbit anti-CRT antibodies.** Immunoblots of total tissue extracts (t) of brain, heart, kidney, and liver, together with the corresponding cytoplasmic fractions (c) and mitochondria (m), were electroblotted and probed with polyclonal rabbit anti-CRT synthetic peptide antibodies. Antibodies used were rabbit anti-rat C-terminal CRT-peptide antibody (A), and anti-N-terminal CRT-peptide antibodies (B), as well as a monoclonal anti-COX mouse antibody (C). In each lane 5 µg of protein was loaded.

Intramitochondrial location of CRT-related proteins

To assess the distribution of the CRT protein within mitochondria, purified rat liver mitochondria were ruptured by osmotic swelling and ultrasonic treatment. Heavy (inner) and lighter (outer) mitochondrial membranes, as well as soluble, non-membraneassociated proteins were separated in sucrose step gradients, and the corresponding protein extracts were finally analyzed by anti-CRT Western blots (Fig. 4). The experiments shown in this figure revealed that both CRT-related polypeptides were highly enriched in the heavy (inner) membrane fraction (lane MIM), while the light (outer) membrane fraction (lane MOM) and the soluble matrix fraction (lane MX) contained virtually no immunoreactive signal. The relative enrichment of the CRT proteins in the heavy fraction can be easily appreciated from a comparison of the signal in the total liver homogenate (Fig 4A, lane liver) and in the inner membrane fraction (Fig. 4, lane MIM). Mitochondrial marker antibodies against COX, as well as against voltage-dependent anion channel (VDAC) were used to probe for mitochondrial inner and outer membrane, respectively.

To confirm the submitochondrial localization of CRT with an independent approach, its accessibility to anti-CRT antibody was determined before and after osmotic rupture of the outer membrane. Mitochondria were incubated with the anti-CRT antibody either in iso-osmolar (250 mM sucrose) or hypo-osmolar medium (50 mM sucrose), followed by antibody detection with protein A-gold (10 nm), using a negative staining technique on whole mitochondria. As shown in Fig. 5, hypo-osmotic treatment caused the formation of peripheral vesicles of outer membrane (arrowheads in A and B), while the inner membrane cristae were still conserved. Significant anti- CRT antibody labeling was seen only under hypo-osmotic conditions and was particularly prominent at the inner membrane (A). Labeling was specific, since it was not observed after treatment with preimmune serum (B), while under iso-osmolar conditions only a few gold particles were seen on the surface of mitochondria (C). Quantification and statistical analysis of the number of gold grains confirmed that significant mitochondrial staining was only seen under Heart, liver, and kidney mitochondria were isolated and carefully purified with PercollTM density gradients to minimize contamination with plasma membrane vesicles and other membranes or organelles. These mitochondria were tested for their ability to accumulate Cr by incubating them in sucrose buffer containing ^{14}C-labeled Cr in a total concentration of 20 mM Cr, which is close to the physiological range for working muscle (2, 3).

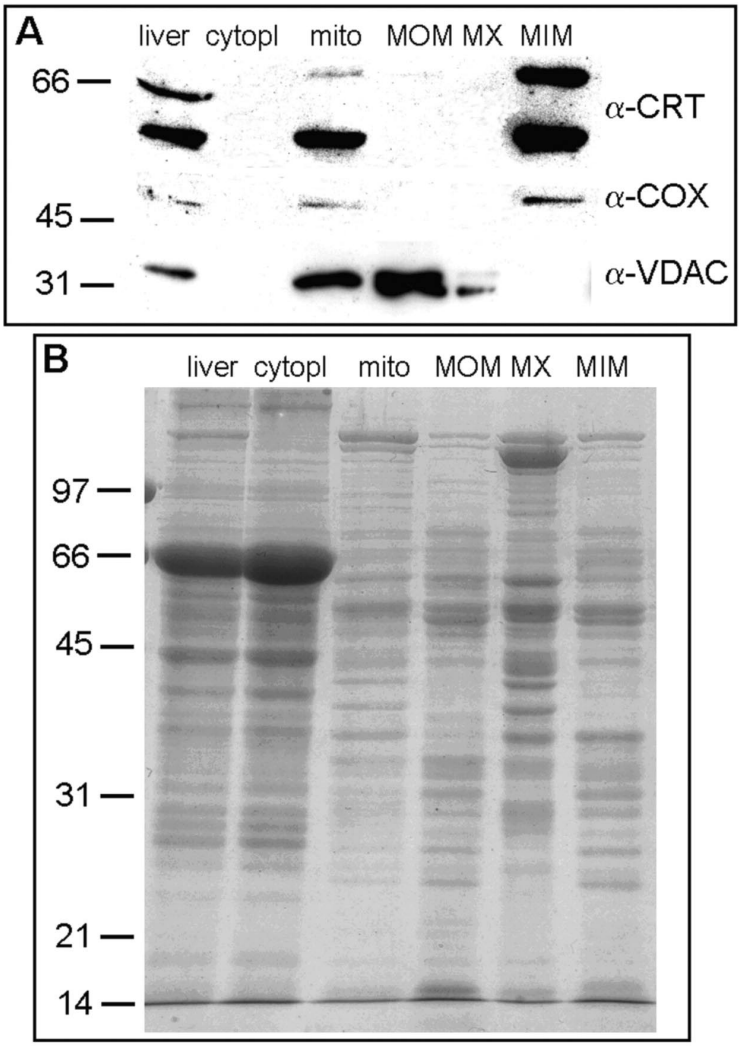

FIGURE 4 **Submitochondrial localization of CRT-related protein by fractionation of mitochondrial membranes**. Rat liver mitochondria were ruptured by a repeated swelling and shrinking procedure followed by ultrasonic treatment according to Ref. 41. Soluble matrix proteins, lighter (outer), as well as heavy (inner), mitochondrial membranes were separated in discontinuous sucrose density gradients and analyzed. The Western blot (10 µg of protein per lane) shows an anti-CRT immunoblot of protein extracts from rat liver total homogenate (liver), soluble cytosolic proteins (cytopl), rat liver mitochondria (mito), mitochondrial outer membrane (MOM), soluble mitochondrial matrix proteins (MX), as well as mitochondrial inner membrane (MIM), indicating the strongest anti-CRT signal in this mitochondrial inner membrane fraction. As controls, anti-COX and anti-voltage-dependent anion channel (α-VDAC) antibodies were used to identify mitochondrial inner and outer membrane, respectively.

Fig. 6 shows that heart, liver, and kidney mitochondria take up Cr with similar kinetics, in a process that leveled off after about 5 min (A). Cr association with the mitochondrial pellet reflected a true transport process, because Cr was sequestered into a sucrose-inaccessible space, as assessed by inclusion of ^{3}H-labeled sucrose into the incubation buffer. The absolute amounts of Cr taken up by heart (Fig. 6A, filled squares), liver (open circles), and

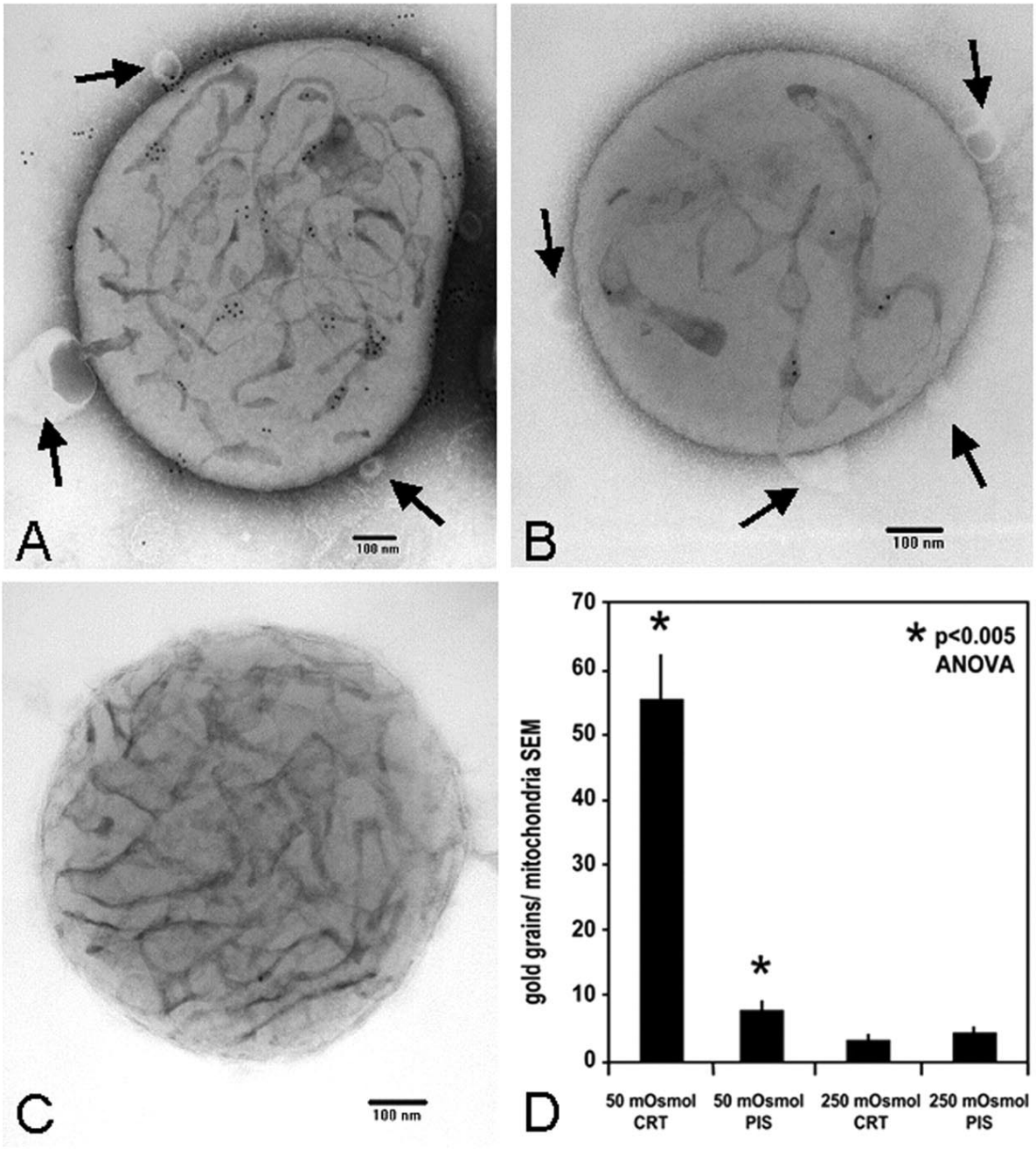

FIGURE 5 **Intramitochondrial localization of CRT-related protein by immunoelectron microscopy.** Rat liver mitochondria (1 mg/ml) were incubated for 1 h at room temperature at different osmolarities with polyclonal rabbit anti-CRT peptide antibody (1:200 dilution) or preimmune serum. Mitochondria were washed three times and incubated for 1 h with protein A-labeled colloidal gold (10 nm) and washed again three times. Mitochondria were then negatively stained with 2% ammonium molybdate, pH 7.4. A, 50 mosmol/kg with anti-CRT peptide antibody; B, 50 mosmol/kg with preimmune serum; C, 250 mosmol/kg with anti-CRT peptide antibody; D, means of gold grains counted per mitochondrion, with 20 mitochondria from two experiments of each condition, were analyzed and plotted accordingly.

kidney mitochondria (open triangles) were about 12, 16, and 19 nmol mg^{-1} mitochondrial protein. Cr uptake followed saturation kinetics with an apparent K_m and V_{max} for Cr transport of 15.90 (± 1.32) mM and 11.79 (± 1.15) nmol mg^{-1} mitochondrial protein min^{-1}, respectively (B). Since creatine uptake is approximately linear over the first 5 min, and because of the rather high S.D. values of initial rate measurements, we determined the initial rates of creatine uptake over the first 3 min.

To address the question of whether Cr uptake into mitochondria could be due to simple diffusion through the inner mitochondrial membrane, or whether it is indeed mediated by a transporter protein, we tested the effect of different sulfhydryl-modifying reagents, like DTNB, DNFB, and NEM. These reagents have been tested earlier for their ability to inhibit enzymatic activities at rather low concentrations (25–27). In our experiments, DTNB and DNFB had rather little effect on Cr uptake. By contrast, NEM inhibited Cr transport significantly in a dose-dependent manner (Fig. 6C). Preincubation of rat heart mitochondria for 10 min in a sucrose medium containing 100 μM NEM decreased Cr uptake by more than 50% of control rates.

The data shown in Fig. 7 demonstrate that Cr uptake is at least in part dependent on the energetic state of mitochondria, that is, energized rat heart mitochondria (5 mM succinate) showed ~20% higher Cr transport activity as compared with partially uncoupled mitochondria (1 mM ADP), whereas the addition of the uncoupler, FCCP, which completely abolishes the mitochondrial membrane potential, led to a ~35% decrease in Cr transport activity, as compared with control rates.

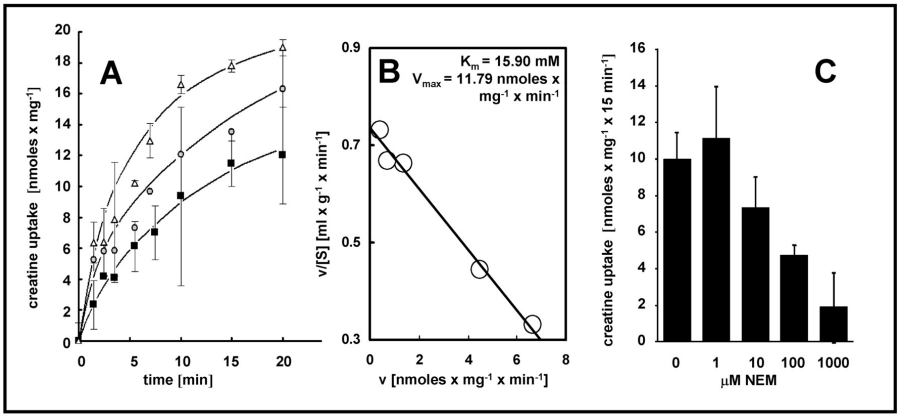

FIGURE 6. **Mitochondrial Cr uptake**. Time course experiments of Cr uptake (A) into isolated mitochondria from rat kidney, liver, and heart, measured at 20 mM external Cr concentration at room temperature in the presence of substrates for oxidative phosphorylation plus ADP. The amount of Cr uptake is expressed as nmol mg^{-1} mitochondrial protein. The graphs correspond to mitochondria from heart (filled black squares), liver (open circles), and kidney (open triangles). Initial rates of Cr uptake were measured for 3 min as a function of Cr concentration at room temperature at 0.53, 1, 2, 10, and 20 mM Cr, respectively. Values are means ± S.E. of measurements from two individual animals in each of which Cr transport was measured in triplicate. Cr uptake values were fitted to Eadie-Hofstee plot (B). Mean (± S.E.) Km and Vmax values fitted from each individual uptake curve were 15.90 (±1.32) mM and 11.79 (±1.15) nmol mg^{-1} mitochondrial protein min^{-1}, respectively. C illustrates inhibition by NEM of Cr uptake into isolated rat heart mitochondria measured for 15 min. Aliquots of mitochondria were preincubated for 10 min with increasing concentrations of NEM, followed by Cr uptake measurements. The amount of Cr uptake is expressed as nmol of Cr mg^{-1} total mitochondrial protein x 15 min^{-1}.

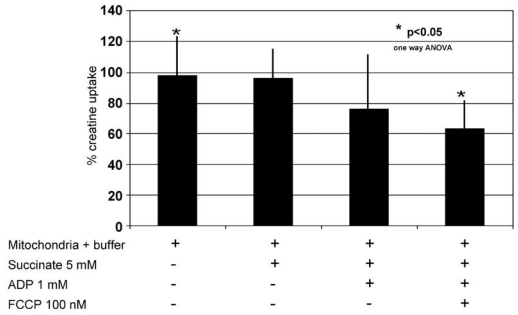

FIGURE 7. **Dependence on mitochondrial membrane potential**. Cr uptake assays were performed at room temperature using highly enriched, PercollTM gradient-purified mitochondrial preparations in transport buffer containing 10 mM Tris/HCl, pH 7.4, supplemented with 250 mM sucrose, 20 mM Cr, and 5 µCi ml^{-1} [^{14}C] Cr, 10 µCi ml^{-1} [^{3}H] sucrose, 2 µM rotenone, 2 mM $MgCl_2$, 10 mM Pi/Tris, 100 µM EGTA at room temperature. Substrates (5 mM succinate, 1 mM ADP) and uncoupler, (FCCP, at final concentration of 100 nM) were added as indicated.

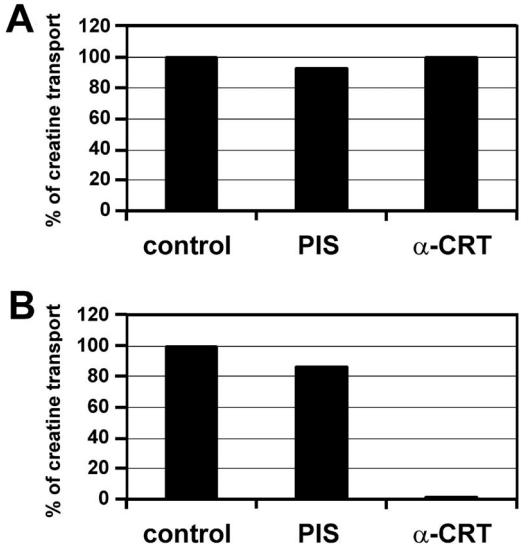

FIGURE 8. **Inhibition of mitochondrial Cr uptake by anti-CRT antibodies**. Mitochondria were pretreated for 1 h at 22 °C in 250 mM (iso-osmotic condition (A) or 50 mM sucrose (hypo-osmotic condition) (B) together with rabbit anti-CRT C-terminal peptide serum, preimmune serum (PIS), or with the same volume of the corresponding sucrose buffer only (control). Subsequently, mitochondria were washed three times with 250 mM sucrose, 10 mM Tris/HCl, pH 7.4, 0.1 mM EDTA and Cr transport assays performed as described in the legend to Fig. 6.

Mitochondrial Cr transport activity was significantly inhibited by the related guanidino compound, arginine, as well as by the amino acid, lysine, but not so by other Cr analogues or amino acids (see Table I). Interestingly, no inhibition of mitochondrial CRT was seen with β-GPA that is known to significantly inhibit sarcolemmal CRT (12, 15).

Finally, the link between the CRT mitochondrial proteins and Cr transport was addressed in the experiments shown in Fig. 8, where incubation of mitochondria with anti-CRT antibody completely inhibited Cr transport in hypo-osmotically treated mitochondria (B, β-CRT column), while uptake was unaffected in iso-osmotic sucrose media (A). These experiments complement the subcellular and submitochondrial localization studies by immunofluorescence and immunoelectron microscopy, respectively, and strongly support the suggestion that mitochondrial Cr transport is likely to be mediated by the ~55 and ~70 CRT-related polypeptides residing in the inner mitochondrial membrane.

Compound	Average	± S.E.	Significance	*n*
	nmol Cr × mg^{-1}			
Control	**19.0**	**± 4.9**		**14**
PCr	**17.1**	**± 6.6**	***p* > 0.3**	**8**
Creatinine	**22.2**	**± 7.9**	***p* > 0.3**	**3**
Cyclo-creatine	**17.7**	**± 1.0**	***p* > 0.3**	**3**
β-GPA	**19.9**	**± 2.2**	***p* > 0.3**	**5**
Arginine	**14.4**	**± 4.4**	***p* < 0.03**	**14**
Lysine	**15.2**	**± 3.8**	***p* < 0.04**	**13**
Proline	**21.6**	**± 2.9**	***p* > 0.3**	**11**
Glutamine	**18.6**	**± 6.3**	***p* > 0.3**	**10**
Ornithine	**16.7**	**± 2.0**	***p* > 0.3**	**3**
Citrulline	**20.0**	**± 1.7**	***p* > 0.3**	**3**
GABA	**16.2**	**± 5.8**	***p* > 0.3**	**4**

TABLE I **Inhibition of Cr uptake by structurally related compounds** Inhibition of uptake of radioactive creatine into mitochondria by various creatine analogues, related guanidino compounds, and amino acids was measured. The Cr uptake assays were performed at room temperature using highly enriched, Percoll™ gradient-purified mitochondrial preparations in transport buffer containing 10 mM Tris/HCl, pH 7.4, supplemented with 250 mM sucrose and 5 μCi ml^{-1} [^{14}C] Cr, 10 μCi ml^{-1} [^{3}H] sucrose, 2 μM rotenone, 2 mM $MgCl_2$, 10 mM Pi/Tris, and 100 μM EGTA (serving as control) and in the presence of 1 mM concentration each of either of the compounds indicated. Statistical evaluation of the measurements (n = number of independent measurements) was done by one way analysis of variance (significance level: 0.05; reached by arginine (< 0.03) and lysine (< 0.04)). GABA, γ-aminobutyric acid.

Discussion

In this paper, we have shown (i) that the two major CRTrelated protein species of ~55 and ~70 kDa, which have been independently identified earlier by various groups (11–16), are associated with the inner mitochondrial membrane, as demonstrated here by immunofluorescence and immunoelectron mi- croscopy, as well as by Western blotting with antibodies made against synthetic N- and C-terminal peptides of CRT and (ii) that heart, kidney, and liver mitochondria are able to transport Cr through a saturable transport system that can be inhibited by the sulfhydryl reagent NEM. Since, after outer membrane rupture, Cr transport could also be completely blocked by anti-CRT antibodies, we suggest that mitochondrial Cr transport is mediated by the ~55- and/or ~70-kDa polypeptide species recognized as the two major signals by anti-N-terminal, as well as anti-C-terminal, anti-CRT antibodies. Although molecular identification of these species as *bona fide* mitochondrial Cr transporter(s) must await purification and reconstitution of these mitochondrial protein(s), as well as protein sequencing of the immunoreactive polypeptides, our results have established that Cr is transported in mitochondria through a specific carrier system. The presented data also indicate that mitochondrial Cr uptake is dependent at least in part on the energetic state of mitochondria and that this Cr transport can be competitively inhibited by arginine and to a lesser extent also by lysine, but not by other Cr analogues or related compounds. This new data provide an explanation for several intriguing findings in the literature and have important implications for our current understanding of intracellular compartmentation of high energy

compounds. Indeed, our results suggest that mitochondria may participate in energy metabolism by regulation of the intracellular distribution of Cr.

CRT isoforms

The classical plasma membrane CRT that is responsible for high affinity uptake of Cr into cells has recently been shown to represent only a minor CRT isoform, in quantitative terms, with an apparent molecular mass of ~58 kDa (15) (see Fig. 9). Often, a polypeptide of unknown identity, showing an apparent molecular mass of 120–130 kDa, has also been recognized by our antibodies as a weak signal in total tissue homogenates (12, 15). The ~58-kDa polypeptides, in contrast to the two mitochondrial polypeptide species of ~55 and ~70 kDa referred to here, is hardly visible on Western blots of total tissue extracts, but can be enriched in preparations of purified plasma membranes, as well as in erythrocytes, but is absent in mitochondria (15). Besides this latter minor CRT species residing in the plasma membrane, we propose here that the two major CRT-related protein species of ~55 and ~70 kDa are residing inside mitochondria in the inner mitochondrial membrane (Fig. 9).

Mitochondrial location of the two major CRT-related protein species

The results obtained from our immunofluorescence studies, as well as immunoelectron microscopic analysis, demonstrate a predominantly mitochondrial location of the two major CRT-related proteins of ~55 and ~70 kDa in heart (Figs. 1 and 2), consistent with earlier results obtained from immunofluorescence work on cross-sections of rat skeletal muscle and myocytes in culture (15). A mitochondrial localization of CRT is independently supported by the finding that slow type-I oxidative muscle fibers stained consistently stronger with anti- CRT antibodies as compared with fast type-II glycolytic fibers (16). This can be explained by the fact that mitochondrial content and volume fraction are significantly higher in type-I *versus* type-II muscle fibers. In addition, the Western blot studies presented here, using isolated mitochondria from rat heart, liver, kidney, and brain, clearly demonstrated an enrichment of both major CRT-related polypeptides in these organelles, which apparently are the mayor site of CRT accumulation. Since the results obtained with liver, brain, and kidney were qualitatively similar to those of cardiac and skeletal muscle, mitochondrial CRT expression is predominant not only in sarcomeric muscle but also in non-muscle tissues, including the liver, which itself is the major organ of Cr biosynthesis (2).

We could further demonstrate that CRT-related polypeptides are exclusively localized in the inner mitochondrial membrane as would be expected for a mitochondrial transporter. Indeed, immunogold labeling of mitochondria was only observed after the outer membrane was permeabilized by hypotonic buffers, and mitochondrial fractionation confirmed that both proteins were highly enriched in the heavy inner membrane fraction that also contained COX subunit I. Additionally, and as would be expected for an integral membrane protein, no CRT was detectable in the soluble fractions of cell homogenates and mitochondria. As judged from the sequence data, no mitochondrial pre- or leader sequence seems to be present in CRT such that the protein would have to find its way into mitochondria by internal sequences that are likely facilitating the import and insertion of CRT(s) into the inner mitochondrial membrane, as, for example, has been shown to be the case also for adenine nucleotide translocase (28), as well as for other mitochondrial membrane proteins (29).

Mitochondrial transport of Cr

Consistent with the presence of an inner membrane Cr transporter, our studies with isolated mitochondria, using ^{14}C-labeled Cr, provide strong evidence that mitochondria are indeed able to accumulate Cr. The apparent K_m of ~15 mM may appear high, but it does in fact match the physiological range of intracellular Cr concentration in muscle (2, 3) (see Fig. 9). Assuming that 1 mg of mitochondrial protein corresponds to a matrix volume of 1 _l, intramitochondrial Cr may reach concentrations of the order of 20 mM. Strong evidence that Cr transport is mediated by a carrier protein comes from the fact that Cr transport activity is inhibited by the sulfhydryl-modifying agent, NEM, which also inhibits a number of other mitochondrial carriers, including the Pi carrier (30). The fact that DTNB and DNFB turned out

to be less inhibitory for mitochondrial Cr uptake than NEM may be explained by accessibility problems due to the larger molecular size and greater hydrophobicity of the former compounds compared with NEM. Interestingly enough, our inhibition studies of mitochondrial Cr transport with creatine analogues, as well as related guanidine compounds, amino acids, and other substrates of the 12-membrane-spanning neurotransmitter transporter family, to which CRT belongs to, indicate that mitochondrial CRT, in contrast to sarcolemmal CRT, seems not to be entirely specific for Cr alone, since arginine and to some extent also lysine showed significant inhibition of Cr uptake. (Table I). The observed difference of inhibition by β-GPA between the plasma membrane CRT (see Refs. 12 and 15) and the mitochondrial CRT, the latter remaining unaffected by this Cr-analogue, indicates that these related CRT isoforms differ in their transport characteristics (Km for Cr) (15), substrate specificity, and susceptibility toward inhibitors, like β-GPA (12, 15). Evidence that the transport activity is mediated by the ~55/ ~70-kDa CRT-related polypeptide species rests on the inhibitory effects of the specific polyclonal anti-CRT antibodies on Cr transport into mitochondria, where a complete blockage of Cr uptake was observed in mitochondria after the outer membrane had been permeabilized by preincubation of mitochondria under hypotonic conditions (Fig. 8), a finding that matches inner membrane staining by the same antibodies (Figs. 4 and 5). As mentioned above, the final molecular identification of the ~55/~70-kDa polypeptide species as the *bona fide* mitochondrial Cr transporters must await purification, sequencing, and reconstitution of these minor mitochondrial protein. The present observations represent an essential step toward this goal.

Implications for Cr compartmentation

These new results shed some light on the possible existence of an intramitochondrial pool of Cr and/or PCr (Fig. 9) and thus may account for a set of interesting earlier observations. For example, during recovery after exhaustive exercise in oxidative type-I, but not in glycolytic type-II muscle fibers (31), the overall PCr concentrations display an overshoot, which may be explained by an accumulation of Cr within mitochondria, which would be trans-phosphorylated to PCr via mitochondrial creatine kinase, suggesting the existence of a PCr/Cr compartment that may be displaced from the overall creatine kinase equilibrium, at least temporarily (32). Earlier observations, showing that mitochondrial Cr content differed considerably in resting as compared with fatigued muscle, suggested that there may be a traffic of Cr across the mitochondrial inner membrane (18). Recent data with skinned muscle fibers indicated that no further Cr can be specifically released from mitochondria of these fibers after their permeabilization with detergents (33). However, an accumulation of PCr in mitochondria is supported by experiments with cell cultures, where isolated mitochondria from cells, after growth factor withdrawal, showed an over 100-fold higher PCr content than control cells (34).

Since our Cr uptake studies with isolated mitochondria were done in the presence of mitochondrial substrates under conditions favoring maximal respiration, it is entirely conceivable that Cr uptake, and possibly also the maintenance of a mitochondrial Cr pool within mitochondria, may depend on the energy charge of mitochondria, *e.g.* would only be observable in actively respiring mitochondria. This is corroborated by our data showing that mitochondrial Cr uptake into isolated mitochondria is significantly hampered after addition of uncoupling agents. The existence of localized creatine kinase isoenzymes forming functionally coupled subcellular microcompartments with ATP-generating and ATP-utilizing processes, possibly involving distinct PCr/Cr pools (3), is also supported by studies on transgenic mice that lack both sarcomeric and mitochondrial creatine kinase (35), which no longer show Cr-stimulated mitochondrial respiration (36). The idea that CRT(s), as well as the creatine kinase substrates themselves, may be compartmentalized has recently gained additional support from *in vivo* experiments. [^{14}C] Cr isotope infusion of fish under different metabolic conditions (resting, actively swimming, exhausted, and recovering), followed by freeze-clamping and analysis of the specific radioactivity of the Cr and PCr pools, showed that a significant fraction of cellular Cr is not freely and rapidly exchanging with exogenously added radioactive Cr and that creatine kinase may not have immediate access to the total pool of PCr and Cr (20), a finding that strongly suggests the existence of at least some

separate intracellular Cr pool(s). Finally, the data presented in this work may provide a likely explanation for the unexpected and anomalous NMR behavior of Cr and of creatine kinase flux measurements *in vivo*, as obtained by ^{1}H NMR (23) and ^{31}P NMR (21, 22, 37), respectively. Finally, experiments with isolated mitochondria to which either PCr, Cr, or none of both had been added showed a rather high Cr background in the latter samples, which was referred to by the authors (46) as "unexplained interference," which in hindsight was probably due to the presence of Cr in freshly isolated mitochondria (18, 19), which, however, was rapidly lost with time, as was probably also the case for chemically skinned muscle fibers, where after the rather lengthy skinning procedure, no more Cr could be released from mitochondria (33). In summary, all these findings appear to imply the presence of intracellular pools of Cr and/or PCr that are not entirely in equilibrium with one another, with one of them likely being mitochondrial origin.

Conclusions and perspectives

A full understanding of the function and the purpose of mitochondrial Cr transport will obviously need a more detailed characterization of the process, as well as the proteins involved, *e.g.* by protein sequencing and thorough studies of the reconstituted CRT protein(s), work which is currently in progress. Open questions are also whether Cr transported into mitochondria is immediately recharged via mitochondrial creatine kinase to PCr (36, 38), *e.g.* for energetic purposes, or whether Cr, a highly abundant zwitterionic guanidino compound in the cytosol, could fulfill some protective role as an osmolyte to guarantee mitochondrial integrity under conditions of cellular stress. Interestingly enough, Cr has been shown to exert marked protection against Ca^{2+}-induced mitochondrial permeability transition pore opening (39), an early event of cellular apoptosis. The importance of assessing the pathway(s) and cellular location of Cr transport is further highlighted by a description of the first patients with an X-linked genetic disease due to defects of the CRT gene (SLC6A8) (40). These patients have a very low concentration of cerebral and cerebellar Cr and display some of the typical symptoms of Cr deficiency, such as general developmental defects and severe speech impairment, hypotonia, intractable epilepsia, with a disease progression eventually leading to brain atrophy (40). Assessing whether impaired mitochondrial transport of Cr is part of the pathogenetic mechanism appears to be of great value for understanding this disease and for fully appreciating the possible role of mitochondria in energy homeostasis beyond the strict requirement for ATP synthesis.

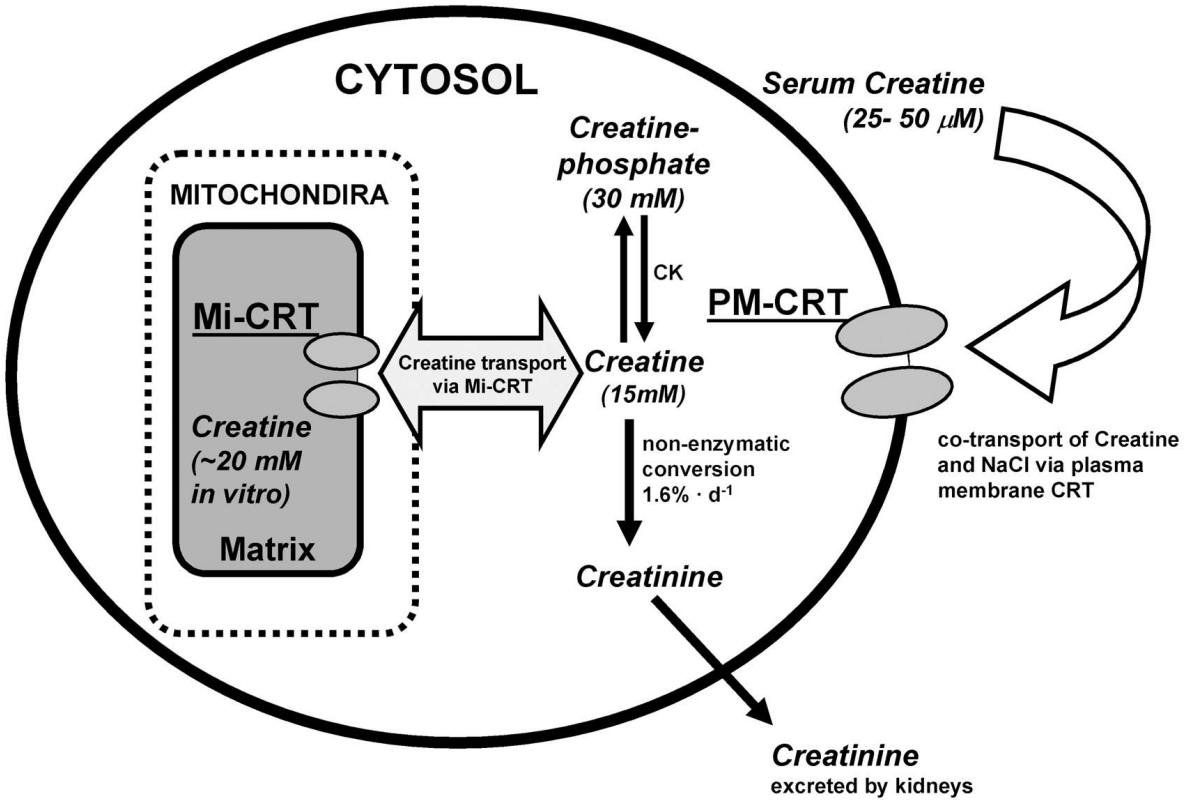

FIGURE 9 **General scheme of cellular Cr transport.** A compartmentation of three Cr pools, that is, in blood serum, cytosol, and mitochondria, are shown. These pools are interconnected via two different CRTs, the high affinity (low K_m) plasma membrane Cr transporter (*PM-CRT*) (15) and the low affinity (high K_m) mitochondrial Cr transporter(s) (*Mi-CRT*). The high Cr concentration gradient (300–600-fold) between serum and cytosol was maintained using an outside-in-directed NaCl gradient, which was used to co-transport Cr across the plasma membrane against a huge Cr concentration gradient. Two-thirds of the Cr that has entered the cytosol becomes transphosphorylated by the creatine kinase reaction to PCr, which is not a substrate of the plasma membrane CRT (44). The strict discrimination of the plasma membrane CRT between Cr and PCr leads to entrapment of PCr inside the cell, since PCr escapes equilibration. This thermodynamically facilitates further Cr uptake by the plasma membrane CRT and helps maintaining the enormous total Cr concentration gradient (600–1,000-fold) across the plasma membrane. The mitochondrial CRTs present in the inner mitochondrial membrane mediate Cr transport into mitochondria. All three Cr compartments are separated by biological membranes, impermeable for Cr and PCr, not being in equilibrium with each other via diffusion. These Cr transporters are likely to be regulated to mediate the exchange and channeling of Cr between these independent compartments, which may differ in their total Cr content, as well as in their PCr/Cr ratios according to their specific metabolic needs. The concentrations of PCr (30 mM) and Cr (15 mM) given here are those of a glycolytic fast twitch skeletal muscle (2, 3), with a typically very high Cr content.

References

1. Ellington, W. R. (2001) *Annu. Rev. Physiol.* 63, **289–325**
2. Wyss, M., and Kaddurah-Daouk, R. (2000) *Physiol. Rev.* 80, **1107–1213**
3. Wallimann, T., Wyss, M., Brdiczka, D., Nicolay, K., and Eppenberger, H. M. (1992) *Biochem. J.* 281, **21–40**
4. Fitch, C. D., and Shields, R. P. (1966) *J. Biol. Chem.* 241, **3611–3614**
5. Barnwell, L. F., Chaudhuri, G., and Townsel, J. G. (1995) *Gene* (*Amst.*) 159, **287–288**
6. Eichler, E. E., Lu, F., Shen, Y., Antonacci, R., Jurecic, V., Doggett, N. A., Moyzis, R. K., Baldini, A., Gibbs, R. A., and Nelson, D. L. (1996) *Hum. Mol. Genet.* 5, **899–912**
7. Iyer, G. S., Krahe, R., Goodwin, L. A., Doggett, N. A., Siciliano, M. J., Funanage, V. L., and Proujansky, R. (1996) *Genomics* 34, **143–146**
8. Nash, S. R., Giros, B., Kingsmore, S. F., Rochelle, J. M., Suter, S. T., Gregor, P., Seldin, M. F., and Caron, M. G. (1994) *Recept. Channels* 2, **165–174**
9. Sandoval, N., Bauer, D., Brenner, V., Coy, J. F., Drescher, B., Kioschis, P., Korn, B., Nyakatura, G., Poustka, A., Reichwald, K., Rosenthal, A., and Platzer, M. (1996) *Genomics* 35, **383–385**
10. Sora, I., Richman, J., Santoro, G., Wei, H., Wang, Y., Vanderah, T., Horvath, R., Nguyen, M., Waite, S., Roeske, W. R., and et al. (1994) *Biochem. Biophys. Res. Commun.* 204, **419–427**
11. Tran, T. T., Dai, W., and Sarkar, H. K. (2000) *J. Biol. Chem.* 275, **35708–35714**
12. Guerrero-Ontiveros, M. L., and Wallimann, T. (1998) *Mol. Cell. Biochem.* 184, **427–437**
13. Neubauer, S., Remkes, H., Spindler, M., Horn, M., Wiesmann, F., Prestle, J., Walzel, B., Ertl, G., Hasenfuss, G., and Wallimann, T. (1999) *Circulation* 100, **1847–1850**
14. Tarnopolsky, M. A., Parshad, A., Walzel, B., Schlattner, U., and Wallimann, T. (2001) *Muscle Nerve* 24, **682–688**
15. Walzel, B., Speer, O., Boehm, E., Kristiansen, S., Chan, S., Clarke, K., Magyar, J., Richter, E. A., and Wallimann, T. (2002) *Am. J. Physiol.* 283, **E390–E401**
16. Murphy, R., McConell, G., Cameron-Smith, D., Watt, K., Ackland, L., Walzel, B., Wallimann, T., and Snow, R. (2001) *Am. J. Physiol.* 280, **C415–C422**
17. Henry, H., O., Speer, O., Braissant, B., Eilers, C., Bachmann, A., and Wallimann, T. (2001) *Cell Biol. Int.* 25, **940**
18. Soboll, S., Conrad, A., Eistert, A., Herick, K., and Kramer, R. (1997) *Biochim. Biophys. Acta* 1320, **27–33**
19. Hebisch, S., Sies, H., and Soboll, S. (1986) *Pfluegers Arch.* 406, **20–24**
20. Hochachka, P. W., and Mossey, M. K. (1998) *Am. J. Physiol.* 274, **R868–R872**
21. Joubert, F., Gillet, B., Mazet, J. L., Mateo, P., Beloeil, J., and Hoerter, J. A. (2000) *Biophys. J.* 79, **1–13**
22. Joubert, F., Vrezas, I., Mateo, P., Gillet, B., Beloeil, J. C., Soboll, S., and Hoerter, J. A. (2001) *Biochemistry* 40, **2129–2137**
23. Kreis, R., Jung, B., Slotboom, J., Felblinger, J., and Boesch, C. (1999) *J. Magn. Reson.* 137, **350–357**
24. Iwata, S., Ostermeier, C., Ludwig, B., and Michel, H. (1995) *Nature* 376, **660–669**
25. Afolayan, A., and Daini, O. A. (1986) *Comp. Biochem. Physiol. B* 85, **463–468**
26. Wolfel, R., Halbrugge, T., and Graefe, K. H. (1989) *Br. J. Pharmacol.* 97, **1308–1314**
27. Yeung, C. H., Majumder, G. C., Rolf, C., Behre, H. M., and Cooper, T. G. (1996) *Mol. Hum. Reprod.* 2, **591–596**
28. Mozo, T., Fischer, K., Flugge, U. I., and Schmitz, U. K. (1995) *Plant J.* 7, **1015–1020**
29. Fiermonte, G., Dolce, V., Arrigoni, R., Runswick, M. J., Walker, J. E., and Palmieri, F. (1999) *Biochem. J.* 344 (Pt. 3), **953–960**
30. Kaplan, R. S., Pratt, R. D., and Pedersen, P. L. (1986) *J. Biol. Chem.* 261, **12767–12773**
31. Sahlin, K., Soderlund, K., Tonkonogi, M., and Hirakoba, K. (1997) *Am. J. Physiol.* 273, **C172–C178**
32. Wallimann, T. (1996) *J. Muscle Res. Cell Motil.* 17, **177–181**
33. Menin, L., Panchichkina, M., Keriel, C., Olivares, J., Braun, U., Seppet, E. K., and Saks, V. A. (2001) *Mol. Cell. Biochem.* 220, **149–159**
34. Vander Heiden, M. G., Chandel, N. S., Li, X. X., Schumacker, P. T., Colombini, M., and Thompson, C. B. (2000) *Proc. Natl. Acad. Sci. U. S. A.* 97, **4666–4671**
35. Steeghs, K., Oerlemans, F., de Haan, A., Heerschap, A., Verdoodt, L., de Bie, M., Ruitenbeek, W., Benders, A., Jost, C., van Deursen, J., Tullson, P., Terjung, R., Jap, P., Jacob, W., Pette, D., and Wieringa, B. (1998) *Mol. Cell Biochem.* 184, **183–194**
36. Kay, L., Nicolay, K., Wieringa, B., Saks, V., and Wallimann, T. (2000) *J. Biol. Chem.* 275, **6937–6944**
37. van Deursen, J., Ruitenbeek, W., Heerschap, A., Jap, P., ter Laak, H., and Wieringa, B. (1994) *Proc. Natl. Acad. Sci. U. S. A.* 91, **9091–9095**
38. Schlattner, U., Forstner, M., Eder, M., Stachowiak, O., Fritz-Wolf, K., and Wallimann, T. (1998) *Mol. Cell. Biochem.* 184, **125–140**
39. O'Gorman, E., Beutner, G., Dolder, M., Koretsky, A. P., Brdiczka, D., and Wallimann, T. (1997) *FEBS Lett.* 414, **253–257**
40. Salomons, G. S., van Dooren, S. J., Verhoeven, N. M., Cecil, K. M., Ball, W. S., Degrauw, T. J., and Jakobs, C. (2001) *Am. J. Hum. Genet.* 68, **1497–1500**
41. Hovius, R., Lambrechts, H., Nicolay, K., and de Kruijff, B. (1990) *Biochim. Biophys. Acta.* 1021, **217–226**
42. Munn, E. A. (1968) *J. Ultrastruct. Res.* 25, **362–380**
43. Muscatello, U., and Horne, R. W. (1968) *J. Ultrastruct. Res.* 25, **73–83**
44. Walzel, B., Boehm, E., Speer, O., Kristiansen, S., Richter, E. A., and Wallimann, T. (2001) *Cell Biol. Int.* 25, **949**

45. Walzel, B., Straumann, N., Hornemann, T., Magyar, J., Kay, L., Kristiansen, S., Richter, E. A., and Wallimann, T. (2000) *Eur. J Med. Res*. 5, Suppl. 1, 28–29
46. Territo, P. R., French, S. A., and Balaban, R. S. (2001) *Cell Calcium* 30, 19–27

CREATINE TRANSPORTER ISOENZYMES: A REAPPRAISAL

Oliver Speer[1§], Lukas J. Neukomm[1§], Robyn M. Murphy[2], Elsa Zanolla[1], Uwe Schlattner[1], Rodney J. Snow[2], and Theo Wallimann[1]

§ These authors have contributed equally to this work.

[1)] *Swiss Federal Institute of Technology, ETH-Zürich, Institute of Cell Biology, ETH-Hönggerberg, CH-8093 Zurich, Switzerland,*

[2)] *School of Health Sciences, Deakin University, 221 Burwood Highway, Burwood, 3125 Australia*

Published in
Molecular and Cellular Biochemistry, in press

Acknowledgement – We are indebted to all members of our research group (Cell Biol. ETH), especially to Dr. Kathryn Adcock for critical reading of the manuscript, Dr. Torsten Kleffmann for help with the ESI-MSMS at the FGCZ, Dr. Thorsten Hornemann, Dr. Dietbert Neumann, Nadine Straumann, Tanja Buerklen, Roland Tuerk for help and stimulating discussion, Dr. Ove Eriksson (Biomedicum Helsinki), and Hugues Henry and Olivier Braissant (CHUV, Lausanne).

This work was supported by the "Swiss Society for Research on Muscle Diseases" (T.W. and O.S), the parents organization "Benni & Co", Germany, the "German Muscle Society" and the ETH-Zurich, as well as by the "Swiss National Foundation" (grant No: 31-62024.00 to T.W.).

Abbreviations: ANT, adenine nucleotide translocator; AGAT, arginine glycine armino-transferase; BC-KADH, branched chain keto acid dehxdrogenase; Cr, creatine; CK, creatine kinase; CrT, creatine transporter; CsA, cyclosporin A; GAA, guanidine acetic acid; GAMT, guanidine-acetate methyl-transferase; β-GPA, β-guanidino propionic acid; α-HCA, α-cyano-4-hydroxycinnamic acid; α-KGDH , α-ketoglutarate dehydrogenase; LC-ESI-MS/MS, liquid-chromatograph-electro-(nano)spray-ionization tandem mass spectroscopy; MALDI TOF, matrix-assisted laser desorption-ionisation and time-of-flight; MCK, muscle type creatine kinase; PDH, pyruvate dehydrogenase; PCr, phospho-creatine; PKC, protein kinase C; PTP, permeability transition pore; TCA, trichloric acid; TFA, trifluoroacetic acid; VDAC, outer mitochondrial membrane voltage dependant anion channel.

Abstract

Creatine (Cr) plays a key role in cellular energy metabolism and is found at high concentrations in metabolically active cells such as skeletal muscle and neurons. These, and a variety of other cells, take up Cr from the extra cellular fluid by a high affinity Na^+/Cl^- - dependent creatine transporter (CrT). Mutations in the *crt* gene, found in several patients, lead to severe retardation of speech and mental development, accompanied by the absence of Cr in the brain.

In order to characterize CrT protein(s) on a biochemical level, antibodies were raised against synthetic peptides derived from the N- and C-terminal cDNA sequences of the putative CrT-1 protein. In total homogenates of various tissues, both antibodies, directed against these different epitopes, recognize the same two major polypetides on Western blots with apparent Mr of 70 and 55 kDa. The C-terminal CrT antibody (α-CrT_{COOH}) immunologically reacts with proteins located at the inner membrane of mitochondria as determined by immuno-electron microscopy, as well as by subfractionation of mitochondria. Cr-uptake experiments with isolated mitochondria showed these organelles were able to transport Cr via a sulfhydryl-reagent-sensitive transporter that could be blocked by anti-CrT antibodies when the outer mitochondrial membrane was permeabilized. We concluded that mitochondria are able to specifically take-up Cr from the cytosol, via a low-affinity CrT, and that the above polypeptides would likely represent mitochondrial CrT(s). However, by mass spectrometry techniques, the immunologically reactive proteins, detected by our anti-CrT antibodies, were identified as E2 components of the α-keto acid dehydrogenase multi enzyme complexes, namely pyruvate dehydrogenase (PDH), branched chain keto acid dehydrogenase (BC-KADH) and α-ketoglutarate dehydrogenase (α-KGDH). The E2 components of PDH are membrane associated, whilst it would be expected that a mitochondrial CrT would be a trans-membrane protein. Results of phase partitioning by Triton X-114, as well as washing of mitochondrial membranes at basic pH, support that these immunologically cross-reactive proteins are as expected for E2 components, that is membrane associated rather than trans-membrane. On the other hand, the fact that mitochondrial Cr uptake into intact mitoplast could be blocked by our α-CrT_{COOH} antibodies, indicate that our antisera contain antibodies reactive to genuine CrT. This is also supported by results from plasma membrane vesicles isolated from human and rat skeletal muscle, where both 55 and 70 kDa polypeptides disappeared and a single polypeptide with an apparent electrophoretic mobility of ~ 65 kDa was enriched.

Due to the fact that all anti-CrT antibodies that were independently prepared by several laboratories seem to cross-react with non-CrT polypeptides, specifically with E2 components of mitochondrial dehydrogenases, further research is required to characterise on a biochemical / biophysical level the CrT polypeptides, e.g. to determine whether the ~ 65 kDa polypeptide is indeed a bona-fide CrT and to identify the mitochondrial transporter that is able to facilitate Cr-uptake into these organelles. Therefore, the anti-CrT antibodies available so far should only be used with these precautions in mind. This holds especially true for quantitation of CrT polypeptides by Western blots, e.g. when trying to answer whether CrT's are up- or down-regulated by certain experimental interventions or under pathological conditions**.**

In conclusion, we still hold to the scheme that besides the high-affinity and high-efficiency plasmalemma CrT there exists an additional low affinity high Km Cr uptake mechanism in mitochondria. However, the exact biochemical nature of these CrT polypeptides, - this holds true for both the plasmalemma CrT, as well as the mitochondrial CrT-, still remains elusive. Finally, we still believe that similar to the creatine kinase (CK) isoenzymes, which are specifically located at different cellular compartments, the substrates of CK are also compartmentalized in cytosolic and mitochondrial pools. This is in line with ^{14}C-Cr-isotope tracing studies and a number of [^{31}P]-NMR magnetization transfer studies, as well as with recent [^{1}H]-NMR spectroscopy data.

Introduction

Recent publications have shed new light on the importance of creatine (Cr). In particular, mutations in the two genes involved in Cr synthesis all lead to an absence of creatine in the brain, which seems to evoke severe disturbances of brain function (1-9). In patients with these inborn errors of creatine metabolism (4, 10-12) several research teams have found treatment with Cr was able to increase the Cr content of the brain. However in patients with mutations of the Cr transporter (CrT) protein no such increase following Cr treatment was observed (2, 7).

This work will briefly discuss creatine metabolism, as well as the identification of the CrT. For more detailed reviews, the reader is directed to (13, 14). The predominant part of this work will present new challenging data on the molecular identification of the creatine transporter isoforms. Creatine supplementation in health and disease will not be mentioned here, but can be found in other parts of this issue or also see (9, 13).

Creatine metabolism

Cr and phospho-creatine (PCr) are guanidino compounds, which together with creatine kinase (CK) isoforms constitute part of the cellular energy network in cells that typically display large fluctuations in energy demand such as skeletal muscle, brain, heart and many other tissues (15-20). In these tissues, Cr is the substrate of creatine kinase, which transfers a phosphate group from ATP to Cr to produce PCr at sites of energy production (mitochondria) and recycles ATP by consuming the PCr at sites of high energy turn over (for review see (16, 21)).

In mammals, the final step of Cr synthesis takes place mainly in the liver and pancreas by the enzyme guanidine-acetate methyl-transferase (GAMT) using the Cr precursor guanidine acetic acid (GAA). GAA itself is synthesised in the kidney by arginine glycine armino-transferase (AGAT) (22-25). Interestingly, tissues, which contain the highest concentrations of PCr and total Cr, do not synthesize their own Cr or do so only to a limited extent (1). This shortcoming is compensated by absorption of Cr into the respective tissues by a specific CrT from the circulating blood (26-29), (for review see (14, 17)). Blood Cr levels are maintained by endogenous Cr synthesis or by ingestion of Cr-containing food (fish and meat).

The creatine transporter

Various cell systems and *in vivo* human studies have shown that the regulation of Cr uptake may be governed by a number of different mechanisms (see (14)). Putative phosphorylation and glycosylation consensus sequences (figure 1) have been identified on the CrT cDNA that suggest the protein may be regulated in either one or both of these ways. Recently, it was shown that CrT protein serine phosphorylation of CrT decreased after starvation in rats with a concomitant increase in Cr uptake into skeletal muscle vesicles (30), whereas tyrosine phosphorylation of CrT is decreased after creatine supplementation (31). These data suggest that changes in the extra- and/or intracellular Cr content alters the phosphorylation state of the CrT, and thereby its activity. In parallel to the

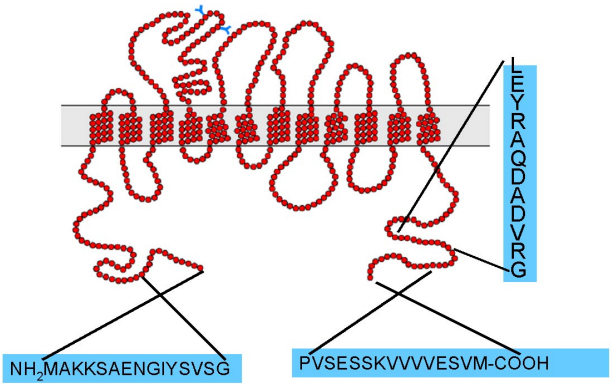

Figure 1 Proposed topology of the hypothetic human creatine transporter 1 protein (hCrT1), adapted from (87). Depicted are the three peptides against which antibodies have been produced (17, 44, 45).

elevated phosphorylation levels, c-Src kinase activity also increases such that it might be speculated that c-Src kinase could possibly tyrosine phosphorylate CrT since this kinase was enriched by immunoprecipitation together with the CrT (30-32).

Recent data obtained with anti-CrT antibodies involving immuno-localization, cell fractionation and Cr uptake studies, suggest the existence of CrT isoforms with localisation in the plasma membrane and with in mitochondria (29, 33). This would support the existence of cytosolic and mitochondrial pools (34, 35).

Inborn errors in CrT

Several mutations of the CrT have been described in humans (2, 3, 7, 36). These patients present with hypotonia, epilepsy and delay in development, speech and expressive language function, and have an absent Cr peak in their brain proton-MR spectra, elevated Cr in blood and in urine (2, 3, 7, 36). Fibroblasts from these patients contained hemizygous nonsense mutations in the CrT gene and were defective in Cr uptake (2, 3). Interestingly, the Xq28 locus - where the *crt1* gene is localized – has been linked to the genes for several neuromuscular disorders, such as Barth syndrome (37-40), causing several authors (17, 41, 42) to speculate that dysfunctional *crt1* gene may be responsible for some of these diseases.

An increased number of families with genetic defects in CrT have been identified. Consequently, it is of interest to study the CrT protein(s) in terms of structure, function and localization, with the aim to study the Cr system and to develop possible diagnostic tests for clinical use. One such approach would be the generation of highly specific antibodies against CrT protein(s) or domains thereof, e.g. for clinical screening by Western blot analysis of patients white blood cells or fibroblasts in the future.

Generation of antibodies against CrT

Antibodies against CrT have been generated independently in several laboratories (17, 43-45). Dodd and coworkers produced a peptide antibody against an over expressed C-terminal polypeptide stretch of 56 amino acids of CrT protein (45) and immuno purified this serum with a heterologously expressed 21 C-terminal polypeptide stretch. This antibody shows 5 signals between 50 and 100 kDa on Western blots. However, only a 90 kDa signal is obtained from HEK293 cells after the enrichment of cell surface exposed proteins via biotinylation and pulled down with Streptavidin coated beads (45). This immunoband represents a glycosylated protein (personal communication). With the same method of antibody production Kekelidze and co-workers obtained three distinct signals at 55, 70 and >100 kDa in a C6 glioma cell line whereas, in a L6 muscle cell line only the 55 and 70 kDa signals were seen (43). Our research group produced sera against N-terminal (NH_2-M-A-K-K-S-A-E-N-G-I-Y-S-V-S-G) or C-terminal peptides (P-V-S-E-S-S-K-V-V-V-V-E-S-V-M-$_{COOH}$) (figure 1) (17). Using these antibodies on Western blot, two main signals at 55 and 70 kDa were obtained in rat muscle, heart, skeletal muscle, brain, liver, kidney, lung, testis and intestine total homogenates. In rat heart, however, a 150 kDa

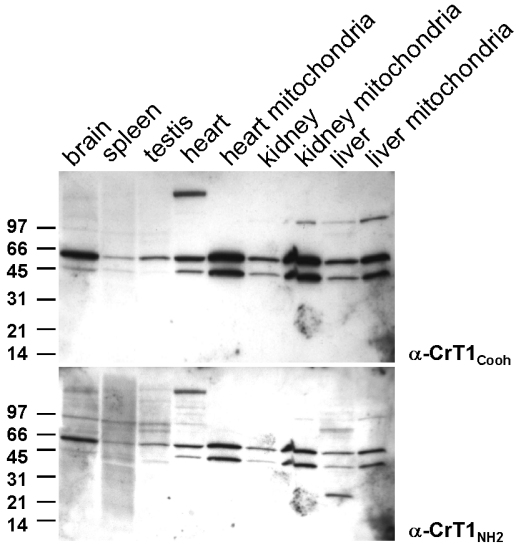

Figure 2 Immuno-blot of total tissue extracts and highly purified mitochondria obtained by fractionated and density gradient centrifugation (20 μg of protein loaded per lane). Proteins were separated by 12% SDS PAGE, transferred to Nitrocellulose membrane. Proteins were detected with anti-CrT C-terminal peptide antibody, and reprobed with anti-CrT N-terminal peptide antibody.

signal has been seen, whereas in enriched sarcolemma fractions from rat skeletal muscle, a single ~ 60 kDa signal has been described (29). In mitochondria isolated from rat gastrocnemius and soleus muscle, heart, brain, and kidney mitochondria both anti-N- and anti-C-terminal peptide antibodies revealed two signals at 55 and 70 kDa (29, 33), whereas in mitochondria from rat liver and kidney a 112 kDa protein was also seen (29).

Tran and co-workers produced another antibody directed against a more internal C-terminal cDNA-derived protein sequences (L-E-Y-R-A-Q-D-A-D-V-R-G) (figure 1) (44). These authors report signals at apparent molecular weight of 55, 60, 75 and >100 kDa in extracts from C_2C_{12} cells. After treatment with tunicamycin (an N-linked glycosylation inhibitor) the 75 kDa signal disappeared, whereas the signal at 60 kDa is significantly increased, suggesting that this could be the core CrT protein. Only the 55 kDa signal, however, is captured by streptavidin after cellular surface biotinylation. This 55 kDa polypeptide is not present at the cell surface after Cyclosporin A treatment (44). These authors discuss the possibility that Cyclosporin A inhibits the chaperone-like cyclophilin, which might be necessary for a correct folding process of CrT in the endoplasmic reticulum.

A commercially available antibody (a 20 amino acid peptide near the cytoplasmic N-terminal of CrT sequence) was used to immune precipitate CrT (30-32). These precipitations where afterwards analysed with phospho-tyrosine and phospho-serine antibodies. So far these authors reported one single representative Western blot signal with apparent Mr of 55 kDa after probing with both phospho-amino acid antibodies (30-32). The actual Western blot signal after probing with α-CrT antibody was reported between 50 and 80 kDa (30).

The common denominator in terms of immune reactivity of all these different antibodies is their consistent detection of strong Western blot signals of two main polypeptides in the range of 55 and 70kDa, with slight variations in the apparent molecular weight, depending on the gel system, the animal species or cell types used. Since the predicted molecular weight of CrT derived from the CrT cDNA was approximately 70kDa, the detection of a strong signal with all of these anti-CrT antibodies at 70 kDa seemed appropriate. Interestingly, with other transporters of the 12-helix membrane transporter family (e.g. the

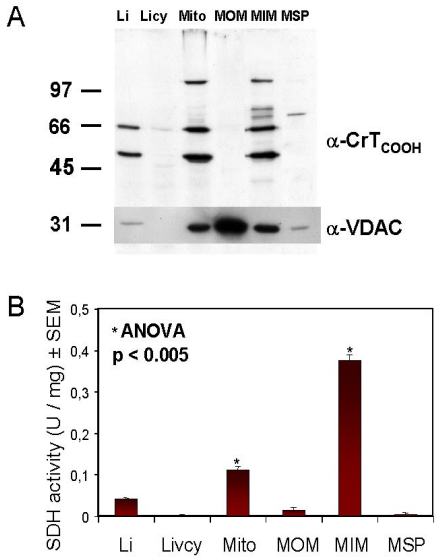

Figure 3 Submitochondrial localization of CrT by fractionation of mitochondrial membranes. After isolation of mitochondria (Mito) and cytoplasm (Licy) from adult rat liver homogenate (Li), mitochondrial outer (MOM) and mitochondrial inner membrane (MIM), as well as soluble mitochondrial proteins (MSP), were enriched by a swelling-shrinkage procedure and a non-linear sucrose ultra-centrifugation (63). 20 µg protein extract each were separated with SDS-PAGE and blotted onto a nitrocellulose membrane. CrT was detected by using polyclonal rabbit α-CrT$_{COOH}$ antibodies and secondary goat α-rabbit coupled HRPO antibodies in liver homogenate, enriched in mitochondria and highly enriched in MIM, but absent in the cytosol and MSP. The same blot was reprobed with α-VDAC monoclonal mouse antibody, a marker for the mitochondrial outer membrane. VDAC was detected highly enriched in the MOM. B) Succinate dehydrogenase (SDH) activity assay of subcellular fractions. SDH as an enzymatic marker for the mitochondrial inner membrane was used to test the enrichment of MIM by measuring the specific SDH activity (U / mg) of the various fractions. Note the almost complete absence of SDH in Licy, MOM and MSP.

serotonin transporter) these highly hydrophobic membrane proteins seem to generally show a rather anomalous electrophoretic behaviour in SDS-PAGE with Mr of over 100kDa observed, as opposed to the expected molecular weight of 70 kDa calculated from the cDNA (46, 47).

Present state of knowledge

Encouraged by these data, and in an attempt to characterize the tissue distribution and subcellular localization of CrT, e.g. on the plasmamembrane, the ER or Golgi etc., we started to use our antibodies for Western blotting, as well as for immuno- and EM localization studies (29, 33). Western blot quantification of the two major polypeptides of 55 kDa and 70 kDa in different muscle types from rats treated either with β–guanidinopropionic acid (β-GPA), a known competitive inhibitor of Cr transport (48), or Cr to deplete or increase intracellular Cr pools, respectively, showed that chronic long-term supplementation by high-dose Cr led to a down-regulation in the accumulation of both of these protein species, whereas the opposite was true after β-GPA treatment (17, 49). Thus, it seemed that CrT expression would respond to interventions affecting Cr synthesis, transport or pool-size. These facts indicated that both of these bands might be CrTs since they responded to interventions affecting cellular Cr levels in the expected manner.

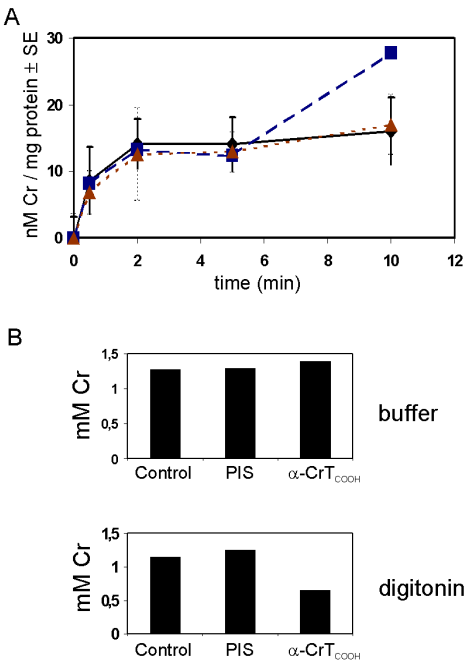

Figure 4 (A) Mitochondrial Cr up-take. Time course experiments of Cr up-take (panel A) into isolated mitochondria from rat heart (■), liver (◆), and kidney (▲), measured at 20 mM of external Cr concentration in the presence of substrates for oxidative phosphorylation. The amount of Cr up-take is expressed as nM / mg total mitochondrial protein. (B) Inhibition of mitochondrial Cr uptake. Mitochondria were pretreated for 1hr at 22°C in 250mM sucrose buffer, or in 250 mM Sucrose buffer containing 100 µg / mg^{-1} protein digitonin, together with rabbit anti-CrT C-terminal peptide serum, pre-immune-serum (PIS) or with the same volume of the corresponding sucrose buffer only (control). Subsequently, mitochondria were washed three times with 250 mM sucrose, 10 mM Hepes KOH, pH 7.4, 0.1 mM EGTA. The Cr transport assays were performed subsequently as in Fig. 6 and described in Material and Methods.

Tissue specific expression of CrT proteins

The first surprise with these antibodies came from Western blot analysis of the tissue distribution as the highest expression of both CrT-species was found in heart. Even though these data corresponded to Northern blot analysis (42 Sora, 1994 #254, 50-52) it was somewhat unexpected, since heart neither expresses the highest levels of CK nor accumulates the highest amount of Cr compared to other tissues (53). One would, perhaps expect fast-twitch glycolytic, white muscle with high concentrations of PCr and total Cr and very high expression levels of cytosolic CK (16) to express the highest levels of CrT. The opposite to this, however, was found in rat skeletal muscle where slow-twitch oxidative muscle showed a greater expression of the CrT compared with the fast-twitch glycolytic muscle (54, 55). On the other hand, cardiac muscle contains the highest proportion of mitochondrial volume fraction of all muscles, and slow-twitch oxidative muscle has a greater mitochondrial number than fast-twitch glycolytic muscle. Strikingly, the liver, despite being the tissue of Cr synthesis, does not express creatine kinase (56). Nevertheless liver was found to express high

concentrations of both immuno-reactive anti CrT bands. By contrast Northern blot analysis provided no evidence of significant levels of CrT mRNA in liver since either no CrT mRNA, or only very low amounts thereof have been reported (42, 50-52, 57, 58). However, this might contradict the physiological role of liver in terms of creatine metabolism, since this organ, as the Cr synthesising organ, must be able to export Cr, however the Na+ gradient would not support the CrT being responsible for the export of Cr.

Localization of the 55 and 70 kDa polypeptide species by cellular fractionation and immune histochemistry

Using the anti-CrT antibodies, two major peptides at 55 and 70 kDa were also detected in brain, spleen, testis, heart, kidney and liver (figure 2). On tissue sections of heart and skeletal muscle analysed by immuno confocal microscopy it was evident that both antibodies recognized proteins within mitochondria (29, 33). By isolation of mitochondria via gradient centrifugation these polypeptide doublets were enriched in the mitochondrial fractions (figure 2). In addition, by immuno electron microscopy, the mitochondrial localisation could also be confirmed. (33). These findings somehow matched parallel findings by Dodd (45) who employed an independently produced antibody, which recognises the transiently expressed CrT as intracellular spots possibly resembling mitochondria. Finally, in our hands, isolated mitochondrial membranes revealed the presence of the 55, 70 and 112 kDa proteins co-purified with the inner mitochondrial membrane (figure 3) and (33).

Mitochondrial creatine uptake

Thus, in the inner mitochondria membrane, there are at least 3 polypeptides, which are recognized by our anti COOH- and NH_2-term CrT sera (figure 3). The presence of a CrT protein within mitochondria seems reasonable, as PCr was found within mitochondria (34, 35). Consequently, it had to be addressed whether mitochondria are indeed able to take up Cr. In fact, our subsequent experiments showed that mitochondria isolated from different tissues were able to take up Cr (figure 4A). According to our recent measurements, this Cr uptake displays a Vmax of 12 nmoles min^{-1} mg^{-1} protein and a Km of 16 mM representing an efficient but low affinity CrT (33). The rather high Km of the mitochondrial Cr uptake seems reasonable, as the CrT in the plasma membrane representing a high-affinity transporter (Km for Cr 20 – 50 µM) is able to efficiently accumulate Cr into the cell leading to an intracellular Cr concentration in muscle in the range of 20-40 mM (13, 16, 29).

Furthermore, the mitochondrial Cr uptake was sensitive to the SH-modifying reagent *N*-ethylmaleimide (NEM) (33). This compound has been tested to inhibit enzymatic activities at low concentrations (59, 60). Most importantly the anti C-terminal CrT sera were also able to inhibit the mitochondrial Cr accumulation, whilst a control antibody had no such effect (figure 4B and (33)). This however was only possible if the outer mitochondrial membrane was disrupted either by digitonin (figure 4 B) or by osmotic shock (33). All these data seem convincing to predict the existence of a mitochondrial Cr uptake protein. Even more, we were convinced that we had identified a new mitochondrial membrane protein, as the physiological characteristics of the mitochondrial Cr uptake were distinct from the Cr transport at the plasma membrane. Raising question to the existence of a specific mitochondrial CrT was that in contrast to the plasmalemmal Cr uptake, mitochondrial Cr uptake activity showed a high Km but was not very effectively inhibited by β-GPA (33). Another finding, which favoured a protein different from plasmalemma CrT, was the sensitivity of mitochondrial creatine transport to the protonophoric uncoupler carbonyl cyanide p-trifluoromethoxyphenyhydrazone (FCCP), which disrupts the mitochondrial membrane potential (33). Furthermore, the question of whether this mitochondrial Cr uptake was via a non-specific amino acid transporter must also be considered given the competitive inhibition of Cr uptake by arginine and lysine (33). Finally, the existence of two CrT mRNAs reported on Northern blots by many groups (28, 42, 50, 52, 57, 58, 61, 62) seemed also to support the existence of at least two different CrT species.

Experimental procedures

Materials

If not otherwise stated all chemicals were purchased from Sigma Chemical Co. (USA). Male Wistar rats (250-300 g) were purchased from BRL (Switzerland).

Tissue extracts and isolation of mitochondria

Male Wistar Rats (3-4 month of age) were anesthetized with diethyl ether and killed by cervical dislocation. Tissue of liver, skeletal and cardiac muscle, kidney, brain, spleen and testis were taken and immediately transferred to ice-cold buffer. Liver, brain, and kidney tissues were homogenized by a teflon/glass potter (Braun-Melsungen, Germany), whereas skeletal and heart muscle was homogenized by a Polytron mixer in 40 ml HEPES-sucrose buffer containing 250 mM sucrose, 10 mM HEPES-HCl pH 7.4, 0.5 % BSA (essentially free of fatty acids) and 1 mM EDTA. The homogenate was centrifuged for 10 min at 700 x g to remove heavy debris as platelets and nuclei. An aliquot from the supernatant was taken for further analysis as the total tissue extract. The supernatant was centrifuged for 10 min at 7,000 x g and the resulting supernatant was stored for subsequent analysis as the soluble cytosolic fraction, while the pellet containing mitochondria was resuspended in 60 ml 250 mM sucrose, 10 mM Tris/HCl pH 7.4, 100 µM EGTA, 25 % Percoll^{TM} (Amersham Pharmacia Biotech, Sweden) and centrifuged for 35 min at 100,000 x g. Percoll^{TM} fractions containing highly purified mitochondria were washed twice with 250 mM sucrose, 10 mM HEPES-HCl pH 7.4, 100 µM EGTA by centrifugation at 7,000 x g for 10 min. Washed mitochondria were then recovered from the pellet and resuspended in 200 µl of the washing buffer.

Western blotting

Extracts were separated in 10-12 % polyacrylamide SDS-gels and trans-blotted onto a nitrocellulose membrane (Schleicher & Schuell, Germany; Geneworks, Australia). The membrane was blocked with 5 % fat-free milk powder in TBS(T) buffer (150 mM NaCl, 25 mM Tris-HCl, pH 7.4, [0.05% Tween]) for 1 hr at room temperature. After washing for 30 min, membranes were incubated with 1:1.000 to 5,000 diluted anti-CrT peptide antibody in TBS buffer for 2 hrs at room temperature. After washing with TBS(T) buffer, the blot was incubated again with a 1:10,000 dilution of goat HRP-conjugated anti-rabbit secondary antibody (Amersham Pharmacia Biotech, Sweden; Silenus, Australia). The immunoreactive bands were visualized using the Renaissance Western Blot Chemiluminescence Reagent Plus Kit (NEN, USA). Images were collected and analysed using a Kodak 1D Image Station.

Isolation of outer and inner membrane from rat liver mitochondria

The isolation of the mitochondrial membranes was done as previously described (63). Briefly, rats were anaesthetized with diethyl ether and killed by cervical dislocation. The liver was taken and immediately transferred to ice-cold homogenization buffer (250 mM sucrose, 10 mM Hepes-KOH pH 7.4, 0.5 % BSA, 1 mM EDTA) and freed from fat and connective tissue. The tissue was homogenized using a glass-teflon potter in homogenization buffer at 0°C. Nuclei and cell debris were pelleted by centrifugation at 700 x g for 10 min, and crude mitochondria were pelleted from the post-nuclear supernatant by centrifugation at 7,000 x g for 10 min. Enriched mitochondria were resuspended in 250 mM sucrose, 10 mM Hepes-KOH, pH 7.4, 0.1 mM EGTA and purified in a 25 % Percoll^{TM} density gradient. Highly enriched mitochondria were carefully collected from the gradient and washed twice in sucrose/Hepes buffer. Protein determination was performed with the BCL Kit (Pierce, USA). Fifty mg of mitochondria were then resuspended in 6 ml of 10 mM KH_2PO_4 buffer, pH 7.5 at 0°C. After 15 min to allow swelling, 6 ml of 10 mM KH_2PO_4 containing 30 % sucrose, 30 % Glycerol, 10 mM $MgCl_2$, 4 mM ATP. After 60 min of incubation at 0°C to allow shrinking the mitochondrial suspension was treated with sonic oscillation using a Brandson sonicator. A first crude inner membrane fraction was pelleted at 12,000 x g for 10 min. The pellet was resuspended in 3 ml 10 mM KH_2PO_4 buffer. Pellet and supernatant were layered onto a discontinuous sucrose gradient consisting out of 51 %, 37 % and 25 % sucrose and

centrifuged in a swinging bucket rotor (SW 40) at 100,000 x g for at least 12 hrs at 4°C. The clear top of the gradient contained the soluble protein fraction, the 25 % - 37 % interphase contained the light outer membrane subfraction, and the 37 % - 51 % interphase contained the pure inner membrane subfraction. The membrane fractions were collected carefully from the gradient, diluted 1:10 in sucrose/Hepes buffer, and pelleted at 100,000 x g, 4°C for 1 h. The pellets were solubilized in sucrose / Hepes and analyzed.

Succinate Dehydrogenase (SDH) enzyme assay

The specific SDH activity was measured indirectly via the increase in the absorption of reduced cytochrome c at 550 nm (ε = 19 mM^{-1} cm^{-1}). 10 µl sample was incubated in 1000 ml 50 mM Na_2HPO_4, 50 mM NaH_2PO_4, pH 7.4, 100 µM cytochrome c, 1 mM KCN, 2.5 mM succinate as described (64).

Plasma membrane giant vesicles preparation

Plasma membrane giant vesicles were prepared from rat (~100 mg – soleus, SOL; ~500 mg white gastrocnemius; WG and mixed muscle) and human (~70-130 mg) skeletal muscle samples as previously described (65). All procedures were undertaken at room temperature, unless otherwise indicated. Freshly extracted samples were rinsed in KCl-Hepes buffer (140 mM KCl, 10 mM Hepes, pH 7.4) and finely cut lengthwise. Muscle pieces were placed in digestion solution (400 µl x 100 mg^{-1} tissue KCl-Hepes buffer with 80 µl collagenase; 1 µl protease inhibitor cocktail; 5 µl phenylmethylsulfonyl fluoride) and incubated at 34°C for 60 – 90 min. Collagenase activity was ceased by the addition of KCl-Hepes-EDTA (10 mM) and vesicles collected with 2-4 subsequent rinses with KCl-Hepes-EDTA buffer, until 10 ml (human and SOL) or 30 ml (WG and mixed) were collected. A solution of 11 % KCl (1.4 M) in Percoll (Amersham Pharmacia Biotech, Sweden) was prepared and added to the muscle solution (2.2 ml x 10 ml^{-1} muscle solution) and mixed by inversion. The mixture was aliquoted into plastic tapered centrifuge tubes (~ 6 ml x $tube^{-1}$), and ~ 2 ml Nycodenz (4 % in KCl-Hepes buffer) was carefully layered on top, followed by ~ 1 ml KCl-Hepes-EDTA buffer. Samples were then spun (60 x g, 45 min, 23°C with the brake off). Vesicles were collected from the Nycodenz layer and washed with an equal volume of KCl-Hepes buffer and spun (900 x g, 10 min, 23°C). The supernatant was aspirated from the pellet of vesicles, and the integrity of the vesicles confirmed under a microscope. Vesicles were then resuspended in a small volume of storage buffer (4 % SDS in 10 mM Tris, 1 mM EDTA) and stored at -20°C until the Western blots were performed.

Red blood cell preparation

Blood (~8 ml) was collected into heparinized tubes and gently mixed before being aliquoted into 1.5 ml microfuge tubes and spun (~ 14,000 x g, 10 min, 4°C). The supernatant was removed and the pellet resuspended in 500 µl isotonic buffer (5 mM Na_2HPO_4 in 0.9 % NaCl, pH 8), spun as above, and the supernatant removed. This washing step was repeated three times. 200 µl aliquots of whole red blood cells (RBC) were then collected from beneath the surface of the pellet, suspended in 500 µl solubilisation buffer (150 mM NaCl, 20 mM Hepes, pH 8, 1 mM EDTA, 0.1 % Triton-X100) and shaken vigourously for 15-25 min at room temperature to release the membrane proteins. The samples were then spun as above and the supernatant collected and stored at -80°C until analyses.

Measurement of Cr transport into mitochondria

Cr uptake assays were performed using highly enriched, Percoll™ gradient purified mitochondrial preparations (adjusted to 10 mg x ml^{-1} protein concentration). The reaction was started by the addition of 10 µl of the mitochondria suspension to 90 µl transport buffer (10 mM Tris/HCl, pH 7.4, supplemented with 250 mM sucrose, 20 mM Cr, and 5 µCi x ml^{-1} [^{14}C]-Cr (American Radiolabeled Chemicals, USA), 10 µCi x ml^{-1} [^{3}H]-sucrose, 5 mM succinate/Tris, 2 µM rotenone, 2 mM $MgCl_2$, 10 mM Pi/Tris, 100 µM EGTA and 2 mM ADP) at RT. The pellet was solubilized in 100 µl of 1 % SDS and counted in 4 ml scintillation

cocktail "Ultima Gold XR" (Packard) in a Packard 1500 Tri-Carb^{TM} liquid scintillation counter. Double-isotope measurement settings were 0-18 eV for the [^{3}H]-isotope and 18-256 eV for the [^{14}C]-isotope. The amount of Cr uptake was calculated as the difference of total Cr subtracted by the Cr present in the space that was also accessible to sucrose. In the experiments with the anti-CrT antibodies, mitochondria (100 µg/mg mitochondrial protein) were preincubated for 1h at 22°C either in 250 mM sucrose +/- 100µg digitonin x mg-1 protein alone or in 250 mM sucrose +/- 100µg digitonin x mg-1 protein together with anti-CrT_{COOH} or preimmune serum (at 1:100 final dilution). Subsequently, mitochondria were washed three times with 250 mM sucrose, 10 mM Tris/HCl, pH 7.4, 0.1 mM EDTA and finally incubated with Cr transport buffer and uptake measured as described above. Mitochondrial volume was estimated with the distribution of tritium labelled water and C^{14} labelled sucrose in mitochondrial pellets, treated in parallel as described above. The final Cr conzentration within mitochondria was estimated with the volume measured as 2µl mg^{-1} mitochondrial protein.

Two dimensional gel electrophoresis

Isoelectric focusing (IEF) was performed according to (66) and the manufacturer's instruction of the IPGphor (Amersham Pharmacia Biotech, Switzerland). Precipitated protein samples were resuspended in rehydration buffer (7 M urea, 2 M thiourea, 2% CHAPS, 0.5% IPG buffer, 60 mM DTT). Samples were sonified in a water bath for 5 min at 30° C, mixed 30 min at 30° C, and centrifuged for 1 min at 13,000 x g. The IPG strip (Immobiline™ DryStrip, 18 cm, Amersham Pharmacia Biotech, Switzerland) was transferred to the focusing tray containing the resuspended sample, and covered with 1-2 ml mineral oil (Amersham Pharmacia Biotech, Switzerland). Isoelectric focusing (IEF) was performed by a five step program: 50V for 10h, 500V for 1h, 1,000V for 1h, 2,000V for 1h, 8,000V for 12h resulting in 92,000 Vh (20° C, 50 µA / Strip). Upon completion of IEF, the IPG strip was incubated for at least 15 min in equilibration buffer (50 mM Tris / HCl pH 8, 8.6 M urea, 30% glycerol, 2% SDS, 60 mM DTT). The second dimension was done in a similar manner to that described under SDS-PAGE. SYPRO® Ruby stained gel spots were cut out of the 2D gel and washed in 80 µl of 0.1M NH_4HCO_3, for 5 min. An equal volume of 100% acetonitrile (ACN) was added. The gel particles were washed by that procedure three times. The gel pieces were dehydrated with 100 µl ACN, and dried in a Speed Vac for 5 min. For reductive alkylation, gel particles were rehydrated in 10 mM DTT in 0.1 M NH_4HCO_3, and incubated for 30 min at 56°C. The excess solution was removed, and the particles were dehydrated with ACN, 5 min. After removing ACN, gel particles were incubated for 20 min in 55 mM iodoacetamide in 0.1 M NH_4HCO_3 in the dark at room temperature to alkylate the proteins. After removing iodoacetamide solution, the particles where washed with 200 µl of 0.1 M NH_4HCO_3, 15 min. The particles were shrunken with ACN, dried under vacuum for 5 min, and put on ice.

In-gel trypsinisation

Samples were rehydrated in the trypsin solution (12.5 ng/µl Trypsin (Promega, Switzerland) in 50 mM NH_4HCO_3) for 30-45 minutes at 4°C. The remaining trypsin solution containing excess trypsin was removed, and the particles were briefly with 50 mM NH_4HCO_3. Subsequently, 50 mM NH_4HCO_3 was added to the gel pieces, just enough to keep them covered during the over night digestion (16-20 h at 37° C).The 'digest solution' containing some tryptic peptides was transferred to a fresh 0.5 ml tube and saved. For basic extraction of peptides 15 µl of 25 mM NH_4HCO_3 was added again to the gel pieces, and incubated for 15 min at 37° C while shaking. After spinning down, an equal volume of ACN was added. After shaking for 15 min at 37° C and sonication for 5 min in a sonication bath at 37° C, liquid was spun down and collected. 50 µl of 5% formic acid was added to the gel particles, and those were incubated for 15 at 37° C while shaking. After spinning down, an equal volume of ACN was added. After shaking for 15 min at 37° C and sonication for 5 min in a sonication bath at 37° C, liquid was spun down and pooled together with the other extracted peptides. Pooled samples were centrifuged at 10,000 x g for 10 min, and the supernatant was frozen in

liquid nitrogen. Samples containing the collected extracted tryptic peptides were dried in a Speed Vac, dissolved in 7 µl of 0.5% acetic acid, and applied to the Liquid Chromatograph.

Mass spectroscopy

Liquid-Chromatograph-Electro-(nano)Spray-Ionization-MS/MS (LC-ESI-MS/MS) with Ion Trap technique was performed at the Functional Genomic Center Zurich (Switzerland) using a LCQ DECA XP (Thermo Finnigan, USA). Data derived from LC-ESI-MS/MS spectrometry were used in Sequest®, a database screening program accessible only in the Functional Genomic Center Zurich (Switzerland). MALDI-TOF (Applied Biosystems, USA) was performed in the Protein Service Lab at the ETH Hoenggerberg. Dried peptides were dissolved in 3 µl ACN : 0.1 TFA, 2:1 (trifluoro acetic acid, Fluka, Switzerland). 2-, 5-dihydrobenzoic acid (DHB, Fluka, Switzerland) served as matrix, which was dissolved in 100 µl of ACN : 0.1 TFA, at 2:1. 2 µl matrix solution were mixed with 1 µl of peptide solution and crystallized. Masses derived from MALDI-TOF-MS spectrometry were analysed in *Mascot* and in *Pep*MAPPER, (www.expasy.ch) to identify the different spots.

Phase partitioning

Phase partitioning was preformed as previously described (67). To achieve this, 72 µg of mitochondrial protein was dissolved in 6 ml 2% Triton X-114 in PBS on ice. After 10 min of sonication and incubation for 1 h on ice, the sample was centrifuged at 14,000 x g for 10 min at 4° C. Heavy debris was sucked off. The supernatant was transferred to a new tube and incubated for 10 min at 37° C. After centrifugation for 10 min at 14,000 x g at RT, the aqueous supernatant and the detergent pellet were precipitated by TCA in H_2O, separated and analyzed by SDS-PAGE.

Membrane washing

Membrane washing was performed as previously described (68, 69). After 10 min of sonication rat heart mitochondria (1 mg/ml) in 100 mM Na_2CO_3, pH 11.0, and incubation for 30 min on ice, membranes were centrifuged for 30 min at 15,000 x g at 4° C. The supernatant was precipitated with 10% TCA in H_2O, and both pellets together were separated and analyzed by SDS PAGE.

Recently obtained insights and new developments

Having identified a new mitochondrial Cr uptake activity that is clearly distinct from the plasma membrane Cr uptake, we tried to identify the molecular identity of this mitochondrial Cr uptake protein. In an attempt to further characterize the two major mitochondrial CrT-related protein species, we started a proteomics approach to identify and partially sequence the two major proteins of 50 and 70 kDa, recognized by our anti-CrT antibodies. Since initial work showed similar results between our COOH- and NH_2-terminal antibodies, most subsequent data has been collected using the α-CrT_{COOH} antibody, unless otherwise stated.

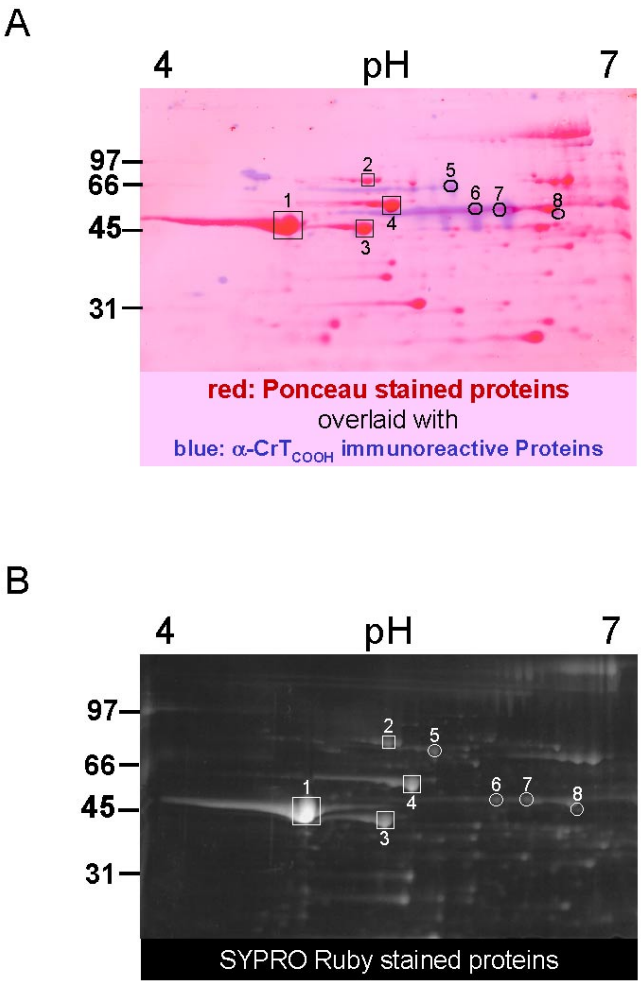

Figure 5 Identification of α-CrT immuno reactive proteins. (A) 2D Western blot against CrT. 2 mg of mitochondrial inner membrane proteins were separated by 2D SDS-PAGE and blotted on a nitrocellulose membrane. The proteins on the membrane were stained with Ponceau (red) and digitized. After destaining, the membrane was incubated with polyclonal rabbit α-CrT_{COOH} antibody and CrT isoforms (blue) were visualized by goat α-rabbit coupled HRPO secondary antibodies. (B) SYPRO Ruby stained 2D Gel. Stained proteins marked with circles were excised and used for digestion, and peptides were then analyzed by LC-ESI-MS/MS.

Identification of α-CrT reactive proteins.

Two dimensional gel electrophoresis, Western blot and advanced liquid chromatography nano-spray ionization tandem mass spectrometry (LC-ESI-MS/MS) were used for the identification of the different α-CrT_{COOH} immuno reactive proteins which were detected in enriched mitochondrial inner membrane preparations (70).

Proteins of the mitochondrial inner membrane were separated by 2D SDS-PAGE transferred to nitrocellulose membrane, stained reversibly with Ponceau and probed by Western blotting with our anti-CrT antibodies. Ponceau stain and Western blot signals were merged after digitalisation (figure 5A red spots represent proteins visualized with Ponceau, blue spots represent the α-CrT_{COOH} Western blot signals). Spots that were recognized by α-CrT_{COOH} antibodies (Figure 5A, spots 5-8), as well as other spots (Figure 5A, spots 1-4), were cut out from paralleled SYPRO Ruby stained 2D gels (figure 5 B) and then digested with

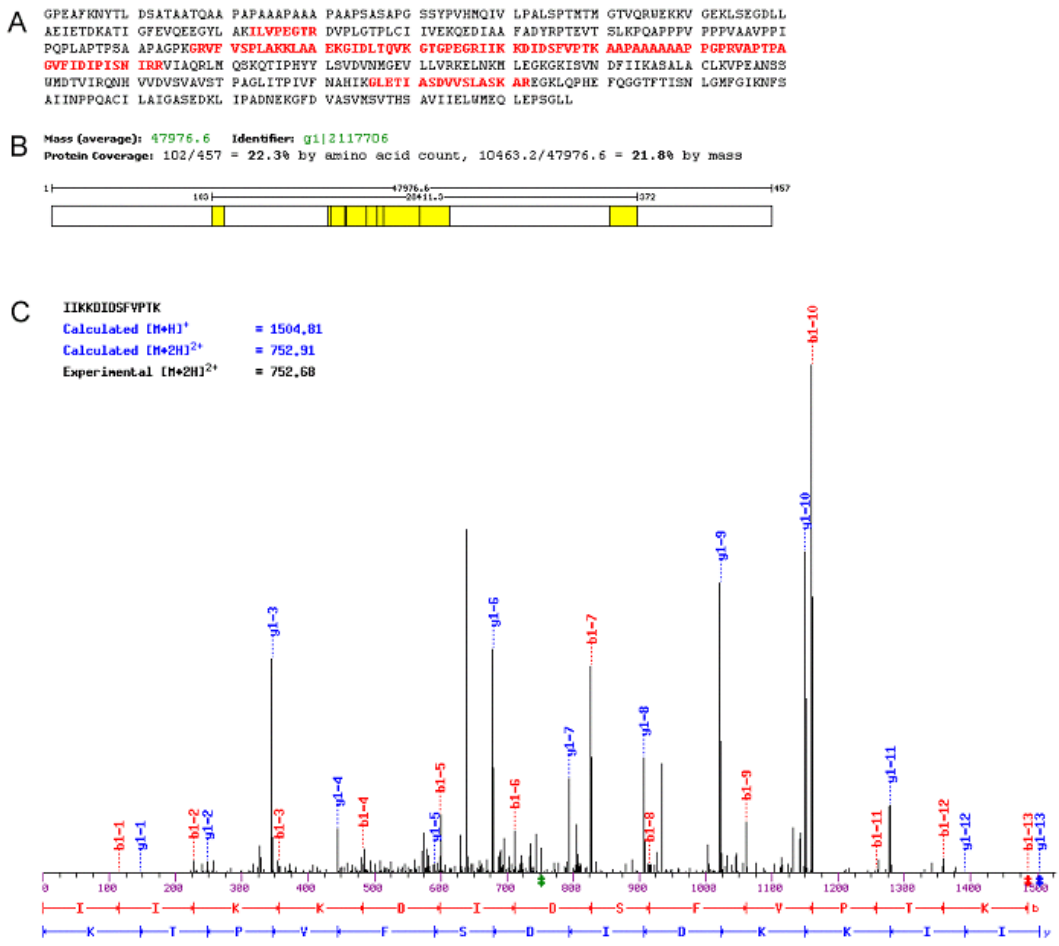

Figure 6 A) Amino acid sequence of spot no. 5. Identified amino acid stretches are shown in red. B) An overall score of the data corresponding to the protein no. 5. Below, different representations of locations within the protein sequences of the identified peptides (yellow) are shown. C) Peptide MS/MS spectrum. A spectrum of one of the identified peptides is shown including the y- and b-ions.

trypsin. The eluted peptides were subsequently analysed by LC-ESI-MS/MS. The MS/MS spectrum of a representative protein, which was identified, is shown in figure 6. Eight protein spots in the region of interest could be identified as shown in figure 5B and listed in table 1.

Using LC-ESI-MS/MS, the α-CrT_{COOH} immuno reactive proteins at 70 and 55 kDa in the mitochondrial inner membrane, which entered the 2 D PAGE, were identified as three dihydrolipoamide acyltransferases (spots 5, 6 and 8 in figure 5 and table 1), which are subunits of different α-keto acid dehydrogenase multi-enzyme complexes. The 70 kDa protein recognized by α-CrT_{COOH} is the dihydrolipoamide S-acetyltransferase (EC 2.3.1.12), a 70 kDa protein of the pyruvate dehydrogenase

complex (PDH), known as the E2 component. Its peptide MS/MS spectrum is shown in Figure 6. One of the 55 kDa α-CrT immuno reactive proteins was identified as the dihydrolipoamide

S-acetyltransferase (EC 2.3.1.61), a 47 kDa protein of the α-ketoglutarate dehydrogenase complex (α-KGDH), also known as the E2 component. The other 55 kDa protein was identified as the dihydrolipoamide branched chain transacylase, a 53 kDa protein of the branched chain keto acid dehydrogenase complex (BC-KADH), also known as the E2 component. Each of these multi enzyme complexes is a constituent of the α-keto acid dehydrogenase multi enzyme complex. The fourth identified protein was aldehyde

dehydrogenase (spot 7, figure 5 and table 1). Four mitochondrial proteins (ATP synthase, HSP60, NADH dehydrogenase Fe-S protein, cytochrome c reductase core protein 1) listed in table 1, which did not react with the α-CrT antibodies were also identified and used as a control for our methods.

Spot No.	Protein (origin, if recognized)	Mass (Dalton)
1	ATP synthase β-chain (EC 3.6.3.14) mitochondrial, fragment (*R. norvegicus*)	56353
2	NADH dehydrogenase (ubiquinone) Fe-S protein 1 (*Mus musculus*)	79417
3	60 kDa heat shock protein, mitochondrial precursor (*R. norvegicus*)	60955
4	ubiquinol-cytochrome c reductase core protein 1	53420
5	Dihydrolipoamide S-acetyltransferase (EC 2.3.1.12) liver (*Rattus norvegicus*)	68764
6	Dihydrolipoamide S-succinyltransferase (EC 2.3.1.61) mitochond. precursor (*R. norvegicus*)	47413
7	Aldehyde dehydrogenase, (EC 1.2.1.3) mitochondrial precursor (*R. norvegicus*)	56488
8	Dihydrolipoamide branched chain transacylase, mitochondrial precursor (*Mus musculus*)	53160

Table 1: Proteins identified by LC-ESI-MS/MS and MALDI-TOF. 2 mg of mitochondrial inner membrane proteins were separated by 2D SDS-PAGE, and stained with SYPRO Ruby (figure 5B). Spots were cut out of the gel, proteins were digested and resulting peptides prepared for LC-ESI-MS/MS or MALDI-TOF. Spots 5 to 8 were identified as being both α-CrT_{COOH} and α-CRT_{NH2} immuno reactive (figure 5A).

Examining the complete CrT sequence or the peptide sequences used for antibody generation (figure 1), no homology with other proteins was found using a BLAST search. Aligning N- and C-terminal CrT peptide sequences (NH_2-M-A-K-K-S-A-E-N-G-I-Y-S-V-S-G and P-V-S-E-S-S-K-V-V-V-V-E-S-V-M-COOH, respectively) with the amino acid sequences of the identified α-keto acid dehydrogenases, however, revealed some sequence homologies, which might also be recognised by the peptide antibodies, thus providing a rational for the observed cross-reactivity of our anti-CrT antibodies. Interestingly, aligning those peptides with HSP60 or ATP synthase gave the same amount of sequence homology, although neither HSP60 nor ATP synthase were recognised by our antibodies (figure 5 A). Consequently, sequence homologies derived from two-dimensional alignments may not entirely explain the cross reactivity of our antibodies with the α-keto acid dehydrogenases.

The major α-CrT immunoreactive polypeptides are soluble.

Three spots that corresponded to α-CrT immuno reactive spots within the range of the upper 70 and the lower 55 kDa bands were identified by LC-ESI-MS/MS as dihydrolipoamide acyltransferases. These three enzymes are not integral membrane-spanning proteins, but all belong to PDH, BC-KADH and α-KGDH multi subunit complexes that are bound to the inner matrix faced leaflet of the inner mitochondrial membrane (71).

Carbonate washing of mitochondrial membranes.

The results derived from LC-ESI-MS/MS suggested that those proteins identified after 2D PAGE would be membrane-associated proteins rather than integral membrane-spanning proteins. After conventional one-dimensional SDS PAGE and Western blotting at least three different α-CrT signals were observed, whereas after 2D PAGE and Western blotting, we could observe only α-CrT reactive proteins with the size of 70 and 55 kDa. It is well known

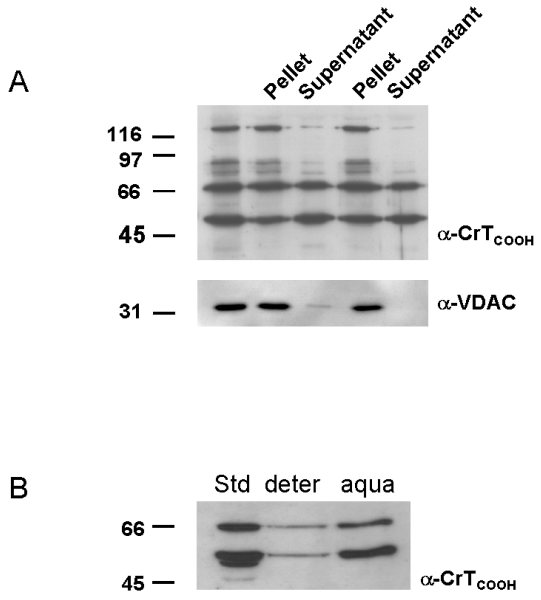

Figure 7 (A). Western blot of rat liver mitochondria washed with 100 mM sodium carbonate at pH 11. After incubation and sonication mitochondria in carbonate, membranes were pelleted and compared to the aqueous supernatant. After separation by SDS-PAGE and Western blotting, membranes were probed with α-CrT$_{COOH}$ and reprobed with α-VDAC antibodies. (B) Phase Partitioning of α-CrT$_{COOH}$ immuno reactive protein bands. 72 µg mitochondrial proteins were incubated in 2% Triton X-114. After centrifugation, the pellet containing integral membrane proteins and detergent (deter), and the supernatant containing aqueous proteins (aqua) were precipitated and compared to 20 µg mitochondrial proteins (Std). After separation and blotting onto a nitrocellulose membrane, the fractions were probed with α-CrT$_{COOH}$ antibodies.

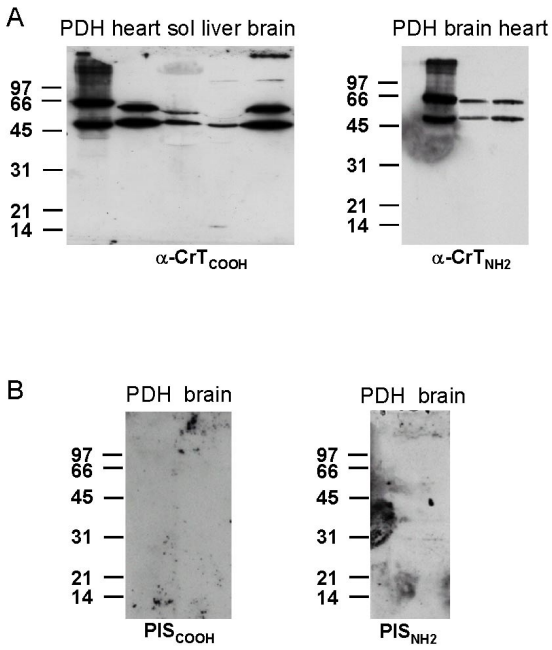

Figure 8 (A) Comparison of purified PDH to rat heart and soleus muscle by Western blot analysis. 3 µg PDH, rat heart and soleus muscle, each 20 µg, were separated by SDS PAGE and Western blotting. Membranes were probed with polyclonal rabbit α-CrT$_{COOH}$ and α-CrT$_{NH2}$ antibodies both 55 and 70 kDa signal were visualized. (B) Purified PDH and brain extracts run on Western blots as above and probed with preimmune serum (PIS) from rabbits injected with either the COOH- or NH_2- terminal peptides.

that highly hydrophobic proteins such as 12 membrane spanning domain-containing proteins, do not enter commercial pre-cast gels for iso-electric focusing (unpublished observation). We therefore concluded that the higher molecular weight signal identified in 1D Western blot at ~ 112 kDa but not seen in the 2D PAGE, using the α-CrT antibodies, represents a typical membrane protein, for which the CrT is a good candidate. To test this hypothesis, mitochondrial membranes were washed with 100 mM sodium carbonate at pH 11. In that buffer system integral membrane proteins cannot be washed off the membranes, whereas membrane-associated proteins should be removed (68, 69).

Rat liver and kidney mitochondria were sonicated and washed in sodium carbonate buffered at pH 11 and membranes were sedimented. Pellets and corresponding supernatant were separated by SDS-PAGE, Western blotted and tested by α-CrT$_{COOH}$ (figure 7 A). Control Western blots were also tested with α-VDAC antibodies. VDAC, a well-known membrane spanning protein of the outer mitochondrial membrane, remained with the mitochondrial membrane pellet. In contrast, the 55 and 70 kDa polypeptides partially separated from the membranes and were detected in both the supernatant and the pellet. Surprisingly the 112 kDa α-CrT reacting proteins did not detach from the mitochondrial

membranes. We therefore concluded that this high Mr protein could be involved in the mitochondrial Cr uptake rather than those of dehydrogenase complexes (55 and 70 kDa).

Our carbonate washing experiments were fully supported by results derived from phase partitioning by Triton X-114 (67), whereby membrane proteins stay in the detergent phase, while soluble proteins are found in the aqueous phase (figure 7B). In these experiments both α-CrT_{COOH} immuno reactive 70 and 55 kDa protein band signals remained in the aqueous phase with a much weaker signal seen in the detergent phase. This indicates that both 70 and 55 kDa α-CrT_{COOH} immuno reactive proteins in mitochondria are not bona fide integral membrane proteins, although the membrane preparation (63) indicated a definite association with the mitochondrial inner membrane.

Comparison with adenine nucleotide translocase (ANT) as a genuine transmembrane protein of the inner mitochondrial membrane, and miCK as a more soluble protein in the inter-membrane space, being weakly associated with both mitochondrial membranes, indicated also in isolated kidney mitochondria that the immuno reactive 55 and 70 kDa "CrT" protein bands do have the behaviour of membrane-attached proteins rather than of integral trans-membrane proteins (not shown).

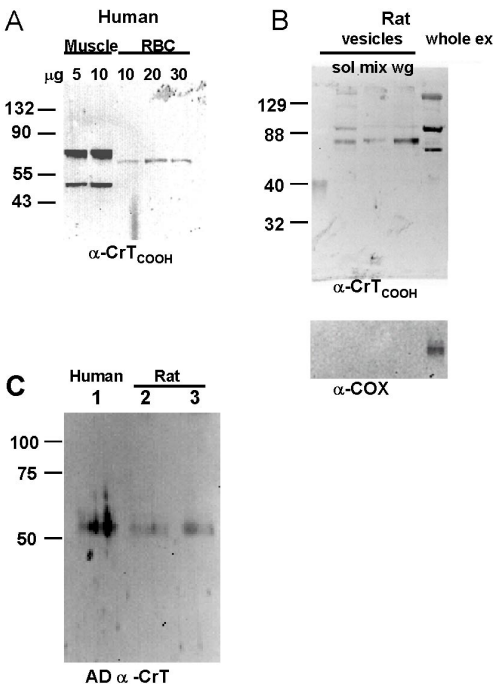

Figure 9 (A) Human skeletal muscle extracts (lanes 1 and 2) and proteins from red blood cell membranes (lanes 3 to 5) were separated by SDS-PAGE and transferred to nitrocellulose membrane. Membranes were probed with polyclonal rabbit α-CrT_{COOH} antibodies. The amount of protein loaded into each lane is indicated. (B).Rat skeletal muscle giant vesicle plasma membrane (lanes 1-3, soleus, mixed muscle and white gastrocnemius, respectively) and whole muscle extracts were separated by SDS-PAGE and transferred to nitrocellulose membrane. Membranes were probed with polyclonal rabbit α-CrT_{COOH} antibodies (top) and cytochrome C oxidase (α-COX, bottom). (C) Giant vesicle plasma membrane preparations from human (lane 1) and rat (lanes 2 and 3) skeletal muscle were separated by SDS-PAGE and transferred to nitrocellulose membrane. Membranes were probed with affinity purified rabbit α-CrT (Alpha Diagnostics, AD). In all figures a molecular weight marker is indicated on the left side of the figure.

α-CrT_{COOH} reactivity with pyruvate dehydrogenase enzyme complexes

A major component of the 70 kDa immuno reactive protein, thought to be the CrT_{70} isoform, was identified here as the E2 component of the PDH. To verify the result derived from LC-ES-MS/MS, 3 µg of PDH purified from porcine liver (Sigma) was compared by Western blot analysis to rat liver homogenate, brain, heart and soleus muscle (figure 8 A). In this purified PDH fraction, our α-CRT antibodies detected two major polypeptide signals, one at about 70 kDa, and the other at about 55 kDa. Both signals in the PDH fraction, when compared to the signals obtained with brain, liver, heart and soleus muscle, support our result derived from LC-ESI-MS/MS. Obviously, our α-CrT_{COOH} and α-CrT_{NH2} antibodies bind to the E2 component of PDH, and probably additionally to one of the other E1 or E3 components of PDH, as indicated by the 55 kDa immuno reactive protein band. As a standard control Western blots of purified PDH and brain extract, show no signals with the preimmune sera of either the COOH- or NH_2 terminal antibodies (figure 8 B).

Protein identified in plasma membrane and red blood cells using α-CrT$_{COOH}$ antibody

To date, a number of studies using our CrT antibodies have reported the presence of CrT in whole cell extracts of human (17, 54, 72, 73) skeletal muscle. It is now evident that the isoforms described in these studies are predominantly of mitochondrial localisation and hence detecting proteins associated with the E2 component of PDH, as described in the beginning of this section. To examine whether a protein localised exclusively to the plasma membrane in both rat and human skeletal muscle was also detectable using our α-CrT$_{COOH}$ antibody, enriched plasma membranes were isolated using the giant vesicles method. A single immunoreactive band was detected on a Western blot in both rat (Figure 9B lanes 1-3) and human (data not shown) skeletal muscle, which differed to the more abundant proteins that have been found to be of mitochondrial origin, and seen in whole muscle extracts (Figure 9A, lanes 1 and 2 and 9B, lane 4). No mitochondrial contamination of the plasma membrane fractions was seen in rat skeletal muscle as assessed by immunoprobing for cytochrome oxidase (Figure 9B, bottom). Therefore, this band may represent the high affinity, low Km CrT expected to be localised to the plasma membrane. In giant vesicles prepared from rat and human skeletal muscle, an immunoreactive band was identified migrating to the same point on the gel using either our α-CrT$_{COOH}$ or the commercially available CrT antibody (Alpha Diagnostics - AD, 10 $\mu g.\mu l^{-1}$ in blocking buffer, Figure 9C).). Examination of the protein isolated from RBC membranes, reveals a single band of ~ 68 kDa using our α-CrT$_{COOH}$ antibody (Figure 9A, lanes 3-5). A single band has also been described previously in rat red blood cells using a similar method of extraction (29). We have preliminary evidence that the immunoreactive band seen in human RBC using the α-CrT$_{COOH}$ Ab is slightly different in apparent molecular weight to the skeletal muscle plasma membrane CrT protein, however further work is required to determine this. Nevertheless, in both rat and human skeletal muscle and RBC, it is apparent that a single membrane associated protein is detected using the anti-CrT$_{COOH}$ antibody, which does not correspond to either of the predominant bands at ~ 55 and 70 kDa that have been discovered to be proteins associated with the E2 component of PDH. It is possible that this protein is the CrT protein, responsible for over 90% of Cr uptake into muscle. Sequencing data, however, is vital to clarify this.

Discussion

A word of caution concerning the major immunoreactivity of anti-CrT antibodies.

Several research groups have independently produced antibodies against the COOH- and/or NH2-terminus of the CrT (17, 43, 44, 74), as well as the commercially available antibody. All antibodies recognise at least one protein, with a molecular weight approximately 55, 70 and over 100 kDa in whole cell extracts. At least our antibodies (17, 29, 33, 54) recognise mitochondrial proteins also at 55 and 70 kDa. We have shown that the main part of these mitochondrial proteins is clearly water-soluble and not membrane spanning. This is supported by carbonate washing and phase partitioning experiments using the inner mitochondrial membrane preparations. With modern protein detection methods these were identified as different E2 components of the α-keto acid dehydrogenase multi enzyme complexes, namely pyruvate dehydrogenase (PDH), branched chain keto acid dehxdrogenase (BC-KADH) and α-ketoglutarate dehydrogenase (α-KGDH). This goes nicely in hand with data seen with confocal microscopy, electron microscopy and biochemical fractionation which all provide evidence that these proteins are localised within mitochondria. Since solubilization of the 55 and 70 kDa protein with carbonate washing was never 100% (figure 7 A), it cannot be excluded that more than one polypeptide is present in each of the two bands. Consequently, it might be that CRT polypeptides could still be hidden there. In addition we have also shown, that these antibodies recognize a protein within muscle plasma membrane, which is distinct from those recognized in mitochondria, shown in Figure 9 and (28, 29). However, so far we have not succeeded in identifying this plasma membrane CrT protein by mass spectrometry or other molecular biology techniques.

Upon close inspection of the PDH subunit sequences, very short stretches of sequence homology are seen with our N-terminal CrT peptides. Homology search with M-A-K-K-S-A-E-N-G-I-Y-S-V-S-G reveals only CrT. However, an alignment of M-A-K-K-S-A-E-N-G-I-Y-S-V-S-G with the Dihydrolipoamide acetyltransferase (EC 2.3.1.12) sequence shows homology of M-A-K-K-S-A-E-N-G-I. But only a homology search with the fused consensus sequence M-A-K-K-S-A-A-E-N-G-I reveals CrT and Dihydrolipoamide acetyltransferase (EC 2.3.1.12) with the same probability. However the homology searches under the same conditions with the C-terminal CrT sequence P-V-S-E-S-S-K-V-V reveals only CrT and GABA transporter. Aligning both termini with the amino acid sequences of the identified proteins might explain the cross-reactivity. However, after aligning both termini with HSP60 one would expect also a cross reactivity with this protein, which is experimentally not observed (figure 5A). These data may explain the very unexpected cross-reactivity, the chances of which, however, would appear to be marginal at first glance. However, the fact that our antibodies clearly cross-react with purified PDH is a clear argument that there is indeed cross-reactivity of our anti-CrT antibodies with this enzyme.

Interestingly, in humans suffering from primary biliary cirrhosis, auto-antibodies against PDH have been detected. Primary biliary cirrhosis is a chronic idiopathic liver disease characterized by the specific destruction of intrahepatic bile ducts (75). This disease is characterized by the presence of anti mitochondrial antibodies in patient sera, and many lines of evidence suggest the involvement of an autoimmune response in the pathogenesis of primary biliary cirrhosis. The major mitochondrial antigens recognized by anti mitochondrial antibodies include the constituents of α-keto acid dehydrogenase complexes, namely the PDH, BC-KADH and the α-KGDH. It has been demonstrated that the E2 components of PDH, α-KGDC and BC-KADH are the major determinants of the anti mitochondrial antibodies in the sera of patients with primary biliary cirrhosis (75-80). These considerations may explain the presence of auto-PDH antibodies in our rabbits, although they were clearly negative before immunisation as seen in figure 8 B, that is, immunisation of the rabbits with these peptides could have led to elicitation of auto-antibodies against PDH.

On the other hand it seems very unlikely that this should happen in several laboratories to the same extent unless the injection of CrT related sequences to generate antibodies against this protein, or the appearance of these antibodies in the animals bloodstream, by some mechanism of cell damage, would lead to the formation of auto-anti-PDH antibodies. This would indicate that anti-CrT antibodies in the blood stream would do some cell damage in the injected animals.

Thus, although our anti-sera and probably also those of other laboratories clearly contain some antibodies against genuine CrT, the most prominent signals on whole cell extracts with these antibodies are always at 55 and 70 kDa. These latter two proteins are more likely to represent subunits of PDH and other keto acid dehydrogenase's and are unlikely to have anything to do with genuine CrT unless unknown CrT species would share the same Mr of 55 and 70 kDa, as discussed above. However as shown with purified plasma membrane, which is free of mitochondria protein, a third protein is detected. This protein is different in its size from those detected in mitochondria and may represent plasma membrane CrT (Figure 9) (28; 29; 54)

Thus, all quantification results of CrT obtained so far with the different anti-CrT antibodies, either directed against synthetic peptides or fusion proteins, should be viewed with caution, due to the fact that the prominent signals at 55 and 70 kDa are at least to a major part due to cross-reactivity of the ant-CrT antibodies with PDH, or may in the worst case have nothing to do with CrT at all. The latter question remains elusive until a clear-cut identification of CrT polypeptides is achieved either from immunoprecipitated material or by 1D SDS-PAGE / mass- spectrometer analysis.

Explanation of the unexpected results by the new data

Assuming now that the two major polypeptides recognized by the anti-CrT antibodies are not related to CrT, but two subunits of mitochondrial keto acid dehydrogenase, peripherally attached to the inner mitochondrial membrane (matrix side), this would explain the preponderance of the 55 and 70 kDa polypeptides seen in heart and liver which are both tissues with high mitochondrial volume content. Additionally, ours and the work of others showing the fibre type dependence of the CrT in both rat (54, 55) and human (73) whole skeletal muscle needs to be re-examined.

The prominent localization signals both by immuno-fluorescence staining (29, 33, 54, 73), as well as be immuno-electron microscopy (33) may now be explained by cross-reactivity of the anti-CrT AB's with mitochondrial keto acid dehydrogenase's. However, on the other hand, mitochondria have been shown recently to possess a Cr uptake system, by simple Cr transport assays, independently of the use of antibodies (33, 35). This Cr uptake, although showing low affinity for Cr, was inhibited by compounds reacting with sulfhydriles, as well as by our anti-C-terminal CrT antibody. However, additional competition experiments have to be performed concerning the specificity of mitochondrial Cr uptake, for it could be, as indicated by its high Km for Cr of 15mM, which corresponds approximately to the internal free Cr concentrations in muscle, that this transporter may not be exclusively for Cr. As indicated by the competitive effect of arginine and lysine on mitochondrial Cr transport (33) it may also transport other related compounds into mitochondria. Again, interestingly, our anti-CrT peptide antibodies have been shown to interfere with mitochondrial Cr uptake so that it has to be assumed that these sera indeed contain anti-CrT activity, the question remaining is whether this activity is related to the two prominent signals of 55 and 70kDa or to some of the low-abundance signals, specifically to a faint immuno-reactive high-Mr polypeptide in the range of 112 kDa that is often seen on Western blots of isolated mitochondria. It is to be expected that the amount of plasma membrane CrT expressed in cells may be very low and thus the signals of genuine CrT seen when enriched plasma membrane is examined may be very weak on Western blots when whole tissue extraction methods are used. Unfortunately though, it seems, that the 55 and 70 kDa signals were so clear-cut and strong that the entire community was mislead to believe that these were the important signals. To sort this multifaceted enigma, which is holding up the entire CrT research community, a new series of

experiments is necessary to identify the genuine CrT isoforms in tissues and in sub cellular fractions.

Conclusions and outlook

Based on our results and those of other groups in the field, we still hold to the general scheme (figure 10) that besides the high-efficiency plasmalemma CrT (26-28, 42, 44, 51, 58, 81-83) there exists an additional low affinity high km CrT in mitochondria (29, 33).

In line with the above observation, *in vivo* isotope tracing studies with labeled Cr have shown that creatine kinase does not have access to the entire cellular Cr and PCr pool(s) (84), which indicates that intracellular Cr and PCr pools may exist that are not in immediate equilibrium with one another. Such interpretations are in agreement with a number of 31P NMR magnetization transfer studies (85), as well as with recent 1H NMR spectroscopy data (86), where monitoring the Cr and PCr levels in human muscle pointed to the existence of a pool of Cr that is not NMR "visible" in resting muscle, but appears in NMR spectra of muscle in ischemic fatigue or post mortem (86).

As far as the identification of CrT species is concerned, the exact protein biochemical nature of these CrT polypeptides, - this holds true also for the plasmalemma CrT, as well as for the mitochondrial CrT-, remains elusive until clear-cut identification and sequence data are available. Until such data are available, we suggest, in light of the facts demonstrated above, that anti-CrT antibodies, if at all, should only be used with these precautions in mind. CrT-quantification as a function of certain interventions, e.g. creatine supplementation or creatine depletion, obtained by α-CrT Western blot quantification have to be considered with caution and need to be re-evaluated in the future, when the molecular identity of CrT isoforms are known.

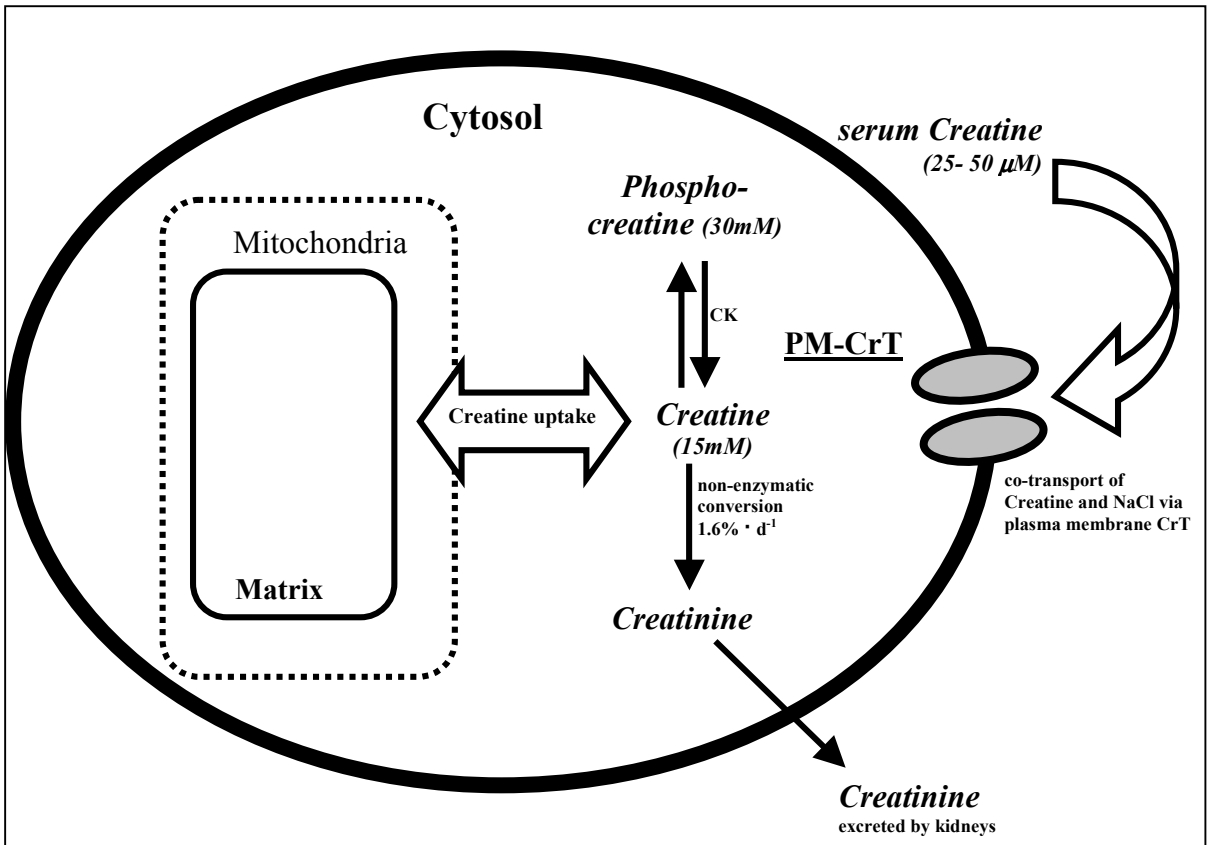

Figure 10 General scheme of cellular Cr transport. A compartmentation of three Cr pools, that is, in blood serum, cytosol, and mitochondria, are shown. These pools are interconnected via two different Cr uptake mechanisms, the high affinity (low *Km*) plasma membrane Cr transporter (*PM-CrT*) (28, 29) and the low affinity (high *Km*) mitochondrial Cr transport (33). The high Cr concentration gradient (300–600-fold) between serum and cytosol was maintained using an outside-in-directed NaCl gradient, which was used to co-transport Cr across the plasma membrane against a huge Cr concentration gradient. Two-thirds of the Cr that has entered the cytosol becomes trans-phosphorylated by the creatine kinase reaction to PCr, which is not a substrate of the plasma membrane CrT . The strict discrimination of the plasma membrane CrT between Cr and PCr leads to entrapment of PCr inside the cell, since PCr escapes equilibration. This thermodynamically facilitates further Cr uptake by the plasma membrane CrT and helps maintaining the enormous total Cr concentration gradient (600–1,000-fold) across the plasma membrane. The mitochondrial CrTs present in the inner mitochondrial membrane mediate Cr transport into mitochondria. Biological membranes, impermeable for Cr and PCr, not being in equilibrium with each other via diffusion, separate all three Cr compartments. These Cr transport mechanisms are likely to be regulated to mediate the exchange and channeling of Cr between these independent compartments, which may differ in their total Cr content, as well as in their PCr/Cr ratios according to their specific metabolic needs. The concentrations of PCr (30 mM) and Cr (15 mM) given here are those of a glycolytic fast twitch skeletal muscle (13, 16), with a typically very high Cr content.

References

1. Braissant, O., Henry, H., Loup, M., Eilers, B., and Bachmann, C. Endogenous synthesis and transport of creatine in the rat brain: an in situ hybridization study(1), Brain Res Mol Brain Res. *86:* 193-201., 2001.
2. Cecil, K. M., Salomons, G. S., Ball, W. S., Jr., Wong, B., Chuck, G., Verhoeven, N. M., Jakobs, C., and DeGrauw, T. J. Irreversible brain creatine deficiency with elevated serum and urine creatine: a creatine transporter defect?, Ann Neurol. *49:* 401-4., 2001.
3. Salomons, G. S., van Dooren, S. J., Verhoeven, N. M., Cecil, K. M., Ball, W. S., Degrauw, T. J., and Jakobs, C. X-linked creatine-transporter gene (SLC6A8) defect: a new creatine- deficiency syndrome, Am J Hum Genet. *68:* 1497-500., 2001.
4. Stockler, S., Hanefeld, F., and Frahm, J. Creatine replacement therapy in guanidinoacetate methyltransferase deficiency, a novel inborn error of metabolism, Lancet. *348:* 789-90., 1996.
5. Stockler, S., Isbrandt, D., Hanefeld, F., Schmidt, B., and von Figura, K. Guanidinoacetate methyltransferase deficiency: the first inborn error of creatine metabolism in man, Am J Hum Genet. *58:* 914-22., 1996.
6. Stockler, S., Marescau, B., De Deyn, P. P., Trijbels, J. M., and Hanefeld, F. Guanidino compounds in guanidinoacetate methyltransferase deficiency, a new inborn error of creatine synthesis, Metabolism. *46:* 1189-93., 1997.
7. Bizzi, A., Bugiani, M., Salomons, G. S., Hunneman, D. H., Moroni, I., Estienne, M., Danesi, U., Jakobs, C., and Uziel, G. X-linked creatine deficiency syndrome: a novel mutation in creatine transporter gene SLC6A8, Ann Neurol. *52:* 227-31., 2002.
8. Cecil, K. M., DeGrauw, T. J., Salomons, G. S., Jakobs, C., Egelhoff, J. C., and Clark, J. F. Magnetic resonance spectroscopy in a 9-day-old heterozygous female child with creatine transporter deficiency, J Comput Assist Tomogr. *27:* 44-7., 2003.
9. Wyss, M. and Schulze, A. Health implications of creatine: can oral creatine supplementation protect against neurological and atherosclerotic disease?, Neuroscience. *112:* 243-60, 2002.
10. Item CB, S.-I. S., Stromberger C, Muhl A, Alessandri MG, Bianchi MC, Tosetti M, Fornai F, Cioni G. Arginine:glycine amidinotransferase deficiency: the third inborn error of creatine metabolism in humans., Am J Hum Genet. *69:* 1127-33, 2001.
11. Stockler, S., Holzbach, U., Hanefeld, F., Marquardt, I., Helms, G., Requart, M., Hanicke, W., and Frahm, J. Creatine deficiency in the brain: a new, treatable inborn error of metabolism, Pediatr Res. *36:* 409-13., 1994.
12. van der Knaap, M. S., Verhoeven, N. M., Maaswinkel-Mooij, P., Pouwels, P. J., Onkenhout, W., Peeters, E. A., Stockler-Ipsiroglu, S., and Jakobs, C. Mental retardation and behavioral problems as presenting signs of a creatine synthesis defect, Ann Neurol. *47:* 540-3., 2000.
13. Wyss, M. and Kaddurah-Daouk, R. Creatine and creatinine metabolism, Physiol Rev. *80:* 1107-213., 2000.
14. Snow, R. J. and Murphy, R. M. Creatine and the creatine transporter: a review, Mol Cell Biochem. *224:* 169-81., 2001.
15. Wallimann, T. and Hemmer, W. Creatine kinase in non-muscle tissues and cells, Mol Cell Biochem. *133-134:* 193-220, 1994.
16. Wallimann, T., Wyss, M., Brdiczka, D., Nicolay, K., and Eppenberger, H. M. Intracellular compartmentation, structure and function of creatine kinase isoenzymes in tissues with high and fluctuating energy demands: the 'phosphocreatine circuit' for cellular energy homeostasis, Biochem J. *281:* 21-40, 1992.
17. Guerrero-Ontiveros ML, W. T. Creatine supplementation in health and disease. Effects of chronic creatine ingestion in vivo: down-regulation of the expression of creatine transporter isoforms in skeletal muscle., Mol Cell Biochem. *184:* 427-37, 1998.
18. Hemmer, W., Riesinger, I., Wallimann, T., Eppenberger, H. M., and Quest, A. F. Brain-type creatine kinase in photoreceptor cell outer segments: role of a phosphocreatine circuit in outer segment energy metabolism and phototransduction, J Cell Sci. *106:* 671-83, 1993.
19. Hemmer, W. and Wallimann, T. Functional aspects of creatine kinase in brain, Dev Neurosci. *15:* 249-60, 1993.
20. Ishida, Y., Riesinger, I., Wallimann, T., and Paul, R. J. Compartmentation of ATP synthesis and utilization in smooth muscle: roles of aerobic glycolysis and creatine kinase, Mol Cell Biochem. *133-134:* 39-50, 1994.
21. Bessman, S. P. and Carpenter, C. L. The creatine-creatine phosphate energy shuttle, Annu Rev Biochem. *54:* 831-62, 1985.
22. Walker, J. B. Creatine: biosynthesis, regulation, and function, Adv Enzymol Relat Areas Mol Biol. *50:* 177-242, 1979.
23. Walker, J. B. and Hannan, J. K. Creatine biosynthesis during embryonic development. False feedback suppression of liver amidinotransferase by N-acetimidoylsarcosine and 1- carboxymethyl-2-iminoimidazolidine (cyclocreatine), Biochemistry. *15:* 2519-22., 1976.
24. Magri, E., Baldoni, G., and Grazi, E. On the biosynthesis of creatine. Intramitochondrial localization of transamidinase from rat kidney, FEBS Lett. *55:* 91-3., 1975.
25. Grazi, E., Magri, E., and Balboni, G. On the control of arginine metabolism in chicken kidney and liver, Eur J Biochem. *60:* 431-6., 1975.

26. Fitch CD, S. R., Payne WF, Dacus JM Creatine metabolism in skeletal muscle. 3. Specificity of the creatine entry process., J Biol Chem. *243:* 2024-7, 1968.
27. Fitch, C. D. and Shields, R. P. Creatine metabolism in skeletal muscle. I. Creatine movement across muscle membranes, J Biol Chem. *241:* 3611-4., 1966.
28. Peral, M. J., Garcia-Delgado, M., Calonge, M. L., Duran, J. M., De La Horra, M. C., Wallimann, T., Speer, O., and Ilundain, A. Human, rat and chicken small intestinal Na(+)-Cl(-)-creatine transporter: functional, molecular characterization and localization, J Physiol. *545:* 133-144., 2002.
29. Walzel, B., Speer, O., Boehm, E., Kristiansen, S., Chan, S., Clarke, K., Magyar, J. P., Richter, E. A., and Wallimann, T. New creatine transporter assay and identification of distinct creatine transporter isoforms in muscle, Am J Physiol Endocrinol Metab. *283:* E390-401., 2002.
30. Zhao, C. R., Shang, L., Wang, W., and Jacobs, D. O. Myocellular creatine and creatine transporter serine phosphorylation after starvation, J Surg Res. *105:* 10-6., 2002.
31. Wang, W., Jobst, M. A., Bell, B., Zhao, C. R., Shang, L. H., and Jacobs, D. O. Cr supplementation decreases tyrosine phosphorylation of the CreaT in skeletal muscle during sepsis, Am J Physiol Endocrinol Metab. *282:* E1046-54., 2002.
32. Wang, W., Shang, L. H., and Jacobs, D. O. Complement regulatory protein CD59 involves c-SRC related tyrosine phosphorylation of the creatine transporter in skeletal muscle during sepsis, Surgery. *132:* 334-40., 2002.
33. Walzel, B., Speer, O., Zanolla, E., Eriksson, O., Bernardi, P., and Wallimann, T. Novel mitochondrial creatine transport activity. Implications for intracellular creatine compartments and bioenergetics, J Biol Chem. *277:* 37503-11., 2002.
34. Hebisch S, S. H., Soboll S *Pflügers Arch. 406:* 20-24, 1986.
35. Soboll, S., Conrad, A., Eistert, A., Herick, K., and Kramer, R. Uptake of creatine phosphate into heart mitochondria: a leak in the creatine shuttle, Biochim Biophys Acta. *1320:* 27-33., 1997.
36. Hahn, K. A., Salomons, G. S., Tackels-Horne, D., Wood, T. C., Taylor, H. A., Schroer, R. J., Lubs, H. A., Jakobs, C., Olson, R. L., Holden, K. R., Stevenson, R. E., and Schwartz, C. E. X-linked mental retardation with seizures and carrier manifestations is caused by a mutation in the creatine-transporter gene (SLC6A8) located in Xq28, Am J Hum Genet. *70:* 1349-56., 2002.
37. Ades, L. C., Gedeon, A. K., Wilson, M. J., Latham, M., Partington, M. W., Mulley, J. C., Nelson, J., Lui, K., and Sillence, D. O. Barth syndrome: clinical features and confirmation of gene localisation to distal Xq28, Am J Med Genet. *45:* 327-34., 1993.
38. Bolhuis, P. A., Hensels, G. W., Hulsebos, T. J., Baas, F., and Barth, P. G. Mapping of the locus for X-linked cardioskeletal myopathy with neutropenia and abnormal mitochondria (Barth syndrome) to Xq28, Am J Hum Genet. *48:* 481-5., 1991.
39. Consalez, G. G., Thomas, N. S., Stayton, C. L., Knight, S. J., Johnson, M., Hopkins, L. C., Harper, P. S., Elsas, L. J., and Warren, S. T. Assignment of Emery-Dreifuss muscular dystrophy to the distal region of Xq28: the results of a collaborative study, Am J Hum Genet. *48:* 468-80., 1991.
40. Thomas, N. S., Williams, H., Cole, G., Roberts, K., Clarke, A., Liechti-Gallati, S., Braga, S., Gerber, A., Meier, C., Moser, H., and et al. X linked neonatal centronuclear/myotubular myopathy: evidence for linkage to Xq28 DNA marker loci, J Med Genet. *27:* 284-7., 1990.
41. Gregor, P., Nash, S. R., Caron, M. G., Seldin, M. F., and Warren, S. T. Assignment of the creatine transporter gene (SLC6A8) to human chromosome Xq28 telomeric to G6PD, Genomics. *25:* 332-3., 1995.
42. Nash, S. R., Giros, B., Kingsmore, S. F., Rochelle, J. M., Suter, S. T., Gregor, P., Seldin, M. F., and Caron, M. G. Cloning, pharmacological characterization, and genomic localization of the human creatine transporter, Receptors Channels. *2:* 165-74, 1994.
43. Kekelidze, T., Khait, I., Togliatti, A., and Holtzman, D. Brain creatine kinase and creatine transporter proteins in normal and creatine-treated rabbit pups, Dev Neurosci. *22:* 437-43., 2000.
44. Tran, T. T., Dai, W., and Sarkar, H. K. Cyclosporin A inhibits creatine uptake by altering surface expression of the creatine transporter, J Biol Chem. *275:* 35708-14., 2000.
45. Dodd, J. R. and Christie, D. L. Cysteine 144 in the third transmembrane domain of the creatine transporter is located close to a substrate-binding site, J Biol Chem. *276:* 46983-8., 2001.
46. Blakely, R. D., De Felice, L. J., and Hartzell, H. C. Molecular physiology of norepinephrine and serotonin transporters, J Exp Biol. *196:* 263-81., 1994.
47. Nelson, N. The family of Na+/Cl- neurotransmitter transporters, J Neurochem. *71:* 1785-803., 1998.
48. Moller, A. and Hamprecht, B. Creatine transport in cultured cells of rat and mouse brain, J Neurochem. *52:* 544-50., 1989.
49. Boehm, E., Chan, S., Monfared, M., Wallimann, T., Clarke, K., and Neubauer, S. Creatine transporter activity and content in the rat heart supplemented by and depleted of creatine, Am J Physiol Endocrinol Metab. *284:* E399-406., 2003.
50. Guimbal, C. and Kilimann, M. W. A Na(+)-dependent creatine transporter in rabbit brain, muscle, heart, and kidney. cDNA cloning and functional expression, J Biol Chem. *268:* 8418-21, 1993.
51. Schloss, P., Mayser, W., and Betz, H. The putative rat choline transporter CHOT1 transports creatine and is highly expressed in neural and muscle-rich tissues, Biochem Biophys Res Commun. *198:* 637-45., 1994.
52. Gonzalez, A. M. and Uhl, G. R. 'Choline/orphan V8-2-1/creatine transporter' mRNA is expressed in nervous, renal and gastrointestinal systems, Brain Res Mol Brain Res. *23:* 266-70., 1994.
53. Neubauer, S., Remkes, H., Spindler, M., Horn, M., Wiesmann, F., Prestle, J., Walzel, B., Ertl, G., Hasenfuss, G., and Wallimann, T. Downregulation of the Na(+)-creatine cotransporter in failing human myocardium and in experimental heart failure, Circulation. *100:* 1847-50, 1999.

54. Murphy, R., McConell, G., Cameron-Smith, D., Watt, K., Ackland, L., Walzel, B., Wallimann, T., and Snow, R. Creatine transporter protein content, localization, and gene expression in rat skeletal muscle, Am J Physiol Cell Physiol. *280:* C415-C422., 2001.
55. Brault, J. J. and Terjung, R. L. Creatine uptake and creatine transporter expression among rat skeletal muscle fiber types, Am J Physiol Cell Physiol. *5:* 5, 2003.
56. Miller, K., Sharer, K., Suhan, J., and Koretsky, A. P. Expression of functional mitochondrial creatine kinase in liver of transgenic mice, Am J Physiol. *272:* C1193-202, 1997.
57. Queiroz, M. S., Shao, Y., Berkich, D. A., Lanoue, K. F., and Ismail-Beigi, F. Thyroid hormone regulation of cardiac bioenergetics: role of intracellular creatine, Am J Physiol Heart Circ Physiol. *283:* H2527-33., 2002.
58. Sora, I., Richman, J., Santoro, G., Wei, H., Wang, Y., Vanderah, T., Horvath, R., Nguyen, M., Waite, S., Roeske, W. R., and et al. The cloning and expression of a human creatine transporter, Biochem Biophys Res Commun. *204:* 419-27, 1994.
59. Afolayan, A. and Daini, O. A. Isolation and properties of creatine kinase from the breast muscle of tropical fruit bat, Eidolon helvum (Kerr), Comp Biochem Physiol B. *85:* 463-8, 1986.
60. Wolfel, R., Halbrugge, T., and Graefe, K. H. Effects of N-ethylmaleimide on 5-hydroxytryptamine transport and sodium content in rabbit platelets, Br J Pharmacol. *97:* 1308-14., 1989.
61. Sandoval, N., Bauer, D., Brenner, V., Coy, J. F., Drescher, B., Kioschis, P., Korn, B., Nyakatura, G., Poustka, A., Reichwald, K., Rosenthal, A., and Platzer, M. The genomic organization of a human creatine transporter (CRTR) gene located in Xq28, Genomics. *35:* 383-5, 1996.
62. Guimbal, C. and Kilimann, M. W. A creatine transporter cDNA from Torpedo illustrates structure/function relationships in the GABA/noradrenaline transporter family, J Mol Biol. *241:* 317-24., 1994.
63. Hovius, R., Lambrechts, H., Nicolay, K., and de Kruijff, B. Improved methods to isolate and subfractionate rat liver mitochondria. Lipid composition of the inner and outer membrane, Biochim Biophys Acta. *1021:* 217-26., 1990.
64. Brdiczka, D., Pette, D., Brunner, G., and Miller, F. [Compartmental dispersion of enzymes in rat liver mitochondria], Eur J Biochem. *5:* 294-304., 1968.
65. Kristiansen, S., Hargreaves, M., and Richter, E. A. Exercise-induced increase in glucose transport, GLUT-4, and VAMP-2 in plasma membrane from human muscle, Am J Physiol. *270:* E197-201., 1996.
66. Gorg, A., Obermaier, C., Boguth, G., Harder, A., Scheibe, B., Wildgruber, R., and Weiss, W. The current state of two-dimensional electrophoresis with immobilized pH gradients, Electrophoresis. *21:* 1037-53. [pii], 2000.
67. Brusca, J. S. and Radolf, J. D. Isolation of integral membrane proteins by phase partitioning with Triton X-114, Methods Enzymol. *228:* 182-93, 1994.
68. Fujiki, Y., Hubbard, A. L., Fowler, S., and Lazarow, P. B. Isolation of intracellular membranes by means of sodium carbonate treatment: application to endoplasmic reticulum, J Cell Biol. *93:* 97-102., 1982.
69. Suzuki, H., Okazawa, Y., Komiya, T., Saeki, K., Mekada, E., Kitada, S., Ito, A., and Mihara, K. Characterization of rat TOM40, a central component of the preprotein translocase of the mitochondrial outer membrane, J Biol Chem. *275:* 37930-6., 2000.
70. Neukomm, L. Identification of antigens recognized by anti-Creatine Transporter antibodies in rat liver mitochondria. Zürich: Swiss Federal technical Highschool, ETH, 2002.
71. Maas, E. and Bisswanger, H. Localization of the alpha-oxoacid dehydrogenase multienzyme complexes within the mitochondrion, FEBS Lett. *277:* 189-90., 1990.
72. Tarnopolsky, P., Walzel, Schlattner, Wallimann Creatine Transporter and Mitochondrial Creatine Kinase Protein Content in Myopathies: Significant Reduction of Creatine Transporters in Myopathies, Muscle and Nerve. *24:* 682-688, 2001.
73. Murphy, R., Tunstall, R., Mehan, K., Cameron-Smith, D., McKenna, M. J., Spriet, L., M., H., and Snow, R. Human skeletal muscle creatine transporter mRNA and protein expression in males and females., Mol Cell Biochem. *244:* 151-157, 2003.
74. Dodd, J. R., Zheng, T., and Christie, D. L. Creatine accumulation and exchange by HEK293 cells stably expressing high levels of a creatine transporter, Biochim Biophys Acta. *1472:* 128-36., 1999.
75. Bassendine, M. F., Jones, D. E., and Yeaman, S. J. Biochemistry and autoimmune response to the 2-oxoacid dehydrogenase complexes in primary biliary cirrhosis, Semin Liver Dis. *17:* 49-60., 1997.
76. Nishio, A., Coppel, R., Ishibashi, H., and Gershwin, M. E. The pyruvate dehydrogenase complex as a target autoantigen in primary biliary cirrhosis, Baillieres Best Pract Res Clin Gastroenterol. *14:* 535-47., 2000.
77. Mackay, I. R., Whittingham, S., Fida, S., Myers, M., Ikuno, N., Gershwin, M. E., and Rowley, M. J. The peculiar autoimmunity of primary biliary cirrhosis, Immunol Rev. *174:* 226-37., 2000.
78. Tanaka, A., Nalbandian, G., Leung, P. S., Benson, G. D., Munoz, S., Findor, J. A., Branch, A. D., Coppel, R. L., Ansari, A. A., and Gershwin, M. E. Mucosal immunity and primary biliary cirrhosis: presence of antimitochondrial antibodies in urine, Hepatology. *32:* 910-5., 2000.
79. Reynoso-Paz, S., Leung, P. S., Van De Water, J., Tanaka, A., Munoz, S., Bass, N., Lindor, K., Donald, P. J., Coppel, R. L., Ansari, A. A., and Gershwin, M. E. Evidence for a locally driven mucosal response and the presence of mitochondrial antigens in saliva in primary biliary cirrhosis, Hepatology. *31:* 24-9., 2000.

80. Yeaman, S. J., Kirby, J. A., and Jones, D. E. Autoreactive responses to pyruvate dehydrogenase complex in the pathogenesis of primary biliary cirrhosis, Immunol Rev. *174:* 238-49., 2000.
81. Saltarelli, M. D., Bauman, A. L., Moore, K. R., Bradley, C. C., and Blakely, R. D. Expression of the rat brain creatine transporter in situ and in transfected HeLa cells, Dev Neurosci. *18:* 524-34, 1996.
82. Loike, J. D., Somes, M., and Silverstein, S. C. Creatine uptake, metabolism, and efflux in human monocytes and macrophages, Am J Physiol. *251:* C128-35., 1986.
83. Dai, W., Vinnakota, S., Qian, X., Kunze, D. L., and Sarkar, H. K. Molecular characterization of the human CRT-1 creatine transporter expressed in Xenopus oocytes, Arch Biochem Biophys. *361:* 75-84., 1999.
84. Hochachka, P. W. and Mossey, M. K. Does muscle creatine phosphokinase have access to the total pool of phosphocreatine plus creatine?, Am J Physiol. *274:* R868-72., 1998.
85. Joubert, F., Gillet, B., Mazet, J. L., Mateo, P., Beloeil, J., and Hoerter, J. A. Evidence for myocardial ATP compartmentation from NMR inversion transfer analysis of creatine kinase fluxes, Biophys J. *79:* 1-13., 2000.
86. Kreis, R., Jung, B., Slotboom, J., Felblinger, J., and Boesch, C. Effect of exercise on the creatine resonances in 1H MR spectra of human skeletal muscle, J Magn Reson. *137:* 350-7., 1999.
87. Zorzano, A., Fandos, C., and Palacin, M. Role of plasma membrane transporters in muscle metabolism, Biochem J. *349 Pt 3:* 667-88., 2000.

ADDITIONAL RESULTS

Identification of the α-CrT reactive, high molecular weight protein

As seen in figure 7, 8 and 9, there was another > 100 kDa polypeptide reacting with the α-CrT_{COOH} serum This could be separated from the α-CrT 55 and 70 kDa polypeptides, identified as PDH (see figure 5), by a floating technique as described in chapter 3. PDH was collected completely within the pellet, whereas the >100 kDa protein was floating to lower density regions of the gradient (figure 11). It was concluded, that this protein might be a membrane protein, as found also by carbonate washing (figure 7). The high molecular weight region was subsequently cut out from a coomassie stained gel, trypsin digested and analysed by MALDI-TOF. With the resulting peak list the carbamoyl-phosphate synthase (CPS) was identified. The amino acid sequence was covered to 24 %, and the identification score reached 140. The CPS was identified from two different mitochondrial membrane preparations each two samples were analyzed.

CPS is a mitochondrial enzyme, highly hydrophobic and associated with the MIM (Powers-Lee SG JBC1987). After computing the hydrophobicity plot (figure 12, inset), CPS appeared to contain two transmembrane domains. The CPS model presented here, depicts CPS with the N- and C-term facing the mitochondiral matrix, whereas the loop between both trans membrane domains is facing the inter membrane space (figure 12). This could be also the part of the protein recognized by the α-CrT antibody on the outer

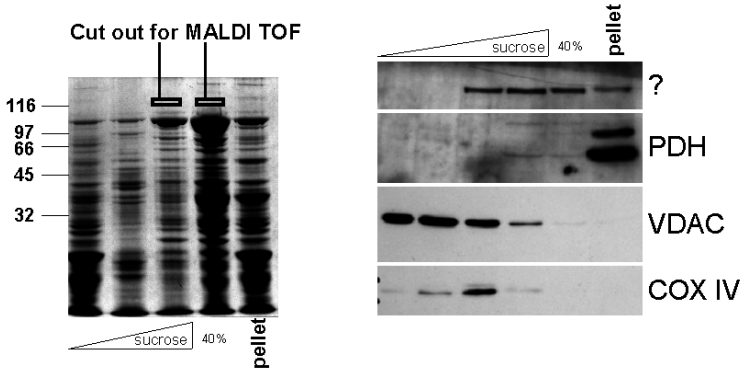

Figure 11 **Separation of different α-CrT reactive proteins.** Isolated liver and kidney mitochondria were diluted with chilled washing buffer to 20 mg/ml mitochondrial proteins and 0.75 % Triton X-100 final concentration. Mitochondria were dissolved on ice in a glace/glace homogeniser. The Triton homogenate was diluted resulting in 40 % Sucrose and 10 mg/ml mitochondrial protein in washing buffer. This 40 % sucrose solution was layered under a linear sucrose gradient (38%- 15%) and centrifuged for at least 20h at 100'000 x g at 4°C. The resulting gradient was aliquoted into 500 µl. After the protein determination, 20 µg protein from each sample was precipitated by standard TCA precipitation, dissolved in SDS buffer, and proceeded to Western blot (see materials and methods chapter 4).

CARBAMOYL-PHOSPHATE SYNTHASE

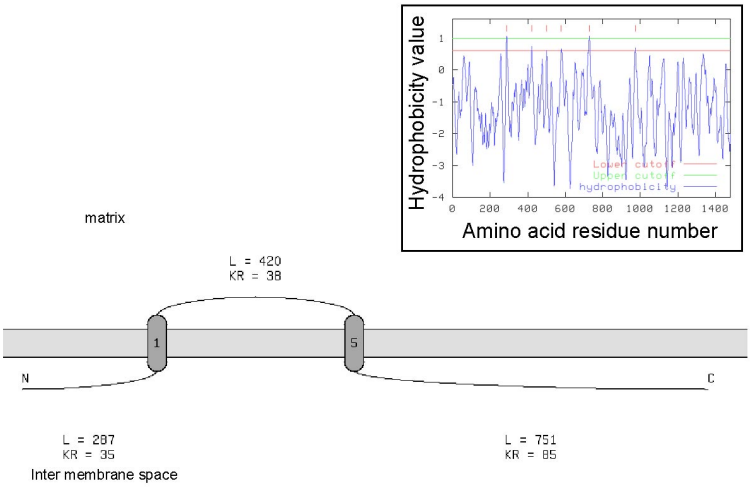

Figure 12. **Hydrophobicity plot and membrane topology of CPS.** The aminoacid sequence of CPS was analysed by the hydrophobicity of each amino acid residue. Thereby relative negative values are given to hydrophilic residues, whereas hydrophobic residues getting number towards positive values. A trans-membrane domain is considered as sure, if an amino acid stretch of at least 10 residues is beyond the lower cut-off value 0.6, as well as containing residues over the higher cut-off value 1. (Inset). For CPS at least two trans-membrane domains were found.

unpublished

surface of the MIM, as presented in Chapter 5, figure 5. Thus remains only one α-CrT reactive polypeptide at 65 kDa, which is, however, only present in muscular plasma membrane (figure 9). We assume, that mitochondria do not contain a protein related to CrT. However, mitochondria take up creatine significantly and highly reproducibly. This creatine uptake was slightly inhibited by FCCP, NEM, α-CrT antibodies, and by arginine. Therefore we started to reinvestigate the mitochondrial creatine uptake, as presented in the next section.

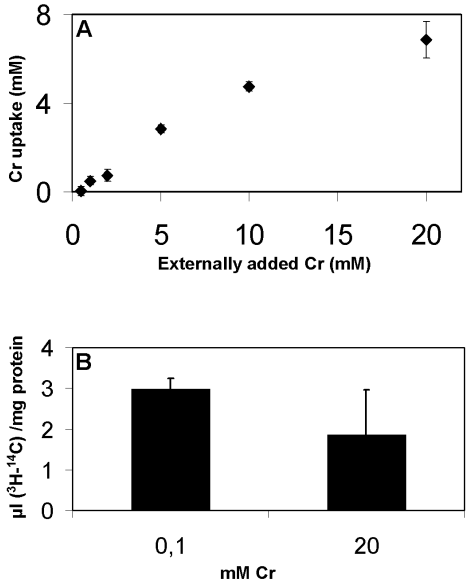

Figure 13. **Intra mitochondrial Cr concentration determination**. Creatine uptake assay and volume measurements were performed as described in material and methods. *Panel A:* Rat liver mitochondria were incubated for 5 min with the indicated Cr concentrations. In parallel mitochondria were incubated with unlabeled Cr and in addition with tritium labelled water and 14C labelled sucrose for the volume determination (see materials and methods). The mitochondrial volume was determined as 2.9 ± 0.25 µl/mg, an decreased slightly but not significant after the addition of 20 mM Cr (*panel B*).

A critical appraisal of mitochondrial creatine uptake

Background

There is no doubt that mitochondria are able to take up creatine, as shown in Chapter 4. However, based on our results obtained with the α-CrT antibodies no Cr transporter protein could be identified within the inner mitochondrial membrane, as was seen earlier in this chapter. Therefore mitochondrial Cr uptake was reinvestigated. First the volume of mitochondria was measured, which lead to an estimation of the intra-mitochondrial Cr concentration accumulated after Cr uptake. Second the release of Cr from mitochondria into the medium was measured after a creatine uptake.

Results

Creatine concentration within mitochondria. We have seen in chapter 4, that the mitochondrial creatine uptake is a high K_m low affinity uptake, in contrast to the Cr uptake by the cytoplasmic membrane. It was of interest to measure mitochondrial volume in parallel to the creatine uptake measurements. Using ^{14}C sucrose and tritium labelled water, liver mitochondria were determined to contain 2.9 ± 0.25 µl water /mg mitochondrial protein. This water permeable and sucrose impermeable volume was named matrix volume. With this volume, the creatine concentration was determined during the Cr transport. These measurements revealed that mitochondria take up, but do not accumulate Cr. As seen in figure 13 the concentration after 5 minutes uptake did stay below the externally given Cr concentrations.

After the findings, that (a) we were not successful in demonstrating a specific CrT molecule within mitochondria, (b) the intra-mitochondrial Cr concentration remained at 30 - 40 % of the external Cr concentration and (c) the dependence of the mitochondrial Cr uptake upon mitochondrial functions such as respiration, oxidative phosphorylation and uncoupling was not significant as seen in Figure 7, Chapter 5. There it was shown that neither the addition of succinate nor the addition of nucleotides changed significantly the mitochondrial Cr uptake in comparison to non-respiring mitochondria. A slight inhibition after uncoupling with FCCP however was seen.

Consequently the question came up whether the mitochondrial Cr uptake is driven by diffusion. Therefore, mitochondria were incubated with ^{14}C labelled Cr and ^{3}H-sucrose (see experimental procedures) for 5 min and washed afterwards either with unlabeled "cold" Cr or with buffer without Cr. The experiment was controlled by adding 0.1 % Triton X100 to dissolve mitochondria completely, which should release all the Cr. Mitochondria were then precipitated by centrifugation and the amount of radioactivity in the precipitates (pellet in figure 14) and super-natants (SN in figure 14) were compared.

As seen in figure 14, under all conditions, nearly 100% of the Cr was released. Also sucrose behaved in a similar manner. However there might be the tendency, that more sucrose was retained by mitochondria by the given time. That means that the off-rate of Cr from mitochondria is such high, that almost all ^{14}C-Cr is found in the medium at the moment the external ^{14}C-Cr is taken away. Cr seems to migrate even faster then sucrose. This finding goes well in hand with the results seen in figure 13: mitochondria take up Cr if high amounts of Cr are present in the medium, but then only up to 30% of the external concentration. This process seems to be equilibrium of binding and release of Cr. The ^{14}C-Cr molecules are randomly distributed. That would mean that once ^{14}C-Cr is changed for "cold" Cr, the ^{14}C-Cr is lost in the ocean of surrounding medium, (seen in figure 14 as the bars Cr SN compared to Cr Pellet).

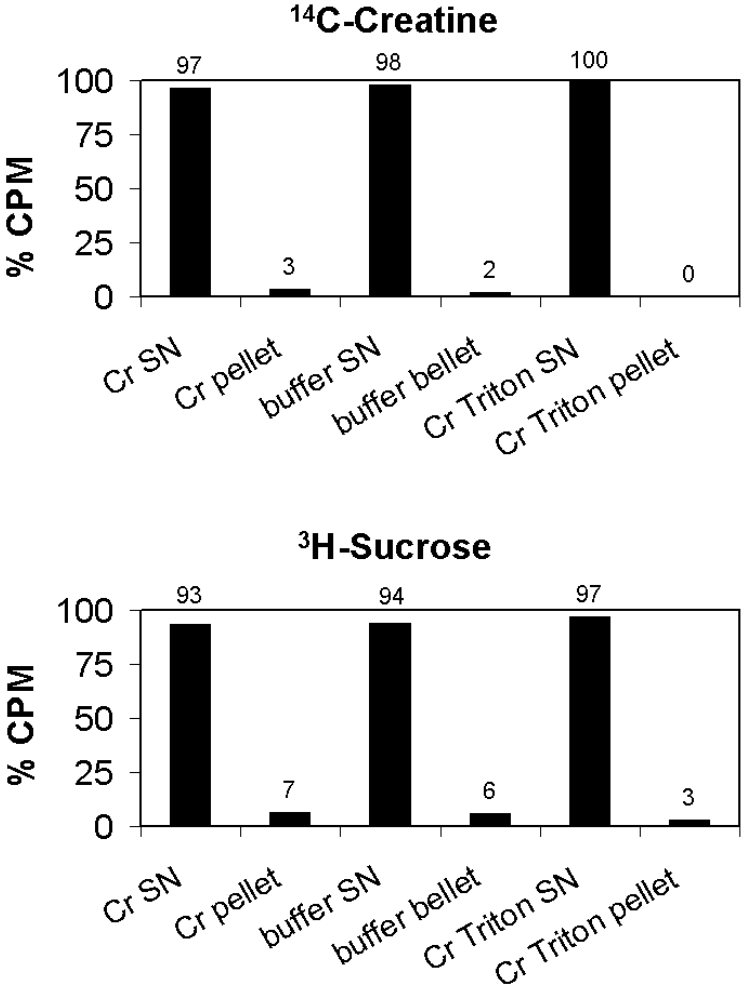

Figure 14. **Pulse chase of mitochondrial creatine uptake**. Creatine uptake assay was performed as described in experimental procedures. Rat liver mitochondria were incubated for 5 min with the 10 mM Cr spiked with 14C-Cr and 3H-sucrose (see text and experimental procedures), precipitated by centrifugation for 1 min at 13000g and resuspended in Hepes sucrose buffer containing succinate, ADP, inorganic phosphate, EGTA. In parallel mitochondria were incubated with 10 mM unlabeled Cr , buffer only and buffer supplemted with 0.1 % Triton X 100 for 5 min. Mitochondria were precipitated again, the supernatants (SN) and the dissolved pellets were analysed in a scintillation counter. The sum of the counted decays per minute (CPM) of a corresponding pair of SN and pellet were set as 100 %. The means of a triplicate experiment are shown. Note that in all conditions nearly 100 percent of the creatine as well as sucrose is set free to the medium.

Discussion

Since mitochondria in the cytosol are surrounded by a high concentration of Cr, which seems to degrease towards the centre of mitochondria. However as the concentration of Cr

inside the cell is in the range of 20 mM (1, 3), and mitochondria absorb Cr to about ~30 % of the external conzentration, mtCK inside mitochondria will still be surrounded by at least ~6 mM Cr. Cr should be small enough to migrate relatively freely into the inter-membrane space and into the cristae lumen of mitochondria.

The concept of a mitochondrial Cr transport has to be discussed again. In Chapter 5, Figure 7 and (2) was shown, that the uncoupler FCCP reduces the mitochondrial Cr uptake about 40 %. We discussed thereafter that the mitochondrial Cr uptake seems to be dependent on membrane potential ($\Delta\Psi_m$).

Remarcably, in Chapter 2 was shown that mitochondria if suspended in buffer do not develop $\Delta\Psi_m$. Once supplemented with a substrate, i.e. succinate $\Delta\Psi_m$ increases clearly (drop of TMRE fluorescenz, *Chapter 2, Figure 2A and 3A*). Thus you have to expect, that the mitochondrial Cr uptake should increase significantly after the addition of succinate. However as seen in Figure 7, Chapter 5 no difference in the Cr uptake between mitochondria with or without succinate was detected. Neither was a change detected after the addition of ADP, which should provoke a drop in $\Delta\Psi_m$, as the ATPsynthase consumes it. I fear that the results in chapter 5 and (2) were not interpreted carefully enough.

The results in figure 13 (*this chapter*) demonstrate that the intra-mitochondrial concentration stays ~70% below the external Cr concentration, after the entire measured "matrix" volume (Figure 13) was taken into count. Besides in Figure 14 it was shown, that the Cr seems to diffuse into and out of mitochondria (*panel A*), equally as sucrose does (*panel B*). As both substances behaved similar in the pulse chase experiment I conclude that the mitochondrial Cr uptake is a diffusion driven Cr influx. Further an increasing Cr concentration leads to a slight, unspecific decrease of the sucrose impermeable volume (figure 13B). That could mean the matrix is shrinking due to osmosis, as high Cr concentrations are presentoutside the matrix. For that Cr does not enter the mitochondrial matrix, similar to sucrose. But why is it then possible to measure a Cr uptake?

In the Cr uptake studies ^{14}C-Cr and ^{3}H-sucrose were used. One difference between sucrose and Cr is size; sucrose is much bigger than Cr. Thus, it might well be that sucrose has access to certain areas of the inter-membrane space, however is too large to follow Cr, which diffuses deeply into the cristae spaces.

While measuring the mitochondrial "matrix" volume, in fact the sucrose impermeable space was measured. However it seems that there is a sucrose impermeable "none-matrix" volume, permeable for Cr, which is actually counting for the net "Cr uptake". This was consequently measured! This sucrose impermeable volume seems to be the cristae volume. If that is the case, the Cr concentrations inside the cristae are probably as high as the external concentration. But counting the Cr, which was taken up on the entire sucrose impermeable volume, it appears to reach only 30 % of the external concentration. It follows, that the matrix counts for 70 % and cristae for 30 % of the sucrose impermeable volume.

Why do FCCP and NEM have an effect on the diffusion of Cr into the cristae? As seen in chapter 3 (*Figure 1 and 2*) FCCP can provoke mitochondrial swelling. Thus also the volume of cristae might be reduced, which will lead to a decreased "Cr uptake". Or even the cristae entrance for sucrose might be extended, resulting also in an apparently reduced Cr uptake. The same might be valid for the NEM effect seen in Chapter 5, figure 6: NEM as a SH-reagent shuts down the entire mitochondrial respiratory chain, which leads to a drop of $\Delta\Psi_m$, and possibly to swelling and rupture of mitochondrial membranes. In fact we never followed the mitochondrial swelling after addition of 0.1 or 1 mM NEM used as seen in Chapter 5, figure 6. I conclude that the effects of FCCP and NEM on the mitochondrial Cr influx were unspecific.

However these new findings cannot explain the inhibition of mitochondrial Cr uptake by α-CrT antibodies, also shown in Chapter 5. Also the inhibition of the Cr uptake by arginine does not make sense in this light. However arginine is decreasing the mitochondrial Cr uptake by less then 40 %. However, inhibitors of the plasma membrane Cr transport decrease the Cr by more then 80 %. Substances such as β-GPA, cyclo-Cr and Cr it self had highly significant effects on the plasma membrane Cr transport (Peral et al. J Physiol 2002). All those substances had no effect on the mitochondrial Cr uptake. Additionally Cyclocreatine is getting to the same places inside mitochondria, namely mtCK, as it was shown in Chapter3

that both, Cr and CycloCr have the same effects on mPT. But there CycloCr is not competing the Cr uptake. That indicates that there is free diffusion into the cristae- and inter-membrane spaces, if not otherwise CycloCr takes different ways. This comparison illustrates that the mitochondrial Cr influx is rather unspecific.

I propose that Cr migrates thru the openings of the critstae, the pediculi into the cristae lumen. This mechanism is sufficient for Cr to get directly to the location of mtCK. MtCK has direct access to matrix ATP via coupling with ANT. Consequently the Cr, surrounding mtCK in the cristae lumen, becomes phosphorylated. PCr is still small enough to migrate out of the cristae space into the inter-membane space thru VDAC into the cytoplasmic space by diffusion, maybe even driven by concentration gradients, or at its best by near-equilibrium reactions catalysed by mtCK, as presented in Chapter 1, Figure 3.

References

1. **Wallimann T and Hemmer W.** Creatine kinase in non-muscle tissues and cells. *Mol Cell Biochem* 133-134: 193-220, 1994.
2. **Walzel B, Speer O, Zanolla E, Eriksson O, Bernardi P, and Wallimann T.** Novel mitochondrial creatine transport activity. Implications for intracellular creatine compartments and bioenergetics. *J Biol Chem* 277: 37503-37511, 2002.
3. **Wyss M and Kaddurah-Daouk R.** Creatine and creatinine metabolism. *Physiol Rev* 80: 1107-1213., 2000.

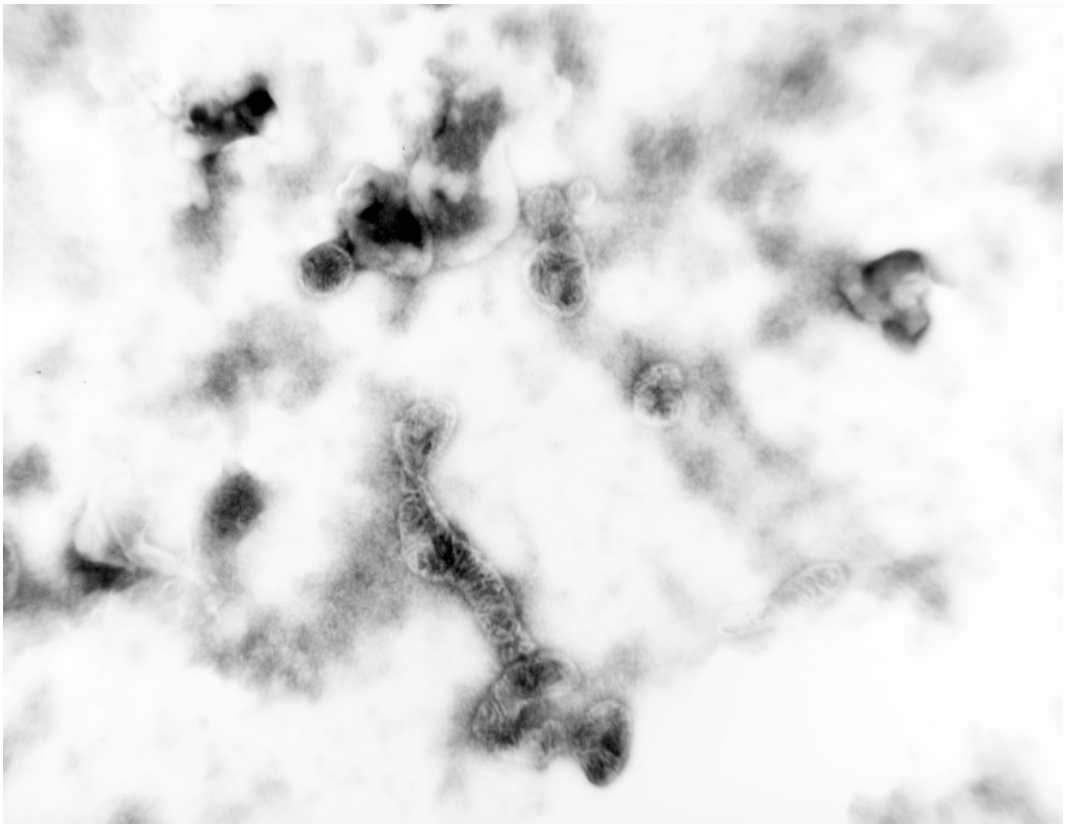

Brain mitochondria, Oliver Speer, April 2001

CONCLUDING REMARKS

In my PhD thesis, the mitochondrial permeability transition (mPT) and novel aspects of mitochondria in creatine metabolism were under investigation. We have characterised a new inhibitor of the mPT, the carbonyl compound methyglyoxal (MG). This compound is an intermediate, which is set free from the glycolytic enzyme triose phosphate isomerase. Therefore, MG is a physiological substance appearing in µM concentrations in the cell *in vivo*. Interestingly, of the 29 tested carbonyl compounds from glucose- and amino acid-metabolism, only MG and its derivative glyoxal had an inhibiting effect on (mPT). *Nota bene*, MG had no influence on vital mitochondrial functions such as oxidative phosphorylation. As mPT inhibitor, MG prevented the release of the apoptogenic protein cytochrome c after Ca^{2+} or ceramide stimuli. Several proteins are known, especially Bcl-2 family members that prevent cytochrome c release. The idea of preventing mitochondria from going into mPT and releasing of apoptogenic factors by a small metabolic intermediate can be considered as a new concept. Furthermore these findings depict how precise and carefully mitochondria are linked into cellular metabolic cross talk.

Small compounds and the mitochondrial permeability transition

The precise target of MG is largely unknown. However, after the analysis of synthetic peptides, it became clear that MG is able to modifie covalently arginine residues. This is confirmed by the characteristics of other synthetic carbonyl compounds such as phenylglyoxal and 2,3-butanedione. With MG and other covalent mPT modifiers, new tools for the identification of proteins involved in mPT might now be available.

Another small compound, creatine, is known to prevent mitochondria from mPT in concert with the corresponding enzyme mtCK. It was already known that creatine prevented uncoupled respiration, caused by mPT induction (6). In mitochondria from transgenic liver over-expressing ubiquitous mtCK creatine, and cyclo-creatine inhibit mitochondrial swelling after mPT induction by Ca^{2+} pulses and uncoupling. No external addition of nucleotides was necessary to achieve those affects. Most importantly, the addition of creatine together with purified mtCK to mitochondria isolated from wild type liver that are expressing no mtCK did not prevent Ca^{2+} induced mitochondrial swelling.

Thus it became clear, that mtCK should be located in a micro-compartment together with the adenine nucleotide translocator (ANT) in order to display full enzyme activity with regard to mPT regulation. Further, it was demonstrated that mitochondria form a defined pool of intra-mitochondrial nucleotides, which seem not to leak out, not even during mitochondrial isolation.

Micro-comparments within mitochondria

While studying mitochondria from mtCK expressing liver, I found that mtCK is located between MIM and MOM, but importantly also inside christae, confirming previous findings (7, 8). By digitonin treatment it was shown, that the mere presence of mtCK increased mitochondrial and christae stability and structural integrity. Thus the idea of micro-compartments within mitochondria was strengthened. It was possible to prepare micro-compartments containing mtCK, ANT, VDAC and components of the respiratory chain by floating of detergent resistant membranes. This approach might represent a novel method to prepare mitochondrial enzyme complexes, eventually containing the mPT pore constituents. However this has to be evaluated very carefully by other robust methods, such as immuno electron microscopy or co-immune precipitation.

Mitochondrial creatine uptake

The location of mtCK inside mitochondrial christae remote from the cytoplasm, begs the question of how the substrate, creatine, reaches its target, mtCK. Indeed it was possible to measure a mitochondrial creatine uptake. This uptake displayed a high K_m and low V_{max}, was inhibited by the uncoupler FCCP but not stimulated by substrates, and inhibited by arginine presumably competitively. These characteristics, however, were very much different from those of the reported plasma membrane transporter. Nevertheless the experimental

facts were convincing enough to conclude that a new mitochondrial creatine tranporter (CrT) identified, as anti-creatine transporter peptide antibodies detected defined polypeptides within the MIM by Western blotting of membrane sub-fractions and immune electron microscopy. This conviction became even greater, after I found that these antibodies inhibited the mitochondrial creatine uptake.

Consequently, those anti-CrT reactive proteins were identified by modern proteomics techniques, 2D gel electrophoresis, MALDI-TOF and ESI-MS/MS. However, none of the candidates was a genuine CrT. We identified dehydrogenase complex components, as well as an enzyme from the Urea cycle, carboamoyl synthase (CPS). To test the findings from the mass spectroscopy data, mitochondrial membranes were washed at high pH. Indubitable, two of the three candidates were not membrane proteins, but only membrane attached polypeptides. The third promising candidate, CPS, might be a membrane protein, as found from its hydrophobic pattern. However, it seems unlikely, that CPS forms a transporter.

A critical view on mitochondrial creatine uptake

Upon closed inspection of the available data on mitochondrial creatine uptake obtained earlier (1, 9) and more recently in our laboratory (10, 12), together with our new data from the pulse chase experiment, as well as quantification of the concentration of creatine taken up by mitochondria with respect to mitochondrial volume, we have to conclude that mitochondrial creatine uptake per se does indeed exists, but this process seems to be a passive diffusion based influx of creatine into the mitochondrial inter-membrane, as well as the inter-cristae space, where the substrate is used by mtCK located in these two compartments.

The fact that total mitochondrial creatine concentrations, when calculated by virtue of total mitochondrial volume measurements, reached only about 30% of the externally added concentration, strongly argues that not the entire mitochondrial volume is uniformly occupied by creatine. The inter-membrane space and intra-cristae space could eventually make up, depending on the source and state of mitochondria, a third of the mitochondrial volume. Thus, the creatine concentration within the inter-membrane space and intra-cristae space could reach the external concentration of creatine surrounding mitochondria.

If this interpretation were correct, creatine would not enter the matrix space. Anyhow this would not make physiological sense, since there is no mtCK located, and in addition this would agree with the results that we, after all, could not find a specific CrT in the inner mitochondrial membrane with our antibodies.

The fact that liver mitochondria, which do not contain mtCK did take-up creatine equally well as mitochondria from tissues, which contain mtCK, was a very unexpected and puzzling finding, because it simply would not make physiological sense. If this can now be explained by passive creatine influx into the inter-membrane and inter-cristae space of any kind of mitochondria this enigma would be solved.

The fact that creatine migrates into the inter-membrane and intra-cristae space, would still make mitochondria to a significant store of total cellular creatine. This intra-mitochondrial creatine then could well behave in certain respects, e.g. speed of exchangeability with the cytosolic creatine pool, as a different entity (2), as well as in NMR-visibility terms (3-5, 11).

The thesis presented here is an example how steep and contorted the path of scientific work can be. New and unexpected findings have to be verified and corroborated by different methods and from different angles of perspectives! After a cumbersome Odyssey, the reward of finally being able to interpret the flood of data and to reach some final conclusions is comforting.

References

1. **Hebisch S SH, Soboll S.** *Pflügers Arch* 406: 20-24, 1986.
2. **Hochachka PW and Mossey MK.** Does muscle creatine phosphokinase have access to the total pool of phosphocreatine plus creatine? *Am J Physiol* 274: R868-872., 1998.
3. **Joubert F, Mazet JL, Mateo P, and Hoerter JA.** 31P NMR detection of subcellular creatine kinase fluxes in the perfused rat heart: contractility modifies energy transfer pathways. *J Biol Chem* 277: 18469-18476, 2002.
4. **Joubert F, Vrezas I, Mateo P, Gillet B, Beloeil JC, Soboll S, and Hoerter JA.** Cardiac creatine kinase metabolite compartments revealed by NMR magnetization transfer spectroscopy and subcellular fractionation. *Biochemistry* 40: 2129-2137, 2001.
5. **Kinsey ST, Locke BR, Penke B, and Moerland TS.** Diffusional anisotropy is induced by subcellular barriers in skeletal muscle. *NMR Biomed* 12: 1-7, 1999.
6. **O'Gorman E BG, Dolder M, Koretsky AP, Brdiczka D, Wallimann T.** The role of creatine kinase in inhibition of mitochondrial permeability transition. *FEBS Lett* 414: 253-257, 1997.
7. **Rojo M, Hovius R, Demel R, Wallimann T, Eppenberger HM, and Nicolay K.** Interaction of mitochondrial creatine kinase with model membranes. A monolayer study. *FEBS Lett* 281: 123-129, 1991.
8. **Rojo M, Hovius R, Demel RA, Nicolay K, and Wallimann T.** Mitochondrial creatine kinase mediates contact formation between mitochondrial membranes. *J Biol Chem* 266: 20290-20295, 1991.
9. **Soboll S, Conrad A, Eistert A, Herick K, and Kramer R.** Uptake of creatine phosphate into heart mitochondria: a leak in the creatine shuttle. *Biochim Biophys Acta* 1320: 27-33., 1997.
10. **Speer O, Neukomm L, Murphy R, Zanolla E, Schlattner U, Snow R, and Wallimann T.** Creatine transporter isozymes: a reappraisal. *Mol Cell Biochem* in press, 2003.
11. **van Dorsten FA, Furter R, Bijkerk M, Wallimann T, and Nicolay K.** The in vitro kinetics of mitochondrial and cytosolic creatine kinase determined by saturation transfer 31P-NMR. *Biochim Biophys Acta* 1274: 59-66, 1996.
12. **Walzel B, Speer O, Zanolla E, Eriksson O, Bernardi P, and Wallimann T.** Novel mitochondrial creatine transport activity. Implications for intracellular creatine compartments and bioenergetics. *J Biol Chem* 277: 37503-37511, 2002.

Bambus, acryl on paper, Oliver Speer, April 2002

Dipl. Biol. Oliver Speer

08.01.1973
German
Single

Magnusstr. 22
CH - 8004 Zürich
Switzerland

+ 41 78 803 02 60
oliver.speer@cell.biol.ethz.ch

Education

01/07/2003	Thesis defence
04/2000 – 07/2003	Ph. D. student in Theo Wallimann´s group, Institute for Cell Biology, ETH Zürich
09/1999	Diploma (very good)
10/1994 – 09/1999	Studying at the Faculty of Biology, University of Konstanz
11/1992 - 01/1994	Civil service in the Hospital of Konstanz
05/1992	Abitur (good), award for the best student in natural sciences.

Working experience

Since 09/2000	ETH Zürich, Institute of Cell Biology, PhD student in Dr. Theo Wallimann's group. Investing the role of mitochondria in creatine synthesis and metabolic regulation.
08/2002 – 09/ 2002	University of Helsinki, visiting Dr. Ove Eriksson. Investigating the rapid suppression of mitochondrial permeability transition by methylglyoxal and the role of reversible arginine modification
05/2000 – 08/2000	University of Helsinki, learning electron microscope techniques with Dr. Ove Eriksson and Dr. Sarah Butcher. Investing the ultrastructure of miCK overexpressing rat liver.
09/1999 – 04/2000	Universitiy of Konstanz, investigating the role of Bax on mitochondria and mechanisms of cytochrome c in Dr. Dieter Brdiczka´s lab.
11/1998 – 09/1999	Diploma in Dr. Michael Ehrmann´s lab, University of Konstanz. Structural and functional mapping of the complex membrane transporter TolC of *E. coli* using a novel target-directed proteolysis technique.
05/ - 06/1998	University of Konstanz, Dr. Pierluigi Nicotera´s group, Measuring mitochondrial membrane potential in Jurkat cells after treatment with nitric oxide.
02/ - 04/1998	University degli studii, Padova, Dr. Paolo Bernardi´s lab, Studding whether a model condition could be identified leading to mobilisation of Cytochrome C to the intermembrane space without rupturing the outer membrane.
06/ - 07/1996	University of Konstanz, Prof. Dr. Dieter Brdiczka´s workgroup, Tissue specific regulations of mitochondrial and cytoplasmic enzymes during creatine depletion.

Techniques

Biochemistry/ cell biology	▶ 2D gel electrophoresis and in gel trypsin digestion ▶ Identifying proteins with MALDI TOF and LC ESI MS/MS ▶ Sub cellular fractionation (mitochondria and nuclei from cultured cells and different tissues) ▶ Measuring different mitochondrial parameters (oxygen consumption, membrane potential, swelling) in vitro and vivo. ▶ Confocal- and immuno fluorescenz microscopy ▶ Enzyme activitiy assays ▶ Cell culturing (Jurkat cells) ▶transport measurements with radioactive labelled substrates
Molecular biology	▶ PCR techniques like cross-over PCR, oligomutagenesis, sequencing, cloning, expression of engineered proteins, ▶ Western blotting
Electron microscopy	▶ negative staining, immuno electron microscopy, tilting series, image processing, 3D reconstruction

Languages

German, English, Italian, French

Other skills

One-week course in project management

One-week course in scientific communication, presenting and writing

Elected student for the council of faculty

Personal interests

Painting, stage design, trainer for swimming, rescue diving, sailing

Zürich, June 2003

Publications

1. **Oliver Speer**, Sarune Morkunaite-Haimi, Julius Liobikas, Marina Franck, Linn Hensbo, Matts D. Linder, Paavo J. K. Kinnunen, Theo Wallimann, and Ove Eriksson Rapid Suppression of Mitochondrial Permeability Transition by Methylglyoxal, Role of Reversible Arginine Modification. *J Biol Chem*, 2003 Jun 18 [Epub ahead of print]

2. **Oliver Speer**, Lukas J. Neukomm, Robyn M. Murphy, Elsa Zanolla, Uwe Schlattner, Rodney J. Snow, and Theo Wallimann
Creatine transporter isoenzymes: a reappraisal. *Moll Cell Biochem* in press.

3. Max Dolder, Bernd Walzel, **Oliver Speer**, Uwe Schlattner, and Theo Wallimann Inhibition of the mitochondrial permeability transition by creatine kinase substrates: requirement for microcompartmentation. *J. Biol. Chem* 2003 May 16;278(20):17760-17766.

4. Tarnopolsky M, Parise G, Fu MH, Brose A, Parshad A, **Speer O**, Wallimann T. Acute and moderate-term creatine monohydrate supplementation does not affect creatine transporter mRNA or protein content in either young or elderly humans. *Mol Cell Biochem*. 2003 Feb; 244(1-2):159-66.

5. Peral MJ, Garcia-Delgado M, Calonge ML, Duran JM, De La Horra MC, Wallimann T**, Speer O**, Ilundain A.
Human, rat and chicken small intestinal Na+ - Cl- -creatine transporter: functional, molecular characterization and localization. *J Physiol.* 2002 Nov 15;545(Pt 1):133-44.

6. Bernd Walzel*, **Oliver Speer***, Else Zanolla, Ove Eriksson, Paolo Bernardi, and Theo Wallimann
Novel Mitochondrial Creatine Transport Activity: Implications for Intracellular Creatine Compartments and Bioenergetics. *J Biol Chem* 2002 Oct 4;277(40):37503-37511
* Contributed equally

7. Bernd Walzel*, **Oliver Speer***, Ernie Boehm, Soren Kristiansen, Sharon Chan, Kierian Clarke, Josef P. Magyar, Erik A. Richter, and Theo Wallimann
New creatine transporter assay and identification of distinct creatine transporter isoforms in muscle. *Am J Physiol Endocrinol Metab.* 2002 Aug;283(2):E390-401.
* Contributed equally

8. Wendt S, Dedeoglu A, **Speer O**, Wallimann T, Beal MF, Andreassen OA.
Reduced creatine kinase activity in transgenic amyotrophic lateral sclerosis mice. *Free Radic Biol Med* 2002 May 1;32(9):920-6

9. Schlattner U, Mockli N, **Speer O**, Werner S, Wallimann T.
Creatine kinase and creatine transporter in normal, wounded, and diseased skin. *J Invest Dermatol.* 2002 Mar;118(3):416-23.

10. Castro-Palomino JC, Simon B, **Speer O**, Leist M, Schmidt RR. Synthesis of ganglioside GD3 and its comparison with bovine GD3 with regard to oligodendrocyte apoptosis mitochondrial damage. *Chemistry* 2001 May 18;7(10):2178-84

International conferences

11/14 – 11/16/2002	3rd EMBL Ph.D. Student International Symposium: ”Life within Boundaries - Membranes & Compartments in Biology”, EMBL, Heidelberg Poster: “Creatine within mitochondrial boundaries”
08/02 – 08/04/2002	SCANDO MIT, Scandinavian Mitochondria Meeting, Tampere, Finland Poster: “Mitochondrial Creatine Transport” and “Mitochondrial kinases prevent GD3 induced permeability transition”
06/29 – 07/3/2002	ELSO Meeting 2002, Nice, France Poster: “Mitochondrial Creatine Transport”
06/13 – 06/17/2001	5th International Muscle Energetics Conference, Burlington, Vermont, USA Poster: “Mitochondrial Creatine Transport”
03/30 – 04/02/2000	“Mitochondrial related disease and myopathies” in Halle, Germany. Poster: “Mitochondrial kinases prevent GD3 induced permeability transition”
06/12 – 06/14/1999	Molecular Basis of Biomembrane Transporters, Bari, Italy. Poster: “Topology of TolC, an Escherichia coli outer membrane protein part of MDR"
06/27 – 07/02/1998	10th EBEC, Göteborg, Sweden, Abstract: BBA, EBEC Short Reports, Volume 10, p. 220
09/18 – 09/21/1997	„New Perspectives in Mitochondrial Research“ in Padova. Poster: „Tissue Specific Compensatory Regulations of Hexokinase, Creatine Kinase and Adenylate Kinase during Creatine Depletion “.

Invited talks

14/03/2003	“Creatine within mitochondrial boundaries” ASP meeting Fulda, invited by Sylvia Stöckler.
16/12/2002	“Creatine uptake into mitochondria” University of Geneva, invited by Jean-Paul Giaccobino.
26/11/2002	“Creatine transport into muscle” Swiss muscle foundation, Swiss Sport School Macolin, invited by Denis Monard.
04.11.1999	“Domain structure and functional analysis of the outer membrane protein TolC by site specific proteolysis, a novel approach.” Max-Planck-Institut für Biochemie, Martinsried. Invited by Jörg Höhfeld.
02.11.1999	“Domain structure and functional analysis of the outer membrane protein TolC by site specific proteolysis, a novel approach.” Theodor-Boveri-Institut für Mikrobiologie der Universität Würzburg. Invited by Roland Benz.
17.09.1999	“Domain structure and functional analysis of the outer membrane protein TolC by site specific proteolysis, a novel approach.” I´IBGC-CNRS Bordeaux, invited by Guy Lauquin

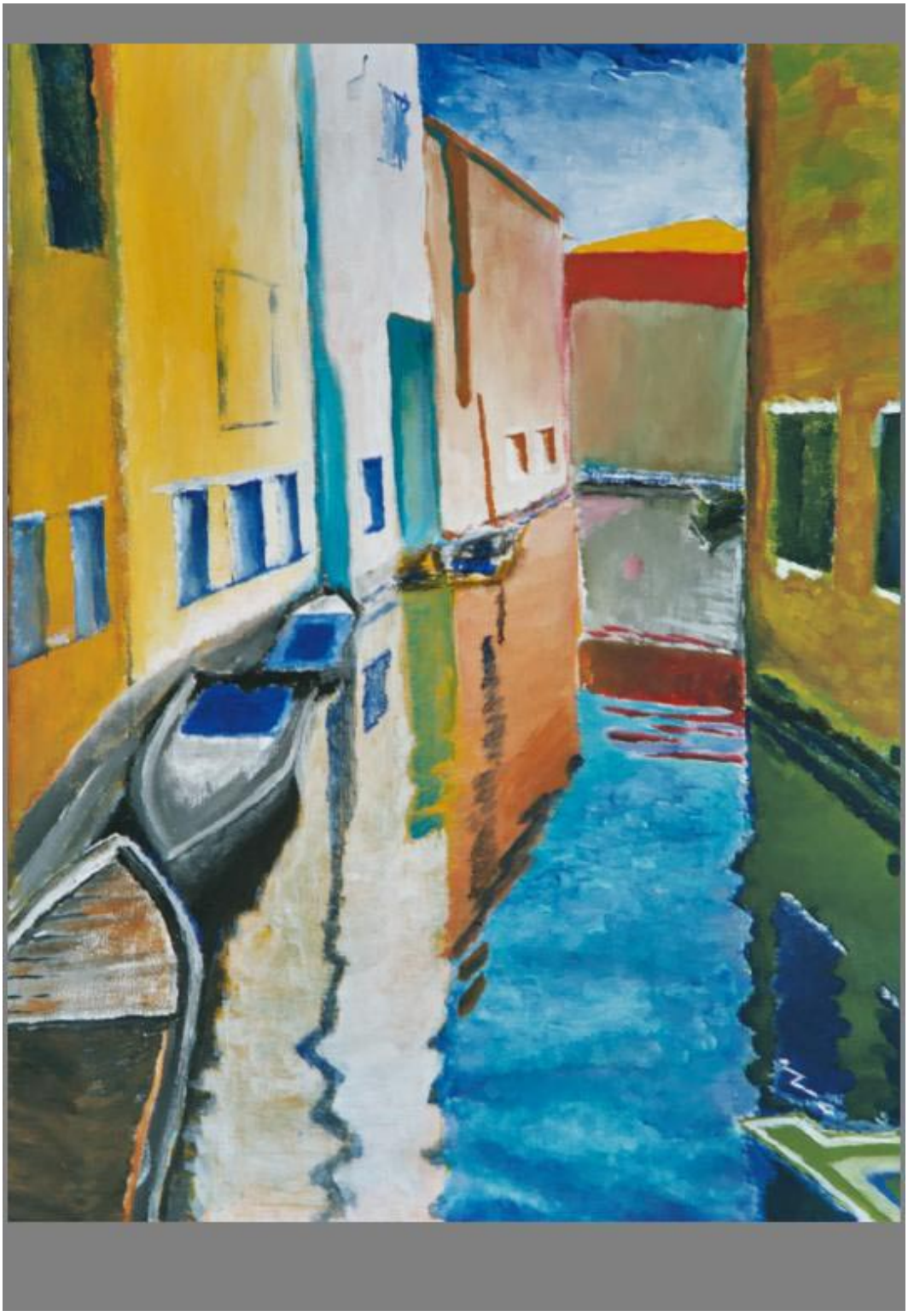

Canale, acryl on canvas, Oliver Speer, June/July 2002